LLNL-TR-862099

Lawrence Livermore National Laboratory

TEX-Hf Assemblies: Highly Enriched Uranium Plates with Hafnium Using Polyethylene Moderator and Polyethylene Reflector

IER-532 CED-4b

Jesse Norris and Eric Aboud (Internal Reviewer)
Lawrence Livermore National Laboratory

Michael Zerkle (External Reviewer)
Naval Nuclear Laboratory

External Audience (Unlimited)

August 1, 2024

Disclaimer

Acknowledgements

This work was supported by the Nuclear Criticality Safety Program (NCSP), funded and managed by the National Nuclear Security Administration for the Department of Energy. The NCSP Critical Experiment Design Team (C_EdT) included[1] Jesse Norris (LLNL, Team Lead), Theresa Cutler (LANL, Experiment Member), Michael Zerkle (NNL, Nuclear Data Advisory Group Member), William Marshall (ORNL, Methods Member), Joetta Goda (LANL, Additional Member), and Catherine Percher (LLNL, Additional Member). Thanks to Eric Aboud (LLNL) and Michael Zerkle (NNL) for serving as internal and external reviewers as part of submission to the Technical Review Group for the International Criticality Safety Benchmark Evaluation Project (ICSBEP).

The benchmark evaluation was submitted as HEU-MET-INTER-013 (HMI-013) to the 2024 ICSBEP Technical Review Group (TRG). It was reviewed and approved with pending subgroup review during the April 2024 meeting hosted by Lawrence Livermore National Laboratory (LLNL) in Livermore, CA. The ICSBEP TRG Subgroup for HMI-013 included[2]: Eric Aboud (LLNL), Kelsey Amundson (LANL), Joetta Goda (LANL), William Marshall (ORNL), Fabian Sommer (GRS), and Michael Zerkle (NNL). In addition to the members of the ICSBEP TRG and Subgroup, the following individuals provided comments[3]: John Bess (JFA), Mariya Brovchenko (IRSN), Geordie McKenzie (LANL), Alfie O'Neill (UK NNL), Kristin Stolte (LANL), Larry Wetzel (LLW), and Nicholas Whitman (LANL).

These experiments were executed at the National Criticality Experiments Research Center (NCERC) under the operation of Los Alamos National Laboratory's (LANL) Advanced Nuclear Technology Group (NEN-2). The NEN-2 experimenters involved in this campaign included Travis Grove, Theresa Cutler, Rene Sanchez, Kelsey Amundson, Nicholas Thompson, Kenneth Valdez, Justin Martin, Jessie Walker, and Alex McSpaden. Hardware design for this experiment, originally designed for TEX-HEU, was performed by Nicholas Wynne, with review by Chris Romero. The experiments were conducted with facility support by NCERC-FO and Mission Support and Test Services (MSTS). The hafnium plates were procured and provided to the NCSP by the Naval Nuclear Laboratory (NNL). All experiment photos are courtesy of NEN-2.

[1] LLNL = Lawrence Livermore National Laboratory; LANL = Los Alamos National Laboratory; NNL = Naval Nuclear Laboratory.
[2] GRS = Gesellschaft für Anlagen und Reaktorsicherheit (Germany).
[3] JFA = JFoster & Associates, LLC; IRSN = Institut de Radioprotection et de Súreté Nucléaire (France); UK NNL = National Nuclear Laboratory (United Kingdom); LLW = LL Wetzel, LLC.

Table of Contents

1.0 Detailed Description **1**
1.1 Overview of the Experiment 1
1.2 Description of Experimental Configuration 2
1.2.1 Design of the Critical Assembly 2
1.2.2 Comet General Purpose Critical Assembly Machine 4
1.2.2.1 Stationary Platform 5
1.2.2.2 Movable Platen 6
1.2.3 Highly Enriched Uranium Plates 7
1.2.4 Hafnium Plates 9
1.2.5 Polyethylene Parts 12
1.2.5.1 Moderator and Reflector Plates 12
1.2.5.2 Reflector Rings 18
1.2.5.3 Reflector Caps 22
1.2.5.4 Bottom Reflector 25
1.2.6 Aluminum Inserts 27
1.2.7 Height Measurements 29
1.2.8 Reactor Period 31
1.2.9 Experimental Configurations 32
1.2.9.1 Case 1 33
1.2.9.2 Case 2 36
1.2.9.3 Case 3 39
1.2.9.4 Case 4 42
1.2.9.5 Case 5 45
1.2.9.6 Case 6 48
1.2.9.7 Case 7 51
1.3 Description of Material Data 54
1.3.1 Highly Enriched Uranium 54
1.3.1.1 ^{235}U Enrichment 56
1.3.1.2 Uranium Impurities 57
1.3.2 Hafnium 57
1.3.2.1 Hafnium Density Measurements 57
1.3.2.2 Hafnium Impurity Analysis 57
1.3.3 Polyethylene 59
1.3.3.1 Polyethylene Density Measurements 59
1.3.3.2 Polyethylene Impurity Analysis 59
1.3.4 Aluminum 60
1.3.5 Comet General Purpose Critical Assembly Machine 60
1.4 Temperature Data 61
1.5 Supplemental Experimental Measurements 61

2.0 Evaluation of Experimental Data **62**
2.1 Reactor Period 63
2.2 Mass Uncertainty 66
2.2.1 Highly Enriched Uranium Mass 66
2.2.2 Hafnium Plate Mass 68
2.2.3 Polyethylene Moderator Mass 69

2.2.4 Polyethylene Reflector Mass 71
2.2.5 Aluminum Insert Mass 73
2.2.6 Membrane Mass 73
2.2.7 Structure Mass 74
2.3 Dimensional Uncertainty 75
2.3.1 Highly Enriched Uranium Plate Dimensions 75
2.3.2 Hafnium Plate Dimensions 76
2.3.3 Polyethylene Plate Dimensions 77
2.3.4 Aluminum Insert Dimensions 79
2.3.5 Core Stack Height 80
2.3.6 Polyethylene Reflector Ring Diameters 82
2.3.7 Polyethylene Reflector Ring Height 83
2.3.8 Membrane Thickness 85
2.3.9 Membrane Lift 86
2.3.10 Positional Uncertainty 87
2.4 Material Uncertainty 88
2.4.1 U-235 Enrichment 88
2.4.2 Highly Enriched Uranium Composition 89
2.4.3 Hafnium Composition 97
2.4.4 Polyethylene Composition 106
2.4.5 Aluminum Composition 109
2.5 Temperature Uncertainty 113
2.5.1 Thermal Contraction 114
2.5.2 Doppler Broadening 115
2.5.3 Thermal Scattering Law 116
2.6 Combined Uncertainty 118
2.6.1 Case 1 119
2.6.2 Case 2 121
2.6.3 Case 3 123
2.6.4 Case 4 125
2.6.5 Case 5 127
2.6.6 Case 6 129
2.6.7 Case 7 131

3.0 Benchmark Specifications 133
3.1 Description of Model 133
3.1.1 Model Simplification and Bias 133
3.1.1.1 HEU Impurity 133
3.1.1.2 Hafnium Impurity 134
3.1.1.3 Polyethylene Impurity 134
3.1.1.4 Aluminum Impurity 135
3.1.1.5 Temperature Correction 135
3.1.1.6 Comet and Room Removal 136
3.1.1.7 Reflector Rings, Caps, and Bottom Reflector 138
3.1.1.8 Average Geometry 138
3.1.2 Summary of Bias Calculations 140
3.2 Dimensions 140
3.2.1 Comet General Purpose Critical Assembly Machine 140

3.2.1.1 Membrane 142
3.2.1.2 Interface Plate 143
3.2.1.3 Adapter Plate 144
3.2.1.4 Adapter Extension 145
3.2.1.5 Comet Movable Platen 146
3.2.1.6 Comet Stationary Platform 147
3.2.2 Highly Enriched Uranium Plates 148
3.2.3 Hafnium Plates 149
3.2.4 Polyethylene Moderator and Reflector Plates 150
3.2.5 Polyethylene Reflector Rings and Caps 151
3.2.6 Polyethylene Bottom Reflector 152
3.2.7 Aluminum Inserts 153
3.2.8 Case Models 153
3.2.8.1 Case 1 154
3.2.8.2 Case 2 157
3.2.8.3 Case 3 160
3.2.8.4 Case 4 163
3.2.8.5 Case 5 166
3.2.8.6 Case 6 169
3.2.8.7 Case 7 172
3.3 Material Data 175
3.3.1 Highly Enriched Uranium 175
3.3.2 Hafnium 176
3.3.3 Polyethylene 178
3.3.4 Aluminum 179
3.4 Temperature Data 179
3.5 Experimental and Benchmark-Model k_{eff} 180

4.0 Results of Sample Calculations **181**

5.0 References **185**

Appendix A Typical Input Listings **186**
A.1 MCNP® 6.2.2 Input Listings 186

Appendix B Design Drawings **187**

Executive Summary

This report documents the integral experiment evaluation and publication for IER-532 (TEX-Hf), Thermal/Epithermal eXperiments (TEX) with highly enriched uranium (HEU) fuel and hafnium (Hf), moderated and reflected by polyethylene. The design of TEX-Hf is a variation of IER-297 (TEX-HEU), with the inclusion of hafnium as a diluent material. The experiment and evaluation include seven configurations, all of which were acceptable as benchmark cases. These benchmark cases provide validation for hafnium in the thermal, intermediate, and fast neutron energy regimes by maximizing the sensitivity in k_{eff} to the hafnium cross sections. The evaluation was reviewed and accepted by the International Criticality Safety Benchmark Evaluation Project (ICSBEP) Technical Review Group on April 17, 2024, and was submitted to the ICSBEP in August 2024 following subgroup approval.

Table 1 reports the benchmark k_{eff}, used to benchmark radiation transport codes. The experimental k_{eff} is calculated from the measured reactor period while the uncertainty is based on a rigorous analysis of 25 uncertainty components[1]. The bias in k_{eff} represents model simplifications for ease of modeling by the end-user[2]. The leading source of uncertainty in the experimental k_{eff} remains the core stack height[3]. Additional sources of uncertainty include the membrane thickness, ^{235}U enrichment, and the polyethylene (^{1}H in CH_2) thermal scattering law due to temperature uncertainty (only for Case 5 which is thermal).

Table 1. Summary of the cases and benchmark k_{eff}, determined by adding the bias to the experimental k_{eff}.

Case	Moderator Thickness (in.)	Neutron Spectrum[(a)]	Experimental k_{eff}	Bias in k_{eff}	Benchmark k_{eff}
1	No moderator.	Fast	1.00101 ± 0.00146	-0.00198 ± 0.00013	0.99903 ± 0.00147
2	0.125	Intermediate	1.00102 ± 0.00157	-0.00194 ± 0.00014	0.99908 ± 0.00158
3	0.250	Intermediate	1.00185 ± 0.00153	-0.00249 ± 0.00015	0.99936 ± 0.00154
4	0.500	Mixed	1.00063 ± 0.00123	-0.00220 ± 0.00015	0.99843 ± 0.00124
5	1.500	Thermal	1.00081 ± 0.00146	0.00096 ± 0.00015	1.00177 ± 0.00147
6[(b)]	0.250	Intermediate	1.00120 ± 0.00141	-0.00177 ± 0.00014	0.99943 ± 0.00142
7[(c)]	No moderator.	Fast	1.00085 ± 0.00136	-0.00142 ± 0.00012	0.99943 ± 0.00137

[(a)] Based on the majority fission fraction (calculation): thermal (<0.625 eV), intermediate (0.625 eV – 100 keV), and fast (>100 keV). The mixed neutron spectrum indicates no majority fission fraction.

[(b)] Hafnium plates are sandwiched between two nominal 0.125 in. thick polyethylene moderator plates.

[(c)] Hafnium plates are bunched as top and bottom reflector surrounding the HEU plates.

Table 2 reports sample calculational results using MCNP® 6.2.2, comparing both ENDF/B-VII.1 and ENDF/B-VIII.0. Notably, ENDF/B-VIII.0 performs better for all cases, except Case 5 (thermal) and Case 7 (fast). The Case 7 experimental configuration places the hafnium plates as top and bottom reflector surrounding the HEU plates. Disagreement with the experiment for both ENDF/B-VII.1 and ENDF/B-VIII.0 could indicate a deficiency in the hafnium scattering cross section or angular distributions. For Case 5, ENDF/B-VIII.0 underpredicts while ENDF/B-VII.1 is in agreement with the experiment. Figure 1 shows a comparison of the calculation-over-experiment (C/E) results from Table 2 for both ENDF/B-VII.1 and ENDF/B-VIII.0, compared against the other HEU benchmark C/E results in the ICSBEP. Figure 2 shows a comparison of the C/E results using ENDF/B-VIII.0 between different radiation transport codes.

[1] These uncertainty components include seven mass, ten dimensional, five material, and three temperature uncertainty components.

[2] The model simplifications include material impurity voiding, room removal, average part dimensions, and temperature correction.

[3] The core stack height measurements have improved since IER-297 (TEX-HEU), having a measurement of uncertainty of at most 0.8 mm, typically less than 0.4 mm (refer to Section 1.2.7 and Section 2.3.5).

Table 2. Sample k_{eff} and C/E results using MCNP® 6.2.2 (red denotes C/E values outside 2σ).

Case	MCNP® 6.2.2 (Continuous Energy ENDF/B-VII.1)		MCNP® 6.2.2 (Continuous Energy ENDF/B-VIII.0)	
	Calculated k_{eff}	C/E	Calculated k_{eff}	C/E
1	1.00071 ± 0.00003	1.00168 ± 0.00147	1.00097 ± 0.00003	1.00194 ± 0.00147
2	0.99733 ± 0.00004	0.99825 ± 0.00158	1.00135 ± 0.00004	1.00227 ± 0.00158
3	0.99596 ± 0.00004	**0.99660 ± 0.00154**	0.99854 ± 0.00004	0.99918 ± 0.00154
4	0.99533 ± 0.00004	**0.99690 ± 0.00124**	0.99574 ± 0.00004	**0.99731 ± 0.00124**
5	1.00298 ± 0.00004	1.00121 ± 0.00147	0.99947 ± 0.00004	0.99770 ± 0.00147
6	0.99608 ± 0.00004	**0.99665 ± 0.00142**	0.99850 ± 0.00004	0.99907 ± 0.00142
7	0.99824 ± 0.00003	0.99881 ± 0.00137	0.99605 ± 0.00003	**0.99662 ± 0.00137**

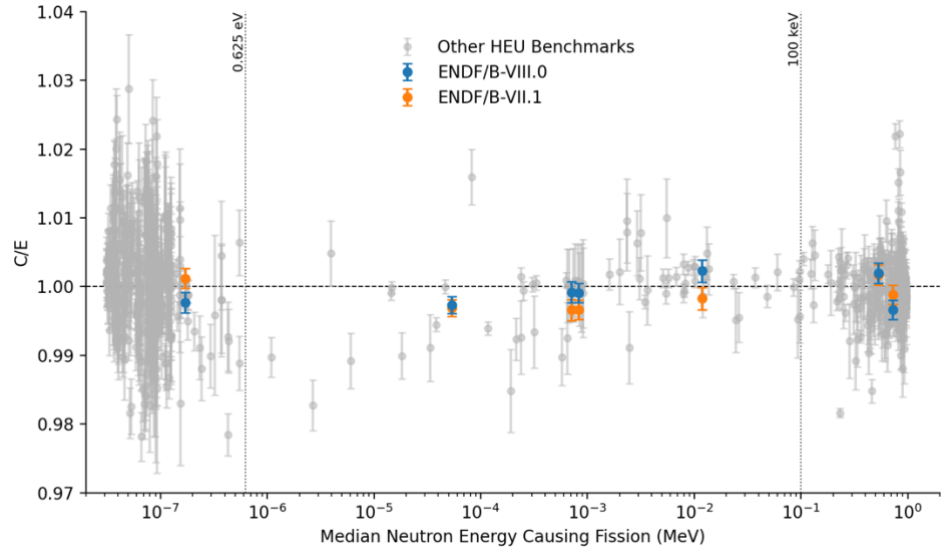

Figure 1: Comparison of C/E results using MCNP® 6.2.2 with ENDF/B-VII.1 and ENDF/B-VIII.0.

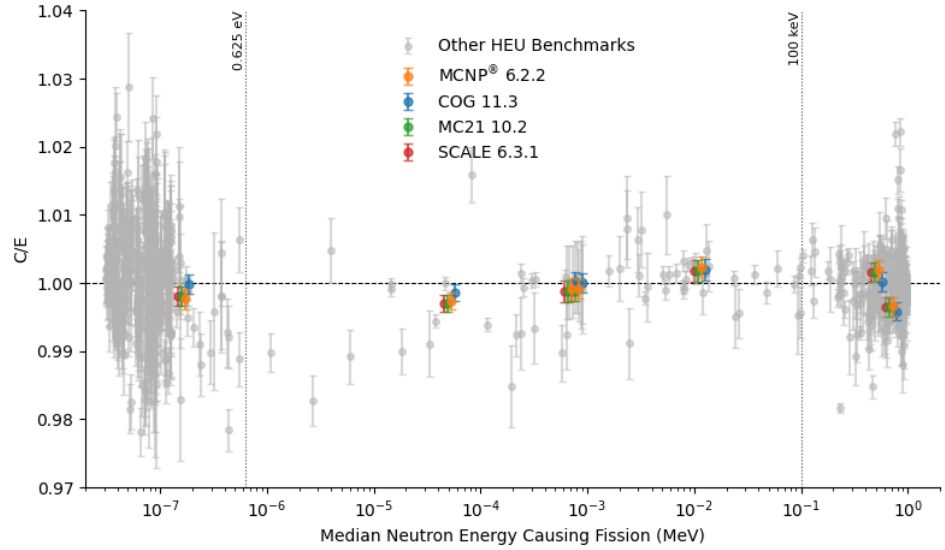

Figure 2: Comparison of C/E results between radiation transport codes with ENDF/B-VIII.0.

NEA/NSC/DOC(95)03/II
Volume II

HEU-MET-INTER-013

TEX-HF ASSEMBLIES: HIGHLY ENRICHED URANIUM PLATES WITH HAFNIUM USING POLYETHYLENE MODERATOR AND POLYETHYLENE REFLECTOR

Evaluator

Jesse Norris
Lawrence Livermore National Laboratory

Internal Reviewer

Eric Aboud
Lawrence Livermore National Laboratory

Independent Reviewer

Michael Zerkle
Naval Nuclear Laboratory

LLNL-TR-862099
Lawrence Livermore National Laboratory
7000 East Avenue, P.O. Box 808, L-198, Livermore, California, USA, 94551

DISCLAIMER

ACKNOWLEDGEMENTS

This work was supported by the Nuclear Criticality Safety Program, funded and managed by the National Nuclear Security Administration for the Department of Energy.

HEU-MET-INTER-013

TEX-HF ASSEMBLIES: HIGHLY ENRICHED URANIUM PLATES WITH HAFNIUM USING POLYETHYLENE MODERATOR AND POLYETHYLENE REFLECTOR

IDENTIFICATION NUMBER: HEU-MET-INTER-013

KEY WORDS: critical experiment, highly enriched uranium, metal, hafnium, diluent, high-density polyethylene, polyethylene-moderated, polyethylene-reflected, Comet, Jemima, acceptable

1.0 DETAILED DESCRIPTION

1.1 Overview of the Experiment

This evaluation documents the Thermal Epithermal eXperiments (TEX) configurations with highly enriched uranium (HEU) and hafnium (Hf), known as TEX-Hf. This experiment is a variation of HEU-MET-MIXED-021 (TEX-HEU Baseline Assemblies) with the addition of hafnium plates as a diluent material [1]. The goal of TEX-HEU was to provide multiple configurations that span the entire neutron energy spectrum. The TEX-Hf experiment furthers this by providing integral experiments for validation of hafnium in the thermal, intermediate, and fast neutron energy regimes by maximizing the sensitivity in k_{eff} to the hafnium isotope cross sections. All seven experimental configurations are judged to be acceptable as benchmark cases. As the neutron spectra of the seven experiments differed, Cases 1 and 7 are cross listed as HEU-MET-FAST-105, Case 4 is cross listed as HEU-MET-MIXED-022, and Case 5 is cross listed as HEU-MET-THERM-037.

The main parameter that is varied between the experimental configurations is the thickness, or presence, of high-density polyethylene moderator plates between the HEU plates. Varying the thickness of these polyethylene plates allows the neutron spectrum to be varied between majority fast (Cases 1 and 7), intermediate (Cases 2, 3, and 6), mixed (Case 4), and thermal (Case 5). These fission fractions are based on calculations and reported in Table 1.

Table 1: Comparison of the polyethylene plate thicknesses and resulting fission fractions grouped by neutron energy regime (based on calculations using MCNP® 6.2.2 with ENDF/B-VIII.0).

Config-uration	Nominal Moderator Thickness, in. (cm)	Calculated Fission Fractions		
		Thermal (<0.625 eV)	Intermediate (0.625 eV - 100 keV)	Fast (>100 keV)
1	-	0.057	0.179	0.764
2	0.125 (0.3175)	0.085	0.511	0.404
3	0.250 (0.6350)	0.155	0.551	0.294
4	0.500 (1.2700)	0.311	0.487	0.203
5	1.500 (3.8100)	0.598	0.279	0.123
6[(a)]	0.250 (0.6350)	0.129	0.575	0.296
7[(b)]	-	0.015	0.136	0.849

[(a)] Hafnium plates are sandwiched between two nominal 0.125 in. thick polyethylene moderator plates (Section 1.2.1).
[(b)] Hafnium plates are bunched as top and bottom reflectors surrounding the HEU plates (Section 1.2.1).

The HEU plates used in this experiment have a long history in critical experiments performed by LANL. The earliest usage of these HEU plates is in the "extension of the earlier Jemima experiments" in 1956[1], using U(93.4) plates with an outer diameter of 15 in. (38.1 cm) and a thickness of 0.118 in. (0.29972 cm) (IEU-MET-FAST-002). Since then, these HEU plates have been used in the Big Ten experiments in the 1970s (IEU-MET-FAST-007), the first three Zeus experiments in 1999-2002 (HEU-MET-INTER-006, HEU-MET-FAST-072, and HEU-MET-FAST-073), and the Nb-1Zr experiment in 2004 (HEU-MET-FAST-047). More recently, these HEU plates have been in the Curie (HEU-MET-INTER-011), TEX-HEU (HEU-MET-MIXED-021), and the Zeus with lead (IEU-MET-FAST-025, HEU-MET-FAST-102) experiments.

These experiments were conducted over seven weeks in August, September, and October of 2022 at the National Criticality Experiments Research Center (NCERC), located inside the Device Assembly Facility at the Nevada National Security Site in the United States of America. The design and execution of the experiments were a collaboration between Lawrence Livermore National Laboratory's (LLNL) Nuclear Criticality Safety Division (NCSD) and Los Alamos National Laboratory's (LANL) Advanced Nuclear Technologies Group (NEN-2), funded by the U.S. Department of Energy's Nuclear Criticality Safety Program. The experiments were designed by Anthony Nelson, Catherine Percher, William Zywiec, and David Heinrichs of LLNL's NCSD. The experiments were observed and documented by Jesse Norris of LLNL's NCSD. The experiments were performed by Theresa Cutler, Travis Grove, Rene Sanchez, Kelsey Amundson, Nicholas Thompson, Jesson Hutchinson, Alexander McSpaden, and Cole Kostelac of LANL's NEN-2. The hafnium plates were provided by Naval Nuclear Laboratory, facilitated by Michael Zerkle.

1.2 Description of Experimental Configuration

1.2.1 Design of the Critical Assembly

Figure 1 shows a rendering of the TEX-HEU experiment design [2]. For TEX-Hf, hafnium plates were placed as a diluent material within this design. The main parameter that is varied between these experimental configurations is the thickness of the polyethylene moderator plates. Varying this thickness allows the neutron spectrum to be varied between majority thermal, intermediate, and fast. The mass of the HEU is changed by adding or removing the HEU plates. Finally, the thickness of the upper reflector is adjusted in increments of 1/32 in. (0.079375 cm) to provide fine reactivity control. The polyethylene ring reflector height is adjusted to match the HEU and polyethylene plate stack to the nearest 1/32 in. (0.079375 cm).

Three different methods of stacking the HEU and hafnium plates were used in this experiment. The first method, referred to as Standard (STD) stacking, placed the hafnium plates between the HEU plates and polyethylene plates, matching the TEX-HEU design with the hafnium diluent between the layers. The second method, referred to as Sandwich (SAND) stacking, placed the hafnium plates between two polyethylene plates, in a flux-trap design. The third method, referred to as Bunched (BUNCH) stacking, placed the hafnium plates in two monoliths, consisting of 12 hafnium plates each, on the top and bottom of the HEU plate stack between the polyethylene reflectors. Figure 2 shows the three different methods of placing the hafnium plates in the experimental configurations. This figure shows, from left to right, the bottom halves of the Case 2, Case 6, and Case 7 configurations. The Standard (left) and Sandwich (center) stacking figures show the bottom halves of the benchmark experimental configurations with the polyethylene side reflector removed. The Bunched (right) stacking figure shows a partial configuration with the polyethylene side reflector removed during its approach to critical.

[1] The "early Jemima experiments" in 1952-1954 used HEU plates having a diameter of 10.50 in. and thickness of 0.800 cm (IEU-MET-FAST-001).

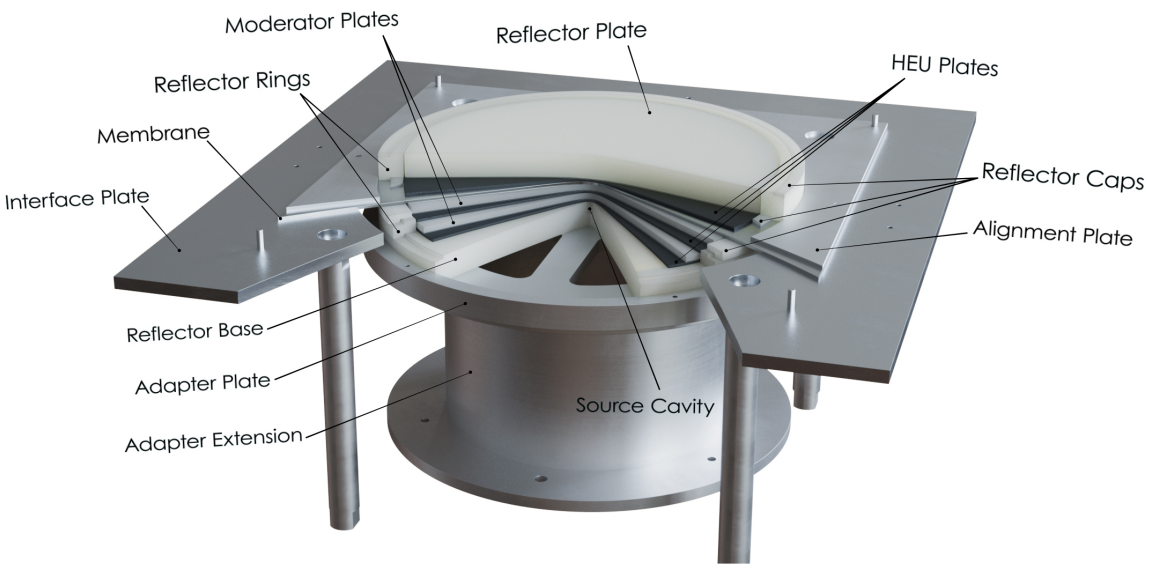

Figure 1: Components of TEX-HEU [2].

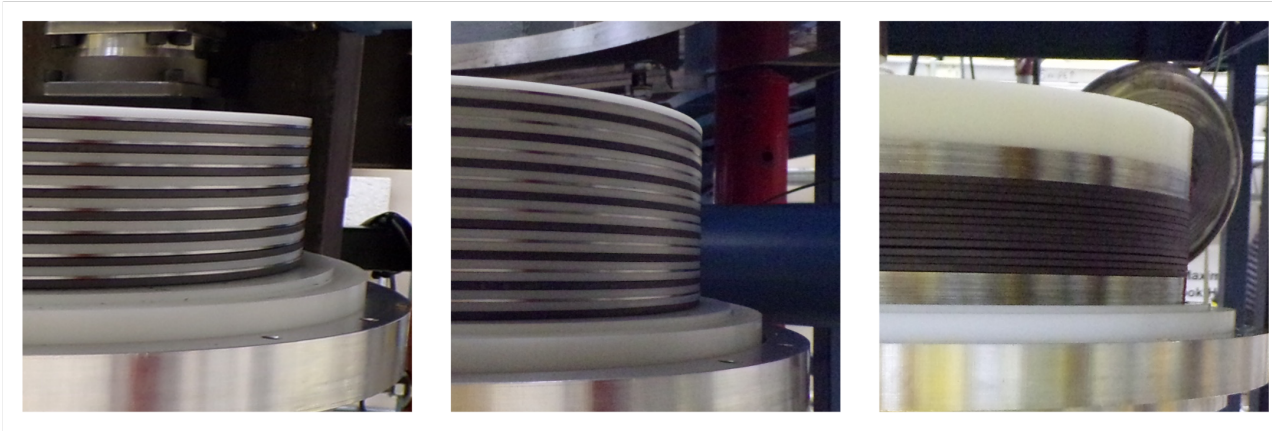

Figure 2: TEX-Hf stacking methods: Standard (left), Sandwich (center), and Bunched (right). These photographs show the HEU plates (black), hafnium plates (silver), and polyethylene plates (white) in the core stack. In the Standard stacking method (left), the stacking order is a repeated HEU plate, hafnium plate, and polyethylene plate (bottom to top). In the Sandwich stacking method (center), the stacking order is a repeated HEU plate, polyethylene plate, hafnium plate, and polyethylene plate (bottom to top). In the Bunched stacking method (right), the hafnium plates are stacked together above and below the HEU plates, surrounded by the polyethylene plates on the top and bottom.

1.2.2 Comet General Purpose Critical Assembly Machine

Comet is a general purpose critical assembly machine used to remotely assemble a critical mass. During assembly, roughly half of the experiment is constructed on the upper experiment platform with the other half on the lower adapter. During operation, the movable platen is extended vertically to bring the two halves of the experiment into contact. Once fully assembled, the two halves are only separated by the membrane.

Figure 3 shows a diagram of Comet, consisting of a surrounding structure, stationary platform, and movable platen. For TEX-HEU and TEX-Hf, additional parts were affixed to Comet: an experiment platform, on to the stationary platform; and a lower adapter, extending the movable platen. The Godiva IV fast burst reactor is located in the same room as Comet, greater than 10 ft (3 m) away. The following sections describe these additional parts on Comet with associated design drawings included in Appendix B.

Figure 3: The Comet general purpose critical assembly machine. The Godiva IV fast burst reactor is located to the right of this photo (out of frame).

1.2.2.1 Stationary Platform

The experiment platform holds the upper half of the experiment, shown in Figure 4. The platform consists of the interface plate and four standoffs, which rigidly attache the interface plate to the stationary platform. The membrane is placed on top of the interface plate, allowing the movable platen to lift the lower half of the experiment as it meets the upper half of the experiment through the membrane. The interface plate uses four pegs to hold the membrane and alignment plate in place while allowing vertical movement. The original drawings of the stationary platform, interface plate, standoffs, and membrane, with dimensions and tolerances, are included in Appendix B.

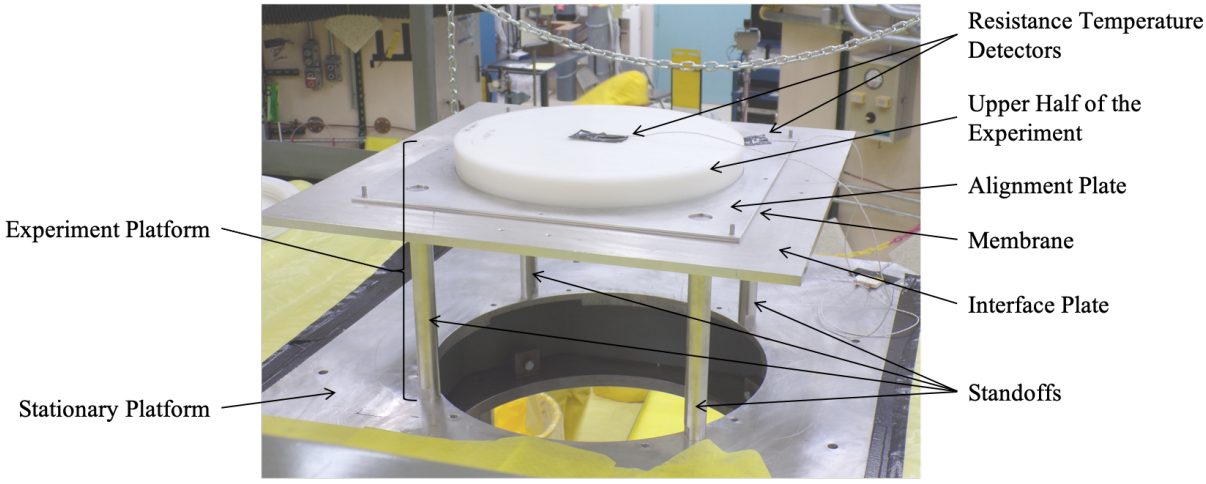

Figure 4: Upper stationary platform of the Comet, with the experiment platform. During the benchmark measurements, the resistance temperature detectors and alignment plate were removed.

The interface plate is a 28 in. × 28 in. × 0.5 in. (71.12 cm × 71.12 cm × 1.27 cm) Al-6061 plate with a 19 in. (48.26 cm) diameter hole through its center. The standoffs are 12 in. (30.48 cm) long Al-6061 cylinders with a 1.25 in. (3.175 cm) diameter. The membrane is a 21 in. × 21 in. (53.34 cm × 53.34 cm) Al-6061 plate with a thickness of 0.125 in. (0.3175 cm), report in Table 2. The membrane includes four small holes, one in each corner, which match the four pegs in the interface plate, ensuring consistent alignment during placement. This design allows the membrane to be lifted up to 0.75 in. (1.905 cm) from the top surface of the interface plate.

Table 2: Membrane nominal dimensions and tolerances.

Part Type	Thickness [in. (cm)]	Side Length [in. (cm)]
Membrane	0.125 ± 0.010 (0.3175 ± 0.0254)	21.000 ± 0.030 53.3400 ± 0.0762

1.2.2.2 Movable Platen

The lower adapter holds the lower half of the experiment, shown in Figure 5. The adapter consists of the adapter plate and the adapter extension, which rigidly attaches the lower adapter to the movable platen. The original drawings of the movable platen, adapter plate, and adapter extension, with dimensions and tolerances, are included in Appendix B.

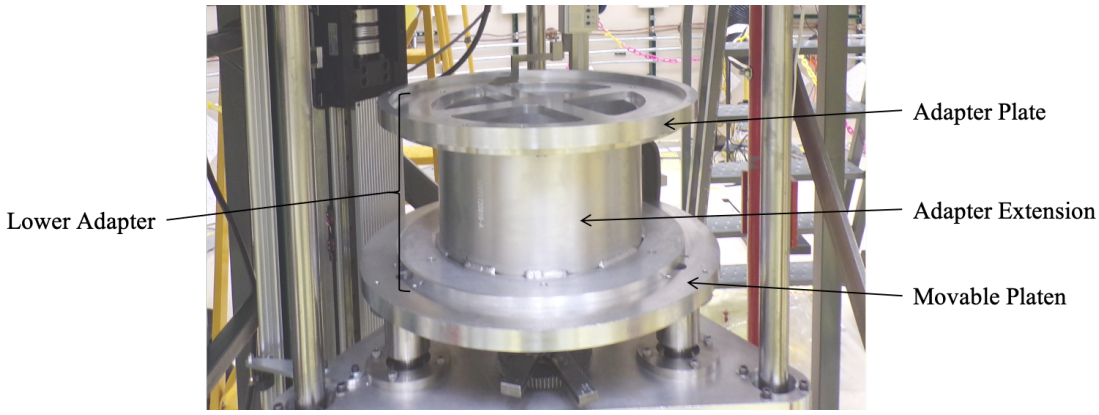

Figure 5: Lower movable platen of Comet, with the lower adapter.

The adapter plate is a 0.53 in. (1.3462 cm) thick cylindrical plate with an 18.5 in. (46.99 cm) outer diameter. This plate includes a 17.15 in. (43.561 cm) inner diameter with an additional 0.47 in. (1.1938 cm) lip height, to hold the bottom polyethylene reflector plate. The adapter extension is an 8 in. (20.32 cm) tall annular cylinder with a wall thickness of 0.25 in. (0.635 cm) and a 12 in. (30.48 cm) outer diameter. This extension includes a 2.5 in. (6.35 cm) wide and 0.5 in. (1.27 cm) thick top and bottom flange to affix it to the adapter plate and the movable platen. Both components of the lower adapter are Al-6061.

In [2], which uses the same adapter as this experiment, the lip of the adapter plate was measured using an electronic height gauge, reproduced in Table 3. The height gauge had a manufacturer reported resolute and indication variability of 0.01 mm and an indication accuracy of ± 0.004 cm for height ranges of 0 in to 12 in (0 cm to 30.48 cm). This lip has an average measured height of 1.247 ± 0.062 cm, which is significantly larger than the indication accuracy of ± 0.004 cm.

Table 3: Adapter plate lip height measurements from [2].

Nominal [in. (cm)]	**Measurement (cm)**
0.47 ± 0.01 (1.1938 ± 0.0254)	1.282
	1.254
	1.273
	1.283
	1.312
	1.136
	1.187
Average (cm)	**1.247 ± 0.062**

1.2.3 Highly Enriched Uranium Plates

The HEU plates are cylindrical U(93+) plates with a nominal diameter of 15 in. (38.1 cm) and thickness of 0.118 in. (0.29972 cm), collectively known as the "Jemima" plates. These plates are either full or annular cylinders with nominal inner diameters of 2.5 in. (6.35 cm), 6 in. (15.24 cm), or 10 in. (25.4 cm). The annulus removes some of the HEU mass resulting in lower and higher mass plate types. The plates are identified in this, and previous evaluations, based on their annulus[2]: 15/0-HEU (Full, HEU1), 15/2.5-HEU (2.5", HEU2, Id. No. 403), 15/6-HEU (6", HEU4, "Six Inch", Id. No. 401), and 15/10-HEU (10", "Ten Inch", Id. No. 402). Each of these four part types are shown in Figure 6. The nominal dimensions and design tolerances of the plate types are reported Table 4.

Table 4: HEU plate nominal dimensions and tolerances (see Fig. 6 for dimensions)[3].

Part Type	**Inner Diameter, *b* [in. (cm)]**	**Outer Diameter, *a* [in. (cm)][(a)]**	**Thickness, *c* [in. (cm)]**
15/0-HEU	-	15 +0.000/-0.005 (38.1 +0.0000/-0.0127)	0.118 (0.29972)
15/2.5-HEU	2.510 +0.005/-0.000 (6.3754 +0.0127/-0.0000)		
15/6-HEU	6.005 +0.005/-0.000 (15.2527 +0.0127/-0.0000)		
15/10-HEU	10.005 +0.005/-0.000 (25.4127 +0.0127/-0.0000)		
6/0-HEU	-	6 +0.000/-0.005 (15.24 +0.0000/-0.0127)	

[(a)] A recent report characterizing the HEU plate dimensions using a coordinate measuring machine included original drawings of the 15/2.5-HEU, 15/6-HEU, and 15/10-HEU plates[4]. These drawings indicate a symmetric tolerance on the outer diameter of ±0.005 in.; which is in disagreement with the asymmetric tolerenace reported in [3, 4, 5]. However, the measurements of the outer diameters in that report indiciate an average outer diameter of 14.996 in. with a range of 14.993 in. to 15.000 in.; which is in agreement with the asymmetric tolerance. Therefore, the reported asymmetric tolerance from [3, 4, 5] is presented.

Table 5 compares the HEU plate masses over time and reports the available thickness measurements. The mass measurements performed during this experiment in 2022 are described in Section 1.3.1. The mass measurements performed in 2020 are reproduced from [2]. No thickness measurements were performed during this experiment. Instead, the thickness measurements reported in [8] performed during MIX-MET-FAST-016 in 2019 are reproduced in Table 5. The measurements were performed using an IP67 Mitutoyo caliper (CD-24"C) with a resolution of ±0.02 in. (±0.0508 cm).

[2]The HEU notation (HEU1, HEU2, and HEU4) is used in the Zeus benchmarks [3, 4, 5] and the Id. No. notation in used in the Big Ten benchmark [6].

[3]The inner and outer diameter dimensions and tolerances are based on descriptions of the 15/0-HEU and 15/2.5-HEU plates in [3] and [4] and the 15/6-HEU plates in [5].

[4]K. Amundson et al. *HEU Pancake (Jemima) Plate Preliminary Characterization Report*. LA-UR-24-20414. Los Alamos National Laboratory, 2024. DOI: 10.2172/2282508.

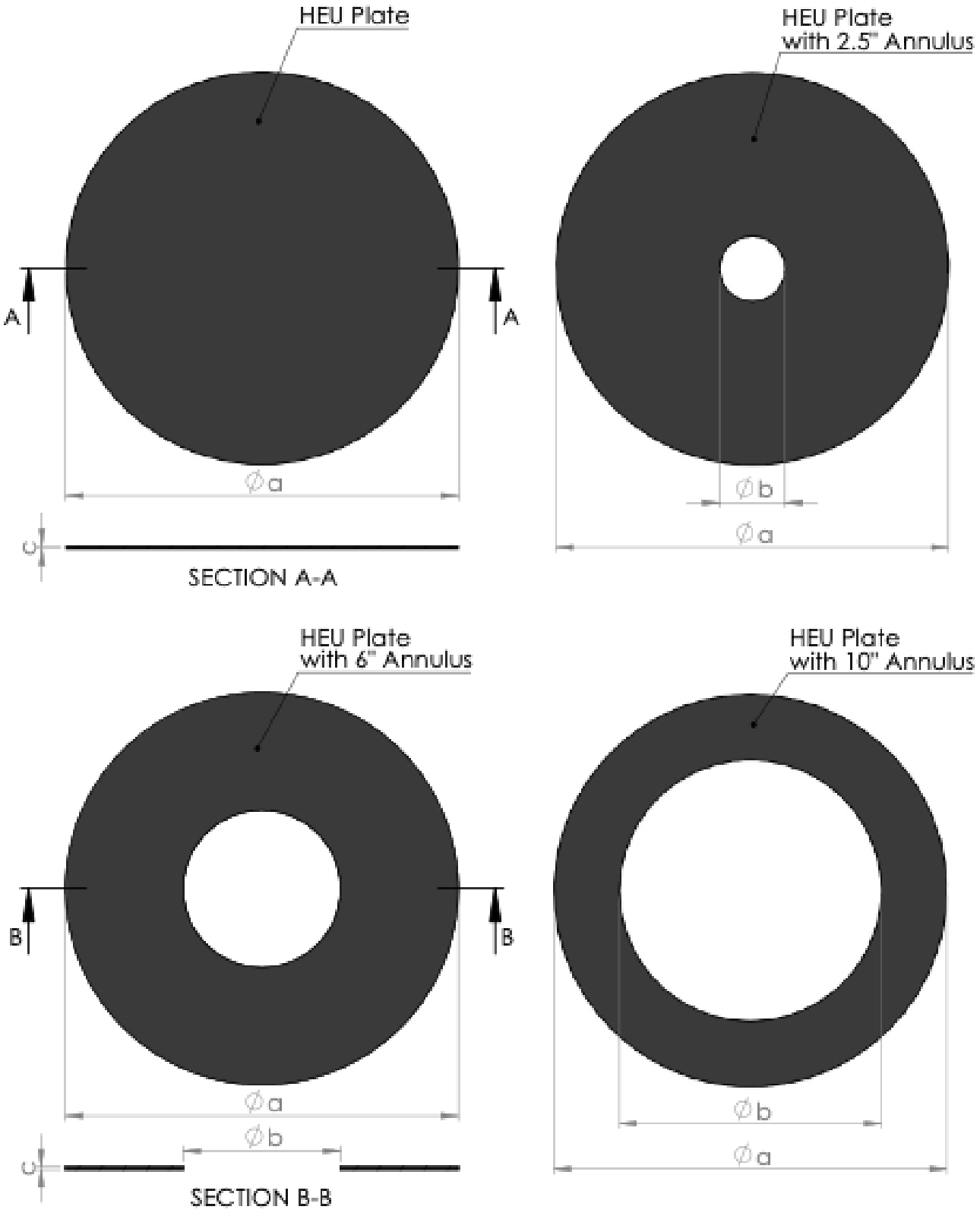

Figure 6: Diagram of the HEU plates, showing four part types.

Table 5: HEU plate mass and dimension measurements (see Fig. 6 for dimensions).

Part Type	Part ID	Mass (g)			Thickness, c [in. (cm)][(b)]
		2022	2020[(a)]	2005[(b)]	
15/0-HEU	11150	6404.7	6410.3	6415.4	0.1218 (0.3095)
	11149	6382.2	6383.6	6409.2	0.1222 (0.3103)
	11147	6512.4	6517.3	6526.2	0.1195 (0.3035)
	11019	6469.2	6470.0	6476.9	0.1190 (0.3023)
	11017	6497.8	6501.6	6518.6	0.1208 (0.3069)
15/2.5-HEU	10491	6391.6	6392.4	6393.8	0.1238 (0.3145)
	10489	6343.7	6343.8	6345.0	0.1232 (0.3128)
	10487	6275.4	6274.9	6276.4	0.1203 (0.3056)
	10475	6228.5	6230.0	6236.2	0.1285 (0.3264)
	10470	6278.6	6279.0	6261.0	0.1227 (0.3116)
	10467	6335.6	6335.8	6336.6	0.1245 (0.3162)
	10464	6258.4	6258.5	6259.3	0.1195 (0.3035)
15/6-HEU	11018	5369.6	5369.9	5375.4	0.1192 (0.3027)
	10935	5434.9	-	5435.9	-
	10933	5437.4	-	5439.9	-
	10932	5432.9	-	5436.5	0.1250 (0.3175)
	10477	5498.9	5499.2	5498.6	0.1235 (0.3137)
	10457	5573.9	5574.1	5574.0	0.1255 (0.3188)
15/10-HEU	10485	3604.3	-	3605.5	-
	10481	3594.3	-	3593.6	0.1205 (0.3061)
	10479	3564.6	3564.7	3565.4	0.1198 (0.3044)
	10473	3606.9	-	3607.3	-
	10472	3586.4	3585.7	3587.2	0.1220 (0.3099)
	10463	3631.7	3631.7	3627.0	0.1233 (0.3133)
	10458	3617.9	-	3618.3	-
6/0-HEU	Q2-16	1075.6	-	1077.8	0.1252 (0.3179)

[(a)] Reproduced from [2].
[(b)] Reproduced from [8].

1.2.4 Hafnium Plates

The hafnium plates are cylindrical with a nominal diameter of 15 in. (38.1 cm) and thickness of 0.04 in. (0.1016 cm), reported in Table 6. The original drawing of the hafnium plates, with dimensions and tolerances, are included in Appendix B.

Table 6: Hafnium plate nominal dimensions and tolerances.

Part Type	Thickness [in. (cm)]	Diameter [in. (cm)]
HF	0.040 ± 0.004 (0.10160 ± 0.01016)	15.000 +0.000/-0.005 (38.100 +0.0000/-0.0127)

Tables 7 and 8 report the mass and dimensional measurements of the hafnium plates. These measurements were provided by the manufacturer during acceptance testing of the plates. The mass measurements were required to be reported to the nearest 0.1 g. The diameter measurements were performed using a caliper with a tolerance of +0.000/-0.005 in. (+0.000/-0.0127 cm). Two methods of measuring the thickness were used: an electronic gauge and an ultrasonic thickness gage (UTG). The thickness measurements reported in Table 7 were performed using the electronic gauge. This measurement procedure involved probing the thickness and recording the minimum and maximum thickness to the nearest 0.001 in. (0.00254 cm). The thickness measurements reported in Table 8 were performed using a 45MG Digital UTG. The measurement procedure involved performing an initial thickness measurement to calibrate the UTG. Then, with the plate flat on a table, the UTG was used to measure the thickness at 10 locations on each plate.

Table 7: Hafnium plate mass and dimensional measurements.

Part ID[(a)]	Mass (g)	Thickness (in.)		Diameter [in. (cm)]
		Min	Max	
HF-01	1590.0	0.0420	0.0430	14.9970 (38.0924)
HF-02	1593.6	0.0420	0.0435	14.9970 (38.0924)
HF-03	1579.7	0.0410	0.0430	14.9990 (38.0975)
HF-04	1614.0	0.0410	0.0450	14.9980 (38.0949)
HF-05	1559.7	0.0410	0.0420	14.9960 (38.0898)
HF-06	1570.2	0.0415	0.0425	14.9960 (38.0898)
HF-07	1564.2	0.0410	0.0420	14.9970 (38.0924)
HF-08	1578.4	0.0415	0.0420	14.9970 (38.0924)
HF-09	1564.9	0.0410	0.0420	14.9950 (38.0873)
HF-10	1584.8	0.0410	0.0430	14.9970 (38.0924)
HF-11	1573.6	0.0415	0.0420	14.9970 (38.0924)
HF-12	1556.1	0.0410	0.0420	14.9980 (38.0949)
HF-13	1555.0	0.0410	0.0420	14.9980 (38.0949)
HF-14	1555.4	0.0410	0.0410	14.9980 (38.0949)
HF-15	1568.6	0.0410	0.0450	14.9950 (38.0873)
HF-16	1559.2	0.0410	0.0430	14.9960 (38.0898)
HF-17	1560.0	0.0410	0.0430	14.9980 (38.0949)
HF-18	1567.0	0.0410	0.0420	14.9970 (38.0924)
HF-19	1570.4	0.0410	0.0420	14.9970 (38.0924)
HF-20	1566.1	0.0410	0.0420	14.9970 (38.0924)
HF-22	1554.7	0.0410	0.0430	14.9960 (38.0898)
HF-23	1559.6	0.0410	0.0430	14.9990 (38.0975)
HF-24	1559.8	0.0410	0.0420	14.9980 (38.0949)
HF-25	1570.9	0.0410	0.0420	14.9950 (38.0873)
HF-26	1573.5	0.0410	0.0420	14.9980 (38.0949)
HF-27	1550.5	0.0400	0.0420	14.9960 (38.0898)

[(a)] HF-21 did not meet certification requirements and is not part of the hafnium plate inventory.

Table 8: Hafnium plate thickness measurements. The reported average thickness is converted to centimeters prior to rounding.

Part ID[(a)]	Measurements (in.)										Thickness [in. (cm)]		
	t_1	t_2	t_3	t_4	t_5	t_6	t_7	t_8	t_9	t_{10}	Min	Max	Average
HF-01	0.0430	0.0422	0.0417	0.0424	0.0432	0.0427	0.0421	0.0419	0.0422	0.0428	0.0417	0.0432	0.0424 (0.1077)
HF-02	0.0423	0.0423	0.0427	0.0424	0.0421	0.0426	0.0429	0.0423	0.0424	0.0427	0.0421	0.0429	0.0425 (0.1079)
HF-03	0.0427	0.0417	0.0422	0.0423	0.0424	0.0419	0.0417	0.0426	0.0418	0.0422	0.0417	0.0427	0.0422 (0.1071)
HF-04	0.0428	0.0431	0.0429	0.0428	0.0432	0.0444	0.0430	0.0426	0.0430	0.0432	0.0426	0.0444	0.0431 (0.1095)
HF-05	0.0417	0.0416	0.0412	0.0415	0.0431	0.0417	0.0413	0.0418	0.0417	0.0414	0.0412	0.0431	0.0417 (0.1059)
HF-06	0.0418	0.0421	0.0428	0.0419	0.0415	0.0417	0.0422	0.0420	0.0419	0.0418	0.0415	0.0428	0.0420 (0.1066)
HF-07	0.0416	0.0414	0.0419	0.0417	0.0413	0.0418	0.0427	0.0418	0.0417	0.0417	0.0413	0.0427	0.0418 (0.1061)
HF-08	0.0420	0.0422	0.0423	0.0423	0.0422	0.0419	0.0422	0.0417	0.0419	0.0422	0.0417	0.0423	0.0421 (0.1069)
HF-09	0.0411	0.0415	0.0422	0.0415	0.0420	0.0422	0.0417	0.0417	0.0414	0.0419	0.0411	0.0422	0.0417 (0.1060)
HF-10	0.0421	0.0417	0.0418	0.0421	0.0423	0.0421	0.0429	0.0429	0.0423	0.0422	0.0417	0.0429	0.0422 (0.1073)
HF-11	0.0425	0.0429	0.0422	0.0418	0.0420	0.0416	0.0415	0.0416	0.0418	0.0421	0.0415	0.0429	0.0420 (0.1067)
HF-12	0.0422	0.0418	0.0413	0.0411	0.0415	0.0417	0.0415	0.0416	0.0416	0.0413	0.0411	0.0422	0.0416 (0.1056)
HF-13	0.0420	0.0417	0.0411	0.0416	0.0429	0.0415	0.0410	0.0417	0.0416	0.0413	0.0410	0.0429	0.0416 (0.1058)
HF-14	0.0415	0.0419	0.0415	0.0413	0.0413	0.0416	0.0417	0.0413	0.0415	0.0414	0.0413	0.0419	0.0415 (0.1054)
HF-15	0.0414	0.0418	0.0436	0.0434	0.0417	0.0415	0.0418	0.0416	0.0415	0.0419	0.0414	0.0436	0.0420 (0.1067)
HF-16	0.0412	0.0415	0.0419	0.0416	0.0414	0.0419	0.0425	0.0415	0.0414	0.0415	0.0412	0.0425	0.0416 (0.1058)
HF-17	0.0417	0.0411	0.0417	0.0420	0.0415	0.0411	0.0414	0.0430	0.0417	0.0412	0.0411	0.0430	0.0416 (0.1058)
HF-18	0.0420	0.0414	0.0415	0.0415	0.0416	0.0417	0.0418	0.0421	0.0416	0.0421	0.0414	0.0421	0.0417 (0.1060)
HF-19	0.0419	0.0414	0.0413	0.0420	0.0422	0.0424	0.0418	0.0417	0.0420	0.0419	0.0413	0.0424	0.0419 (0.1063)
HF-20	0.0419	0.0417	0.0416	0.0418	0.0422	0.0415	0.0414	0.0416	0.0419	0.0420	0.0414	0.0422	0.0418 (0.1061)
HF-22	0.0418	0.0428	0.0414	0.0414	0.0418	0.0415	0.0414	0.0408	0.0410	0.0416	0.0408	0.0428	0.0416 (0.1055)
HF-23	0.0417	0.0417	0.0414	0.0413	0.0413	0.0414	0.0411	0.0415	0.0417	0.0415	0.0411	0.0417	0.0415 (0.1053)
HF-24	0.0420	0.0415	0.0412	0.0418	0.0421	0.0415	0.0411	0.0424	0.0415	0.0415	0.0411	0.0424	0.0417 (0.1058)
HF-25	0.0420	0.0415	0.0417	0.0421	0.0420	0.0419	0.0417	0.0419	0.0418	0.0420	0.0415	0.0421	0.0419 (0.1063)
HF-26	0.0418	0.0416	0.0414	0.0418	0.0420	0.0420	0.0419	0.0424	0.0424	0.0421	0.0414	0.0424	0.0419 (0.1065)
HF-27	0.0411	0.0412	0.0411	0.0418	0.0422	0.0413	0.0408	0.0409	0.0414	0.0416	0.0408	0.0422	0.0413 (0.1050)

[(a)] HF-21 did not meet certification requirements and is not part of the hafnium plate inventory.

1.2.5 Polyethylene Parts

The polyethylene parts include moderator (MOD) plates, reflector (REF) plates, a bottom reflector (BOTREF), and reflector rings (RING) and caps (CAP, BOTCAP). Figure 7 shows a diagram of how these parts fit together. The moderator plates are interstitial to the core stack while all other parts are used to create a nominal 1 in. (2.54 cm) reflector surrounding the core stack. The bottom reflector, reflector rings, and reflector caps include step joints, allowing the parts to easily mate while also reducing neutron streaming paths. As shown in Fig. 7, the BOTCAP and 0-CAP parts are used to fill in the step joints to complete the reflectors. The polyethylene parts are all high density polyethylene.

All parts were weighed and measured, using a coordinate measuring machine (CMM), by LLNL's Dimensional Inspection Laboratory prior to the experiment. The dimensional measurements performed by the CMM report minimum, maximum, and average values for the diameters and a single value for the thicknesses. The diameter measurements result from measuring many cord lengths of the diameter. The thickness measurements result from creating a best-fit plane of the top surface using many points measured at that surface. The thickness represents the distance between the base and this plane. The following sections report the mass and dimensional measurements for the polyethylene parts.

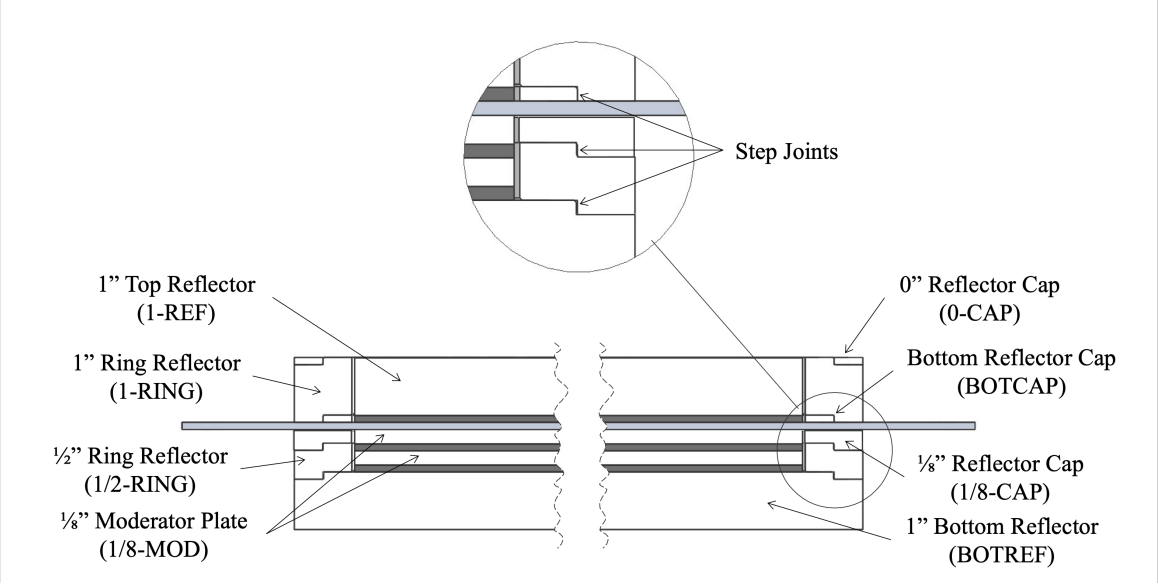

Figure 7: Diagram of the polyethylene parts.

1.2.5.1 Moderator and Reflector Plates

The polyethylene moderator and reflector plates are cylindrical with a nominal diameter of 15 in. (38.1 cm) and varying thicknesses, reported in Table 9. Figure 8 shows a schematic of the moderator and reflector plate part. The moderator plates are placed between the HEU plates with four nominal thicknesses: 0.125 in. (0.3175 cm), 0.25 in. (0.635 cm), 0.5 in. (1.27 cm), and 1.5 in. (3.81 cm). The reflector plates are used as the top reflector and provide fine reactivity control with three nominal thicknesses: 0.03125 in. (0.079375 cm), 0.0625 in. (1.5875 cm), and 1 in. (2.54 cm). The moderator plates were also used in the top reflector. The original drawings of the moderator plates, with dimensions and tolerances, are included in Appendix B.

Tables 10, 11, 12, 13, and 14 report the mass and dimensional measurements of the polyethylene moderator and reflector plates. A description of these measurements is included in Section 1.2.5.

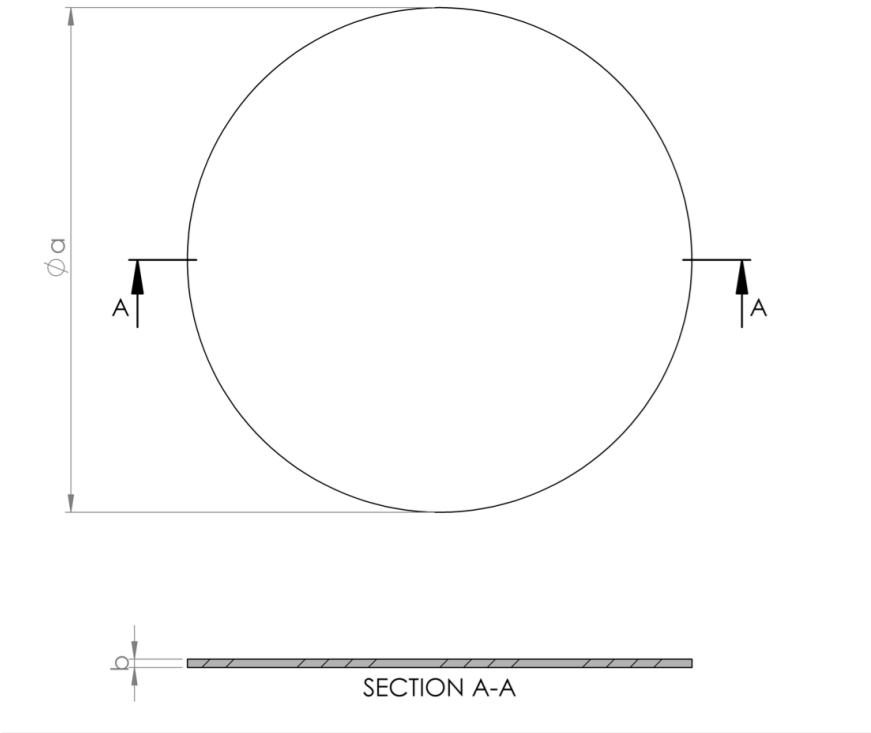

Figure 8: Schematic of the polyethylene moderator and reflector plate.

Table 9: Polyethylene moderator and reflector plate nominal dimensions (see Fig. 8 for dimensions).

Part Type	**Thickness, *b* [in. (cm)]**	**Diameter, *a* [in. (cm)]**
1/8-MOD	0.125 ± 0.005 (0.3175 ± 0.0127)	15.000 ± 0.010 (38.1000 ± 0.0254)
1/4-MOD	0.250 ± 0.005 (0.6350 ± 0.0127)	
1/2-MOD	0.500 ± 0.005 (1.2700 ± 0.0127)	
1.5-MOD	1.500 ± 0.005 (3.8100 ± 0.0127)	
1/32-REF	0.03125 ± 0.00005 (0.079375 ± 0.000127)	
1/16-REF	0.0625 ± 0.0005 (0.15875 ± 0.00127)	
1-REF	1.000 ± 0.005 (2.5400 ± 0.0127)	

Table 10: Mass and dimension measurements of the 1/8-MOD parts (see Fig. 8 for dimensions).

Part ID	Mass (g)	Thickness, *b* [in. (cm)]	Diameter, *a* [in. (cm)]		
			Min	Max	Average
1/8-MOD-1	343.0	0.1249 (0.3172)	14.9894	14.9979	14.9948 (38.0868)
1/8-MOD-2	342.1	0.1259 (0.3198)	14.9895	14.9991	14.9947 (38.0865)
1/8-MOD-3	344.0	0.1253 (0.3183)	14.9894	14.9993	14.9950 (38.0873)
1/8-MOD-4	344.3	0.1251 (0.3178)	14.9878	14.9999	14.9944 (38.0858)
1/8-MOD-5	343.0	0.1246 (0.3165)	14.9913	14.9995	14.9955 (38.0886)
1/8-MOD-6	344.7	0.1255 (0.3188)	14.9934	15.0018	14.9965 (38.0911)
1/8-MOD-7	345.0	0.1248 (0.3170)	14.9908	15.0017	14.9959 (38.0896)
1/8-MOD-8	345.2	0.1251 (0.3178)	14.9901	15.0003	14.9956 (38.0888)
1/8-MOD-9	343.4	0.1248 (0.3170)	14.9885	14.9969	14.9940 (38.0848)
1/8-MOD-10	343.5	0.1266 (0.3216)	14.9904	15.0004	14.9962 (38.0903)
1/8-MOD-11	343.2	0.1249 (0.3172)	14.9901	14.9998	14.9954 (38.0883)
1/8-MOD-12	344.6	0.1264 (0.3211)	14.9876	15.0001	14.9951 (38.0876)
1/8-MOD-13	343.9	0.1250 (0.3175)	14.9895	15.0002	14.9945 (38.0860)
1/8-MOD-14	345.4	0.1259 (0.3198)	14.9908	15.0006	14.9964 (38.0909)
1/8-MOD-15	345.3	0.1256 (0.3190)	14.9927	14.9986	14.9961 (38.0901)
1/8-MOD-16	343.8	0.1247 (0.3167)	14.9931	15.0005	14.9972 (38.0929)
1/8-MOD-17	344.0	0.1253 (0.3183)	14.9921	14.9991	14.9957 (38.0891)
1/8-MOD-18	344.7	0.1255 (0.3188)	14.9917	15.0000	14.9964 (38.0909)
1/8-MOD-19	350.8	0.1275 (0.3239)	14.9917	15.0013	14.9967 (38.0916)
1/8-MOD-20	350.2	0.1280 (0.3251)	14.9888	14.9980	14.9943 (38.0855)
1/8-MOD-21	350.6	0.1285 (0.3264)	14.9893	14.9995	14.9953 (38.0881)
1/8-MOD-22	351.0	0.1274 (0.3236)	14.9905	15.0001	14.9961 (38.0901)
1/8-MOD-23	351.4	0.1274 (0.3236)	14.9899	14.9998	14.9955 (38.0886)
1/8-MOD-24	351.4	0.1271 (0.3228)	14.9916	14.9987	14.9958 (38.0893)
1/8-MOD-25	349.4	0.1268 (0.3221)	14.9903	14.9995	14.9951 (38.0876)
1/8-MOD-26	351.9	0.1269 (0.3223)	14.9919	15.0000	14.9957 (38.0891)
1/8-MOD-27	349.3	0.1263 (0.3208)	14.9937	15.0004	14.9965 (38.0911)
1/8-MOD-28	349.3	0.1272 (0.3231)	14.9922	15.0015	14.9974 (38.0934)
1/8-MOD-29	347.9	0.1314 (0.3338)	14.9894	14.9999	14.9957 (38.0891)
1/8-MOD-30	348.3	0.1283 (0.3259)	14.9908	15.0003	14.9950 (38.0873)
1/8-MOD-31	351.1	0.1268 (0.3221)	14.9886	14.9990	14.9953 (38.0881)
1/8-MOD-32	348.8	0.1270 (0.3226)	14.9890	14.9992	14.9952 (38.0878)
1/8-MOD-33	350.0	0.1271 (0.3228)	14.9892	14.9990	14.9948 (38.0868)
1/8-MOD-34	351.3	0.1277 (0.3244)	14.9880	14.9979	14.9942 (38.0853)
1/8-MOD-35	351.2	0.1288 (0.3272)	14.9909	14.9984	14.9957 (38.0891)
1/8-MOD-36	348.3	0.1306 (0.3317)	14.9908	15.0015	14.9965 (38.0911)
1/8-MOD-37	347.3	0.1293 (0.3284)	14.9922	15.0009	14.9963 (38.0906)
1/8-MOD-38	351.1	0.1321 (0.3355)	14.9923	15.0008	14.9973 (38.0931)
1/8-MOD-39	350.5	0.1276 (0.3241)	14.9864	15.0007	14.9946 (38.0863)

Table 11: Mass and dimension measurements of the 1/4-MOD parts (see Fig. 8 for dimensions).

Part ID	Mass (g)	Thickness, *b* [in. (cm)]	Diameter, *a* [in. (cm)]		
			Min	Max	Average
1/4-MOD-1	690.2	0.2512 (0.6380)	14.9835	14.9910	14.9879 (38.0693)
1/4-MOD-2	689.1	0.2532 (0.6431)	14.9821	14.9912	14.9866 (38.0660)
1/4-MOD-3	688.0	0.2497 (0.6342)	14.9804	14.9915	14.9853 (38.0627)
1/4-MOD-4	689.7	0.2558 (0.6497)	14.9824	14.9903	14.9868 (38.0665)
1/4-MOD-5	689.2	0.2555 (0.6490)	14.9822	14.9923	14.9869 (38.0667)
1/4-MOD-6	687.5	0.2539 (0.6449)	14.9806	14.9909	14.9862 (38.0649)
1/4-MOD-7	688.4	0.2531 (0.6429)	14.9792	14.9872	14.9843 (38.0601)
1/4-MOD-8	689.2	0.2524 (0.6411)	14.9786	14.9903	14.9855 (38.0632)
1/4-MOD-9	688.8	0.2540 (0.6452)	14.9850	14.9913	14.9883 (38.0703)
1/4-MOD-10	689.5	0.2514 (0.6386)	14.9792	14.9887	14.9844 (38.0604)
1/4-MOD-11	688.1	0.2499 (0.6347)	14.9790	14.9885	14.9849 (38.0616)
1/4-MOD-12	688.5	0.2516 (0.6391)	14.9842	14.9909	14.9872 (38.0675)
1/4-MOD-13	689.4	0.2511 (0.6378)	14.9806	14.9899	14.9864 (38.0655)
1/4-MOD-14	689.5	0.2507 (0.6368)	14.9803	14.9897	14.9858 (38.0639)
1/4-MOD-15	689.1	0.2515 (0.6388)	14.9806	14.9893	14.9858 (38.0639)
1/4-MOD-16	688.2	0.2532 (0.6431)	14.9815	14.9924	14.9872 (38.0675)
1/4-MOD-17	687.6	0.2605 (0.6617)	14.9796	14.9899	14.9851 (38.0622)
1/4-MOD-18	688.9	0.2530 (0.6426)	14.9812	14.9898	14.9859 (38.0642)
1/4-MOD-19	688.2	0.2547 (0.6469)	14.9769	14.9887	14.9838 (38.0589)
1/4-MOD-20	688.7	0.2599 (0.6601)	14.9814	14.9890	14.9860 (38.0644)
1/4-MOD-21	686.9	0.2600 (0.6604)	14.9804	14.9877	14.9840 (38.0594)
1/4-MOD-22	688.2	0.2605 (0.6617)	14.9817	14.9889	14.9851 (38.0622)
1/4-MOD-23	688.0	0.2499 (0.6347)	14.9775	14.9879	14.9841 (38.0596)
1/4-MOD-24	688.3	0.2528 (0.6421)	14.9810	14.9878	14.9854 (38.0629)
1/4-MOD-25	687.6	0.2525 (0.6414)	14.9800	14.9903	14.9849 (38.0616)
1/4-MOD-26	688.4	0.2542 (0.6457)	14.9812	14.9907	14.9860 (38.0644)
1/4-MOD-27	687.9	0.2574 (0.6538)	14.9803	14.9881	14.9849 (38.0616)
1/4-MOD-28	687.9	0.2595 (0.6591)	14.9820	14.9887	14.9857 (38.0637)
1/4-MOD-29	688.0	0.2621 (0.6657)	14.9830	14.9924	14.9864 (38.0655)
1/4-MOD-30	688.3	0.2594 (0.6589)	14.9837	14.9914	14.9870 (38.0670)
1/4-MOD-31	688.2	0.2515 (0.6388)	14.9821	14.9892	14.9861 (38.0647)
1/4-MOD-32	688.2	0.2509 (0.6373)	14.9807	14.9910	14.9859 (38.0642)
1/4-MOD-33	688.3	0.2511 (0.6378)	14.9815	14.9922	14.9871 (38.0672)
1/4-MOD-34	687.7	0.2581 (0.6556)	14.9810	14.9887	14.9849 (38.0616)
1/4-MOD-35	688.2	0.2583 (0.6561)	14.9830	14.9918	14.9879 (38.0693)
1/4-MOD-36	688.1	0.2576 (0.6543)	14.9833	14.9900	14.9875 (38.0683)

Table 12: Mass and dimension measurements of the 1/2-MOD parts (see Fig. 8 for dimensions).

Part ID	Mass (g)	Thickness, *b* [in. (cm)]	Diameter, *a* [in. (cm)]		
			Min	Max	Average
1/2-MOD-1	1377.9	0.5079 (1.2901)	14.9884	14.9953	14.9925 (38.0810)
1/2-MOD-2	1377.8	0.5047 (1.2819)	14.9866	14.9957	14.9909 (38.0769)
1/2-MOD-3	1385.0	0.5095 (1.2941)	14.9880	14.9951	14.9914 (38.0782)
1/2-MOD-4	1378.1	0.5044 (1.2812)	14.9877	14.9974	14.9926 (38.0812)
1/2-MOD-5	1380.2	0.5033 (1.2784)	14.9882	14.9950	14.9913 (38.0779)
1/2-MOD-6	1378.2	0.5003 (1.2708)	14.9870	14.9955	14.9910 (38.0771)
1/2-MOD-7	1383.7	0.5068 (1.2873)	14.9882	14.9963	14.9917 (38.0789)
1/2-MOD-8	1386.3	0.5047 (1.2819)	14.9854	14.9925	14.9888 (38.0716)
1/2-MOD-9	1385.4	0.5035 (1.2789)	14.9867	14.9912	14.9888 (38.0716)
1/2-MOD-10	1379.6	0.5045 (1.2814)	14.9861	14.9939	14.9890 (38.0721)
1/2-MOD-11	1384.5	0.5068 (1.2873)	14.9849	14.9937	14.9889 (38.0718)
1/2-MOD-12	1376.8	0.5005 (1.2713)	14.9867	14.9937	14.9901 (38.0749)
1/2-MOD-13	1385.5	0.5061 (1.2855)	14.9900	14.9961	14.9923 (38.0804)
1/2-MOD-14	1378.1	0.5079 (1.2901)	14.9841	14.9947	14.9884 (38.0705)
1/2-MOD-15	1381.5	0.5060 (1.2852)	14.9839	14.9936	14.9896 (38.0736)
1/2-MOD-16	1378.8	0.5063 (1.2860)	14.9848	14.9943	14.9891 (38.0723)
1/2-MOD-17	1378.8	0.5075 (1.2891)	14.9856	14.9942	14.9886 (38.0710)
1/2-MOD-18	1384.9	0.5127 (1.3023)	14.9840	14.9949	14.9892 (38.0726)
1/2-MOD-19	1380.5	0.5105 (1.2967)	14.9825	14.9922	14.9871 (38.0672)
1/2-MOD-20	1378.2	0.5016 (1.2741)	14.9862	14.9924	14.9893 (38.0728)
1/2-MOD-21	1379.3	0.5005 (1.2713)	14.9867	14.9921	14.9896 (38.0736)
1/2-MOD-22	1377.0	0.5030 (1.2776)	14.9858	14.9925	14.9888 (38.0716)
1/2-MOD-23	1385.3	0.5104 (1.2964)	14.9858	14.9934	14.9896 (38.0736)
1/2-MOD-24	1378.2	0.5092 (1.2934)	14.9854	14.9937	14.9887 (38.0713)
1/2-MOD-25	1385.6	0.5109 (1.2977)	14.9842	14.9920	14.9890 (38.0721)
1/2-MOD-26	1377.8	0.5066 (1.2868)	14.9837	14.9928	14.9870 (38.0670)
1/2-MOD-27	1385.1	0.5082 (1.2908)	14.9833	14.9934	14.9886 (38.0710)
1/2-MOD-28	1377.3	0.4996 (1.2690)	14.9855	14.9931	14.9889 (38.0718)
1/2-MOD-29	1376.3	0.5041 (1.2804)	14.9874	14.9942	14.9901 (38.0749)
1/2-MOD-30	1377.5	0.5084 (1.2913)	14.9857	14.9935	14.9900 (38.0746)
1/2-MOD-31	1377.8	0.5051 (1.2830)	14.9878	14.9952	14.9915 (38.0784)
1/2-MOD-32	1381.2	0.5073 (1.2885)	14.9862	14.9937	14.9889 (38.0718)

Table 13: Mass and dimension measurements of the 1.5-MOD parts (see Fig. 8 for dimensions).

Part ID	Mass (g)	Thickness, *b* [in. (cm)]	Diameter, *a* [in. (cm)]		
			Min	Max	Average
1.5-MOD-1	4150.8	1.4998 (3.8095)	14.9962	15.0107	15.0035 (38.1089)
1.5-MOD-2	4132.6	1.5100 (3.8354)	14.9968	14.9977	14.9933 (38.0830)
1.5-MOD-3	4125.6	1.5087 (3.8321)	14.9846	14.9962	14.9988 (38.0970)
1.5-MOD-4	4136.2	1.5146 (3.8471)	14.9879	15.0005	14.9946 (38.0863)
1.5-MOD-5	4147.2	1.4945 (3.7960)	14.9967	15.0075	15.0038 (38.1097)
1.5-MOD-6	4173.6	1.5086 (3.8318)	14.9811	14.9896	14.9859 (38.0642)
1.5-MOD-7	4167.4	1.5241 (3.8712)	14.9851	14.9984	14.9913 (38.0779)
1.5-MOD-8	4175.3	1.5105 (3.8367)	14.9803	14.9896	14.9856 (38.0634)
1.5-MOD-9	4135.6	1.5027 (3.8169)	14.9879	14.9949	14.9917 (38.0789)
1.5-MOD-10	4168.4	1.5103 (3.8362)	14.9784	14.9898	14.9841 (38.0596)
1.5-MOD-11	4171.2	1.5263 (3.8768)	14.9827	14.9948	14.9887 (38.0713)
1.5-MOD-12	4146.4	1.5188 (3.8578)	14.9915	15.0022	14.9965 (38.0911)

Table 14: Mass and dimension measurements of the reflector plate parts (see Fig. 8 for dimensions).

Part ID	Mass (g)	Thickness, *b* [in. (cm)]	Diameter, *a* [in. (cm)]		
			Min	Max	Average
1/32-REF-1	85.0	0.0334 (0.0848)	14.9832	14.9996	14.9908 (38.0766)
1/32-REF-2	85.9	0.0325 (0.0826)	14.9833	14.9983	14.9905 (38.0759)
1/16-REF-1	182.4	0.0728 (0.1849)	14.9831	14.9890	14.9858 (38.0639)
1/16-REF-2	182.9	0.0671 (0.1704)	14.9829	14.9884	14.9856 (38.0634)
1-REF-1	2766.9	0.9995 (2.5387)	14.9860	14.9934	14.9902 (38.0751)
1-REF-2	2767.2	1.0015 (2.5438)	14.9844	14.9922	14.9883 (38.0703)

1.2.5.2 Reflector Rings

The polyethylene reflector rings are annular cylinders with varying thicknesses and a nominal inner and outer diameter of 15.1 in. (38.354 cm) and 17.1 in. (43.434 cm), respectively. Figure 9 shows a schematic of the reflector ring part. The reflector rings have four nominal thicknesses: 0.25 in. (0.635 cm), 0.5 in. (1.27 cm), 1 in. (2.54 cm), and 3 in. (7.62 cm). The reflector rings stack around the core stack to provide a nominal 1 in. (2.54 cm) reflector. They are designed to interlock, using step joints, which keep the rings in alignment as they are stacked and reduce neutron streaming paths, shown in Fig. 7. The step joints have a nominal height of 0.125 in. (0.3175 cm). On the lower half of the experiment, the reflector rings interlock with the bottom reflector (BOTREF). On the upper half of the experiment, the reflector rings sit on the bottom reflector cap (BOTCAP).

Table 15 reports the mass and dimensional measurements of the polyethylene reflector rings. A description of these measurements is included in Section 1.2.5.

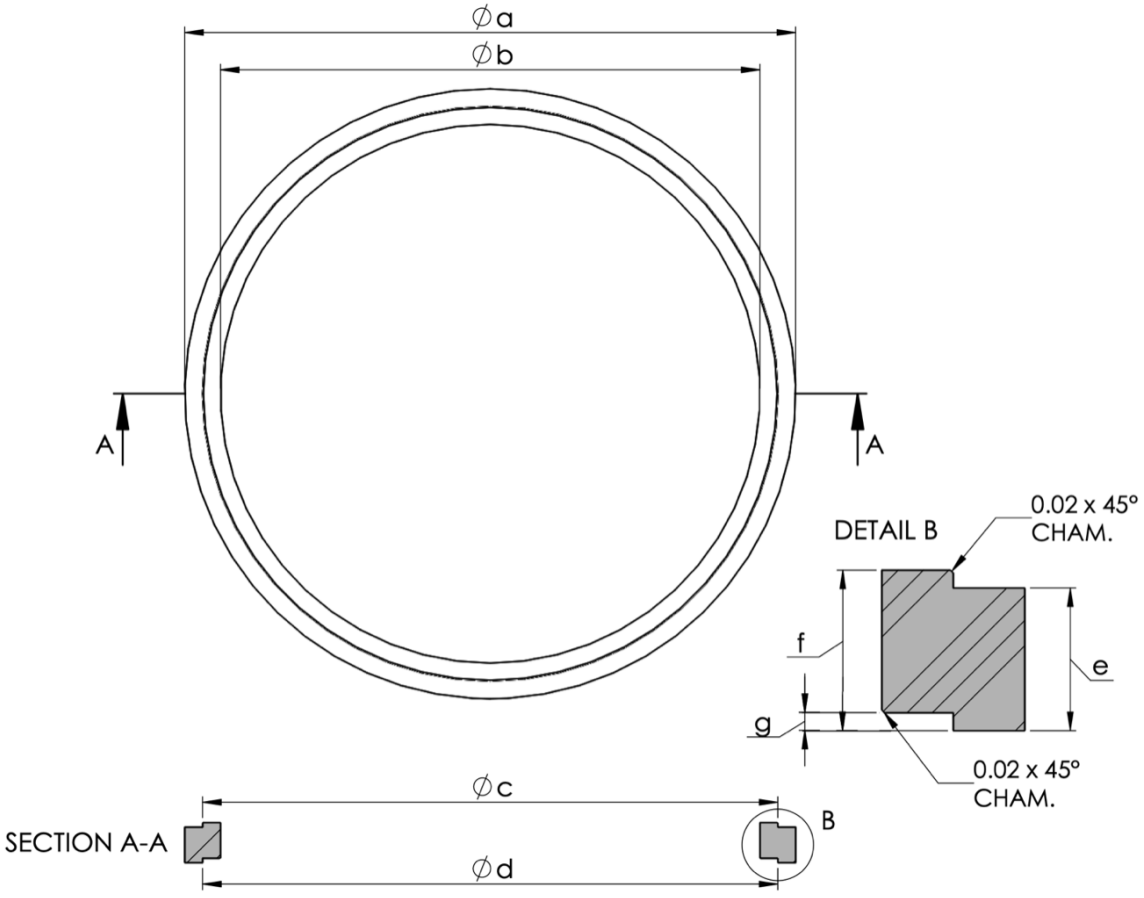

Figure 9: Schematic of the polyethylene reflector ring (dimensions in inches).

Table 15: Mass and dimensions of the reflector ring parts (see Fig. 9 for dimensions).

Part ID	Mass (g)	Outer Diameter, *a* [in. (cm)]			Inner Diameter, *b* [in. (cm)]		
		Min	Max	Average	Min	Max	Average
1/4-RING-1	199.1	17.0822	17.1050	17.0933 (43.4170)	15.0657	15.0912	15.0789 (38.3004)
1/4-RING-2	198.9	17.0821	17.1019	17.0927 (43.4155)	15.0690	15.0925	15.0813 (38.3065)
1/4-RING-3	198.7	17.0816	17.1060	17.0939 (43.4185)	15.0699	15.0912	15.0811 (38.3060)
1/4-RING-4	199.4	17.0838	17.1047	17.0937 (43.4180)	15.0681	15.0897	15.0792 (38.3012)
1/2-RING-1	394.1	17.0770	17.0870	17.0818 (43.3878)	15.0620	15.0728	15.0670 (38.2702)
1/2-RING-2	394.4	17.0802	17.0854	17.0830 (43.3908)	15.0660	15.0729	15.0682 (38.2732)
1/2-RING-3	392.9	17.0806	17.0855	17.0828 (43.3903)	15.0652	15.0721	15.0680 (38.2727)
1/2-RING-4	393.3	17.0793	17.0865	17.0822 (43.3888)	15.0650	15.0703	15.0676 (38.2717)
1-RING-1	805.8	17.0787	17.0852	17.0824 (43.3893)	15.0605	15.0691	15.0660 (38.2676)
1-RING-2	805.8	17.0745	17.0781	17.0767 (43.3748)	15.0572	15.0629	15.0609 (38.2547)
1-RING-3	805.8	17.0808	17.0888	17.0837 (43.3926)	15.0622	15.0700	15.0666 (38.2692)
1-RING-4	804.9	17.0696	17.0766	17.0729 (43.3652)	15.0509	15.0606	15.0560 (38.2422)
1-RING-5	804.8	17.0812	17.0868	17.0839 (43.3931)	15.0671	15.0714	15.0691 (38.2755)
1-RING-6	805.8	17.0775	17.0810	17.0788 (43.3802)	15.0595	15.0647	15.0624 (38.2585)
3-RING-1	2384.7	17.0879	17.0916	17.0898 (43.4081)	15.0875	15.0912	15.0896 (38.3276)
3-RING-2	2387.0	17.0877	17.0923	17.0896 (43.4076)	15.0891	15.0932	15.0910 (38.3311)
3-RING-3	2388.8	17.0872	17.0938	17.0915 (43.4124)	15.0880	15.0913	15.0898 (38.3281)
3-RING-4	2388.1	17.0887	17.0928	17.0912 (43.4116)	15.0873	15.0922	15.0905 (38.3299)
3-RING-5	2384.2	17.0855	17.0915	17.0888 (43.4056)	15.0894	15.0928	15.0913 (38.3319)
3-RING-6	2384.7	17.0861	17.0933	17.0892 (43.4066)	15.0877	15.0933	15.0909 (38.3309)

Table 15 (continued): Mass and dimensions of the reflector ring parts (see Fig. 9 for dimensions).

Part ID	Top Step Diameter, *c* [in. (cm)]			Bottom Step Diameter, *d* [in. (cm)]		
	Min	**Max**	**Average**	**Min**	**Max**	**Average**
1/4-RING-1	16.0527	16.0778	16.0654 (40.8061)	16.0876	16.1120	16.0990 (40.8915)
1/4-RING-2	16.0532	16.0787	16.0654 (40.8061)	16.0906	16.1096	16.1003 (40.8948)
1/4-RING-3	16.0491	16.0743	16.0630 (40.8000)	16.0896	16.1120	16.1010 (40.8965)
1/4-RING-4	16.0509	16.0746	16.0634 (40.8010)	16.0895	16.1082	16.0993 (40.8922)
1/2-RING-1	16.0480	16.0596	16.0537 (40.7764)	16.0836	16.0956	16.0895 (40.8673)
1/2-RING-2	16.0507	16.0575	16.0533 (40.7754)	16.0871	16.0919	16.0894 (40.8671)
1/2-RING-3	16.0471	16.0528	16.0496 (40.7660)	16.0894	16.0965	16.0922 (40.8742)
1/2-RING-4	16.0495	16.0543	16.0515 (40.7708)	16.0880	16.0938	16.0904 (40.8696)
1-RING-1	16.0564	16.0653	16.0615 (40.7962)	16.0800	16.0845	16.0824 (40.8493)
1-RING-2	16.0517	16.0575	16.0550 (40.7797)	16.0897	16.0939	16.0923 (40.8744)
1-RING-3	16.0590	16.0661	16.0628 (40.7995)	16.0799	16.0862	16.0823 (40.8490)
1-RING-4	16.0420	16.0531	16.0485 (40.7632)	16.0989	16.1075	16.1037 (40.9034)
1-RING-5	16.0624	16.0693	16.0653 (40.8059)	16.0850	16.0906	16.0880 (40.8635)
1-RING-6	16.0554	16.0604	16.0581 (40.7876)	16.0915	16.0967	16.0934 (40.8772)
3-RING-1	16.0726	16.0780	16.0742 (40.8285)	16.0975	16.1006	16.0993 (40.8922)
3-RING-2	16.0713	16.0748	16.0729 (40.8252)	16.0982	16.1025	16.1000 (40.8940)
3-RING-3	16.0685	16.0751	16.0713 (40.8211)	16.0970	16.1014	16.0994 (40.8925)
3-RING-4	16.0714	16.0751	16.0738 (40.8275)	16.0981	16.1035	16.1007 (40.8958)
3-RING-5	16.0710	16.0733	16.0720 (40.8229)	16.0994	16.1029	16.1014 (40.8976)
3-RING-6	16.0710	16.0736	16.0722 (40.8234)	16.1022	16.1048	16.1033 (40.9024)

Table 15 (continued): Mass and dimensions of the reflector ring parts (see Fig. 9 for dimensions).

Part ID	**Outer Edge Height, *e* [in. (cm)]**	**Inner Edge Height, *f* [in. (cm)]**	**Bottom Step Height, *g* [in. (cm)]**
1/4-RING-1	0.2568 (0.6523)	0.3727 (0.9467)	0.1205 (0.3061)
1/4-RING-2	0.2585 (0.6566)	0.3748 (0.9520)	0.1209 (0.3071)
1/4-RING-3	0.2575 (0.6541)	0.3721 (0.9451)	0.1205 (0.3061)
1/4-RING-4	0.2566 (0.6518)	0.3711 (0.9426)	0.1199 (0.3045)
1/2-RING-1	0.5027 (1.2769)	0.6140 (1.5596)	0.1198 (0.3043)
1/2-RING-2	0.5042 (1.2807)	0.6156 (1.5636)	0.1205 (0.3061)
1/2-RING-3	0.5053 (1.2835)	0.6166 (1.5662)	0.1179 (0.2995)
1/2-RING-4	0.5050 (1.2827)	0.6156 (1.5636)	0.1184 (0.3007)
1-RING-1	1.0016 (2.5441)	1.1275 (2.8639)	0.1219 (0.3096)
1-RING-2	1.0036 (2.5491)	1.1256 (2.8590)	0.1196 (0.3038)
1-RING-3	1.0014 (2.5436)	1.1268 (2.8621)	0.1219 (0.3096)
1-RING-4	1.0052 (2.5532)	1.1232 (2.8529)	0.1161 (0.2949)
1-RING-5	0.9991 (2.5377)	1.1252 (2.8580)	0.1205 (0.3061)
1-RING-6	1.0036 (2.5491)	1.1255 (2.8588)	0.1190 (0.3023)
3-RING-1	2.9952 (7.6078)	3.1229 (7.9322)	0.1231 (0.3127)
3-RING-2	2.9957 (7.6091)	3.1223 (7.9306)	0.1230 (0.3124)
3-RING-3	2.9974 (7.6134)	3.1235 (7.9337)	0.1232 (0.3129)
3-RING-4	2.9953 (7.6081)	3.1223 (7.9306)	0.1225 (0.3112)
3-RING-5	2.9961 (7.6101)	3.1243 (7.9357)	0.1231 (0.3127)
3-RING-6	2.9951 (7.6076)	3.1226 (7.9314)	0.1224 (0.3109)

1.2.5.3 Reflector Caps

The polyethylene reflector caps are rings with varying thicknesses and a nominal inner and outer diameter of 15.1 in. (38.354 cm) and 17.1 in. (43.434 cm), respectively. The polyethylene bottom reflector caps (BOTCAP) are rings with a nominal thickness of 0.125 in. (0.3175 cm) and inner and outer diameter of 15.1 in. (38.354 cm) and 16.08 in. (40.8432 cm), respectively. Figures 10 and 11 show a schematic of the reflector cap part types. The reflector caps provide fine height adjustment on the top of the reflector rings while the bottom reflector caps serve as the base for the first reflector ring in upper half of the experiment on the membrane. The reflector caps allow the ring reflector to be brought to within 0.03125 in. (0.079375 cm) of the top reflector height. Like the polyethylene reflector rings, the step joints have a nominal height of 0.125 in. (0.3175 cm). There is also a zero-height reflector cap (0-CAP) with a nominal thickness of 0.125 in. (0.3175 cm) and inner and outer diameter of 16.08 in. (40.8432 cm) and 17.1 in. (43.434 cm), respectively. The zero-height reflector cap finishes the top of the reflector rings without adding any additional height.

Tables 16 and 17 report the mass and dimensional measurements of the polyethylene reflector caps. A description of these measurements is included in Section 1.2.5.

Table 16: Mass and dimensions of the 0-BOTCAP and 0-CAP parts (see Fig. 11 for dimensions).

Part ID	**Mass (g)**	**Outer Diameter, *a* [in. (cm)]**	**Inner Diameter, *b* [in. (cm)]**	**Outer Edge Height, *d* [in. (cm)]**
0-BOTCAP-1	48.2	16.0530 (40.7746)	15.0660 (38.2676)	0.1310 (0.3327)
0-BOTCAP-2	48.0	16.0530 (40.7746)	15.0650 (38.2651)	0.1250 (0.3175)
0-CAP-1	50.7	17.0465 (43.2981)	16.0785 (40.8394)	0.1260 (0.3200)
0-CAP-2	50.8	17.0460 (43.2968)	16.0770 (40.8356)	0.1255 (0.3188)
0-CAP-3	50.9	17.0470 (43.2994)	16.0710 (40.8203)	0.1250 (0.3175)

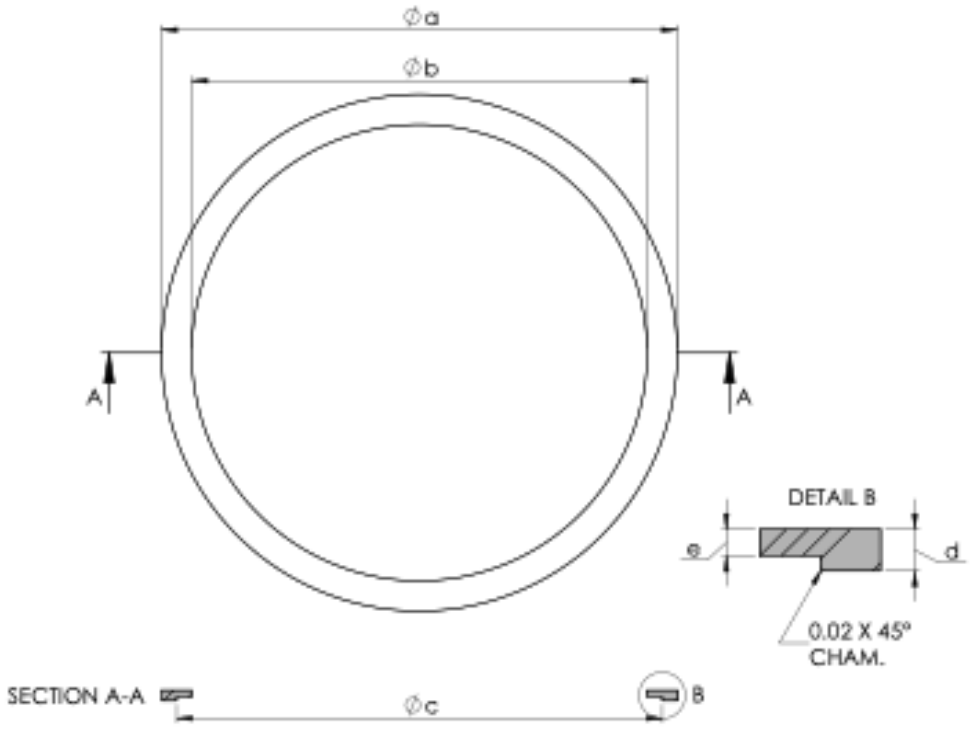

Figure 10: Diagram of the reflector cap (dimensions in inches)

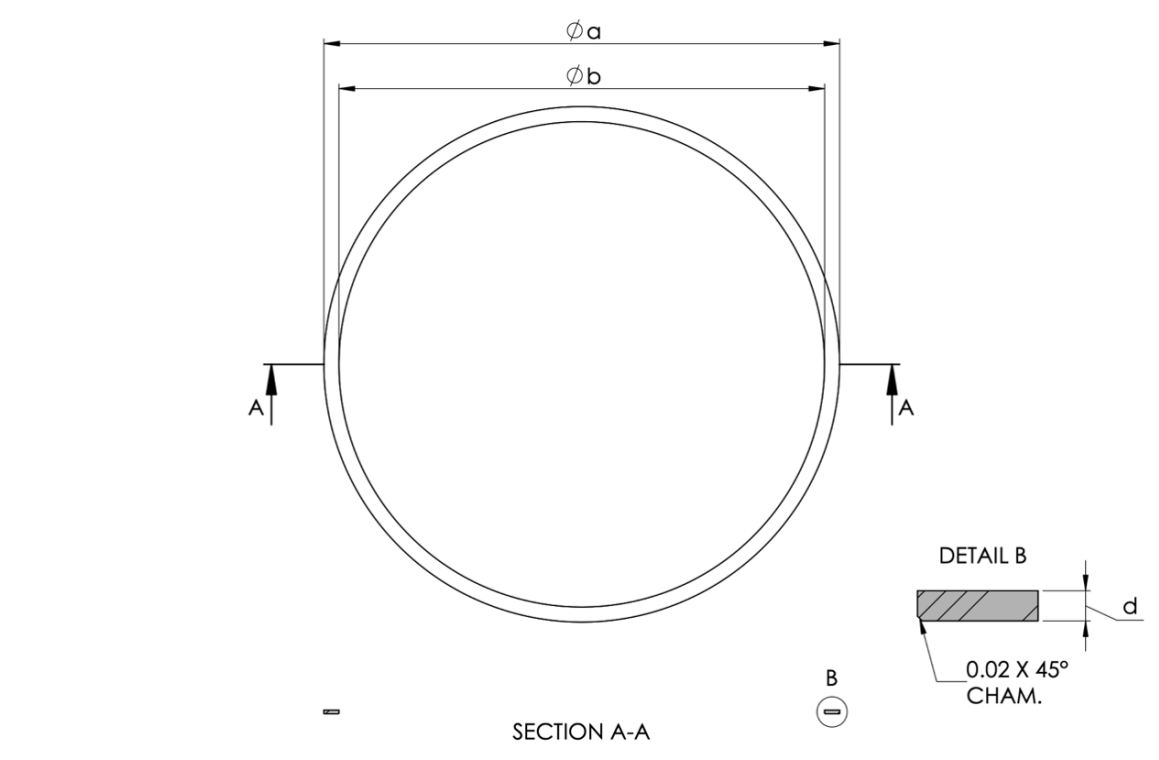

Figure 11: Diagram of the 0-BOTCAP and 0-CAP parts (dimensions in inches).

Table 17: Mass and dimensions of the reflector cap parts (see Fig. 10 for dimensions).

Part ID	Mass (g)	Outer Diameter, *a* [in. (cm)]			Inner Diameter, *b* [in. (cm)]		
		Min	Max	Average	Min	Max	Average
1/32-CAP-1	76.8	17.0612	17.0763	17.0689 (43.3550)	15.0604	15.0828	15.0738 (38.2875)
1/32-CAP-2	76.8	17.0620	17.0804	17.0711 (43.3606)	15.0645	15.0875	15.0769 (38.2953)
1/32-CAP-3	76.9	17.0651	17.0758	17.0710 (43.3603)	15.0731	15.0847	15.0773 (38.2963)
1/16-CAP-1	101.5	17.0457	17.1074	17.0794 (43.3817)	15.0554	15.1168	15.0842 (38.3139)
1/16-CAP-2	101.2	17.0690	17.0906	17.0803 (43.3840)	15.0741	15.0933	15.0850 (38.3159)
1/16-CAP-3	101.0	17.0496	17.1070	17.0765 (43.3743)	15.0456	15.1037	15.0773 (38.2963)
3/32-CAP-1	127.9	17.0414	17.1020	17.0725 (43.3642)	15.0511	15.1100	15.0807 (38.3050)
3/32-CAP-2	126.7	17.0687	17.0734	17.0713 (43.3611)	15.0821	15.0893	15.0850 (38.3159)
3/32-CAP-3	127.5	17.0620	17.0836	17.0728 (43.3649)	15.0676	15.0920	15.0796 (38.3022)
1/8-CAP-1	149.0	17.0753	17.0845	17.0788 (43.3802)	15.0748	15.0873	15.0824 (38.3093)
1/8-CAP-2	148.9	17.0692	17.0909	17.0791 (43.3809)	15.0748	15.0921	15.0817 (38.3075)
1/8-CAP-3	149.0	17.0582	17.0977	17.0781 (43.3784)	15.0652	15.1004	15.0815 (38.3070)
5/32-CAP-1	173.7	17.0691	17.0927	17.0788 (43.3802)	15.0714	15.0913	15.0836 (38.3123)
5/32-CAP-2	173.7	17.0668	17.0892	17.0775 (43.3769)	15.0752	15.0944	15.0847 (38.3151)
5/32-CAP-3	172.9	17.0664	17.0908	17.0787 (43.3799)	15.0733	15.0934	15.0848 (38.3154)
3/16-CAP-1	198.2	17.0697	17.0946	17.0797 (43.3824)	15.0708	15.0966	15.0851 (38.3162)
3/16-CAP-2	194.1	17.0714	17.0906	17.0806 (43.3847)	15.0781	15.0972	15.0867 (38.3202)
3/16-CAP-3	193.9	17.0754	17.0867	17.0808 (43.3852)	15.0828	15.0950	15.0876 (38.3225)
7/32-CAP-1	225.4	17.0781	17.0919	17.0860 (43.3984)	15.0790	15.0933	15.0861 (38.3187)
7/32-CAP-2	225.2	17.0662	17.0774	17.0706 (43.3593)	15.0692	15.0857	15.0780 (38.2981)
7/32-CAP-3	225.6	17.0548	17.0841	17.0686 (43.3542)	15.0602	15.0909	15.0774 (38.2966)

Table 17 (continued): Mass and dimensions of the reflector cap parts (see Fig. 10 for dimensions).

Part ID	Top Step (Male) Diameter, *c* [in. (cm)]			Outer Edge Height, *d* [in. (cm)]	Inner Edge Height, *e* [in. (cm)]
	Min	Max	Average		
1/32-CAP-1	16.0833	16.1000	16.0930 (40.8762)	0.1647 (0.4183)	0.0344 (0.0874)
1/32-CAP-2	16.0874	16.1030	16.0950 (40.8813)	0.1649 (0.4188)	0.0351 (0.0892)
1/32-CAP-3	16.0906	16.0989	16.0943 (40.8795)	0.1664 (0.4227)	0.0350 (0.0889)
1/16-CAP-1	16.0727	16.1328	16.1012 (40.8970)	0.1953 (0.4961)	0.0681 (0.1730)
1/16-CAP-2	16.0898	16.1123	16.1025 (40.9004)	0.1912 (0.4856)	0.0673 (0.1709)
1/16-CAP-3	16.0673	16.1258	16.0999 (40.8937)	0.1904 (0.4836)	0.0729 (0.1852)
3/32-CAP-1	16.0645	16.1234	16.0946 (40.8803)	0.2431 (0.6175)	0.1006 (0.2555)
3/32-CAP-2	16.0948	16.1025	16.0978 (40.8884)	0.2443 (0.6205)	0.1000 (0.2540)
3/32-CAP-3	16.0813	16.1057	16.0930 (40.8762)	0.2451 (0.6226)	0.1005 (0.2553)
1/8-CAP-1	16.0928	16.1036	16.0993 (40.8922)	0.2531 (0.6429)	0.1292 (0.3282)
1/8-CAP-2	16.0913	16.1076	16.0981 (40.8892)	0.2540 (0.6452)	0.1290 (0.3277)
1/8-CAP-3	16.0838	16.1214	16.1011 (40.8968)	0.2535 (0.6439)	0.1281 (0.3254)
5/32-CAP-1	16.0874	16.1091	16.0999 (40.8937)	0.2832 (0.7193)	0.1618 (0.4110)
5/32-CAP-2	16.0905	16.1128	16.1009 (40.8963)	0.2836 (0.7203)	0.1620 (0.4115)
5/32-CAP-3	16.0889	16.1098	16.1009 (40.8963)	0.2824 (0.7173)	0.1606 (0.4079)
3/16-CAP-1	16.0891	16.1102	16.1020 (40.8991)	0.3147 (0.7993)	0.1935 (0.4915)
3/16-CAP-2	16.0982	16.1164	16.1070 (40.9118)	0.3116 (0.7915)	0.1866 (0.4740)
3/16-CAP-3	16.1019	16.1163	16.1086 (40.9158)	0.3116 (0.7915)	0.1856 (0.4714)
7/32-CAP-1	16.0990	16.1155	16.1073 (40.9125)	0.3444 (0.8748)	0.2290 (0.5817)
7/32-CAP-2	16.0823	16.0973	16.0904 (40.8696)	0.3517 (0.8933)	0.2242 (0.5695)
7/32-CAP-3	16.0723	16.1012	16.0887 (40.8653)	0.3531 (0.8969)	0.2251 (0.5718)

1.2.5.4 Bottom Reflector

The polyethylene bottom reflector is a cylindrical plate with a nominal 17.1 in. (43.434 cm) diameter and 1 in. (2.54 cm) thickness, reported in Table 18. Figure 12 shows a schematic of the bottom reflector plate part. The plate features a step joint along its outer diameter on the top face. This step joint serves as the base for the lower reflector ring as described in Section 1.2.5.2 and similar to the base provided by the BOTCAP part as described in Section 1.2.5.3. Like the membrane for the upper half of the experimental configuration, the bottom reflector provides the base for the lower half of the experimental configuration. The bottom reflector sits in the lower adapter plate on the Comet lower movable platen, held in place by the lip of the adapter plate. There is a small hole in the center of the top face of the plate to hold the neutron source present during the approach to critical. It was empty during all benchmark measurements.

Figure 12: Diagram of the bottom reflector plate (dimensions in inches)

Table 18: Mass and dimensions of the BOTREF parts (see Fig. 12 for dimensions).

Part ID	Mass (g)	Outer Diameter, *a* [in. (cm)]			Step Diameter, *b* [in. (cm)]		
		Min	Max	Average	Min	Max	Average
BOTREF-1	3543.2	17.0711	17.0820	17.0761 (43.3733)	16.0507	16.0634	16.0572 (40.7853)
BOTREF-2	3544.9	17.0715	17.0814	17.0814 (43.3868)	16.0468	16.0592	16.0536 (40.7761)

Part ID	Thickness, *c* [in. (cm)]	Outer Edge Height, *d* [in. (cm)]	Source Diameter, *e* [in. (cm)]	Source Depth, *f* [in. (cm)]
BOTREF-1	1.0110 (2.5679)	0.8909 (2.2629)	0.2810 (0.7137)	0.4959 (1.2596)
BOTREF-2	1.0225 (2.5972)	0.9057 (2.3005)	0.2814 (0.7148)	0.5043 (1.2809)

1.2.6 Aluminum Inserts

The aluminum inserts are Al-6061 disks with a nominal thickness of 0.125 in. (0.3175 cm) and varying diameters, reported in Table 19. The inserts were placed in the annuli of the HEU plates, to prevent the possibility of any sagging in the polyethylene moderator and reflector plates due to weight. The inserts are nominally 0.1 in. (0.254 cm) smaller in diameter than the corresponding HEU plate annuli: 2.5-DISK for 15/2.5-HEU, 6-DISK for 15/6-HEU, and 10-DISK for 15/10-HEU.

Table 20 reports the mass and dimensional measurements of the aluminum inserts. The dimensional measurements of the diameters and thicknesses were performed by LLNL's Dimensional Inspection Laboratory using a caliper having a precision of 0.0005 in..

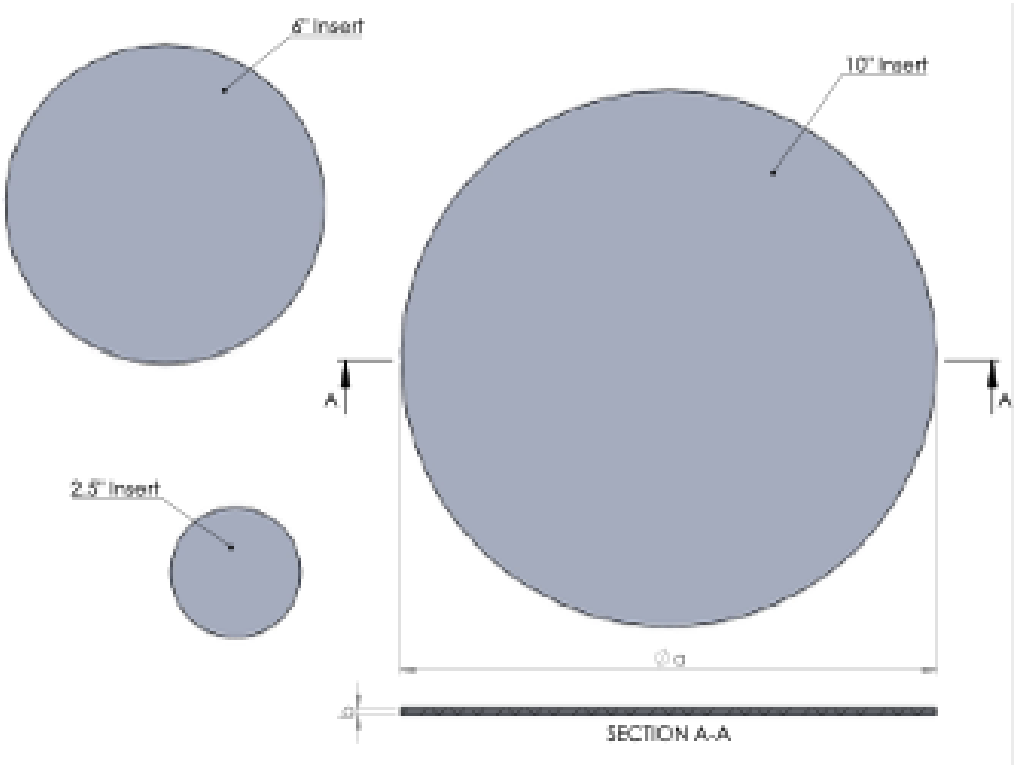

Figure 13: Schematic of the aluminum inserts.

Table 19: Aluminum insert nominal dimensions.

Part Type	**Diameter, *a* [in. (cm)]**	**Thickness, *b* [in. (cm)]**
2.5-DISK	2.4 (6.096)	0.125 (0.3175)
6-DISK	5.9 (14.986)	
10-DISK	9.9 (25.146)	

Table 20: Mass and dimensions of the aluminum insert parts (see Fig. 13)

Part Type	Mass (g)	Thickness, *b* [in. (cm)]	Diameter, *a* [in. (cm)]		
			Min	Max	Average
2.5-DISK-1	24.6	0.1240 (0.3150)	2.3945	2.3945	2.3945 (6.0820)
2.5-DISK-2	24.8	0.1245 (0.3162)	2.3955	2.3960	2.3958 (6.0858)
2.5-DISK-3	24.7	0.1245 (0.3162)	2.3960	2.3960	2.3960 (6.0858)
2.5-DISK-4	24.9	0.1255 (0.3188)	2.3960	2.3960	2.3960 (6.0858)
2.5-DISK-5	24.9	0.1250 (0.3175)	2.3950	2.3950	2.3950 (6.0833)
2.5-DISK-6	25.0	0.1255 (0.3188)	2.3940	2.3950	2.3945 (6.0833)
2.5-DISK-7	24.9	0.1250 (0.3175)	2.3950	2.3955	2.3953 (6.0846)
2.5-DISK-8	24.8	0.1250 (0.3175)	2.3945	2.3950	2.3948 (6.0833)
2.5-DISK-9	24.6	0.1240 (0.3150)	2.3945	2.3950	2.3948 (6.0833)
2.5-DISK-10	24.9	0.1250 (0.3175)	2.3955	2.3955	2.3955 (6.0846)
6-DISK-1	149.9	0.1240 (0.3150)	5.8935	5.8945	5.8940 (14.9720)
6-DISK-2	149.7	0.1235 (0.3137)	5.8915	5.8915	5.8915 (14.9644)
6-DISK-3	151.1	0.1250 (0.3175)	5.8915	5.8915	5.8920 (14.9644)
6-DISK-4	151.3	0.1250 (0.3175)	5.8930	5.8935	5.8933 (14.9695)
6-DISK-5	150.1	0.1240 (0.3150)	5.8905	5.8915	5.8910 (14.9644)
6-DISK-6	150.4	0.1245 (0.3162)	5.8920	5.8925	5.8923 (14.9670)
10-DISK-1	423.9	0.1240 (0.3150)	9.8915	9.8920	9.8918 (25.1257)
10-DISK-2	424.0	0.1245 (0.3162)	9.8920	9.8935	9.8928 (25.1295)
10-DISK-3	426.5	0.1250 (0.3175)	9.8925	9.8925	9.8925 (25.1270)
10-DISK-4	426.3	0.1250 (0.3175)	9.8925	9.8930	9.8928 (25.1282)
10-DISK-5	426.9	0.1255 (0.3188)	9.8880	9.8900	9.8890 (25.1206)
10-DISK-6	427.1	0.1250 (0.3175)	9.8935	9.8940	9.8938 (25.1308)
10-DISK-7	426.5	0.1250 (0.3175)	9.8910	9.8920	9.8915 (25.1257)
10-DISK-8	426.2	0.1250 (0.3175)	9.8915	9.8920	9.8918 (25.1257)
10-DISK-9	425.3	0.1245 (0.3162)	9.8915	9.8925	9.8920 (25.1270)
10-DISK-10	423.1	0.1245 (0.3162)	9.8900	9.8925	9.8913 (25.1270)

1.2.7 Height Measurements

The need for accurate height measurements was determined during the design of the experiment and confirmed to be the primary source of experimental uncertainty in [2]. A Westward Electronic Height Gauge (Model No. 2YND5) was used to perform the stack height measurements. The manufacturer of the gauge reports an indication accuracy of ±0.04 mm and resolution of 0.01 mm. These height measurements were performed during the experiment, while the experimental configurations were separated on Comet immediately after the benchmark period measurements. Measurements were taken of both the upper and lower core stacks and reflector rings for each experimental configuration.

For the upper stack, the height gauge was placed on the membrane. To perform the measurement, the height gauge was zeroed next to the reflector ring, on the membrane. For the lower stack, the height gauge was either held in place or clamped to the movable platen. To perform the measurement, the height gauge was zeroed next to the reflector ring, on the lip of the adapter plate. Figure 14 shows a picture of this procedure on the lower stack. The lip of the adapter plate is nominally 0.47 in. (1.1938 cm), reported in Section 1.2.2.2. Therefore, all lower stack height measurements need to account for this lip height to determine the true stack height.

Once the height gauge was zeroed, the scribe was raised, and the height gauge was rotated over the desired measurement location. Once in position, the scribe was lowered to measure either the core stack or the reflector ring. After the measurement was taken, the height gauge was again rotated to the location where it was zeroed, and a remeasurement of that position was performed. This remeasurement of the zero location was used to check the drift of the height gauge as the scribe was raised and lowered and the height gauge itself is rotated. If this drift exceed 0.10 mm, then the measurement was performed again. Typically, the drift was less than 0.05 mm.

Five positions were measured for the upper and lower core stack heights, shown in Figure 15. A single height measurement was performed for the upper and lower reflector rings. On the lower reflector ring, this measurement was done to ensure that the reflector ring was at the same height or slightly lower than the core stack, ensuring no gap was present at the center of the core stack due to the lower reflector ring. This requirement was not necessary for the upper reflector ring.

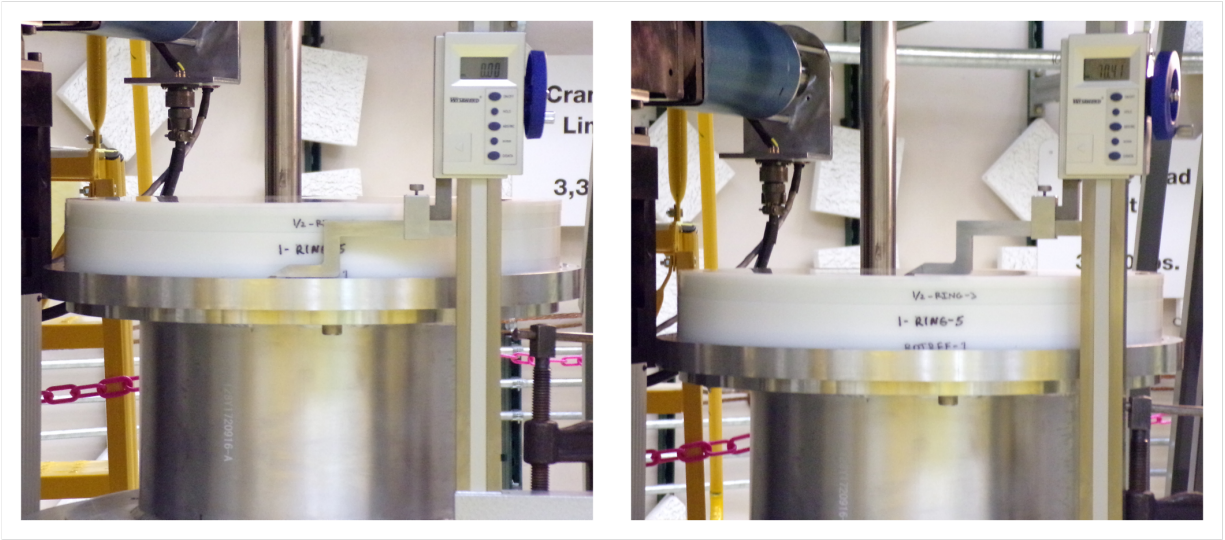

Figure 14: Height gauge measuring the stack height of the lower half of the experiment, where it must be zeroed on the lip of the lower adapter plate.

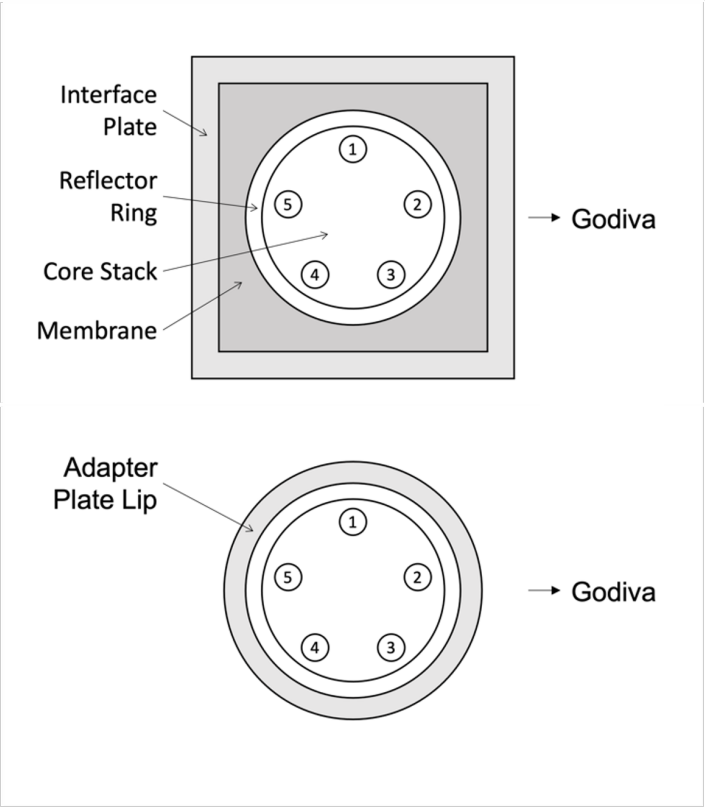

Figure 15: Upper (top) and lower (bottom) stack height measurement locations.

Table 21 summarizes of the measured upper and lower core stack and reflector ring heights. The individual height measurements are reported for each experimental configuration throughout Section 1.2.9. The core stack height measurements represent the average and standard deviation of the five measurements. The lower height measurements do not account for the height of the adapter plate lip.

Table 21: Summary of upper and lower core stack and reflector ring height measurements.

Config-uration	Upper (cm)		Lower (cm)[(a)]	
	Core Stack	Reflector Ring	Core Stack	Reflector Ring
1	8.307 ± 0.016	8.484	6.519 ± 0.018	6.467
2	7.675 ± 0.026	7.913	7.376 ± 0.038	7.272
3	9.201 ± 0.021	9.122	7.688 ± 0.014	7.649
4	9.673 ± 0.014	9.752	9.819 ± 0.018	9.791
5	25.533 ± 0.034	25.548	22.580 ± 0.029	22.408
6	8.001 ± 0.029	8.030	9.883 ± 0.026	9.774
7	7.417 ± 0.011	7.483	6.508 ± 0.031	6.421

[(a)] The lower height measurements do not account of the adapter plate lip (see Fig. 14).

1.2.8 Reactor Period

Reactor period measurements of the experimental configurations were performed using four ^{3}He proportional counters, referred to as the start-up (SU) detectors, and three compensated ion chambers, referred to as the linear channels (LC). Figure 16 shows an example of the period measurement for the Case 3 experimental configuration. At about 400 s, the SU detectors begin to saturate due to the high neutron count rates, seen in the plot as the discontinuities. Saturation of the SU detectors occurred while measuring all the experimental configurations.

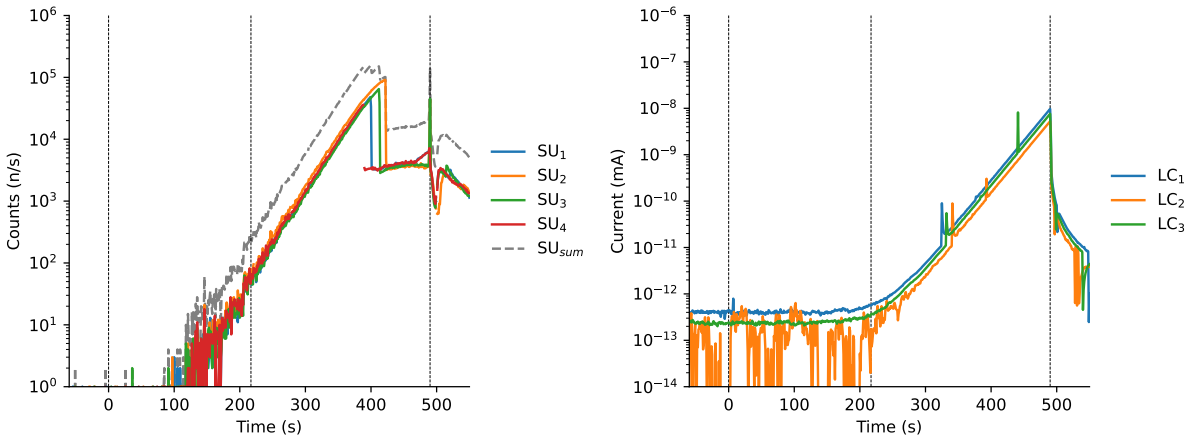

Figure 16: Example period measurement of the Case 3 experimental configuration, showing the SUs (left) and LCs (right). The first vertical dashed line (∼220 s) represents the two halves making contact while the second vertical dashed line (∼490 s) represents the separation of the two halves.

Table 22 reports the measured reactor periods and estimated excess reactivities from the Comet logbook. The SU measurements are reported as the sum of all four ^{3}He proportional counters (SU_{sum}), to improve the counting statistics. The estimated excess reactivity is based on a preliminary fit of the measured neutron count rate data. Typically, this fit is performed over the final minute, or less, of count rate data, prior to separation of the two halves of the experimental configuration. Care was taken to ensure the fit of the SU_{sum} measurement only included data prior to the first SU detector saturating.

Table 22: Benchmark period measurements, in seconds (s), and estimated excess reactivity, in cents (¢).

Config-uration	Measured Reactor Period & Estimated Excess Reactivity [s (¢)][(a)]			
	SU_{sum}	LC_1	LC_2	LC_3
1	61.41 (13.71)	59.08 (14.09)	59.71 (13.99)	58.80 (14.14)
2	65.66 (13.07)	64.97 (13.17)	65.15 (13.15)	64.40 (13.26)
3	26.76 (23.45)	25.43 (24.15)	25.52 (24.10)	25.32 (24.21)
4	127.86 (7.83)	122.75 (8.10)	123.50 (8.06)	122.51 (8.11)
5	92.16 (10.15)	84.30 (10.87)	85.04 (10.80)	84.06 (10.89)
6	53.59 (15.09)	50.57 (15.70)	50.96 (15.61)	50.53 (15.70)
7	78.10 (11.51)	73.63 (12.03)	74.15 (11.96)	73.62 (12.03)

[(a)] Based on preliminary fits of the measured neutron count rate data as reported in the Comet logbook.

In addition to the benchmark period measurements, reproducibility measurements of Cases 1, 3, 5, and 6 were performed to measure the potential impact of inconsistencies when assembling the experimental configurations. Table 23 reports the measured reactor periods and estimated excess reactivity for the reproducibility measurements of the select experimental configurations. The reproducibility measurements were performed by completely disassembling the experimental configuration then reassembling it, placing the parts in the same order and orientation. The reproducibility of Cases 1, 3, and 5 was measured to characterize the majority fast, intermediate, and thermal neutron energy spectra configurations. The reproducibility of Case 6 was measured as it used the Sandwich stacking method, instead of the Standard stacking method, as described in Section 1.2.1.

Table 23: Reproducibility period measurements, in seconds (s), and estimated excess reactivity, in cents (¢). No reproducibility measurements were performed for Cases 2, 4, or 7.

Configuration	Measured Reactor Period & Estimated Excess Reactivity [s (¢)][a]			
	SU_{sum}	LC_1	LC_2	LC_3
1	73.44 (12.05)	72.04 (12.22)	71.68 (12.27)	71.92 (12.24)
3	26.42 (23.62)	25.18 (24.28)	25.24 (24.25)	25.06 (24.35)
5	77.31 (11.60)	74.70 (11.90)	75.30 (11.83)	74.64 (11.91)
6	53.47 (15.11)	50.64 (15.68)	50.91 (15.63)	50.56 (15.70)

[a] Based on preliminary fits of the measured neutron count rate data as reported in the Comet logbook.

1.2.9 Experimental Configurations

The following sections describe the seven experimental configurations. Each section includes a to-scale rendering of the experimental configuration, the height measurements (described in Section 1.2.7), and a listing and diagram of the parts used in the experimental configuration. The rendering shows a cross section of the upper and lower halves of the experimental configuration, separated by the membrane. Table 24 summarizes the characteristics of the experimental configurations.

Table 24: Overview of the experimental configurations.

Configuration	Number of HEU Plates	Total HEU Mass (kg)	Total Hf Mass (kg)	Nominal Moderator Thickness [in. (cm)]	Nominal Top Reflector Thickness [in. (cm)]
1	25	135.5	38.7	-	1.15625 (2.93688)
2	16	99.4	24.2	0.125 (0.3175)	0.87500 (2.22250)
3	13	82.8	19.4	0.250 (0.6350)	0.96875 (2.46063)
4	10	63.9	14.5	0.500 (1.2700)	1.00000 (2.54000)
5	11	70.4	16.1	1.500 (3.8100)	1.50000 (3.81000)
6[a]	14	88.4	21.0	0.250 (0.6350)	0.96875 (2.46063)
7[b]	22	124.7	33.9	-	1.18750 (3.01625)

[a] Hafnium plates are sandwiched between two nominal 0.125 in. thick polyethylene moderator plates (Section 1.2.1).
[b] Hafnium plates are bunched as top and bottom reflectors surrounding the HEU core (Section 1.2.1).

1.2.9.1 Case 1

The Case 1 experimental configuration includes 25 HEU plates, 24 hafnium plates, no moderator plates, and a nominal 1.15625 in. (2.93688 cm) top reflector. These 25 HEU plates consisted of six 15/0-HEU, seven 15/2.5-HEU, five 15/6-HEU, and seven 15/10-HEU plates, for a total HEU mass of 135.5 kg. This configuration uses the Standard stacking method, described in Section 1.2.1.

Figure 17 shows a rendering of the Case 1 experimental configuration. Table 25 reports the height measurements of the upper and lower core stacks and reflector rings, described in Section 1.2.7. Figure 18 and Tables 26 and 27 list the parts used in the experimental configuration. The measured reactor period is reported in Section 1.2.8.

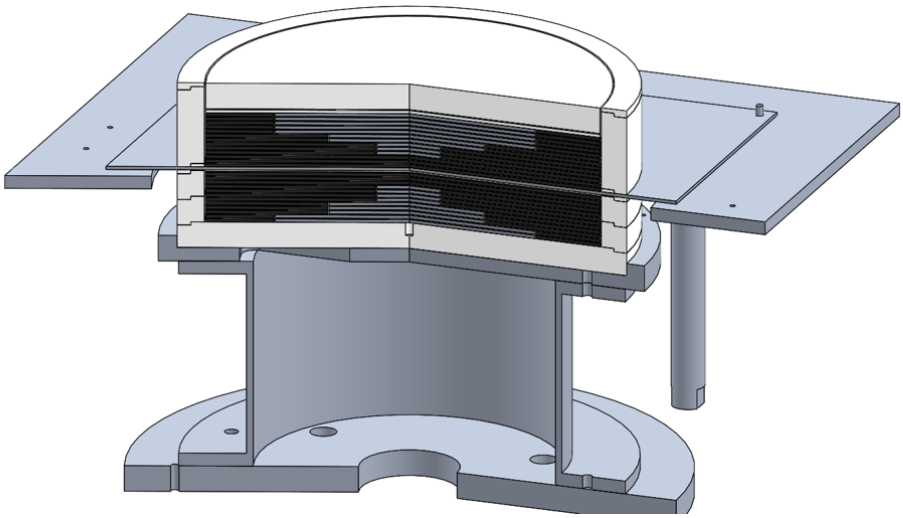

Figure 17: Rendering of the Case 1 experimental configuration.

Table 25: Height measurements of the core stacks (left) and reflector rings (right) for Case 1.

Position	Core Stack Height (cm)	
	Upper	Lower
1	8.301	6.531
2	8.284	6.525
3	8.312	6.525
4	8.328	6.527
5	8.312	6.487
Average	**8.307 ± 0.016**	**6.339 ± 0.018**

Reflector Ring Height (cm)	
Upper	Lower
8.484	6.467

Table 26: Parts used in the upper (left) and lower (right) core stacks of Case 1, using the Standard stacking method.

Layer	Upper Core Stack
28	1-REF-1
27	1/32-REF-1
26	1/8-MOD-2
25	10479 (10-DISK-7)
24	HF-25
23	10481 (10-DISK-6)
22	HF-24
21	10485 (10-DISK-5)
20	HF-23
19	10473 (10-DISK-4)
18	HF-22
17	10463 (10-DISK-3)
16	HF-20
15	10935 (6-DISK-5)
14	HF-19
13	10933 (6-DISK-4)
12	HF-18
11	10470 (2.5-DISK-7)
10	HF-17
9	10475 (2.5-DISK-6)
8	HF-16
7	10489 (2.5-DISK-5)
6	HF-15
5	11018 (Q2-16)
4	HF-14
3	11017
2	HF-13
1	11150

Part	Lower Core Stack
25	HF-12
24	11019
23	HF-11
22	11147
21	HF-10
20	11149
19	HF-09
18	10467 (2.5-DISK-4)
17	HF-08
16	10464 (2.5-DISK-3)
15	HF-07
14	10487 (2.5-DISK-2)
13	HF-06
12	10491 (2.5-DISK-1)
11	HF-05
10	10932 (6-DISK-3)
9	HF-04
8	10457 (6-DISK-2)
7	HF-03
6	10477 (6-DISK-1)
5	HF-02
4	10458 (10-DISK-2)
3	HF-01
2	10472 (10-DISK-1)
1	BOTREF-1

Table 27: Parts used in the upper (left) and lower (right) reflector rings of Case 1.

Layer	Upper Reflector Ring
3	5/32-CAP-1
2	3-RING-1
1	0-BOTCAP-1

Layer	Lower Reflector Ring
3	1/32-CAP-2
2	1-RING-1
1	1-RING-3

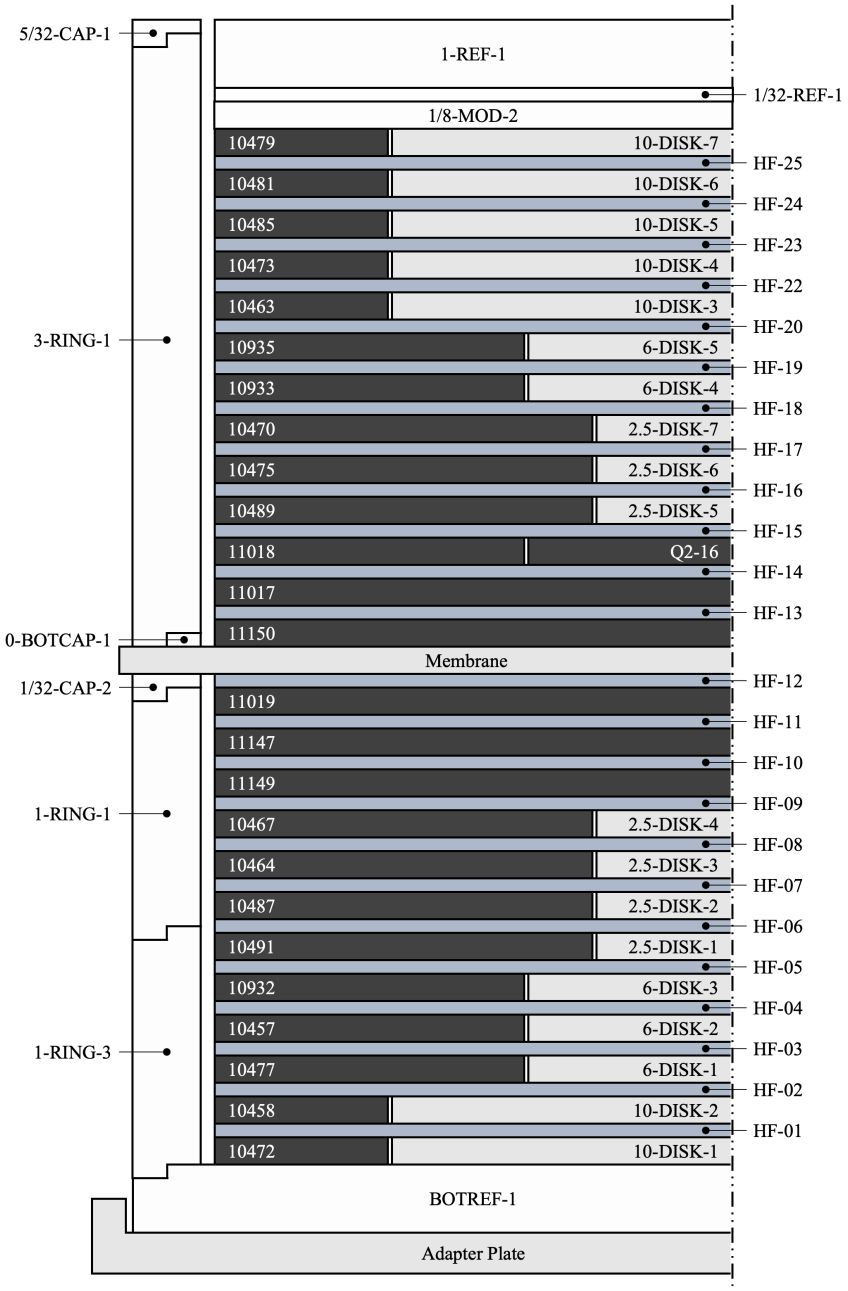

Figure 18: Axisymmetric diagram of the Case 1 experimental configuration (not to scale).

1.2.9.2 Case 2

The Case 2 experimental configuration includes 16 HEU plates, 15 hafnium plates and 0.125 in. (0.3175 cm) nominal moderator plates between each HEU plate, and a nominal 0.875 in. (2.2225 cm) top reflector. These 16 HEU plates consist of six 15/0-HEU plates, seven 15/2.5-HEU plates, and three 15/6-HEU plates, for a total HEU mass of 99.4 kg. This configuration uses the Standard stacking method, described in Section 1.2.1.

Figure 19 shows a rendering of the Case 2 experimental configuration. Table 28 reports the height measurements of the upper and lower core stacks and reflector rings, described in Section 1.2.7. Figure 18 and Tables 29 and 30 list the parts used in the experimental configuration. The measured reactor period is reported in Section 1.2.8.

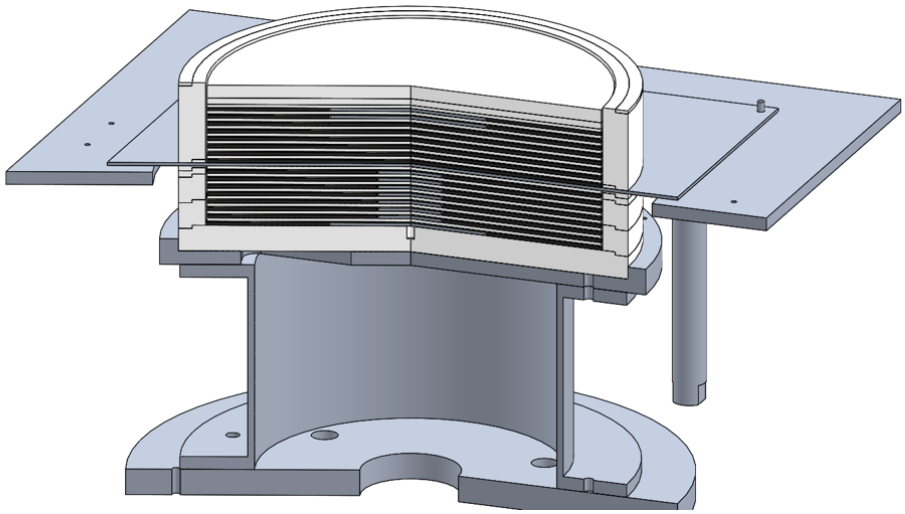

Figure 19: Rendering of the Case 2 experimental configuration, using the Standard stacking method.

Table 28: Height measurements of the core stacks (left) and reflector rings (right) for Case 2.

Position	Core Stack Height (cm)	
	Upper	Lower
1	7.701	7.340
2	7.646	7.348
3	7.679	7.363
4	7.649	7.403
5	7.699	7.428
Average	**7.675 ± 0.026**	**7.376 ± 0.038**

Reflector Ring Height (cm)	
Upper	Lower
7.913	7.272

Table 29: Parts used in the upper (left) and lower (right) core stacks of Case 2.

Layer	Upper Core Stack
25	1/2-MOD-1
24	1/4-MOD-1
23	1/8-MOD-16
22	10477 (6-DISK-3)
21	1/8-MOD-15
20	HF-15
19	10935 (6-DISK-2)
18	1/8-MOD-14
17	HF-14
16	11018 (Q2-16)
15	1/8-MOD-13
14	HF-13
13	11150
12	1/8-MOD-12
11	HF-12
10	11149
9	1/8-MOD-11
8	HF-11
7	11019
6	1/8-MOD-10
5	HF-10
4	11017
3	1/8-MOD-9
2	HF-09
1	11147

Layer	Lower Core Stack
25	1/8-MOD-8
24	HF-08
23	10464 (2.5-DISK-7)
22	1/8-MOD-7
21	HF-07
20	10475 (2.5-DISK-6)
19	1/8-MOD-6
18	HF-06
17	10470 (2.5-DISK-5)
16	1/8-MOD-5
15	HF-05
14	10489 (2.5-DISK-4)
13	1/8-MOD-4
12	HF-04
11	10491 (2.5-DISK-3)
10	1/8-MOD-3
9	HF-03
8	10467 (2.5-DISK-2)
7	1/8-MOD-2
6	HF-02
5	10487 (2.5-DISK-1)
4	1/8-MOD-1
3	HF-01
2	10457 (6-DISK-1)
1	BOTREF-1

Table 30: Parts used in the upper (left) and lower (right) reflector rings of Case 2.

Layer	Upper Reflector Ring
3	0-CAP-1
2	3-RING-1
1	0-BOTCAP-2

Layer	Lower Reflector Ring
4	1/16-CAP-1
3	1/4-RING-3
2	1-RING-1
1	1-RING-3

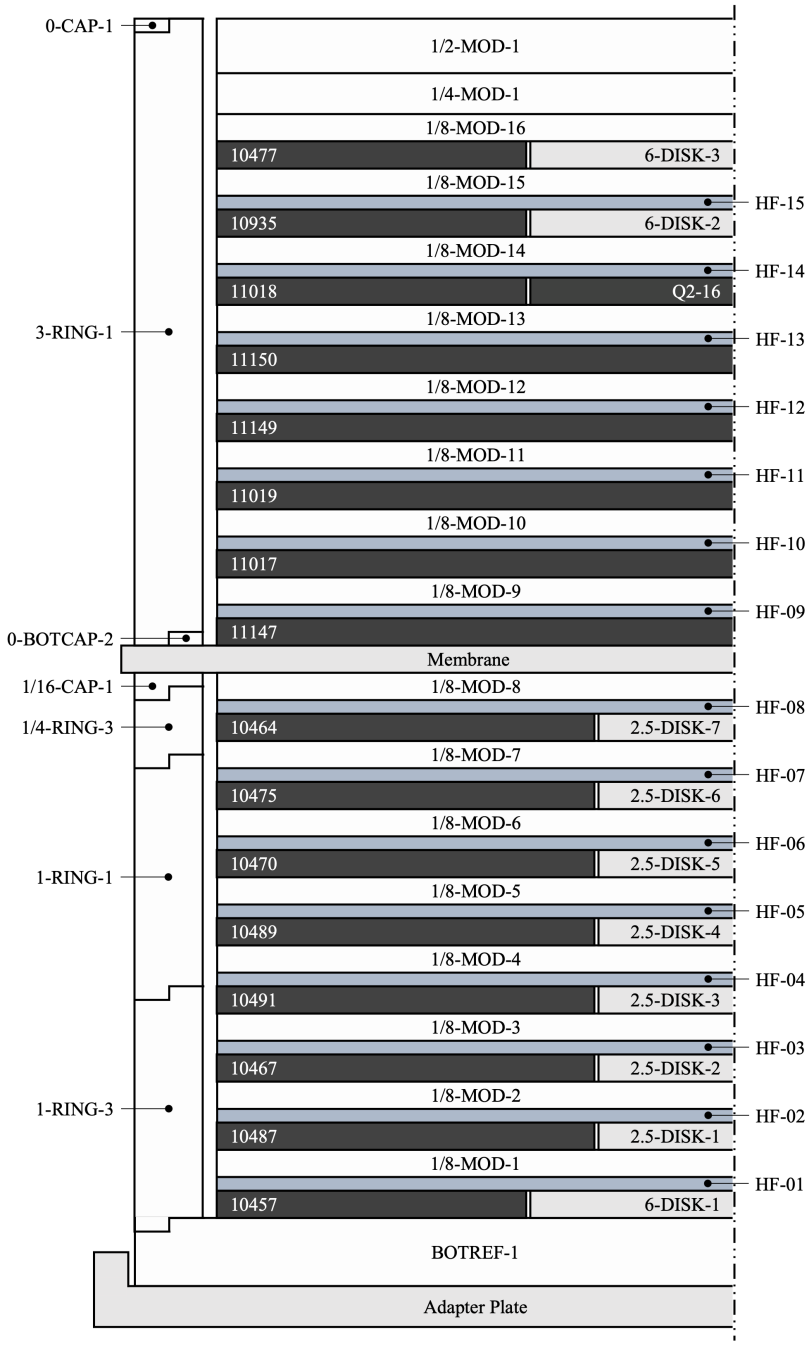

Figure 20: Axisymmetric diagram of the Case 2 experimental configuration (not to scale).

1.2.9.3 Case 3

The Case 3 experimental configuration includes 13 HEU plates, 12 hafnium plates and 0.25 in. (0.635 cm) nominal moderator plates between each HEU plate, and a nominal 0.96875 in. (2.46063 cm) top reflector. These 13 HEU plates consist of six 15/0-HEU plates and seven 15/2.5-HEU plates, for a total HEU mass of 82.8 kg. This configuration uses the Standard stacking method, described in Section 1.2.1.

Figure 21 shows a rendering of the Case 3 experimental configuration. Table 31 reports the height measurements of the upper and lower core stacks and reflector rings, described in Section 1.2.7. Figure 22 and Tables 32 and 33 list the parts used in the experimental configuration. The measured reactor period is reported in Section 1.2.8.

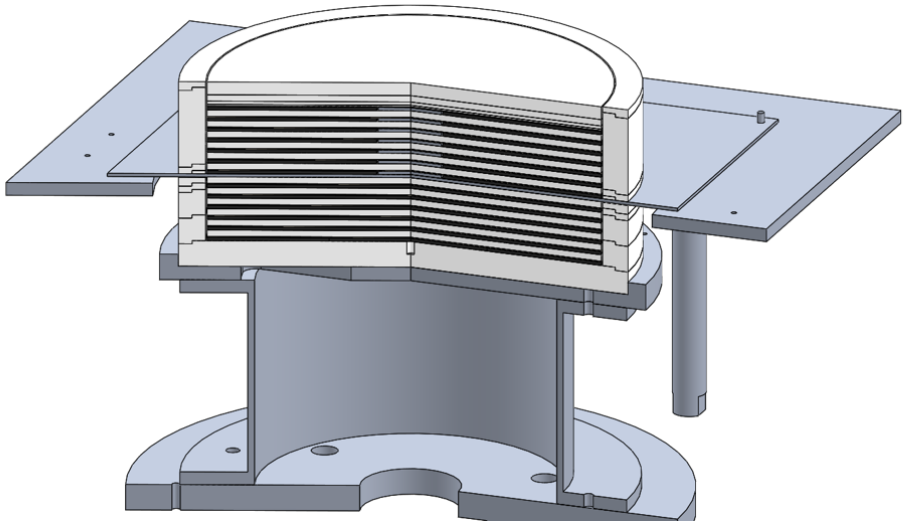

Figure 21: Rendering of the Case 3 experimental configuration, using the Standard stacking method.

Table 31: Height measurements of the core stacks (left) and reflector rings (right) for Case 3.

Position	Core Stack Height (cm)	
	Upper	Lower
1	9.183	7.677
2	9.211	7.708
3	9.232	7.692
4	9.182	7.690
5	9.196	7.671
Average	**9.201 ± 0.021**	**7.688 ± 0.014**

Reflector Ring Height (cm)	
Upper	Lower
9.122	7.649

Table 32: Parts used in the upper (left) and lower (right) core stacks of Case 3.

Layer	Upper Core Stack
24	1/2-MOD-1
23	1/4-MOD-13
22	1/8-MOD-1
21	1/16-REF-1
20	1/32-REF-1
19	10475 (2.5-DISK-8)
18	1/4-MOD-12
17	HF-12
16	10464 (2.5-DISK-3)
15	1/4-MOD-11
14	HF-11
13	10470 (2.5-DISK-9)
12	1/4-MOD-5
11	HF-10
10	10489 (2.5-DISK-10)
9	1/4-MOD-10
8	HF-09
7	10491 (2.5-DISK-4)
6	1/4-MOD-4
5	HF-08
4	10467 (2.5-DISK-6)
3	1/4-MOD-9
2	HF-07
1	10487 (2.5-DISK-5)

Layer	Lower Core Stack
19	1/4-MOD-8
18	HF-06
17	11149
16	1/4-MOD-7
15	HF-05
14	11147
13	1/4-MOD-6
12	HF-04
11	11019
10	1/4-MOD-3
9	HF-03
8	11017
7	1/4-MOD-2
6	HF-02
5	11150
4	1/4-MOD-1
3	HF-01
2	11018 (Q2-16)
1	BOTREF-1

Table 33: Parts used in the upper (left) and lower (right) reflector rings of Case 3.

Layer	Upper Reflector Ring
4	7/32-CAP-2
3	3-RING-1
2	1/4-RING-3
1	0-BOTCAP-1

Layer	Lower Reflector Ring
4	7/32-CAP-1
3	1/4-RING-1
2	1-RING-5
1	1-RING-3

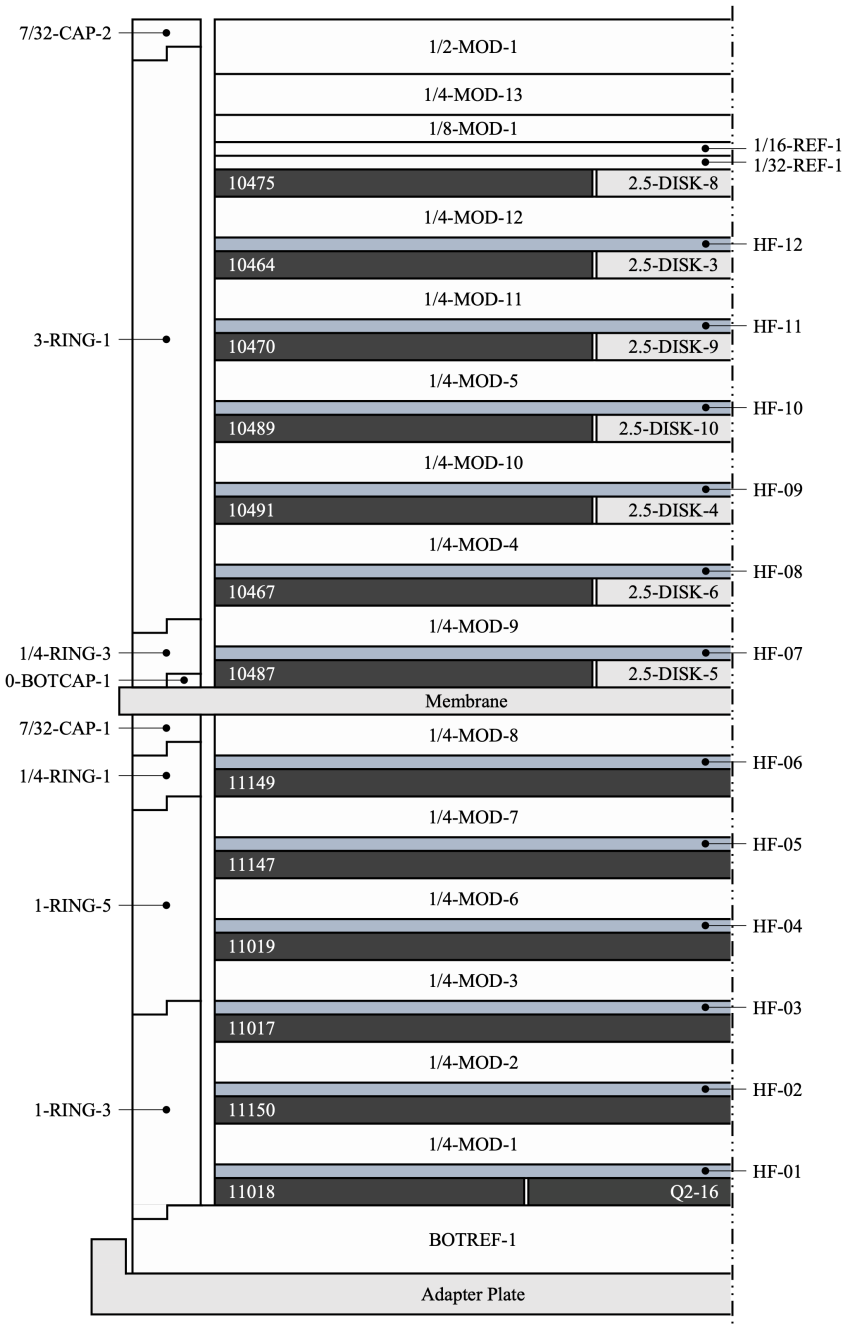

Figure 22: Axisymmetric diagram of the Case 3 experimental configuration (not to scale).

1.2.9.4 Case 4

The Case 4 experimental configuration includes 10 HEU plates, nine hafnium plates and 0.5 in. (1.27 cm) nominal moderator plates between each HEU plate, and a nominal 1.0 in. (2.54 cm) top reflector. These 10 HEU plates consist of five 15/0-HEU plates and five 15/2.5-HEU plates, for a total HEU mass of 63.9 kg. This configuration uses the Standard stacking method, described in Section 1.2.1.

Figure 23 shows a rendering of the Case 4 experimental configuration. Table 34 reports the height measurements of the upper and lower core stacks and reflector rings, described in Section 1.2.7. Figure 24 and Tables 35 and 36 list the parts used in the experimental configuration. The measured reactor period is reported in Section 1.2.8.

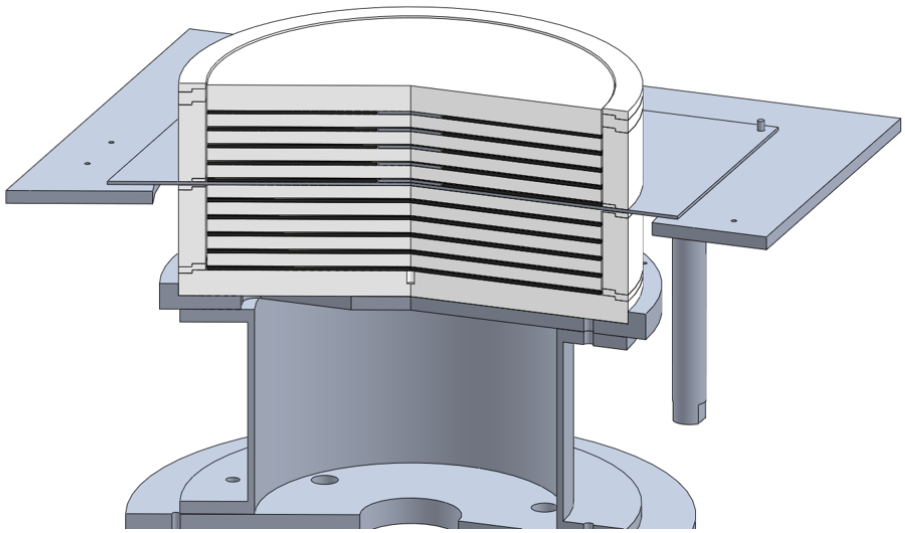

Figure 23: Rendering of the Case 4 experimental configuration, using the Standard stacking method.

Table 34: Height measurements of the core stacks (left) and reflector rings (right) for Case 4.

Position	Core Stack Height (cm)	
	Upper	Lower
1	9.671	9.839
2	9.657	9.829
3	9.665	9.790
4	9.680	9.819
5	9.694	9.818
Average	**9.673 ± 0.014**	**9.819 ± 0.018**

Reflector Ring Height (cm)	
Upper	Lower
9.752	9.791

Table 35: Parts used in the upper (left) and lower (right) core stacks of Case 4.

Layer	Upper Core Stack
14	1-REF-1
13	10470 (2.5-DISK-5)
12	1/2-MOD-9
11	HF-09
10	10489 (2.5-DISK-4)
9	1/2-MOD-8
8	HF-08
7	10491 (2.5-DISK-3)
6	1/2-MOD-7
5	HF-07
4	10467 (2.5-DISK-2)
3	1/2-MOD-6
2	HF-06
1	10487 (2.5-DISK-1)

Layer	Lower Core Stack
16	1/2-MOD-5
15	HF-05
14	11147
13	1/2-MOD-4
12	HF-04
11	11149
10	1/2-MOD-3
9	HF-03
8	11019
7	1/2-MOD-2
6	HF-02
5	11017
4	1/2-MOD-1
3	HF-01
2	11150
1	BOTREF-1

Table 36: Parts used in the upper (left) and lower (right) reflector rings of Case 4.

Layer	Upper Reflector Ring
4	7/32-CAP-1
3	1/2-RING-4
2	3-RING-6
1	0-BOTCAP-1

Layer	Lower Reflector Ring
3	1/16-CAP-3
2	3-RING-1
1	1/4-RING-2

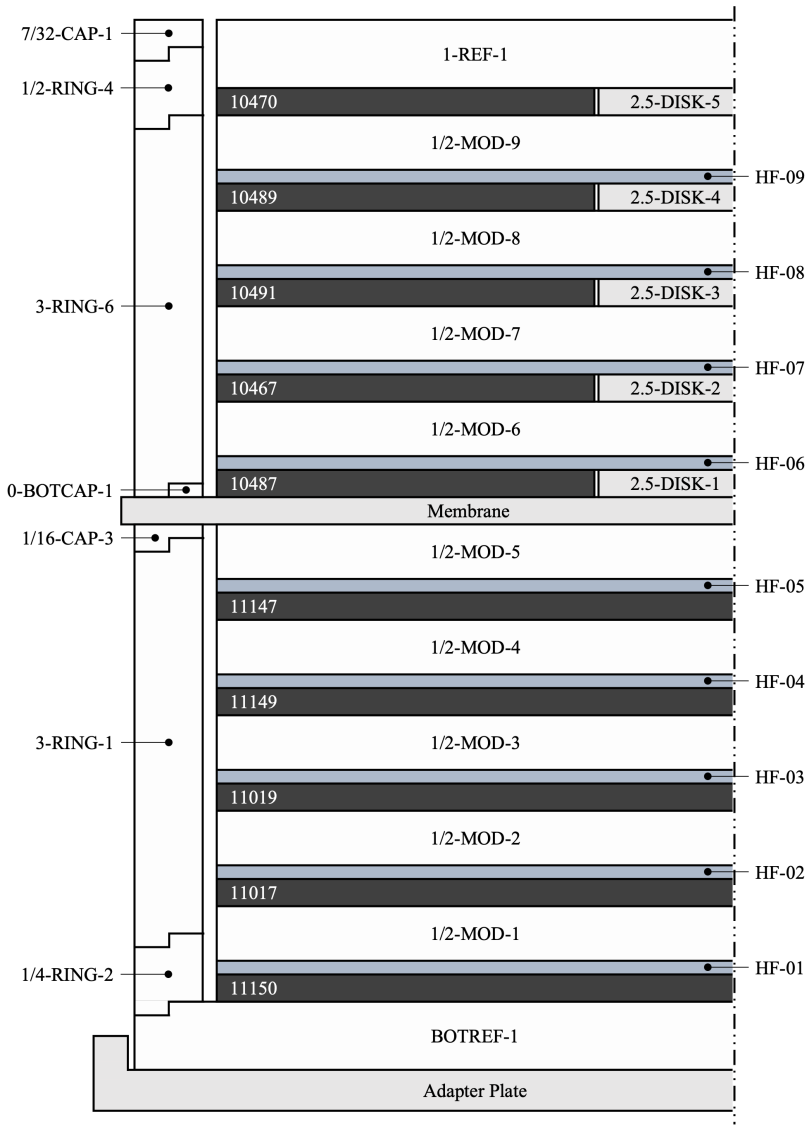

Figure 24: Axisymmetric diagram of the Case 4 experimental configuration (not to scale).

1.2.9.5 Case 5

The Case 5 experimental configuration includes 11 HEU plates, 10 hafnium plates and 1.5 in. (3.81 cm) nominal moderator plates between each HEU plate, and a nominal 1.5 in. (3.81 cm) top reflector. These 11 HEU plates consist of six 15/0-HEU plates and five 15/6-HEU plates, for a total HEU mass of 70.4 kg. This configuration uses the Standard stacking method, described in Section 1.2.1.

Figure 25 shows a rendering of the Case 5 experimental configuration. Table 37 reports the height measurements of the upper and lower core stacks and reflector rings, described in Section 1.2.7. Figure 26 and Tables 38 and 39 list the parts used in the experimental configuration. The measured reactor period is reported in Section 1.2.8.

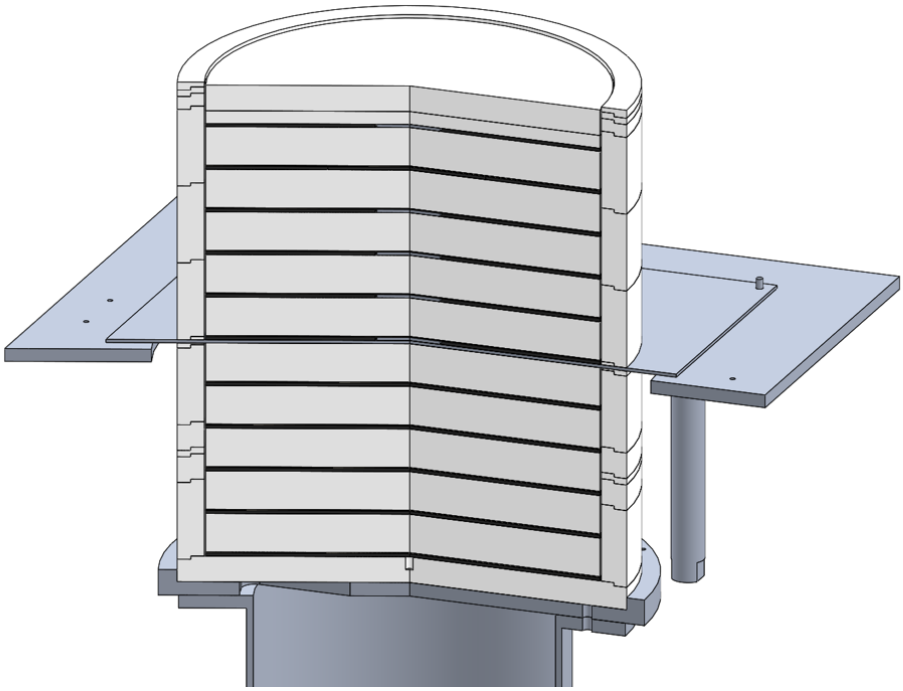

Figure 25: Rendering of the Case 5 experimental configuration, using the Standard stacking method.

Table 37: Height measurements of the core stacks (left) and reflector rings (right) for Case 5.

Position	Core Stack Height (cm)	
	Upper	Lower
1	25.495	22.601
2	25.522	22.616
3	25.512	22.562
4	25.570	22.578
5	25.568	22.544
Average	**25.533 ± 0.034**	**22.580 ± 0.029**

Reflector Ring Height (cm)	
Upper	Lower
25.548	22.408

Table 38: Parts used in the upper (left) and lower (right) core stacks of Case 5.

Layer	Upper Core Stack
18	1-REF-1
17	1/2-MOD-1
16	10470 (2.5-DISK-5)
15	1.5-MOD-11
14	HF-10
13	11018 (Q2-16)
12	1.5-MOD-10
11	HF-09
10	10489 (2.5-DISK-4)
9	1.5-MOD-9
8	HF-08
7	10491 (2.5-DISK-3)
6	1.5-MOD-8
5	HF-07
4	10467 (2.5-DISK-2)
3	1.5-MOD-7
2	HF-06
1	10487 (2.5-DISK-1)

Layer	Lower Core Stack
16	1.5-MOD-6
15	HF-05
14	11147
13	1.5-MOD-5
12	HF-04
11	11149
10	1.5-MOD-4
9	HF-03
8	11019
7	1.5-MOD-3
6	HF-02
5	11017
4	1.5-MOD-1
3	HF-01
2	11150
1	BOTREF-1

Table 39: Parts used in the upper (left) and lower (right) reflector rings of Case 5.

Layer	Upper Reflector Ring
7	3/16-CAP-1
6	1/4-RING-3
5	1/2-RING-2
4	3-RING-3
3	3-RING-6
2	3-RING-2
1	0-BOTCAP-1

Layer	Lower Reflector Ring
6	1/16-CAP-2
5	3-RING-4
4	1-RING-3
3	1/4-RING-1
2	1-RING-1
1	3-RING-1

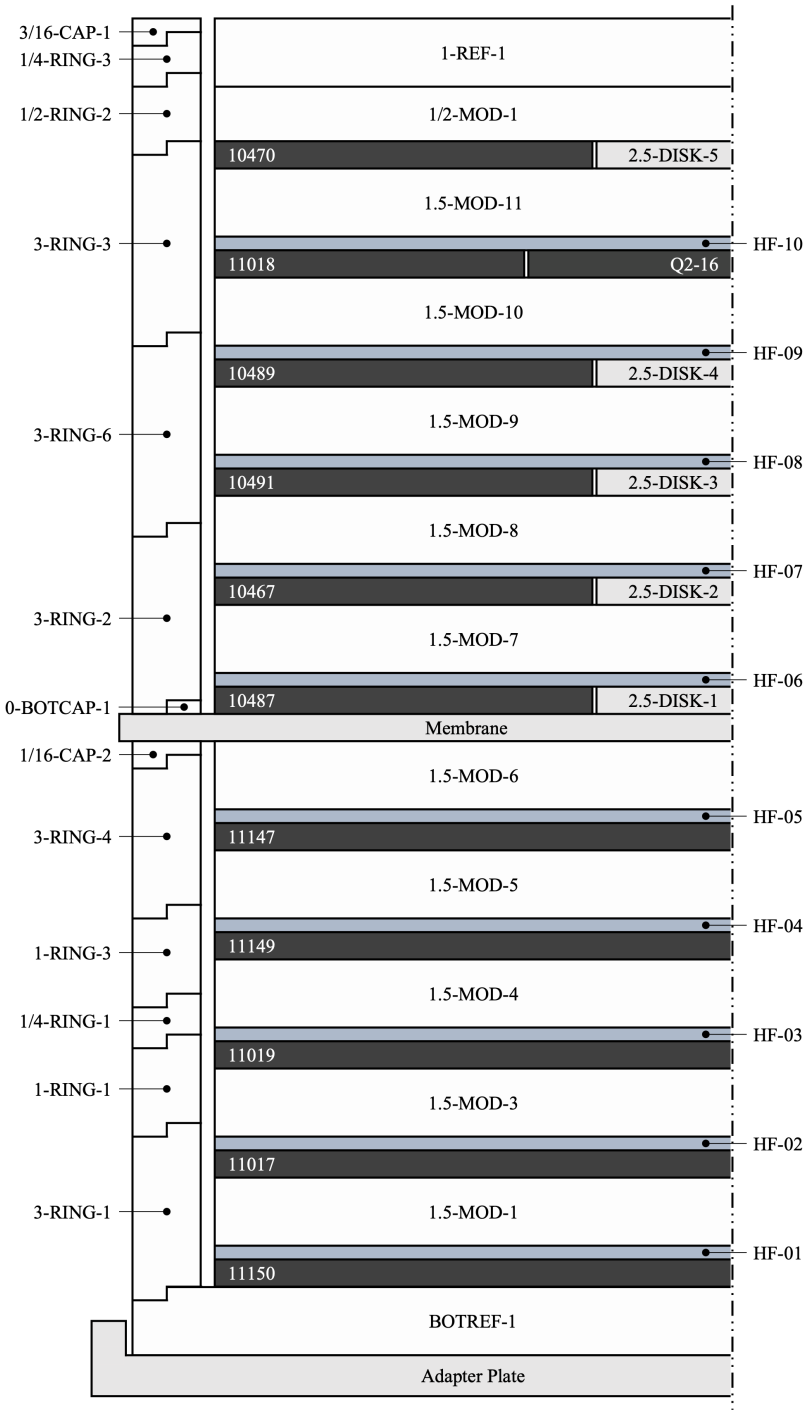

Figure 26: Axisymmetric diagram of the Case 5 experimental configuration (not to scale).

1.2.9.6 Case 6

The Case 6 experimental configuration includes 14 HEU plates, 13 hafnium plates, 26 0.125 in. (0.3175 cm) nominal moderator plates between each HEU plate, and a nominal 0.96875 in. (2.46063 cm) top reflector. These 14 HEU plates consist of six 15/0-HEU plates, seven 15/2.5-HEU plates, and one 15/6-HEU plate, for a total HEU mass of 88.4 kg. This configuration uses the Sandwich stacking method, described in Section 1.2.1.

Figure 27 shows a rendering of the Case 6 experimental configuration. Table 40 reports the height measurements of the upper and lower core stacks and reflector rings, described in Section 1.2.7. Figure 28 and Tables 41 and 42 list the parts used in the experimental configuration. The measured reactor period is reported in Section 1.2.8.

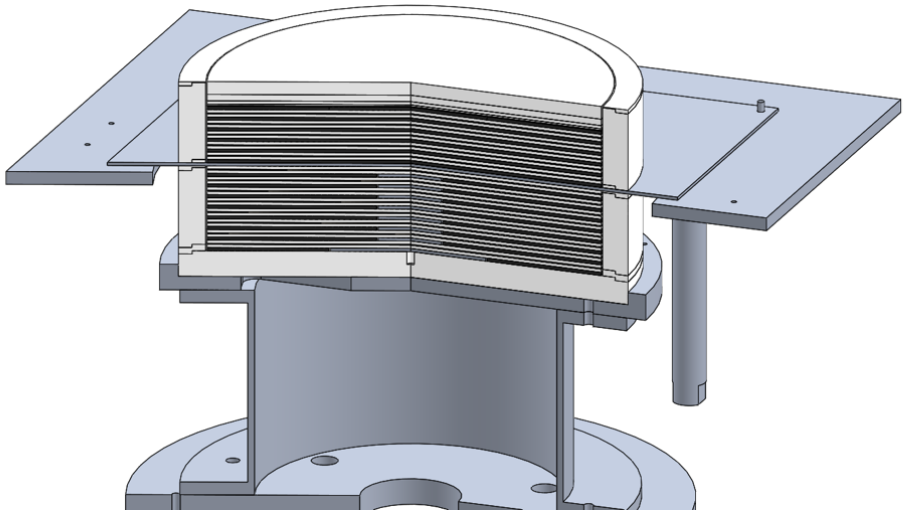

Figure 27: Rendering of the Case 6 experimental configuration, using the Sandwich stacking method.

Table 40: Height measurements of the core stacks (left) and reflector rings (right) for Case 6.

Position	Core Stack Height (cm)	
	Upper	Lower
1	7.999	9.891
2	7.969	9.852
3	7.980	9.912
4	8.019	9.902
5	8.040	9.859
Average	**8.001 ± 0.029**	**9.883 ± 0.026**

Reflector Ring Height (cm)	
Upper	Lower
8.030	9.774

Table 41: Parts used in the upper (left) and lower (right) core stacks of Case 6.

Layer	Upper Core Stack
26	1/2-MOD-1
25	1/4-MOD-1
24	1/8-MOD-14
23	1/16-REF-1
22	1/32-REF-1
21	11018 (Q2-16)
20	1/8-MOD-31
19	HF-13
18	1/8-MOD-13
17	11150
16	1/8-MOD-30
15	HF-12
14	1/8-MOD-12
13	11149
12	1/8-MOD-29
11	HF-11
10	1/8-MOD-11
9	11019
8	1/8-MOD-28
7	HF-10
6	1/8-MOD-10
5	11017
4	1/8-MOD-27
3	HF-09
2	1/8-MOD-9
1	11147

Layer	Lower Core Stack
33	1/8-MOD-26
32	HF-08
31	1/8-MOD-8
30	10464 (2.5-DISK-7)
29	1/8-MOD-25
28	HF-07
27	1/8-MOD-7
26	10475 (2.5-DISK-6)
25	1/8-MOD-24
24	HF-06
23	1/8-MOD-6
22	10470 (2.5-DISK-5)
21	1/8-MOD-23
20	HF-05
19	1/8-MOD-5
18	10489 (2.5-DISK-4)
17	1/8-MOD-22
16	HF-04
15	1/8-MOD-4
14	10491 (2.5-DISK-3)
13	1/8-MOD-21
12	HF-03
11	1/8-MOD-3
10	10467 (2.5-DISK-2)
9	1/8-MOD-20
8	HF-02
7	1/8-MOD-2
6	10487 (2.5-DISK-1)
5	1/8-MOD-19
4	HF-01
3	1/8-MOD-1
2	10457 (6-DISK-1)
1	BOTREF-1

Table 42: Parts used in the upper (left) and lower (right) reflector rings of Case 6.

Layer	Upper Reflector Ring
3	1/32-CAP-1
2	3-RING-2
1	0-BOTCAP-1

Layer	Lower Reflector Ring
3	1/16-CAP-1
2	3-RING-1
1	1/4-RING-3

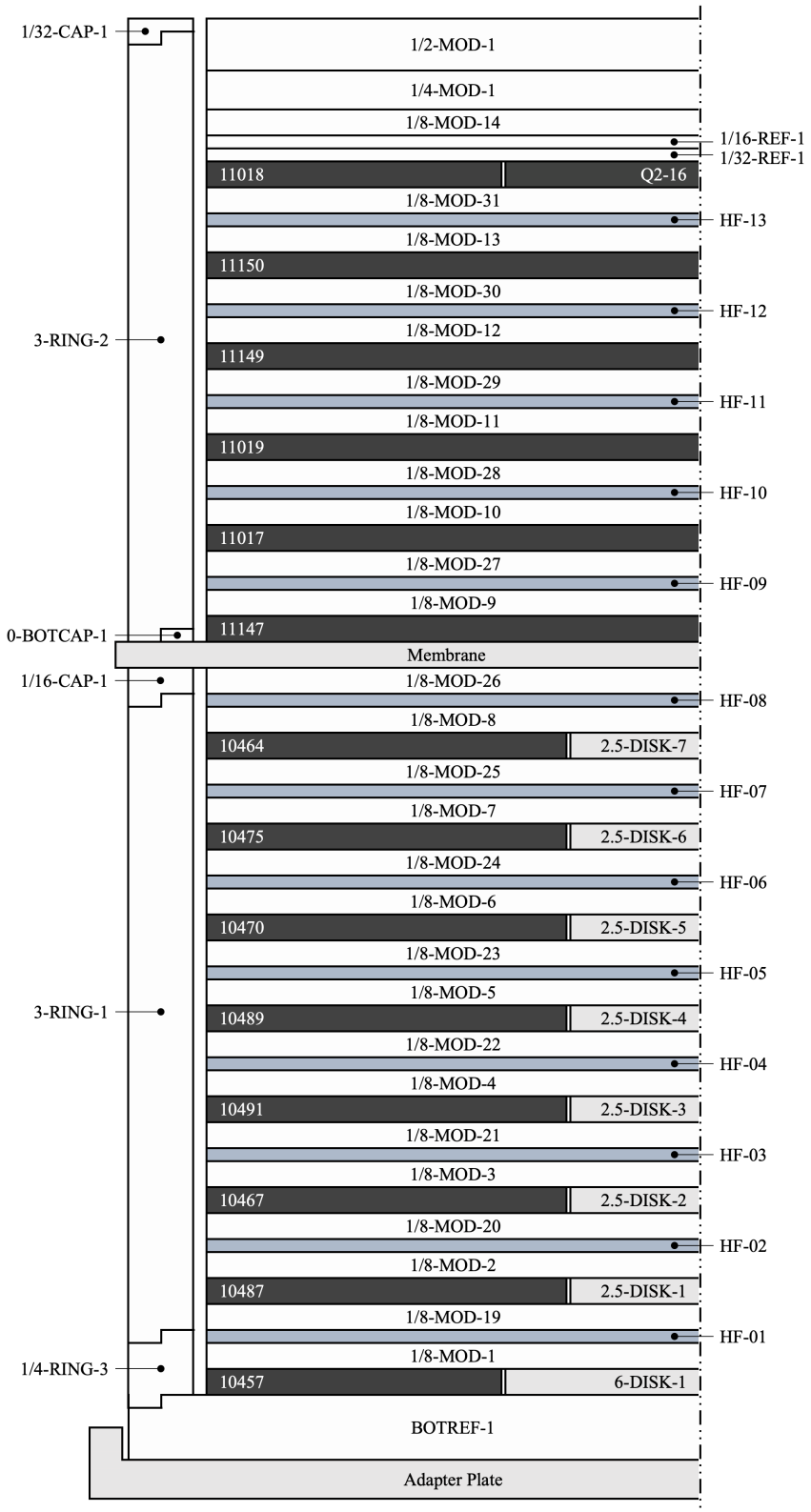

Figure 28: Axisymmetric diagram of the Case 6 experimental configuration (not to scale).

1.2.9.7 Case 7

The Case 7 experimental configuration includes 22 HEU plates, no moderator, a nominal 1.1875 in. (3.01625 cm) top reflector, and a nominal 0.48 in. (1.2192 cm) top and bottom hafnium reflector consisting of 12 hafnium plates each. These 22 HEU plates consist of six 15/0-HEU plates, seven 15/2.5-HEU plates, five 15/6-HEU plate, and four 15/10-HEU plates, for a total HEU mass of 124.7 kg. This configuration uses the Bunched stacking method, described in Section 1.2.1.

Figure 29 shows a rendering of the Case 7 experimental configuration. Table 43 reports the height measurements of the upper and lower core stacks and reflector rings, described in Section 1.2.7. Figure 30 and Tables 44 and 45 list the parts used in the experimental configuration. The measured reactor period is reported in Section 1.2.8.

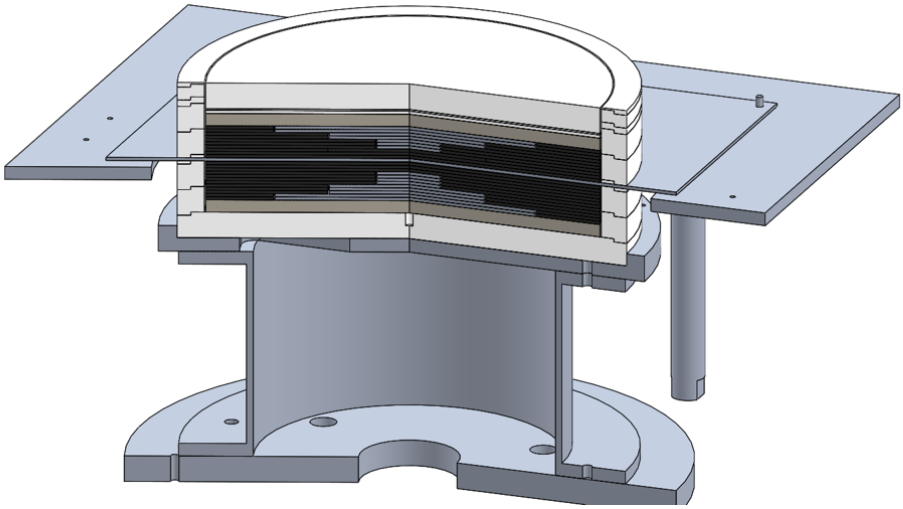

Figure 29: Rendering of the Case 7 experimental configuration, using the Bunched stacking method.

Table 43: Height measurements of the core stacks (left) and reflector rings (right) for Case 7.

Position	Core Stack Height (cm)	
	Upper	Lower
1	7.404	6.540
2	7.408	6.479
3	7.423	6.529
4	7.432	6.471
5	7.418	6.519
Average	**7.417 ± 0.011**	**6.508 ± 0.031**

Reflector Ring Height (cm)	
Upper	Lower
7.483	6.421

Table 44: Parts used in the upper (left) and lower (right) core stacks of Case 7.

Layer	Upper Core Stack
25	1-REF-1
24	1/16-REF-1
23	1/8-MOD-1
22	HF-25
21	HF-24
20	HF-23
19	HF-22
18	HF-20
17	HF-19
16	HF-18
15	HF-17
14	HF-16
13	HF-15
12	HF-14
11	HF-13
10	10473 (10-DISK-4)
9	10463 (10-DISK-3)
8	10935 (6-DISK-5)
7	10933 (6-DISK-4)
6	10470 (2.5-DISK-7)
5	10475 (2.5-DISK-6)
4	10489 (2.5-DISK-5)
3	11018 (Q2-16)
2	11017
1	11150

Layer	Lower Core Stack
25	11019
24	11147
23	11149
22	10467 (2.5-DISK-4)
21	10464 (2.5-DISK-3)
20	10487 (2.5-DISK-2)
19	10491 (2.5-DISK-1)
18	10932 (6-DISK-3)
17	10457 (6-DISK-2)
16	10477 (6-DISK-1)
15	10458 (10-DISK-2)
14	10472 (10-DISK-1)
13	HF-12
12	HF-11
11	HF-10
10	HF-09
9	HF-08
8	HF-07
7	HF-06
6	HF-05
5	HF-04
4	HF-03
3	HF-02
2	HF-01
1	BOTREF-1

Table 45: Parts used in the upper (left) and lower (right) reflector rings of Case 7.

Layer	Upper Reflector Ring
6	1/16-CAP-1
5	1/2-RING-1
4	1/4-RING-1
3	1-RING-3
2	1-RING-4
1	0-BOTCAP-1

Layer	Lower Reflector Ring
3	0-CAP-2
2	1-RING-5
1	1-RING-1

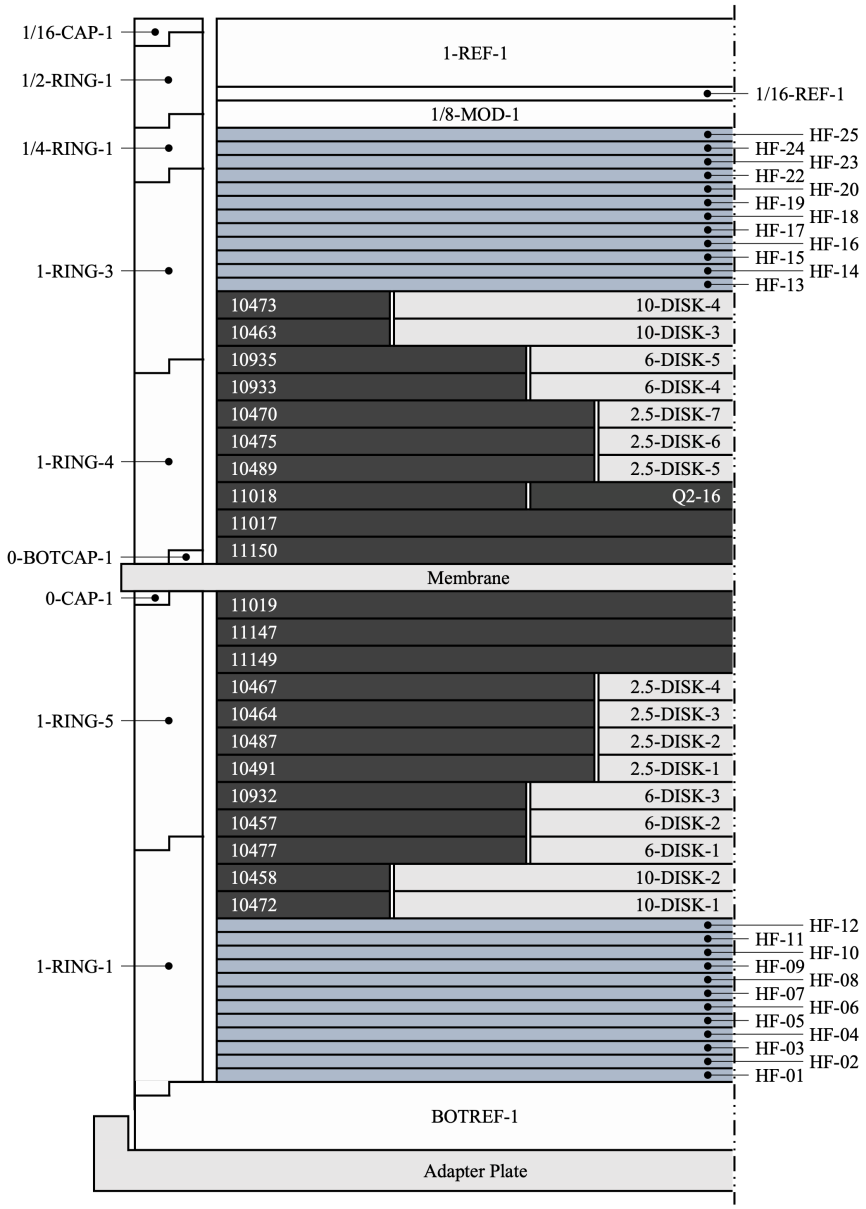

Figure 30: Axisymmetric diagram of the Case 7 experimental configuration (not to scale).

1.3 Description of Material Data

The following material descriptions are reproduced from [2]. Except for the hafnium plates, all other materials used in this experiment are the same as [2].

1.3.1 Highly Enriched Uranium

Sections 1.3.1.1 and 1.3.1.2 summarize and reproduce relevant material descriptions from [6] and [4], which use the same HEU plates. The 15/2.5-HEU, 15/6-HEU, and 15/10-HEU plate types, identified as Id No. 403, 401, and 402, are used in [6]. The 15/0-HEU and 15/2.5-HEU plate types, identified as HEU1 and HEU2, are used in [4].

Mass measurements of the HEU plates were performed using a Mettler Toledo SB16001 High Capacity Precision Balance under the NCERC Calibration Program (Cal No. 012708). The calibration for this balance was certified on May 17, 2022, and was valid through May 17, 2023. These measurements were taken on October 17, 2022. The manufacturer of the SB16001 reports a maximum capacity of 16,100 grams, precision of ± 0.1 grams, and linearity of ± 0.3 grams. The measurement procedure required the HEU plates be weighed in a plastic bag to contain any contamination. Each bag was weighed before placing the HEU plate in it. Then the weight of the HEU plate inside the bag was measured. After performing this measurement, the balance was checked to ensure the measurement returned to zero with the HEU plate and bag removed.

Prior to performing the HEU plate mass measurements, two known check weights were measured on the balance. Table 46 summarizes these measurements, chosen to encompass the HEU plate masses.

Table 46: Check weight measurements used to generate the calibration curve.

Mass (g)			Notes
Check Weight	**Measured**	**Difference[(a)]**	
2000.0	2000.2	0.2	2 kg weight
7000.0	7000.8	0.8	2 kg + 5 kg weights

[(a)] (Measured) - (Check Weight)

Based on these measurements, the following calibration curve was generated

$$f(m) = 0.00012 \cdot m - 0.04 \tag{1}$$

where m is the mass, in grams, and $f(m)$ is the calibration curve, as a function of mass, used to correct the mass measurement, valid between 2 kg and 7 kg. This calibration curve is used to correct the HEU plate masses reported in Table 46.

Table 47: HEU plate mass measurements and mass corrections.

Part Type	Part ID	Mass (g)			Corrected Mass (g)[b]
		Bag	Plate & Bag	Plate[a]	
15/0-HEU	11150	96.4	6501.8	6405.4	6404.7
	11149	100.8	6483.7	6382.9	6382.2
	11147	95.9	6609.0	6513.1	6512.4
	11019	95.9	6565.8	6469.9	6469.2
	11017	100.5	6599.0	6498.5	6497.8
15/2.5-HEU	10491	98.6	3703.3	3604.7	3604.3
	10489	99.6	3694.3	3594.7	3594.3
	10487	103.2	3668.2	3565.0	3564.6
	10475	98.0	3705.3	3607.3	3606.9
	10470	95.2	3682.0	3586.8	3586.4
	10467	98.2	3730.3	3632.1	3631.7
	10464	95.8	3714.1	3618.3	3617.9
15/6-HEU	11018	101.4	6493.7	6392.3	6391.6
	10935	100.5	6444.9	6344.4	6343.7
	10933	97.1	6373.2	6276.1	6275.4
	10932	96.7	6325.9	6229.2	6228.5
	10477	95.9	6375.2	6279.3	6278.6
	10457	98.2	6434.5	6336.3	6335.6
15/10-HEU	10485	100.0	6359.1	6259.1	6258.4
	10481	100.7	5470.9	5370.2	5369.6
	10479	97.6	5533.1	5435.5	5434.9
	10473	95.6	5533.6	5438.0	5437.4
	10472	101.2	5534.7	5433.5	5432.9
	10463	95.9	5595.4	5499.5	5498.9
	10458	100.8	5675.3	5574.5	5573.9
6/0-HEU	Q2-16	102.7	1178.4	1075.7	1075.6

[a] (Plate & Bag Mass) - (Bag Mass) = (Plate Mass)
[b] Corrected using the calibration curve reported in Eq. 1.

1.3.1.1 ^{235}U Enrichment

Table 48 reproduces the mass spectrometry measurements from [6] and [4], reporting the uranium isotopic content of the HEU plates. The measurements are reported as atomic ratios relative to ^{235}U and the uncertainties are at the 95% confidence level (2σ), as noted in [6].

Table 48: HEU plate uranium isotopic content measurements.

Part Type	Part ID	Uranium Isotope (Atom Ratio Relative to ^{235}U)			
		^{234}U	^{235}U	^{236}U	^{238}U
15/10-HEU	10458	0.0111 ± 0.0002	1.00	<2E-5	0.0577 ± 0.0012
15/6-HEU	10493	0.0115 ± 0.0001	1.00	(8.40 ± 0.42)E-4	0.0592 ± 0.0002
	10932	0.0108 ± 0.0001	1.00	(3.50 ± 0.04)E-3	0.0586 ± 0.0002
	11018	0.0110 ± 0.0001	1.00	(5.56 ± 0.06)E-3	0.0555 ± 0.0002

Table 49 reproduces the relevant HEU plate enrichments from [6] and [4]. The enrichments were obtained from Material Controls and Accountability for the plates used in the Big Ten assembly and a letter from Dixon Callihan (ORNL) to Hugh Paxton (LANL) dated May 20, 1960. The HEU plates in [6] are not individually identified, instead it lists individual enrichment values grouped by part type. Some of the HEU plate Part IDs in [4] are prefaced with "B10" which has been removed in favor of the ending 5-digit identifier.

Table 49: HEU plate ^{235}U enrichment.

Part Type	Part ID	Enrichment
15/0-HEU	11150	93.17
	11149	93.24
	11147	93.17
	11019	93.18
	11017	93.31
15/2.5-HEU	10491	93.37
	10489	93.39
	10487	93.26
	10475	93.40
	10470	93.41
	10467	93.41
	10464	93.38
6/0-HEU	Q2-16	-

Part Type	Part ID	Enrichment
15/6-HEU	11018	93.19
	10935	93.18
	10933	93.16
	10932	93.15
	10477	93.35
	10457	93.44
15/10-HEU	10485	93.24
	10481	93.23
	10479	-
	10473	-
	10472	-
	10463	-
	10458	93.4

1.3.1.2 Uranium Impurities

Table 50 reproduces the HEU plate impurity measurements from [6] and [4]. The analysis reports did not distinguish whether the impurities were atom fractions or mass fractions. Therefore, the reported impurities are assumed to be by weight, as is done in [6].

Table 50: Measured HEU plate impurities.

Impurity (ppm U)	15/0-HEU			15/6-HEU	
	11147	**11149**	**11150**	**10932**	**10933**
Li	<0.1	<0.1	<0.1	<0.1	<0.1
Be	<0.1	<0.1	<0.1	<0.1	<0.1
B	0.6	0.6	0.3	0.2	<0.1
C	1100	270	320	170	170
Na	<1	<1	<1	<1	<1
Mg	<1	<1	<1	<1	1
Al	50	40	20	150	100
Si	300	400	210	80	130
Ca	<2	<2	<2	<2	<2
V	<20	<20	<20	<20	<20
Cr	5	15	5	2	3
Mn	4	7	6	7	6
Fe	100	190	90	70	30
Co	<5	<5	<5	<5	<5
Ni	20	30	20	15	15
Cu	6	5	4	4	3
Mo	50	<25	<25	-	-
Sn	<1	<1	<1	-	-
Pb	5	<1	<1	-	-

1.3.2 Hafnium

The following sections report density measurements and impurity analysis of the hafnium plates. These measurements were performed and certified by the manufacturer prior to the experiment.

1.3.2.1 Hafnium Density Measurements

Table 51 reports the measured densities of the hafnium plates as reported by the manufacturer.

1.3.2.2 Hafnium Impurity Analysis

Table 52 reports the measured elemental impurity content of the hafnium material used to produce the hafnium plates, including the maximum specification. Measurements were performed with three samples of the ingot used to produce the plates and one sample from the product. The maximum specification allowed for 0.2305 Wt.% (2305 ppm) impurities, 4.5 Wt.% zirconium, and the remainder as hafnium.

Table 51: Hafnium plate density measurements.

Part ID	Density (g/cm^3)	Part ID	Density (g/cm^3)
HF-01	12.9	HF-14	13.1
HF-02	13.0	HF-15	12.6
HF-03	13.0	HF-16	12.8
HF-04	13.0	HF-17	12.8
HF-05	13.0	HF-18	13.0
HF-06	13.1	HF-19	13.1
HF-07	13.0	HF-20	13.0
HF-08	13.1	HF-22	12.8
HF-09	13.0	HF-23	12.8
HF-10	13.0	HF-24	13.0
HF-11	13.1	HF-25	13.1
HF-12	13.0	HF-26	13.1
HF-13	12.9	HF-27	13.1

Table 52: Hafnium impurity analysis results from samples of the ingot and product.

Element	Elemental Composition (%)				
	Spec. Max.	Ingot			Product
Hf	Balance	-	-	-	-
Zr	4.5	2.6	2.7	2.7	2.7
Al	0.010	<0.0025	<0.0025	<0.0025	<0.0025
C	0.015	0.003	0.003	0.003	0.004
Cr	0.010	<0.003	-	<0.003	<0.003
Cu	0.010	<0.002	<0.002	<0.002	<0.002
H	0.0025	<0.0003	-	<0.0003	<0.0003
Fe	0.050	0.014	0.015	0.016	0.016
Mo	0.0020	<0.0010	<0.0010	<0.0010	<0.0010
Ni	0.0050	<0.0025	-	<0.0025	<0.0025
Nb	0.010	<0.005	<0.005	<0.005	<0.005
N	0.010	0.005	-	0.005	0.004
O	0.040	0.021	-	0.021	0.017
Si	0.010	<0.0025	-	<0.0025	<0.0025
Ta	0.020	<0.001	<0.001	<0.001	<0.001
Sn	0.0050	<0.0010	-	<0.0010	<0.0010
Ti	0.010	<0.002	<0.002	<0.002	<0.002
W	0.0150	<0.002	<0.002	<0.002	<0.0020
U	0.0010	<0.0002	-	<0.0002	<0.0002
V	0.0050	<0.0010	-	<0.0010	<0.0010

1.3.3 Polyethylene

1.3.3.1 Polyethylene Density Measurements

The density of the polyethylene was analyzed at LLNL by performing high-precision volume and mass measurements of small samples taken from seven different polyethylene parts. The volume measurements were performed using a Micromeritics AccuPyc II gas displacement pycnometry system. The system used a 100 cm^3 sample chamber and was calibrated using a 51.08755 cm^3 calibration ball prior to each series of sample measurements. Each volume measurement was performed 10 times per sample. The mass measurements were performed on a balance with a precision of 10 µg. Each sample was weighed three times.

Table 53 reports the results of density measurements performed on the seven polyethylene samples. The uncertainty in the mass and volume measurements is reported as the standard deviation of the three mass measurements and 10 volume measurements. These uncertainties are then propagated in quadrature to determine the standard deviation of the calculated density.

Table 53: Polyethylene part density measurements.

Part ID	Mass (g)	Volume (cm^3)	Density (g/cm^3)
0-CAP-3	39.92816 ± 0.00003	41.1483 ± 0.0047	0.9703 ± 0.0001
3/32-CAP-3	48.90154 ± 0.00004	50.4268 ± 0.0033	0.9698 ± 0.0001
1-RING-6	44.30622 ± 0.00001	45.6667 ± 0.0063	0.9702 ± 0.0001
1/8-MOD-38	46.37212 ± 0.00007	48.1521 ± 0.0047	0.9630 ± 0.0001
1/4-MOD-36	58.59803 ± 0.00001	61.2725 ± 0.0043	0.9564 ± 0.0001
1/2-MOD-32	57.58423 ± 0.00007	60.1526 ± 0.0022	0.9573 ± 0.0000
1.5-MOD-12	42.35975 ± 0.00002	44.2152 ± 0.0059	0.9580 ± 0.0001

1.3.3.2 Polyethylene Impurity Analysis

Elemental analysis by Inductively Coupled Plasma Mass Spectrometry (ICP-MS) was performed on a 246.97 µg sample of the polyethylene. This process involved adding the sample to a digestion pressure vessel with 10 mL of 6M nitric acid (HNO_3) and then digesting it in a MARS6 Microwave Digestion System (Model 910900) following the CEM "Polyethylene" procedure in the semi-quantitative, MS/MS mode. The measured elemental impurities are reported in Table 54. The selection criteria required >5000 counts per second, elements included in the analysis were as follows: Mg, V, Mn, Ni, Cu, Zn, Ga, Zr, Mo, Sn, La, and Pb.

Table 54: Polyethylene impurity analysis results. Elements not meeting the selection criteria are not reported.

Elemental Impurity	Unit	Average	Standard Deviation
Na	$\mu g\,g^{-1}$	14.38	1.82
Al	$\mu g\,g^{-1}$	23.92	1.74
Si	$mg\,g^{-1}$	1.17	0.06
Cr	$ng\,g^{-1}$	921.35	7.08

1.3.4 Aluminum

All aluminum parts in the experimental configuration are Aluminum Alloy 6061 (Al-6061). Table 55 presents handbook data for Al-6061[5].

Table 55: Elemental composition limits for Aluminum Alloy 6061.

Element	Wt.%
Al[(a)]	95.8 - 98.6
Mg	0.8 - 1.2
Si	0.4 - 0.8
Cu	0.15 - 0.4
Cr	0.04 - 0.35

[(a)] Aluminum content reported is calculated as the remainder.

Element	Wt.%
Fe	Max 0.7
Zn	Max 0.25
Mn	Max 0.15
Ti	Max 0.15
Other, each	Max 0.05
Other, total	Max 0.15

1.3.5 Comet General Purpose Critical Assembly Machine

The additional parts on Comet, described in Section 1.2.2, used in the TEX-HEU and TEX-Hf experiments were weighed and reported in [2]. These parts include the membrane, the experiment platform, and the lower adapter. The weights are reported in Table 56 and were measured during the TEX-HEU experiment using a Mettler Toledo SB16001 High Capacity Precision Balance under the NCERC Calibration Program (Cal No. 012708). The calibration for this balance was certified on May 2, 2019, and was valid through May 2, 2020. These measurements were taken on February 24, 2020. The manufacturer of the SB16001 reports a maximum capacity of 16,100 grams, precision of 0.1 grams, and linearity of 0.3 grams. All parts are Al-6061.

Table 56: Mass measurements of the additional parts on Comet.

Part Type		Mass (g)
Membrane		2396.1
Experiment Platform	Interface Plate	11242.5
	Standoffs	633.8
		634.4
		634.0
		635.0
Lower Adpater	Adapter Plate	5014.7
	Adapter Extension	8365.3

[5] *ASTM B209M-14, Standard Specification for Aluminum and Aluminum-Alloy Sheet and Plate (Metric).* West Conshohocken, PA: ASTM International. DOI: 10.1520/b0209m-14.

1.4 Temperature Data

The temperature of each experimental configuration was measured by placing two resistance temperature detectors (RTDs) on the upper half of the experiment. Figure 3 shows the RTDs that were placed on top of the polyethylene reflector (RTD #1) and the aluminum membrane (RTD #2), which was in direct contact with an HEU plate. These RTDs were only put in place during the approach to critical and the initial critical configuration, to ensure no measurable change in temperature. They were removed during the reassembly of the experimental configuration prior to the reactivity measurement for the benchmark configuration. In addition to the RTDs on the upper half of the experiment, there was one RTD placed on the Comet support structure (RTD #3) and one RTD measuring the ambient air temperature (RTD #5).

Table 57 reports the temperature measurements taken during the benchmark period measurements, including the Comet structure (RTD #3) and ambient air (RTD #5).

Table 57: Temperature measurements of the experimental configurations.

Case	Temperature (°C)	
	Comet (RTD #3)	Ambient (RTD #5)
1	16.0	13.3
2	16.6	14.2
3	18.3	16.8
4	16.4	14.1
5	16.7	14.0
6	15.5	13.4
7	16.0	13.6

1.5 Supplemental Experimental Measurements

No additional experimental measurements were performed.

2.0 EVALUATION OF EXPERIMENTAL DATA

Each configuration was evaluated using MCNP® 6.2 with ENDF/B-VIII.0 neutron cross section libraries[6,7], using the re-release of the NJOY2016 processed thermal scattering law library[8]. The calculations are typically run with 1,000 generations of 500,000 particles per generation, skipping the first 50 generations, resulting in a total of 475 million active histories and a typical statistical uncertainty of ±0.00003 to ±0.00004 (3 pcm to 4 pcm) in k_{eff}. Therefore, the threshold for negligible is defined to be less than or equal to 0.00004 (4 pcm) in k_{eff}, which represents the propagated uncertainty in Δk_{eff} given a statistical uncertainty of ±0.00003.

For a given parameter i with a mean value $x_{0,i}$ and a perturbation δx_i, the resulting effect in k_{eff} is calculated using

$$\Delta k_{\text{eff},i} = \frac{k_{\text{eff}}(x_{0,i} + \delta x_i) - k_{\text{eff}}(x_{0,i} - \delta x_i)}{2} \tag{2}$$

The effect of the perturbation in k_{eff} for parameter i is symmetric unless otherwise stated. The standard uncertainty in k_{eff}, $u_{k,i}$, is then calculated by scaling the evaluated uncertainty in parameter i, u_i, using the sensitivity in k_{eff} to the perturbation δx_i from Eq. 2, defined as

$$u_{k,i} = u_i \left(\frac{\Delta k_{\text{eff},i}}{\delta x_i} \right) \tag{3}$$

When the sensitivity in k_{eff} to parameter i, as defined in Eq. 2, can be assumed to be independent for multiple perturbations δx_i, Eq. 3 may be represented as

$$u_{k,i} = u_i \sqrt{N} \left(\frac{\Delta k_{\text{eff},i}}{\Delta x_i} \right) \tag{4}$$

where $u_i\sqrt{N}$ is the resulting sum in quadrature of N independent uncertainties in parameter i, u_i, and Δx_i is the sum of the individual perturbations δx_i. This form is useful when evaluating the uncertainty in a parameter i involving multiple parts of a similar type, allowing N perturbations to be performed with a single calculation. This approach is used for components of the mass uncertainty in Section 2.2, dimensional uncertainty in Section 2.3, and material uncertainty in Section 2.4.

[6] Christopher John Werner et al. *MCNP User's Manual Code Version 6.2*. LA-UR-17-29981. Los Alamos National Laboratory, 2017.

[7] J. L. Conlin et al. *Release of ENDF/B-VIII.0-Based ACE Data Files*. LA-UR-18-24034. Los Alamos National Laboratory, 2018. DOI: 10.2172/1438139.

[8] D. K. Parsons and C. A. Toccoli. *Re-Release of the ENDF/B VIII.0 S(α,β) Data Processed by NJOY2016*. LA-UR-20-24456. Los Alamos National Laboratory, 2020. DOI: 10.2172/1634930.

2.1 Reactor Period

Reactor period measurements of the experimental configurations are described in Section 1.2.8. As noted in the description of the reactor period measurements, the four ^{3}He proportional counters (SU) typically saturated prior to the end of the experimental measurements, as shown in Fig. 16 of Section 1.2.8. Therefore, only the data from the compensated ion chambers (LC) is considered for the benchmark reactor period.

The measurements reported in Table 22 of Section 1.2.8 are based on preliminary fits of the neutron count rate data performed during the experiment and documented in the Comet logbook. Table 58 reports the final fits of the neutron count rate data following the conclusion of the experiment. The uncertainty in the fits are negligible for all measurements. The LC_{avg} is the average and standard deviation of the three LC detectors and represents the evaluated benchmark reactor periods.

Table 58: Measured reactor period based on exponential fitting of the neutron count rate data.

Case	Reactor Period (s)			
	LC_1	LC_2	LC_3	LC_{avg}
1	58.7	58.6	58.6	58.6 ± 0.1
2	63.4	63.6	63.1	63.4 ± 0.2
3	25.0	24.7	24.9	24.9 ± 0.1
4	122.6	123.2	122.6	122.8 ± 0.4
5	84.3	84.5	83.6	84.2 ± 0.5
6	50.0	49.9	49.7	49.8 ± 0.1
7	71.6	71.6	71.2	71.5 ± 0.2
1[(a)]	71.0	71.7	70.8	71.2 ± 0.5
3[(a)]	25.5	24.9	25.1	25.1 ± 0.3
5[(a)]	75.3	75.1	74.4	74.9 ± 0.5
6[(a)]	50.3	50.4	49.9	50.2 ± 0.2

[(a)] Reproducibility measurement.

The measured reactor period is used to estimate the excess reactivity of the experimental configuration using the following form of the Inhour equation

$$\rho(T) = \frac{\Lambda}{T\beta_{\text{eff}}} + \sum_{i=1}^{6} \frac{a_i}{(1+\lambda_i T)} \tag{5}$$

where $\rho(T)$ is the excess reactivity, as a function of the measured reactor period T, Λ is the mean generation time, and a_i and λ_i are the abundance ($\beta_i/\beta_{\text{eff}}$) and decay constant of the i^{th} delayed neutron precursor group, respectively.

The ENDF/B-VIII.0 six-group delayed neutron abundances and decay constants[9] for ^{235}U were used and are reproduced in Table 59. The ENDF-6 Delayed Neutron Data format does not store values for the uncertainties in the parameters. Therefore, the uncertainties in the abundances and decay constants are based on the six-

[9]ENDF-6 Formats Manual, File 1, Delayed Neutron Data (MT=455). DOI: 10.2172/1425114

group parameters for ^{235}U as recommended by Tuttle[10]. These delayed neutron abundances, decay constants, and uncertainties are similar to, but not the same as, the six-group parameters as reported by Keepin for fast ^{235}U fission[11].

Table 59: ENDF/B-VIII.0 six-group delayed neutron abundances and decay constants for ^{235}U.

Group	**Abundance, a_i**	**Decay Constant, λ_i (s^{-1})**
1	0.036 ± 0.004	0.0133 ± 0.0003
2	0.236 ± 0.007	0.0309 ± 0.0012
3	0.179 ± 0.024	0.1134 ± 0.0040
4	0.327 ± 0.010	0.2925 ± 0.0120
5	0.170 ± 0.012	0.8575 ± 0.1200
6	0.051 ± 0.004	2.7297 ± 0.5500

The delayed neutron fraction, β_{eff}, and the mean generation time, Λ, are system-dependent. Furthermore, no measurements were performed to infer these quantities experimentally. Therefore, β_{eff} and Λ must be based on calculation. To do so, the iterated fission probability method, as implemented in the KOPTS card of MCNP® 6.2, was used. The results of these calculations using the benchmark models are reported in Table 60. The uncertainties in these calculated parameters are based on the Monte Carlo statistical uncertainty of the calculation, which are less than ± 0.3 % for all calculations.

Table 60: Delayed neutron fraction and mean generation time (based on calculations using MCNP® 6.2 with ENDF/B-VIII.0).

Case	**Delayed Neutron Fraction, β_{eff}**	**Mean Generation Time, Λ (s)**
1	0.00674 ± 0.00002	8.619E−7 ± 1.627E-9
2	0.00719 ± 0.00002	1.008E−6 ± 1.280E-9
3	0.00725 ± 0.00002	1.466E−6 ± 1.230E-9
4	0.00732 ± 0.00002	3.296E−6 ± 1.440E-9
5	0.00707 ± 0.00002	2.327E−5 ± 5.940E-9
6	0.00717 ± 0.00002	1.195E−6 ± 1.210E-9
7	0.00656 ± 0.00002	1.751E−7 ± 5.671E-10

Table 61 reports the results of the experimental configurations. The excess reactivity is calculated using Eq. 5 with the LC_{avg} period. The uncertainty in the excess reactivity is propagated from the delayed neutron parameters (Table 59), calculated β_{eff} and Λ (Table 60), and standard deviation of LC_{avg} (Table 61). Finally, the following relationship is used to determine the k_{eff} of the experimental configurations

$$\rho(\$) = \frac{k_{\text{eff}} - 1}{k_{\text{eff}}\ \beta_{\text{eff}}} \tag{6}$$

[10] R. J. Tuttle. "Delayed-Neutron Data for Reactor-Physics Analysis". *Nuclear Science and Engineering* 56.1 (1975), pp. 37–71. DOI: 10.13182/NSE75-A26620.

[11] G. R. Keepin. *Physics of Nuclear Kinetics*. Reading, Massachusetts: Wesley Publishing Company, 1956.

where $\rho(\$)$ is the excess reactivity in dollars and β_{eff} is the delayed neutron fraction (Table 60).

Table 61: Measured reactor period, excess reactivity, and k_{eff} for the experimental configurations.

Case	Reactor Period (s)[(a)]	Excess Reactivity ($)	Experimental k_{eff}
1	58.6 ± 0.1	0.144 ± 0.006	1.00101 ± 0.00004
2	63.4 ± 0.2	0.141 ± 0.006	1.00102 ± 0.00005
3	24.9 ± 0.1	0.255 ± 0.011	1.00185 ± 0.00008
4	122.8 ± 0.4	0.085 ± 0.005	1.00063 ± 0.00004
5	84.2 ± 0.5	0.115 ± 0.007	1.00081 ± 0.00006
6	49.8 ± 0.1	0.167 ± 0.007	1.00120 ± 0.00005
7	71.5 ± 0.2	0.130 ± 0.006	1.00085 ± 0.00004

[(a)] Based on LC_{avg} reported in Table 61.

In addition to the reactor period measurements of the seven experimental configurations documented in this evaluation, four additional period measurements were performed to characterize the reproducibility of the experimental configurations. These reproducibility measurements were performed for the Case 1, 3, 5, and 6 experimental configurations by completely disassembling, then reassembling and remeasuring the reactor period.

Table 62 reports the measured results of the reproducibility measurements. Only Case 1 had a statistically significant difference in the calculated excess reactivity of the reproducibility measurements outside one sigma. Based on the majority of the reproducibility measurements having a statistically insignificant change in reactivity, the reproducibility uncertainty in the experimental measurements is judged to be negligible. Therefore, the k_{eff} in Table 61 represents the experimental k_{eff}, including the uncertainty in the period measurement.

Table 62: Measured reactor period, excess reactivity, and k_{eff} for the reproducibility measurements. No reproducibility measurements were performed for Cases 2, 4, or 7.

Case	Reactor Period (s)[(a)]	Excess Reactivity ($)	Experimental k_{eff}
1	71.2 ± 0.5	0.130 ± 0.009	-0.014 ± 0.010
3	25.1 ± 0.3	0.254 ± 0.016	-0.001 ± 0.019
5	74.9 ± 0.5	0.125 ± 0.008	0.010 ± 0.011
6	50.2 ± 0.2	0.166 ± 0.008	-0.001 ± 0.010

[(a)] Based on LC_{avg} reported in Table 61.

2.2 Mass Uncertainty

All mass uncertainties are evaluated by perturbing the mass at a constant volume, requiring the part density to be adjusted in order to conserve mass. Where individual part measurements are performed, the evaluated uncertainty is typically based on the distribution of the individual part measurements within a given part type. Unless noted otherwise, this evaluated uncertainty represents the standard deviation,

$$\sigma = \sqrt{\sum_{i=1}^{N} (x_i - \bar{x})^2} \tag{7}$$

where $\bar{x}$ is the average mass of the part type and σ is the resulting uncertainty for the part type, assuming N parts of that part type, each having a measured mass x_i. This assumes the mass measurements within a given part type are independent, which is valid given that each part is measured individually. While the same instrument is typically used to measure a given set of parts, the random uncertainty component associated with that instrument is assumed to be significantly less than the uncertainty in the distribution of the part masses and can therefore be ignored.

As described in Section 2.0, the perturbations related to mass uncertainties are performed by collectively perturbing all parts of a given part type at once, unless noted otherwise. This allows Eq. 4 to be used in determining the standard uncertainty in k_{eff}.

2.2.1 Highly Enriched Uranium Mass

Mass measurements of the HEU plates are reported in Table 5 of Section 1.2.3, including measurements from 2022 (this experiment), 2020 [2], and 2005. The measurements from 2022 and 2020 were performed using a balance with a reported linearity of ± 0.3 g, representing the uncertainty in the measurement.

Table 63 compares the differences in the measured HEU plate masses from the 2022 and 2020 measurements, using the 2005 measurements for plates that were not measured in 2020. The measurements have an average difference of -1.2 ± 1.7 g, with almost all plates decreasing in mass. This decrease is likely due to oxidization of the bare HEU metal over time. Based on this comparison, the evaluated uncertainty in HEU plate mass is ± 1.7 g. This uncertainty is significantly larger than the measurement uncertainty of ± 0.3 g.

Table 63: Difference in the HEU plate mass measurements.

Part Type	Part ID	Difference (g)
6/0-HEU	Q2-16[a]	-2.2
15/0-HEU	11150	-5.6
	11149	-1.4
	11147	-4.9
	11019	-0.8
	11017	-3.8
15/2.5-HEU	10491	-0.8
	10489	-0.1
	10487	0.5
	10475	-1.5
	10470	-0.4
	10467	-0.2
	10464	-0.1
15/6-HEU	11018	-0.3
	10935[a]	-1.0
	10933[a]	-2.5
	10932[a]	-3.6
	10477	-0.3
	10457	-0.2
15/10-HEU	10485[a]	-1.2
	10481[a]	0.7
	10479	-0.1
	10473[a]	-0.4
	10472	0.7
	10463	0.0
	10458[a]	-0.4
Average Difference (g)		**−1.2 ± 1.7**

[a] Compared to the mass measurement performed in 2005.

Table 64 summarizes the HEU plate mass uncertainty calculation parameters and sensitivity in k_{eff}. The total HEU mass is the sum of all HEU plates in the experimental configurations. The calculations vary the HEU mass by collectively perturbing the mass of all HEU plates in the experimental configurations by ±6.0 g. Therefore, the standard uncertainty in k_{eff} is calculated using Eq. 4 where N is the number of HEU plates in the experimental configuration and u_i is the evaluated uncertainty in the HEU plate mass of ±1.7 g. Table 64 is reproduced alongside the other evaluated uncertainties in Section 2.6.

Table 64: Summary of sensitivity in k_{eff} to uncertainties in the HEU plate mass.

Case	Number of Plates	Total HEU Mass (g)	Parameter Variation in Calculation	Calculated Effect in k_{eff}	Standard Uncertainty	Standard Uncertainty in k_{eff}
1	26	135407.1	$\pm 6.0 \times 26$	±0.00134	$\pm 1.7\sqrt{26}$	±0.00007
2	17	99330.7	$\pm 6.0 \times 17$	±0.00093	$\pm 1.7\sqrt{17}$	±0.00006
3	14	82823.0	$\pm 6.0 \times 14$	±0.00078	$\pm 1.7\sqrt{14}$	±0.00006
4	10	63890.9	$\pm 6.0 \times 10$	±0.00054	$\pm 1.7\sqrt{10}$	±0.00005
5	12	70336.1	$\pm 6.0 \times 12$	±0.00033	$\pm 1.7\sqrt{12}$	Negligible
6	15	88396.9	$\pm 6.0 \times 15$	±0.00075	$\pm 1.7\sqrt{15}$	±0.00005
7	23	124643.9	$\pm 6.0 \times 23$	±0.00137	$\pm 1.7\sqrt{23}$	±0.00008

2.2.2 Hafnium Plate Mass

Mass measurements of the hafnium plates are reported in Table 7 of Section 1.2.4. These measurements were reported by the manufacturer to the nearest 0.1 g. Therefore, the evaluated uncertainty in the hafnium plate mass is ± 0.1 g per plate. Table 65 summarizes the hafnium plate mass measurements, reporting the average and standard deviation of the measurements.

Table 65: Average hafnium plate mass.

Part Type	N	Mass (g)
HF	26	1569.2 ± 14.4

Table 66 summarizes the hafnium plate mass uncertainty calculation parameters and sensitivity in k_{eff}. The total hafnium mass is the sum of all hafnium plates in the experimental configurations. The calculations vary the hafnium mass by collectively perturbing the mass of all hafnium plates in the experimental configurations by ± 14.4 g. Therefore, the standard uncertainty in k_{eff} is calculated using Eq. 4 where N is the number of hafnium plates in the experimental configuration and u_i is the evaluated uncertainty in the hafnium plate mass of ± 0.1 g. Table 66 is reproduced alongside the other evaluated uncertainties in Section 2.6.

Table 66: Summary of sensitivity in k_{eff} to uncertainties for the hafnium plate mass.

Case	Number of Plates	Total Hafnium Mass (g)	Parameter Variation in Calculation	Calculated Effect in k_{eff}	Standard Uncertainty	Standard Uncertainty in k_{eff}
1	24	37675.9	$\pm 14.4 \times 24$	± 0.00007	$\pm 0.1\sqrt{24}$	Negligible
2	15	23608.2	$\pm 14.4 \times 15$	± 0.00060	$\pm 0.1\sqrt{15}$	Negligible
3	12	18929.2	$\pm 14.4 \times 12$	± 0.00116	$\pm 0.1\sqrt{12}$	Negligible
4	9	14214.7	$\pm 14.4 \times 9$	± 0.00193	$\pm 0.1\sqrt{9}$	Negligible
5	10	15799.5	$\pm 14.4 \times 10$	± 0.00282	$\pm 0.1\sqrt{10}$	Negligible
6	13	20484.2	$\pm 14.4 \times 13$	± 0.00113	$\pm 0.1\sqrt{13}$	Negligible
7	24	37675.9	$\pm 14.4 \times 24$	± 0.00068	$\pm 0.1\sqrt{24}$	Negligible

2.2.3 Polyethylene Moderator Mass

Mass measurements of the polyethylene moderator plates are reported in Tables 13, 10, 11, and 12. These measurements were performed using a balance with a precision of 0.1 g. Table 67 summarizes the polyethylene moderator plate mass measurements, reporting the average and standard deviation of the masses by part type. The uncertainties are represented as the standard deviation of the mass measurements from parts of the same type.

Table 67: Average polyethylene moderator plate mass by part type.

Part Type	N	Mass (g)
1/4-MOD	36	688.4 ± 0.7
1/2-MOD	32	1380.6 ± 3.3
1.5-MOD	12	4152.5 ± 17.9

Figure 31 shows a plot of the polyethylene moderator plate mass measurements by part type. There is a clear grouping in the 1/8-MOD parts between 1/8-MOD-{1-18} and 1/8-MOD-{19-39}. This grouping in likely due to the parts being produced from different sheets of stock material. Table 68 reports the average and standard deviation of these two 1/8-MOD part groups which represents the true spread in mass of the 1/8-MOD parts. While there may also be grouping in the 1/4-MOD and 1/2-MOD parts, neither is as relevant or clear as the 1/8-MOD grouping.

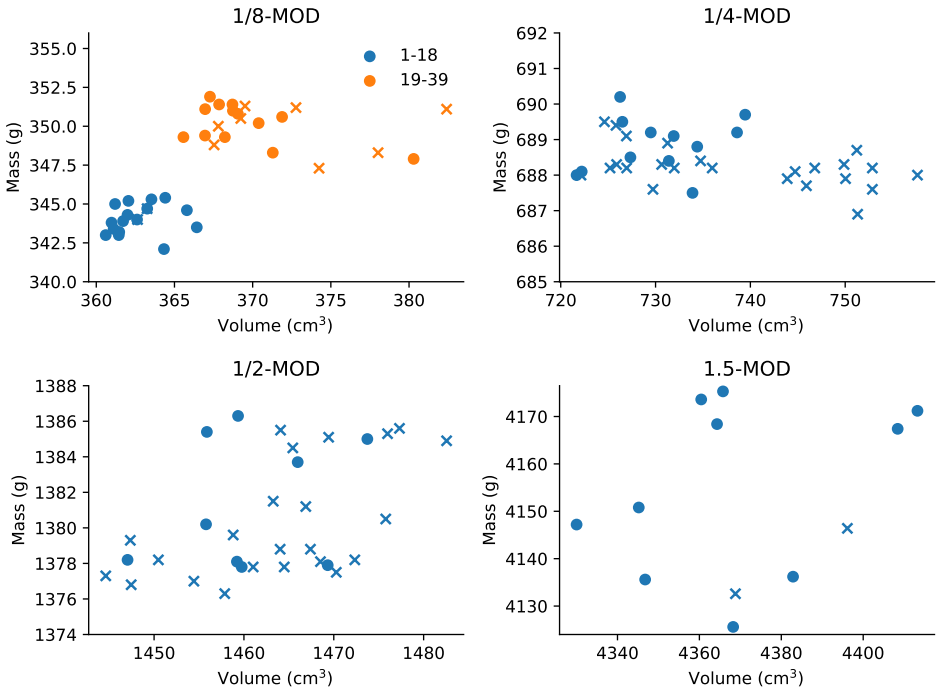

Figure 31: Polyethylene moderator plate masses grouped by part type. The y-axes are chosen to be $\pm 0.5\%$ of the average (expect for 1/8-MOD), to better visualize the spread across parts of different types. The x markers show the parts that are not used in the experimental configurations.

Table 68: Average polyethylene moderator plate mass of the 1/8-MOD groupings.

Part ID	N	Mass (g)
1/8-MOD-{1-18}	18	344.1 ± 0.9
1/8-MOD-{19-38}	21	350.1 ± 1.3

These two groups in the 1/8-MOD parts were discovered during experiment design and were incorporated into the experiment plan in order to prevent non-uniformity in the polyethylene moderator plate mass distribution for Cases 2 and 6. In Case 2, only the 1/8-MOD-{1-15} parts were used. In Case 6, the 1/8-MOD-{1-13} and 1/8-MOD-{19-31} parts were used and stacked such that one part from each group was used in each unit as shown in Figure 28 (e.g., 1/8-MOD-1 with 1/8-MOD-19, 1/8-MOD-2 with 1/8-MOD-20, and so on).

The evaluated uncertainties in the polyethylene moderator plate types are: ± 0.9 g for 1/8-MOD-{1-18}; ± 1.3 g for 1/8-MOD-{19-38}; ± 0.7 g for 1/4-MOD; ± 3.3 g for 1/2-MOD; and ± 17.9 g for 1.5-MOD. Table 69 summarizes the polyethylene moderator plate mass uncertainty calculation parameters and sensitivity in k_{eff}. The total moderator mass is the sum of all polyethylene moderator plates in the experimental configurations. The calculations vary the moderator mass by collectively perturbing the mass of all polyethylene moderator plates in the experimental configurations by their respective evaluated uncertainties. Therefore, the standard uncertainty in k_{eff} is calculated using Eq. 4 where N is the number of polyethylene moderator plates in the experimental configuration and u_i is the evaluated uncertainty for the polyethylene moderator plate type used in the experimental configuration. Table 69 is reproduced alongside the other evaluated uncertainties in Section 2.6.

Table 69: Summary of sensitivity in k_{eff} to uncertainties for the polyethylene moderator plate mass.

Case	Number of Plates	Total Moderator Mass (g)	Parameter Variation in Calculation	Calculated Effect in k_{eff}	Standard Uncertainty	Standard Uncertainty in k_{eff}
1	No polyethylene moderator plates.					-
2	15	5160.6	$\pm 0.9 \times 15$	± 0.00075	$\pm 0.9\sqrt{15}$	± 0.00019
3	12	8266.2	$\pm 0.7 \times 12$	± 0.00033	$\pm 0.7\sqrt{12}$	± 0.00010
4	9	12432.6	$\pm 3.3 \times 9$	± 0.00115	$\pm 3.3\sqrt{9}$	± 0.00038
5	10	41551.3	$\pm 17.9 \times 10$	± 0.00030	$\pm 17.9\sqrt{10}$	± 0.00009
6	26	9022.5	$\pm 1.3 \times 26$	± 0.00117	$\pm 1.3\sqrt{26}$	± 0.00023
7	No polyethylene moderator plates.					-

2.2.4 Polyethylene Reflector Mass

Figure 32 shows a diagram of the polyethylene reflector components. The top reflector consists of the REF and MOD plates. The upper and lower reflector rings consist of the interlocking RING and CAP parts. The base of the upper reflector ring is the BOTCAP part. The base of the lower reflector ring is the bottom reflector, which is the BOTREF-1 plate for all experimental configurations.

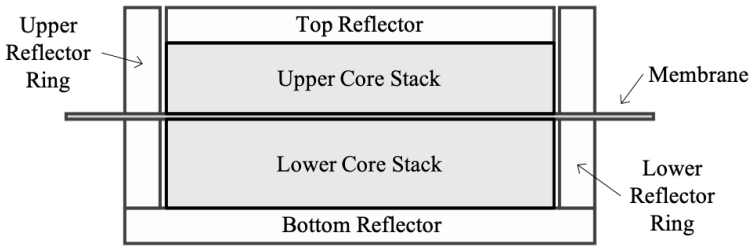

Figure 32: Diagram of the reflector components surrounding the upper and lower core stacks.

Mass measurements of the polyethylene reflector parts are report in Table 14 (REF), Table 15 (RING), Table 16 (CAP and BOTCAP), Table 17 (CAP), and Table 18 (BOTREF). These measurements were performed using a balance with a precision of 0.1 g. Table 70 summarizes the polyethylene reflector part mass measurements, reporting the average and standard deviation of the masses by part type. The uncertainties are represented as the standard deviation of the mass measurements from parts of the same type.

Table 70: Average polyethylene reflector part mass by part type (s).

Part Type	N	Mass (g)
1/32-REF	2	85.5 ± 0.6
1/16-REF	2	182.7 ± 0.4
1-REF	2	2767.1 ± 0.2
1/4-RING	4	199.0 ± 0.3
1/2-RING	4	393.7 ± 0.7
1-RING	6	805.5 ± 0.5
3-RING	6	2386.3 ± 2.0
0-BOTCAP	2	48.1 ± 0.1
0-CAP	3	50.8 ± 0.1
1/32-CAP	3	76.8 ± 0.1
1/16-CAP	3	101.2 ± 0.3
1/8-CAP	3	149.0 ± 0.1
5/32-CAP	3	173.4 ± 0.5
3/16-CAP[(a)]	3	195.4 ± 2.4
7/32-CAP	3	225.4 ± 0.2
BOTREF	2	3544.1 ± 1.2

[(a)] Large spread due to the 3/16-CAP-1 part having a higher mass than the others.

The uncertainties in the reflector part mass measurements are typically less than ± 0.7 g, except for the higher mass parts (3-RING, BOTREF). The exception to this is the 3/16-CAP part type, which has a spread of ± 2.4 g.

This spread is due to the 3/16-CAP-1 part, which is about 4.0 g higher than the other two 3/16-CAP parts. However, this higher mass is consistent with its dimensional measurements which are slightly larger in the Step Height than the other two parts. Furthermore, the 3/16-CAP-1 part is the only part of that type used in the experimental configurations, meaning the uncertainty in the 3/16-CAP-1 part is better represented by the ± 0.1 g precision of the balance used to weight it.

Based on these, the evaluated uncertainties in the reflector part mass components are: ± 2.0 g for the 3-RING and BOTREF parts and ± 0.7 g for all other parts. These evaluated uncertainties are significantly larger than the measurement precision of ± 0.1 g. The top reflectors also consist of the 1/8-MOD, 1/4-MOD, and 1/2-MOD plates, with mass uncertainties evaluated in Section 2.2.3. Table 71 reports the total reflector masses for the experimental configurations.

Table 71: Total masses of the reflector components.

Case	Reflector Component (g)				Total Mass (g)
	Top Plate	Upper Ring	Lower Ring	Bottom Plate[(a)]	
1	3194.0 ± 1.2	2606.6 ± 2.2	1688.4 ± 1.2	3543.2 ± 2.0	11032.2 ± 3.5
2	2411.9 ± 1.2	2483.4 ± 1.2	1911.8 ± 1.4	3543.2 ± 2.0	10350.3 ± 3.0
3	2677.7 ± 1.6	2856.8 ± 2.3	2035.1 ± 1.4	3543.2 ± 2.0	11112.8 ± 3.7
4	2766.9 ± 0.7	3051.6 ± 2.3	2684.6 ± 2.2	3543.2 ± 2.0	12046.3 ± 3.9
5	4144.8 ± 1.0	8000.0 ± 3.7	6684.7 ± 2.5	3543.2 ± 2.0	22372.7 ± 5.0
6	2680.9 ± 1.6	2512.0 ± 2.2	2684.9 ± 2.2	3543.2 ± 2.0	11421.0 ± 4.1
7	3292.3 ± 1.2	2353.6 ± 1.7	1661.3 ± 1.2	3543.2 ± 2.0	10850.5 ± 3.1

[(a)] All cases use the BOTREF-1 part as the bottom reflector plate.

Table 72 summarizes the polyethylene reflector mass uncertainty calculation parameters and sensitivity in k_{eff}. The total reflector mass is the sum of all reflector parts, as reported in Table 71. The calculations vary the reflector mass by collectively perturbing the mass of all reflector part in the experimental configurations by ± 0.5 %. This large perturbation was chosen to improve the statistics in Δk_{eff} used in Eq. 3. Therefore, the standard uncertainty in k_{eff} is calculated using Eq. 4 where N is the number of reflector parts in the experimental configuration and u_i is the evaluated uncertainty in the total polyethylene reflector mass reported in Table 71. Table 72 is reproduced alongside the other evaluated uncertainties in Section 2.6.

Table 72: Summary of sensitivity in k_{eff} to uncertainties for the polyethylene reflector mass.

Case	Number of Parts	Total Reflector Mass (g)	Parameter Variation in Calculation	Calculated Effect in k_{eff}	Standard Uncertainty	Standard Uncertainty in k_{eff}
1	10	11032.2	± 0.5 %	± 0.00115	$\pm 3.5\sqrt{10}$	± 0.00007
2	11	10350.3		± 0.00122	$\pm 3.0\sqrt{11}$	± 0.00007
3	14	11112.8		± 0.00113	$\pm 3.7\sqrt{14}$	± 0.00008
4	9	12046.3		± 0.00089	$\pm 3.9\sqrt{9}$	± 0.00006
5	16	22372.7		± 0.00033	$\pm 5.0\sqrt{16}$	Negligible
6	12	11421.0		± 0.00096	$\pm 4.1\sqrt{12}$	± 0.00007
7	13	10850.5		± 0.00052	$\pm 3.1\sqrt{13}$	Negligible

2.2.5 Aluminum Insert Mass

Mass measurements of the aluminum inserts are reported in Table 20. These measurements were performed using a balance with a precision of 0.1 g. Table 73 summarizes the aluminum insert mass measurements by part type, reporting the average and standard deviation of the measurements.

Table 73: Average aluminum insert mass by part type.

Part Type	N	Mass (g)
2.5-DISK	10	24.8 ± 0.1
6-DISK	6	150.4 ± 0.7
10-DISK	10	425.6 ± 1.4

Table 74 summarizes the aluminum insert mass uncertainty calculation parameters and sensitivity in k_{eff}. The total insert mass is the sum of all aluminum inserts in the experimental configurations. The calculations vary the insert mass by collectively perturbing the mass of all aluminum inserts in the experimental configurations by ± 3.0 g. Therefore, the standard uncertainty in k_{eff} is calculated using Eq. 4 where N is the number of aluminum inserts in the experimental configuration and u_i is the evaluated uncertainty in the aluminum insert mass of ± 0.5 g. Table 66 is reproduced alongside the other evaluated uncertainties in Section 2.6.

Table 74: Summary of sensitivity in k_{eff} to uncertainties for the aluminum insert mass.

Case	Number of Inserts	Total Insert Mass (g)	Parameter Variation in Calculation	Calculated Effect in k_{eff}	Standard Uncertainty	Standard Uncertainty in k_{eff}
1	19	3907.1	$\pm 3.0 \times 19$	± 0.00036	$\pm 0.5\sqrt{19}$	Negligible
2	10	624.5	$\pm 3.0 \times 10$	± 0.00010	$\pm 0.5\sqrt{10}$	Negligible
3	7	173.8	$\pm 3.0 \times 7$	± 0.00003	$\pm 0.5\sqrt{7}$	Negligible
4	5	123.9	$\pm 3.0 \times 5$	± 0.00001	$\pm 0.5\sqrt{5}$	Negligible
5	5	123.9	$\pm 3.0 \times 5$	± 0.00005	$\pm 0.5\sqrt{5}$	Negligible
6	8	323.7	$\pm 3.0 \times 8$	± 0.00002	$\pm 0.5\sqrt{8}$	Negligible
7	16	2626.6	$\pm 3.0 \times 16$	± 0.00033	$\pm 0.5\sqrt{16}$	Negligible

2.2.6 Membrane Mass

The mass measurement of the membrane is reported in Table 56. This measurement was performed using a balance with a reported linearity of ± 0.3 g, representing the uncertainty in the measurement. Therefore, the evaluated uncertainty in the membrane mass is ± 0.3 g.

Table 75 summarizes the membrane mass uncertainty calculation parameters and sensitivity in k_{eff}. The calculations vary the membrane mass by perturbing its mass by ± 20.0 g. This large perturbation was chosen to improve the statistics in Δk_{eff} used in Eq. 3. The standard uncertainty in k_{eff} is calculated using Eq. 3 where u_i is the evaluated uncertainty in the membrane mass of ± 0.3 g. Table 75 is reproduced alongside the other evaluated uncertainties in Section 2.6.

Table 75: Summary of sensitivity in k_{eff} to uncertainties in the membrane mass.

Case	Membrane Mass (g)	Parameter Variation in Calculation	Calculated Effect in k_{eff}	Standard Uncertainty	Standard Uncertainty in k_{eff}
1	2396.1	±20.0	±0.00003	±0.3	Negligible
2			±0.00010		Negligible
3			±0.00005		Negligible
4			±0.00001		Negligible
5			±0.00006		Negligible
6			±0.00007		Negligible
7			±0.00006		Negligible

2.2.7 Structure Mass

The structure consists of the stationary platform, movable platen, and the additional parts affixed to Comet for the TEX-HEU and TEX-Hf experiments. The additional parts are described in Section 1.2.2 and include seven components: the interface plate, the adapter and extension, and four standoffs. The mass measurements of these additional parts are reported in Table 56. These measurements were performed using a balance with a linearity of ±0.3 g, representing the uncertainty in the measurement. No mass measurements are available for the stationary platform and movable platen.

Table 76 summarizes the structure mass uncertainty calculation parameters and sensitivity in k_{eff}. The calculations vary the structure mass by perturbing its mass by ±10 %. This large perturbation was chosen to improve the statistics in the Δk_{eff} used in Eq. 2. The standard uncertainty in k_{eff} is calculated using Eq. 3 where u_i is the evaluated uncertainty in the structure mass of ±0.1 %. Table 76 is reproduced alongside the other evaluated uncertainties in Section 2.6.

Table 76: Summary of sensitivity in k_{eff} to uncertainties for the structure mass.

Case	Structure Mass (g)	Parameter Variation in Calculation	Calculated Effect in k_{eff}	Standard Uncertainty	Standard Uncertainty in k_{eff}
1	27159.7[(a)] (Section 1.3.5)	±10 %	±0.00143	±0.1 %	Negligible
2			±0.00116		Negligible
3			±0.00098		Negligible
4			±0.00093		Negligible
5			±0.00017		Negligible
6			±0.00077		Negligible
7			±0.00087		Negligible

[(a)] Does not include the mass of the lower movable platen or upper stationary platform, which were not measured but are perturbed in density.

2.3 Dimensional Uncertainty

All dimensional uncertainties are evaluated by perturbing the dimensions at a constant mass, requiring the part density to be adjusted in order to conserve mass. The dimensional uncertainties are based on both measured quantities and tolerances from engineering drawings.

As described in Section 2.0, the perturbations related to dimensional uncertainties are performed by collectively perturbing all parts of a given part type at once, unless noted otherwise. This allows Eq. 4 to be used in determining the standard uncertainty in k_{eff}.

2.3.1 Highly Enriched Uranium Plate Dimensions

Due to the dependence of the core stack height on the thickness of the HEU plates, the uncertainty in the plate thickness is evaluated as part of the core stack height uncertainty in Section 2.3.5. This section only evaluates the uncertainty in the inner and outer diameters of the plates.

The nominal dimensions and tolerances of the HEU plates are reported in Table 4 of Section 1.2.3. No verification measurements could be performed on the inner and outer diameters of the HEU plates. Thickness measurements of the HEU plates are reported in Table 5 of Section 1.2.3. Table 77 summarizes the nominal HEU plate diameters and average measured thickness. The tolerance of the diameters has been converted from one-sided to symmetric by selecting the midpoint of the tolerance interval and halving it. The uncertainty in the thickness is reported as the standard deviation of all available thickness measurements, regardless of part type. Therefore, the evaluated uncertainty in the HEU plate diameters and thickness are ± 0.00635 cm and ± 0.0060 cm, respectively. The uncertainty in the diameters is assumed be uniform within the tolerance interval.

Table 77: HEU plate average thickness and nominal diameters by part type.

Part Type	N	Diameter (cm)		Thickness (cm)
		Inner	Outer	
15/0-HEU	5	-	38.0937 ± 0.0064	0.3108 ± 0.0057
15/2.5-HEU	7	6.3818 ± 0.0064		
15/6-HEU	6	15.2591 ± 0.0064		
15/10-HEU	7	25.4191 ± 0.0064		
6/0-HEU	1	-	15.2337 ± 0.0064	

Table 78 summarizes the HEU plate diameter uncertainty calculation parameters and sensitivity in k_{eff}. The calculations vary the parameter by collectively perturbing all HEU plate diameters by ± 0.02 cm. This perturbation is performed for both the inner and outer diameters at the same time but in opposite directions such that the outer diameter is increased by 0.02 cm and the inner diameter is decreased by 0.02 cm, and vice versa. Since the evaluated uncertainty in the diameters represents a uniform tolerance interval, the standard uncertainty is $\pm 0.00635/\sqrt{12}$ cm or approximately ± 0.002 cm. Therefore, the standard uncertainty in k_{eff} is calculated using Eq. 4 where N is the number of HEU plates in the experimental configuration and u_i is the evaluated uncertainty in the HEU plate diameter of ± 0.002 cm. Table 78 is reproduced alongside the other evaluated uncertainties in Section 2.6.

Table 78: Summary of sensitivity in k_{eff} to uncertainties for the HEU plate diameters.

Case	Number of Plates	Parameter Value (cm)	Parameter Variation in Calculation	Calculated Effect in k_{eff}	Standard Uncertainty	Standard Uncertainty in k_{eff}
1	26	Varies (Table 77)	$\pm 0.02(26)$	± 0.00103	$\pm 0.002\sqrt{26}$	Negligible
2	17		$\pm 0.02(17)$	± 0.00066	$\pm 0.002\sqrt{17}$	Negligible
3	14		$\pm 0.02(14)$	± 0.00057	$\pm 0.002\sqrt{14}$	Negligible
4	10		$\pm 0.02(10)$	± 0.00020	$\pm 0.002\sqrt{10}$	Negligible
5	12		$\pm 0.02(12)$	± 0.00030	$\pm 0.002\sqrt{12}$	Negligible
6	15		$\pm 0.02(15)$	± 0.00065	$\pm 0.002\sqrt{15}$	Negligible
7	23		$\pm 0.02(23)$	± 0.00175	$\pm 0.002\sqrt{23}$	Negligible

2.3.2 Hafnium Plate Dimensions

Due to the dependence of the core stack height on the thickness of the hafnium plates, the uncertainty in the plate thickness is evaluated as part of the core stack height uncertainty in Section 2.3.5. The following analysis is limited to the uncertainty in the diameter of the hafnium plates.

The nominal and measured dimensions of the hafnium plates are reported in Tables 6, 7, and 8 of Section 1.2.4. Table 79 summarizes the hafnium plate dimensional measurements, reporting the average thickness and diameter. The uncertainties are reported as the standard deviation of the measurements. The average diameter is based on the measurements reported in Table 7, performed using a caliper with a resolution of 0.0127 cm. The average thickness is based on the measurements reported in Table 8, involved ten measurements of each plate using an ultrasonic thickness gage. Therefore, the evaluated uncertainty in the hafnium plate diameter and thickness are ± 0.003 cm and ± 0.001 cm, respectively.

Table 79: Average hafnium plate dimensions.

Part Type	N	Thickness (cm)			Diameter (cm)
		Min	Max	Average	
HF	26	0.1036	0.1128	0.1064 ± 0.0010	38.0924 ± 0.0029

Table 80 summarizes the hafnium plate diameter uncertainty calculation parameters and sensitivity in k_{eff}. The calculations vary the parameter by collectively perturbing the each hafnium plate diameter by ± 0.02 cm. Therefore, the standard uncertainty in k_{eff} is calculated using Eq. 4 where N is the number of hafnium plates in the experimental configuration and u_i is the evaluated uncertainty in the hafnium plate diameter of ± 0.002 cm. Table 80 is reproduced alongside the other evaluated uncertainties in Section 2.6.

Table 80: Summary of sensitivity in k_{eff} to uncertainties in the hafnium plate diameters.

Case	Number of Plates	Parameter Value (cm)	Parameter Variation in Calculation	Calculated Effect in k_{eff}	Standard Uncertainty	Standard Uncertainty in k_{eff}
1	24	38.0924	$\pm 0.02(24)$	± 0.00039	$\pm 0.003\sqrt{24}$	Negligible
2	15		$\pm 0.02(15)$	± 0.00013	$\pm 0.003\sqrt{15}$	Negligible
3	12		$\pm 0.02(12)$	± 0.00005	$\pm 0.003\sqrt{12}$	Negligible
4	9		$\pm 0.02(9)$	± 0.00020	$\pm 0.003\sqrt{9}$	Negligible
5	10		$\pm 0.02(10)$	± 0.00044	$\pm 0.003\sqrt{10}$	Negligible
6	13		$\pm 0.02(13)$	± 0.00010	$\pm 0.003\sqrt{13}$	Negligible
7	24		$\pm 0.02(24)$	± 0.00014	$\pm 0.003\sqrt{24}$	Negligible

2.3.3 Polyethylene Plate Dimensions

Due to the dependence of the core stack height on the thickness of the polyethylene plates, the uncertainty in the plate thickness is evaluated as part of the core stack height uncertainty in Section 2.3.5. The following analysis is limited to the uncertainty in the diameter of the polyethylene plates.

The polyethylene plates include the moderator (MOD), top reflector (REF), and bottom reflector (BOTREF) part types. The nominal and measured dimensions of the MOD and REF plates are reported in Tables 9, 14, 13, 10, 11, and 12 of Section 1.2.5.1. The nominal and measured dimensions of the BOTREF plates are reported in Table 18 of Section 1.2.5.4. Table 81 summarizes the polyethylene plate dimension measurements, reporting the average thickness and diameter by part type. The diameter of the BOTREF plates in Table 81 corresponds to the outer diameter in Table 18. The uncertainties are reported as the standard deviation of the measured dimensions for each part type. These measurements were performed using a coordinate measuring machine, as described in Section 1.2.5.

Table 81: Average polyethylene moderator and reflector plate by part type.

Part Type	N	Thickness (cm)	Diameter (cm)		
			Min	Max	Average
1/8-MOD	39	0.3221 ± 0.0047	38.0655	38.0840	38.0888 ± 0.0022
1/4-MOD	36	0.6464 ± 0.0093	38.0413	38.0619	38.0642 ± 0.0030
1/2-MOD	32	1.2850 ± 0.0084	38.0556	38.0746	38.0739 ± 0.0037
1.5-MOD	12	3.8373 ± 0.0237	38.0451	38.0919	38.0826 ± 0.0168
1/32-REF	2	0.0837 ± 0.0016	38.0573	38.0576	38.0763 ± 0.0005
1/16-REF	2	0.1777 ± 0.0102	38.0566	38.0571	38.0637 ± 0.0004
1-REF	2	2.5413 ± 0.0036	38.0604	38.0644	38.0727 ± 0.0034
BOTREF	2	2.5825 ± 0.0207	43.3606	43.3616	43.3800 ± 0.0095

The evaluated uncertainty in the polyethylene plate diameter and thickness are reported in Table 82. These uncertainties are based on the standard deviations of the average part types reported in Table 81.

Table 82: Evaluated uncertainty in the polyethylene plate thickness and diameter by part type.

Part Type	Evaluated Uncertainty (cm)	
	Thickness	Diameter
1/8-MOD	±0.005	±0.005
1/4-MOD	±0.010	
1/2-MOD	±0.010	
1.5-MOD	±0.025	±0.020
1/32-REF	±0.010	±0.010
1/16-REF		
1-REF		
BOTREF	±0.020	

Table 83 summarizes the polyethylene moderator and reflector plate diameter uncertainty calculation parameters and sensitivity in k_{eff}. The calculations vary the parameter by collectively perturbing all polyethylene plate diameters by ±0.02 cm. Therefore, the standard uncertainty in k_{eff} is calculated using Eq. 4 where N is the number of polyethylene plates in the experimental configuration and u_i is the evaluated uncertainty in the polyethylene plate diameter as reported in Table 82. Table 83 is reproduced alongside the other evaluated uncertainties in Section 2.6.

Table 83: Summary of sensitivity in k_{eff} to uncertainties in the polyethylene moderator and reflector plate diameters.

Case	Number of Plates	Parameter Value (cm)	Parameter Variation in Calculation	Calculated Effect in k_{eff}	Standard Uncertainty	Standard Uncertainty in k_{eff}
1	4	Varies (Table 81)	±0.02(4)	±0.00006	$\pm 0.010\sqrt{4}$	Negligible
2	19		±0.02(19)	±0.00044	$\pm 0.005\sqrt{19}$	Negligible
3	18		±0.02(18)	±0.00060	$\pm 0.005\sqrt{18}$	Negligible
4	11		±0.02(11)	±0.00086	$\pm 0.005\sqrt{11}$	±0.00007
5	13		±0.02(13)	±0.00051	$\pm 0.020\sqrt{13}$	±0.00015
6	32		±0.02(32)	±0.00617	$\pm 0.005\sqrt{32}$	±0.00028
7	4		±0.02(4)	±0.00003	$\pm 0.010\sqrt{4}$	Negligible

2.3.4 Aluminum Insert Dimensions

Due to the dependence of the core stack height on the thickness of the aluminum inserts, the uncertainty in the insert thickness is evaluated as part of the core stack height uncertainty in Section 2.3.5. The following analysis is limited to the uncertainty in the diameter of the aluminum inserts.

The nominal and measured dimensions of the aluminum inserts are reported in Tables 19 and 20 of Section 1.2.6. Table 84 summarizes the dimensional measurements, reporting the average thickness and diameter by part type. The uncertainties are reported as the standard deviation of the measurements, which are significantly larger than the 0.00127 cm precision of the caliper used to perform the measurements. Therefore, the evaluated uncertainty in the aluminum insert diameter and thickness are ± 0.0015 cm and ± 0.005 cm, respectively, for all part types.

Table 84: Average aluminum insert dimensions by part type.

Part Type	N	Thickness (cm)	Diameter (cm)		
			Min	Max	Average
2.5-DISK	10	0.3170 ± 0.0014	6.0808	6.0858	6.0838 ± 0.0015
6-DISK	6	0.3158 ± 0.0015	14.9619	14.9695	14.9665 ± 0.0028
10-DISK	10	0.3170 ± 0.0011	25.1155	25.1295	25.1254 ± 0.0032

Table 85 summarizes the aluminum insert diameter uncertainty calculation parameters and sensitivity in k_{eff}. The calculations vary the parameter by collectively perturbing all aluminum insert diameters by ± 0.01 cm. Therefore, the standard uncertainty in k_{eff} is calculated using Eq. 4 where N is the number of aluminum inserts in the experimental configuration and u_i is the evaluated uncertainty in the aluminum insert diameter of ± 0.005 cm. Table 85 is reproduced alongside the other evaluated uncertainties in Section 2.6.

Table 85: Summary of sensitivity in k_{eff} to uncertainties in the aluminum insert diameters.

Case	Number of Inserts	Parameter Value (cm)	Parameter Variation in Calculation	Calculated Effect in k_{eff}	Standard Uncertainty	Standard Uncertainty in k_{eff}
1	19	Varies (Table 84)	$\pm 0.01(19)$	± 0.00003	$\pm 0.005\sqrt{19}$	Negligible
2	10		$\pm 0.01(10)$	± 0.00006	$\pm 0.005\sqrt{10}$	Negligible
3	7		$\pm 0.01(7)$	± 0.00001	$\pm 0.005\sqrt{7}$	Negligible
4	5		$\pm 0.01(5)$	± 0.00010	$\pm 0.005\sqrt{5}$	Negligible
5	5		$\pm 0.01(5)$	± 0.00009	$\pm 0.005\sqrt{5}$	Negligible
6	8		$\pm 0.01(8)$	± 0.00001	$\pm 0.005\sqrt{8}$	Negligible
7	16		$\pm 0.01(16)$	± 0.00005	$\pm 0.005\sqrt{16}$	Negligible

2.3.5 Core Stack Height

The core stack height measurements are described in Section 1.2.7. These measurements are reported for each experimental configuration in the subsections of Section 1.2.9 and summarized in Table 21 of Section 1.2.7. The measurements were performed at five specific locations for the upper and lower core stacks of each experimental configuration, shown in Figure 15 of Section 1.2.7. The uncertainty in the core stack height measurement is based on the standard deviation of these five measurements.

The lower core stack height measurement was taken relative to the lip of the adapter plate, as shown in Figure 14 of Section 1.2.7. The lip of the adapter plate is described in Section 1.2.2.2 with measurements reported in Table 3. The lip has a nominal height of 1.1938 ± 0.0254 cm, based on the engineering drawing in Figure 63 of Appendix B, and a measured height of 1.247 ± 0.062 cm, based on seven measurements perform at various locations. These two values differ by 0.0532 ± 0.0670 cm. Therefore, the lip is evaluated to have a height of 1.247 ± 0.067 cm.

Table 86 reports the measured core stack heights, including the adapter plate lip height in the lower core stack height measurements. The uncertainty in the lip height is the largest source of uncertainty in the lower core stack height measurement, making the total uncertainty in the lower core stack height much larger than the upper core stack height.

Table 86: Summary of upper and lower core stack height measurements.

Case	Core Stack Height (cm)	
	Upper	Lower[(a)]
1	8.307 ± 0.016	7.713 ± 0.069
2	7.675 ± 0.026	8.570 ± 0.077
3	9.201 ± 0.021	8.881 ± 0.069
4	9.673 ± 0.014	11.013 ± 0.069
5	25.533 ± 0.034	23.774 ± 0.073
6	8.001 ± 0.029	11.077 ± 0.072
7	7.417 ± 0.011	7.701 ± 0.074

[(a)] Includes the evaluated adapter plate lip height.

The core stacks consist of the HEU plates, hafnium plates, polyethylene moderator and reflector plates, and aluminum inserts, each of which has a measured thickness as reported in the subsections of Section 1.2. This individual part thicknesses can be used to calculate the expected core stack height for a given set of parts. Table 87 reports the calculated core stack heights and difference compared to the measured core stack heights. It should be expected that the sum of the individual parts is less than or equal to the measured core stack height, within uncertainty. If this sum of individual parts is less than the measured core stack height, accounting for the propagated statistical uncertainty in the difference, this would indicate the presence of gaps between the layers. These gaps could be introduced by parts not being completely flat. This behavior is seen for all of the lower core stack heights and some of the upper core stack height, but not always within the statistical uncertainty of the difference. However, this difference can still serve to inform the uncertainty in the core stack height.

Table 87: Comparison of the calculated and measured upper and lower core stack heights. The calculated core stack heights are based on the individual part measurements.

Case	Upper Core Stack (cm)		Lower Core Stack (cm)	
	Calculated[a]	Difference[b]	Calculated[a]	Difference[b]
1	8.331 ± 0.027	0.024 ± 0.031	7.616 ± 0.026	-0.150 ± 0.074
2	7.703 ± 0.043	0.028 ± 0.050	8.515 ± 0.032	-0.108 ± 0.083
3	9.240 ± 0.050	0.039 ± 0.054	8.907 ± 0.056	-0.027 ± 0.089
4	9.667 ± 0.033	-0.007 ± 0.036	11.064 ± 0.053	-0.002 ± 0.087
5	25.501 ± 0.077	-0.032 ± 0.084	23.755 ± 0.090	-0.072 ± 0.116
6	8.119 ± 0.054	0.118 ± 0.061	11.105 ± 0.042	-0.025 ± 0.083
7	7.475 ± 0.026	0.058 ± 0.029	7.616 ± 0.026	-0.139 ± 0.078

[a] Sum of the individual part thicknesses, with propagated uncertainty based on uncertainty in part thicknesses.
[b] (Calculated) - (Measured), refer to Table 86 for measured core stack heights.

The calculated upper core stack height varies when compared to the measured upper core stack height across the experimental configurations. There is no statistical difference between the calculated and measured upper core stack heights for Cases 1 through 5. For Cases 6 and 7, there is a statistically significant difference between the calculated and measured upper core stack heights greater than one-sigma. However, the calculated upper core stack height is greater than the measured upper core stack height. If there were gaps present, the opposite would be the case.

The calculated lower core stack heights are consistently less than the measured lower core stack heights. While this would indicate the presence of gaps, only Cases 1, 2, and 7 have a statistically significant difference with none being more than one-sigma. Additionally, this is complicated by the large uncertainty in the evaluated adapter plate lip height, which is in disagreement with its as-designed height.

Table 88 compares the calculated and measured total core stack heights, which are the sum of the upper and lower core stacks. The total core stack height is proportional to the total neutron leakage of the system which drives the large effect in k_{eff} when perturbing core stack height. This parameter is important when evaluating the upper and lower core stack height measurements.

Table 88: Comparison of the calculated and measured total core stack height.

Case	Total Core Stack (cm)		
	Measured	Calculated	Difference[a]
1	16.073 ± 0.071	15.947 ± 0.037	-0.127 ± 0.080
2	16.298 ± 0.081	16.218 ± 0.053	-0.080 ± 0.097
3	18.135 ± 0.072	18.147 ± 0.075	0.012 ± 0.104
4	20.739 ± 0.071	20.731 ± 0.062	-0.008 ± 0.094
5	49.361 ± 0.080	49.256 ± 0.119	-0.105 ± 0.143
6	19.132 ± 0.078	19.224 ± 0.068	0.092 ± 0.103
7	15.172 ± 0.075	15.091 ± 0.037	-0.081 ± 0.083

[a] (Calculated) - (Measured), refer to Table 86 for measured core stack heights.

The calculated total core stack height is only statistically significant for Case 1, but not more than one-sigma.

Therefore, the uncertainty in the upper and lower core stack heights is based on the propagated uncertainty in the difference of the calculated and measured core stack heights reported in Table 87. Since the total measured core stack height is in agreement with the total calculated core stack height, there is no justification for including gaps in the experimental configurations.

Table 89 summarizes the upper and lower core stack height uncertainty calculation parameters and sensitivity in k_{eff}. The calculations vary the parameter by perturbing the thickness[12] of each part within the stack based on the evaluated uncertainty in the part thickness as reported in Table 77 for the HEU plates, Table 79 for the hafnium plates, Table 82 for the polyethylene plates, and Table 84 for the aluminum inserts. The standard uncertainty in k_{eff} is calculated using Eq. 3 where u_i is the evaluated uncertainty in the core stack height measurements reported in Table 87. Table 89 is reproduced alongside the other evaluated uncertainties in Section 2.6.

Table 89: Summary of sensitivity in k_{eff} to uncertainties in the upper and lower core stack height.

Parameter (unit of measured)	Case	Parameter Value	Parameter Variation in Calculation	Calculated Effect in k_{eff}	Standard Uncertainty	Standard Uncertainty in k_{eff}
Upper Core Stack Height (cm)	1	8.307	±0.141	±0.00217	±0.031	±0.00048
	2	7.675	±0.213	±0.00288	±0.050	±0.00068
	3	9.201	±0.243	±0.00207	±0.054	±0.00046
	4	9.673	±0.123	±0.00153	±0.036	±0.00045
	5	25.533	±0.327	±0.00363	±0.084	±0.00093
	6	8.001	±0.273	±0.00229	±0.061	±0.00051
	7	7.417	±0.132	±0.00186	±0.029	±0.00041
Lower Core Stack Height (cm)	1	7.713	±0.128	±0.00221	±0.074	±0.00128
	2	8.570	±0.160	±0.00257	±0.083	±0.00133
	3	8.881	±0.245	±0.00381	±0.089	±0.00138
	4	11.013	±0.211	±0.00251	±0.087	±0.00103
	5	23.774	±0.361	±0.00225	±0.116	±0.00072
	6	11.077	±0.240	±0.00346	±0.083	±0.00120
	7	7.701	±0.128	±0.00191	±0.078	±0.00117

2.3.6 Polyethylene Reflector Ring Diameters

The polyethylene reflector rings includes the ring (RING) and cap (CAP, BOTCAP) part types. This dimensional uncertainty evaluates the uncertainty in the inner and outer diameters of the upper and lower reflector rings. Since the RING parts make up the majority of the upper and lower reflector rings, while the CAP parts provide only minor height adjustment, the uncertainty is the reflector ring diameter is based only on the RING parts.

The measured diameters of the polyethylene rings are reported in Table 15 of Section 1.2.5.2. Table 90 summarizes the dimensional measurements, reporting the average dimension by part type. As discussed in Section 1.2.5, these measurements were performed using a coordinate measuring machine (CMM) by LLNL's Dimensional Inspection Laboratory. The uncertainties are reported as the standard deviation of the measurements. The uncertainties in the inner and outer diameters are less than 0.003 cm for the 1/4-RING, 1/2-RING,

[12] As noted in Section 2.3, all dimensional perturbations are performed at a constant mass by adjusting density.

and 3-RING part types. The much larger uncertainty of 0.012 cm for the 1-RING parts is due to the 1-RING-2 and 1-RING-4 parts, of which 1-RING-4 part was only used in Case 7. Otherwise, the standard deviation of the diameter measurements for the 1-RING part type is 0.006 cm. Furthermore, the the 1-RING-4 part is only one of six parts in the Case 7 reflector ring. Therefore, the evaluated uncertainty in the reflector ring inner and outer diameters is ± 0.006 cm.

Table 90: Average polyethylene ring inner and outer diameters by part type.

Part ID	N	Inner Diameter (cm)			Outer Diameter (cm)		
		Min	Max	Average	Min	Max	Average
1/4-RING	4	43.3873	43.3929	38.3035 ± 0.0032	43.3873	43.3929	43.4172 ± 0.0013
1/2-RING	4	43.3756	43.3847	38.2720 ± 0.0013	43.3756	43.3847	43.3894 ± 0.0014
1-RING	6	43.3568	43.3862	38.2613 ± 0.0120	43.3568	43.3862	43.3825 ± 0.0112
3-RING	6	43.3972	43.4053	38.3299 ± 0.0017	43.3972	43.4053	43.4086 ± 0.0028

Table 91 summarizes the polyethylene reflector ring diameter uncertainty calculation parameters and sensitivity in k_{eff}. The calculations vary the parameter by collectively perturbing all polyethylene ring diameters by ± 0.02 cm. Therefore, the standard uncertainty in k_{eff} is calculated using Eq. 4 where N is the number of polyethylene ring parts in the experimental configuration and u_i is the evaluated uncertainty in the polyethylene ring diameter of ± 0.006 cm. Table 91 is reproduced alongside the other evaluated uncertainties in Section 2.6.

Table 91: Summary of sensitivity in k_{eff} to uncertainties in the reflector ring diameters.

Case	Number of Parts	Parameter Variation in Calculation	Calculated Effect in k_{eff}	Standard Uncertainty	Standard Uncertainty in k_{eff}
1	3	± 0.02	± 0.00081	± 0.006	± 0.00014
2	4	± 0.02	± 0.00047	± 0.006	± 0.00007
3	5	± 0.02	± 0.00041	± 0.006	± 0.00006
4	4	± 0.02	± 0.00046	± 0.006	± 0.00007
5	10	± 0.02	± 0.00012	± 0.006	Negligible
6	3	± 0.02	± 0.00048	± 0.006	± 0.00008
7	6	± 0.02	± 0.00059	± 0.006	± 0.00007

2.3.7 Polyethylene Reflector Ring Height

The polyethylene reflector rings includes the ring (RING) and cap (CAP, BOTCAP) part types. These parts are used to assemble the upper and lower reflector rings in each experimental configuration. This dimensional uncertainty evaluates the uncertainty in the height of the upper and lower reflector rings, based on measurements.

The reflector ring height measurements are reported for each experimental configuration in the subsections of Section 1.2.9. These measurements use a similar produced as the core stack height measurements described in Section 1.2.7. However, the reflector ring height measurements were only performed at a single location. The same height gauge, as described in Section 1.2.7, with a manufacturer reported indication accuracy of ± 0.04 mm was used for the reflector ring height measurements.

As described in Section 1.2.5, the CAP part allowed the height of the reflector ring to be made within approximately 0.079375 cm of the core stack. As part of the experiment procedure, the lower reflector ring was always shorter than the lower core stack. If the lower reflector ring extended above the lower core stack, there would be a gap between the top of the lower core stack and the bottom of the membrane, the highest worth location of the core stack. This was confirmed both visually and by measuring the height of the lower reflector ring during the experiment. Therefore, no gaps exist in the center of the core stack due to the lower reflector ring.

The upper reflector ring did not have the same requirement. Furthermore, it was preferred to use fewer parts in the reflector ring to avoid possible neutron streaming paths at the step joint. This resulted in some of the upper reflector ring heights being greater than 0.079375 cm of the upper core stack height. This can be seen in the Case 2, which uses the 3-RING-1 and 0-CAP-1 parts for the upper reflector ring, extending approximately 2.5 mm above the upper core stack. The upper reflector ring extending above the upper core stack was not a concern as the top of the upper core stack was the top polyethylene reflector, meaning additional height in the upper reflector ring had a negligible impact on reactivity.

Table 92 reports the upper and lower reflector ring height measurements. The uncertainty in the reflector ring heights is based on the measurement uncertainty of the electronic height gauge. The lower reflector ring height represents the height of the lower reflector ring, including the bottom reflector plate, relative to the lip of the adapter plate, as discussed in Section 2.3.5. For the purpose of this uncertainty analysis, only the uncertainty in the reflector ring height is needed, not the calculated height of the lower reflector. Therefore, the evaluated uncertainty in the upper and lower reflector ring heights is the measurement uncertainty of ± 0.004 cm.

Table 92: Summary of upper and lower reflector ring height measurements.

Case	Reflector Ring Height (cm)	
	Upper	**Lower**
1	8.484 ± 0.004	6.467 ± 0.004
2	7.913 ± 0.004	7.272 ± 0.004
3	9.122 ± 0.004	7.649 ± 0.004
4	9.752 ± 0.004	9.791 ± 0.004
5	25.548 ± 0.004	22.408 ± 0.004
6	8.030 ± 0.004	9.774 ± 0.004
7	7.483 ± 0.004	6.421 ± 0.004

Table 93 summarizes the upper and lower reflector ring height uncertainty calculation parameters and sensitivity in k_{eff}. The calculations vary the parameter by perturbing the reflector height by ± 0.15875 cm. The standard uncertainty in k_{eff} is calculated using Eq. 3 where u_i is the evaluated uncertainty in the reflector ring height of ± 0.004 cm. Table 93 is reproduced alongside the other evaluated uncertainties in Section 2.6.

Table 93: Summary of sensitivity in k_{eff} to uncertainties in the upper and lower reflector ring height.

Parameter (unit of measured)	Case	Parameter Value	Parameter Variation in Calculation	Calculated Effect in k_{eff}	Standard Uncertainty	Standard Uncertainty in k_{eff}
Upper Reflector Ring Height (cm)	1	8.484	±0.15875	±0.00013	±0.004	Negligible
	2	7.913		±0.00288		Negligible
	3	9.122		±0.00207		Negligible
	4	9.752		±0.00153		Negligible
	5	25.548		±0.00363		Negligible
	6	8.030		±0.00229		Negligible
	7	7.483		±0.00186		Negligible
Lower Reflector Ring Height (cm)	1	6.467	±0.15875	±0.00003	±0.004	Negligible
	2	7.272		±0.00257		Negligible
	3	7.649		±0.00381		Negligible
	4	9.791		±0.00251		Negligible
	5	22.408		±0.00225		Negligible
	6	9.774		±0.00346		Negligible
	7	6.421		±0.00191		Negligible

2.3.8 Membrane Thickness

The nominal dimensions of the membrane are reported in Table 2. These dimension are based on the engineering drawing in Fig. 63 of Appendix B. No other dimensional measurements were documented. The drawing reports a thickness tolerance of ±0.010 in. (±0.0254 cm). Therefore, the evaluated uncertainty in the membrane thickness is based on this tolerance. The same membrane was used in all experimental configurations.

Two approaches were used to evaluate the uncertainty in the membrane thickness. Both approaches perturb the membrane thickness by ±0.0254 cm, representing the reported tolerance. The first approach performs this perturbation at a constant mass, requiring the density of the membrane to be varied from 2.4560 $g\,cm^{-3}$ to 2.8832 $g\,cm^{-3}$. The second approach performs this perturbation at a constant density, conserving the density of 2.6525 $g\,cm^{-3}$, calculated based on the mass measurements and drawing dimensions. Table 94 shows the calculated effect in k_{eff} to the membrane thickness perturbation for these two approaches. The constant density perturbation has consistently smaller effect in k_{eff}. Furthermore, given that the membrane is Al-6061, which has a density of 2.70 $g\,cm^{-3}$, the range of densities required for the constant mass perturbation (2.4560 $g\,cm^{-3}$ to 2.8832 $g\,cm^{-3}$) are non-physical. Therefore, the constant density approach is used for the membrane thickness uncertainty evaluation.

Table 94: Calculated effect in k_{eff} to the membrane thickness perturbation using the constant mass and constant density approaches.

Case	Parameter Variation in Calculation (cm)	Calculated Effect in k_{eff}	
		Constant Mass	Constant Density
1	±0.0254	±0.00148	±0.00119
2		±0.00132	±0.00090
3		±0.00118	±0.00083
4		±0.00102	±0.00073
5		±0.00061	±0.00059
6		±0.00105	±0.00083
7		±0.00178	±0.00140

Table 95 summarizes the membrane thickness uncertainty calculation parameters and sensitivity in k_{eff}. The calculations vary the parameter by perturbing the membrane thickness by ±0.0254 cm. Since the evaluated uncertainty in the thickness represents a uniform tolerance interval, the standard uncertainty is $\pm 0.0254/\sqrt{12}$ cm or approximately ±0.0073 cm. The standard uncertainty in k_{eff} is calculated using Eq. 3 where u_i is the evaluated uncertainty in the membrane thickness of ±0.0073 cm. Table 95 is reproduced alongside the other evaluated uncertainties in Section 2.6.

Table 95: Summary of sensitivity in k_{eff} to uncertainties in membrane thickness.

Case	Parameter Value (cm)	Parameter Variation in Calculation	Calculated Effect in k_{eff}	Standard Uncertainty	Standard Uncertainty in k_{eff}
1	0.3175	±0.0254	±0.00119	±0.0073	±0.00034
2			±0.00090		±0.00026
3			±0.00083		±0.00024
4			±0.00073		±0.00021
5			±0.00059		±0.00017
6			±0.00083		±0.00024
7			±0.00140		±0.00040

2.3.9 Membrane Lift

The membrane lift represents the magnitude at which the membrane was lifted off of the interface plate during full-closure of the vertical lift machine. For this experiment, full-closure ranged from a lift of 0.050 inches to 0.350 inches (0.127 cm to 0.889 cm), typically with a target of 0.200 inches (0.508 cm). Therefore, the evaluated uncertainty in the membrane lift is ±0.100 inches (±0.254 cm).

Table 96 summarizes the membrane lift uncertainty calculation parameters and sensitivity in k_{eff}. The calculations vary the parameter by perturbing the membrane lift by ±0.254 cm. Since the evaluated uncertainty in the lift represents a tolerance interval, the standard uncertainty is $\pm 0.254/\sqrt{12}$ cm or approximately ±0.073 cm. The standard uncertainty in k_{eff} is calculated using Eq. 3 where u_i is the evaluated uncertainty in the membrane lift of ±0.073 cm. Table 96 is reproduced alongside the other evaluated uncertainties in Section 2.6.

Table 96: Summary of sensitivity in k_{eff} to uncertainties in the membrane lift.

Case	Parameter Value (cm)	Parameter Variation in Calculation	Calculated Effect in k_{eff}	Standard Uncertainty	Standard Uncertainty in k_{eff}
1	0.3175	±0.254	±0.00011	±0.073	Negligible
2			±0.00004		Negligible
3			±0.00008		Negligible
4			±0.00010		Negligible
5			±0.00002		Negligible
6			±0.00002		Negligible
7			±0.00004		Negligible

2.3.10 Positional Uncertainty

The core stack consists of HEU plates, hafnium plates, and polyethylene moderator and reflector plates with a nominal outer diameter of 15 in. (38.1 cm). The stack is surrounded by polyethylene reflector rings with a nominal inner diameter of 15.1 in. (38.354 cm). Therefore, there exists a gap around the core stack and reflector ring. Similarly, the aluminum inserts have an outer diameter nominally 0.1 in. (0.254 cm) smaller than the inner diameter of their respective HEU annuli. During the execution of the experiment, care was taken to push the core stack and inserts to one side within the reflector. However, this alignment was done by hand and could have shifted during the execution of the experiment. Furthermore, any shifting of the plates in the core stacks would result in misalignment within the core stacks or between the upper and lower halves of the core stack as they were brought together on Comet.

The uncertainty in the core stack position is ±0.025 in. (±0.0635 cm) from the axial center of the reflector rings. This uncertainty represents the upper and lower bounds of a tolerance interval where the core stack could shift within the reflector rings, based on the nominal dimensions. The uncertainty in the aluminum insert position is ±0.05 in. (±0.127 cm) from the axial center of the core stack. This uncertainty represents the upper and lower bounds of a tolerance interval where the aluminum inserts could shift within the annuli of the HEU plates, based on nominal dimensions.

This uncertainty was evaluated in [2] and shown to be negligible for all experimental configurations. Therefore, this uncertainty is judged to be negligible in this experiment.

2.4 Material Uncertainty

The material uncertainties were analyzed using two methods. The first was a direct perturbation method used to evaluate the sensitivity to the ^{235}U enrichment. The second was an adjoint-based sensitivity method used to evaluate the sensitivities to material constituents and impurities[13].

The adjoint-based sensitivity method was used to analyze the impurities by calculating a relative uncertainty in k_{eff} for each isotopic and then adding the individual contributions in quadrature to determine an overall relative uncertainty in k_{eff} for all the impurities in the material. The uncertainty from the adjoint-based sensitivity method is represented as a fractional standard deviation (FSD), defined as the calculated uncertainty divided by its associated sensitivity. The control parameter adjusted (CPA) renormalization method was used. For this renormalization, the majority constituent is each material was chosen as the balance. These are uranium (U) in the HEU plates, hafnium (Hf) in the hafnium plates, CH_2 in the polyethylene, and aluminum (Al) in the aluminum membrane, structure, and inserts. The calculations were performed using the KSEN card in MCNP® 6.2 with ENDF/B-VIII.0 cross sections.

2.4.1 U-235 Enrichment

The uranium isotopic distribution in the HEU is based on the mass spectrometry measurements reported in Table 48 of Section 1.3.1.1. This mass spectrometry data is available for four plates, all of which were used in this experiment. Table 97 summarizes the uranium composition, reporting the average and standard deviation of the measurements. The reported isotopic range is relative to ^{235}U to match Table 48. Based on these measurements, the HEU is 93.232 ± 0.392 % enriched, by weight.

Table 97: Measured HEU isotopic content.

Element	Range (ng/g)	Elemental Composition (Wt.%)	
		Average	Uncertainty
U-234	10.8 - 11.5	1.03046E-02	±2.76710E−04
U-235	-	9.32324E-01	±3.91961E−03
U-236	0.02 - 5.56	2.32202E-03	±2.37288E−03
U-238	57.7 - 59.2	5.50498E-02	±7.31459E−04

In addition to the mass spectrometry measurements which can be used to infer the ^{235}U enrichment, individual plate enrichment values are available for the HEU plates used in the Big Ten experiment, based on Material Control & Accountability records. These values are reported in previous benchmarks and are reproduced in Table 48 of Section 1.3.1.1. Based on these values, the HEU is 93.287 ± 0.103 % enriched, by weight.

The calculated ^{235}U enrichments, based on the mass spectrometry measurements and data available from Material Controls and Accountability (MC&A), are consistent and in good agreement. However, the uncertainty of the mass spectrometry measurements is four times larger than the uncertainty of the MC&A enrichments. Therefore, the ^{235}U enrichment is based on the isotopic distribution reported in Table 97, from the mass spectrometry measurements, with an evaluated uncertainty of ± 0.103 %, based on the distribution of MC&A enrichments.

Table 98 summarizes the ^{235}U enrichment uncertainty calculation parameters and sensitivity in k_{eff}. The cal-

[13] J. A. Favorite et al. "Adjoint Based Sensitivity and Uncertainty Analysis for Density and Composition: A User's Guide". *Nuclear Science and Engineering* 185.3 (2017), pp. 384–405. DOI: 10.1080/00295639.2016.1272990.

culations vary the parameter by collectively perturbing the ^{235}U enrichment for all HEU plates by $\pm 0.103\,\%$. Therefore, the standard uncertainty in k_{eff} is calculated using Eq. 4 where N is the number of HEU plates in the experimental configuration and u_i is the evaluated uncertainty in the ^{235}U enrichment of $\pm 0.103\,\%$. This perturbation using ^{238}U as the balance isotope, no adjustment are made to ^{234}U or ^{236}U. Table 98 is reproduced alongside the other evaluated uncertainties in Section 2.6.

Table 98: Summary of sensitivity in k_{eff} to uncertainties in the ^{235}U enrichment.

Case	Number of Plates	^{235}U Enrichment (Wt.%)	Parameter Variation in Calculation	Calculated Effect in k_{eff}	Standard Uncertainty	Standard Uncertainty in k_{eff}
1	26	93.232	±0.103	±0.00158	$\pm 0.103/\sqrt{26}$	±0.00031
2	17		±0.103	±0.00125	$\pm 0.103/\sqrt{17}$	±0.00030
3	14		±0.103	±0.00121	$\pm 0.103/\sqrt{14}$	±0.00032
4	10		±0.103	±0.00089	$\pm 0.103/\sqrt{10}$	±0.00028
5	12		±0.103	±0.00062	$\pm 0.103/\sqrt{12}$	±0.00018
6	15		±0.103	±0.00132	$\pm 0.103/\sqrt{15}$	±0.00034
7	23		±0.103	±0.00166	$\pm 0.103/\sqrt{23}$	±0.00035

2.4.2 Highly Enriched Uranium Composition

The HEU composition is based on the impurity analysis reported in Table 50 of Section 1.3.1.2. The impurity analysis was performed on five HEU plates. Based on these measurements, there is less than 2000 $\mu g\,g^{-1}$ U (parts-per-million U) of impurities. Table 99 presents the elemental composition for the HEU, treating U as the remainder. For elements measured to be less than a given threshold (Li, Be, Na, Mg, Ca, V, Co, and Sn), the lower bound is assumed to be 0. For these eight elements, the impurity content is assumed to be a uniform distribution centered at the midpoint within the range. For the two elements (Mo and Pb), not included with HEU plates 10932 and 10933, the average impurity content and uncertainty in the average is based only on the measurements of HEU plates 11147, 11149, and 11150. For the remaining elements, the uncertainty in the average impurity content is the standard deviation of the five measurements.

Table 99: HEU impurity content, elemental composition, and uncertainties.

Element	Range (ug/g)	Elemental Composition (Wt.%)	
		Average	Uncertainty
U[(a)]	-	9.99114E+01	-
Li	0.1	5.00000E-06	±1.44338E−06
Be	0.1	5.00000E-06	±1.44338E−06
B	0.1 - 0.6	3.60000E-05	±2.30217E−05
C	170 - 1100	4.06000E-02	±3.93357E−02
Na	1	5.00000E-05	±1.44338E−05
Mg	1	5.00000E-05	±1.44338E−05
Al	20 - 150	7.20000E-03	±5.26308E−03
Si	80 - 400	2.24000E-02	±1.28957E−02
Ca	2	1.00000E-04	±2.88675E−05
V	20	1.00000E-03	±2.88675E−04
Cr	2 - 15	6.00000E-04	±5.19615E−04
Mn	4 - 7	6.00000E-04	±1.22474E−04
Fe	30 - 190	9.60000E-03	±5.89915E−03
Co	5	2.50000E-04	±7.21688E−05
Ni	15 - 30	2.00000E-03	±6.12372E−04
Cu	3 - 6	4.40000E-04	±1.14018E−04
Mo	0 - 50	3.33333E-03	±1.44338E−03
Sn	0 - 1	5.00000E-05	±1.44338E−05
Pb	0 - 5	2.33333E-04	±2.30940E−04

[(a)] Treated as the remainder.

Table 100 summarizes the HEU composition uncertainty calculation parameters and sensitivity in k_{eff}. The calculated effect in k_{eff} is based on the sum of the effect in k_{eff} to the constrained sensitivities as described in Section 2.4. The standard uncertainty is based on the impurity content reported in Table 99. Table 100 is reproduced alongside the other evaluated uncertainties in Section 2.6.

Table 100: Summary of sensitivity in k_{eff} to uncertainties in the HEU composition.

Case	Number of Plates	Parameter Value (Wt.%)	Calculated Effect in k_{eff}	Standard Uncertainty	Standard Uncertainty in k_{eff}
1	26	Varies (Table 99)	±0.00023	Varies (Table 99)	±0.00005
2	17		±0.00017		Negligible
3	14		±0.00014		Negligible
4	10		±0.00011		Negligible
5	12		±0.00006		Negligible
6	15		±0.00015		Negligible
7	23		±0.00025		Negligible

The following tables report the unconstrained and constrained elemental density sensitivities for the HEU composition, calculated as described in Section 2.4. These tables include: Table 101 for Case 1, Table 102 for Case 2, Table 103 for Case 3, Table 104 for Case 4, Table 105 for Case 5, Table 106 for Case 6, and Table 107 for Case 7.

Table 101: Elemental density sensitivities in k_{eff} for the HEU composition in Case 1.

Element	**Unconstrained Sensitivity, $S_{k,i}$**	**FSD, $S_{k,i}/\sigma(S_{k,i})$**	**Constrained Sensitivity, $S_{k,i}^{CPA}$**	**u_k/k**
U	5.8719E-01	0.0006	-	-
Li	-2.7260E-08	0.0003	-5.6646E-08	1.6352E-08
Be	-4.2434E-08	0.1543	-7.1820E-08	2.0733E-08
B	1.3990E-07	1.5602	-7.1680E-08	4.5839E-08
C	1.6640E-05	0.2776	-2.2197E-04	2.1506E-04
Na	-1.3765E-07	0.9298	-4.3151E-07	1.2457E-07
Mg	1.0744E-07	1.4727	-1.8642E-07	5.3814E-08
Al	1.6386E-06	1.3529	-4.0677E-05	2.9734E-05
Si	8.8102E-06	0.4155	-1.2284E-04	7.0718E-05
Ca	7.1100E-08	3.6020	-5.1661E-07	1.4913E-07
V	1.4036E-06	0.7499	-4.4735E-06	1.2914E-06
Cr	-7.7534E-07	0.6495	-4.3016E-06	3.7253E-06
Mn	-1.0973E-06	0.6410	-4.6236E-06	9.4378E-07
Fe	4.7716E-06	0.4990	-5.1649E-05	3.1738E-05
Co	2.4672E-07	1.7910	-1.2226E-06	3.5292E-07
Ni	4.2386E-07	3.0803	-1.1330E-05	3.4692E-06
Cu	-6.0805E-07	0.9950	-3.1940E-06	8.2766E-07
Mo	-2.6743E-07	6.5669	-1.9858E-05	1.2461E-05
Sn	1.6733E-07	1.2432	-1.2652E-07	3.6525E-08
Pb	-1.7143E-07	2.6067	-1.5428E-06	1.3711E-06
Total	**5.8722E-01**	**0.0006**	**-**	**2.3093E-04**

Table 102: Elemental density sensitivities in k_{eff} for the HEU composition in Case 2.

Element	**Unconstrained Sensitivity, $S_{k,i}$**	**FSD, $S_{k,i}/\sigma(S_{k,i})$**	**Constrained Sensitivity, $S_{k,i}^{CPA}$**	**u_k/k**
U	4.3478E-01	0.0006	-	-
Li	-9.5127E-09	0.8468	-3.1271E-08	9.0271E-09
Be	-3.4425E-08	0.1177	-5.6183E-08	1.6219E-08
B	-2.4383E-07	0.1728	-4.0049E-07	2.5611E-07
C	9.8459E-06	0.3279	-1.6683E-04	1.6164E-04
Na	2.0725E-08	7.8302	-1.9686E-07	5.6828E-08
Mg	1.5534E-08	8.9035	-2.0205E-07	5.8326E-08
Al	2.2812E-06	0.5545	-2.9051E-05	2.1236E-05
Si	5.0915E-06	0.4006	-9.2385E-05	5.3186E-05
Ca	-1.9406E-07	0.4427	-6.2922E-07	1.8164E-07
V	-5.6279E-07	1.4693	-4.9144E-06	1.4187E-06
Cr	-1.0902E-08	42.9388	-2.6219E-06	2.2706E-06
Mn	-2.1261E-06	0.3754	-4.7371E-06	9.6695E-07
Fe	2.3303E-06	0.7961	-3.9445E-05	2.4239E-05
Co	-1.0234E-06	0.4113	-2.1113E-06	6.0948E-07
Ni	5.2140E-07	2.0324	-8.1819E-06	2.5052E-06
Cu	6.3562E-07	0.7693	-1.2791E-06	3.3146E-07
Mo	2.4319E-06	0.5277	-1.2074E-05	7.5761E-06
Sn	-7.4838E-08	1.5397	-2.9242E-07	8.4414E-08
Pb	4.7329E-07	0.7031	-5.4209E-07	4.8176E-07
Total	**4.3480E-01**	**0.0006**	**-**	**1.7340E-04**

Table 103: Elemental density sensitivities in k_{eff} for the HEU composition in Case 3.

Element	**Unconstrained Sensitivity, $S_{k,i}$**	**FSD, $S_{k,i}/\sigma(S_{k,i})$**	**Constrained Sensitivity, $S_{k,i}^{CPA}$**	**u_k/k**
U	3.5928E-01	0.0005	-	-
Li	-1.4381E-08	0.0001	-3.2361E-08	9.3418E-09
Be	2.8346E-08	1.4189	1.0366E-08	2.9925E-09
B	-1.6147E-07	0.4315	-2.9093E-07	1.8604E-07
C	9.7899E-06	0.2368	-1.3621E-04	1.3196E-04
Na	-1.4480E-07	0.5031	-3.2460E-07	9.3703E-08
Mg	-1.7346E-08	5.5306	-1.9714E-07	5.6910E-08
Al	4.0899E-07	2.2561	-2.5482E-05	1.8627E-05
Si	3.7022E-06	0.4517	-7.6847E-05	4.4241E-05
Ca	-4.6155E-08	1.8313	-4.0575E-07	1.1713E-07
V	3.4779E-07	1.9117	-3.2481E-06	9.3766E-07
Cr	1.0702E-07	2.9909	-2.0505E-06	1.7758E-06
Mn	-5.0597E-07	1.4020	-2.6635E-06	5.4369E-07
Fe	1.7422E-06	0.7656	-3.2779E-05	2.0142E-05
Co	-8.0468E-07	0.4457	-1.7037E-06	4.9181E-07
Ni	1.3368E-06	0.7189	-5.8551E-06	1.7927E-06
Cu	-6.3883E-07	0.5073	-2.2210E-06	5.7554E-07
Mo	-6.3771E-07	1.5309	-1.2624E-05	7.9216E-06
Sn	-5.6171E-08	1.5620	-2.3597E-07	6.8118E-08
Pb	-1.0396E-08	24.1981	-8.4945E-07	7.5491E-07
Total	**3.5929E-01**	**0.0005**	**-**	**1.4211E-04**

Table 104: Elemental density sensitivities in k_{eff} for the HEU composition in Case 4.

Element	**Unconstrained Sensitivity, $S_{k,i}$**	**FSD, $S_{k,i}/\sigma(S_{k,i})$**	**Constrained Sensitivity, $S_{k,i}^{CPA}$**	**u_k/k**
U	2.6753E-01	0.0006	-	-
Li	9.9308E-09	1.5504	-3.4574E-09	9.9806E-10
Be	-8.3289E-09	1.3082	-2.1717E-08	6.2692E-09
B	-3.4416E-07	0.0845	-4.4056E-07	2.8173E-07
C	1.8026E-06	0.9232	-1.0691E-04	1.0358E-04
Na	4.5732E-08	1.8841	-8.8150E-08	2.5447E-08
Mg	-7.3610E-09	9.1876	-1.4124E-07	4.0773E-08
Al	4.4319E-07	1.5661	-1.8836E-05	1.3769E-05
Si	2.0601E-06	0.6455	-5.7919E-05	3.3344E-05
Ca	1.3222E-08	8.0426	-2.5454E-07	7.3480E-08
V	-2.4173E-07	2.0979	-2.9194E-06	8.4275E-07
Cr	-1.3944E-07	1.6389	-1.7460E-06	1.5121E-06
Mn	-2.7296E-07	1.6292	-1.8795E-06	3.8366E-07
Fe	2.1106E-06	0.4952	-2.3595E-05	1.4499E-05
Co	-3.0591E-07	0.9906	-9.7532E-07	2.8155E-07
Ni	-1.2236E-06	0.5137	-6.5789E-06	2.0144E-06
Cu	-3.4691E-07	0.8320	-1.5251E-06	3.9519E-07
Mo	-1.2681E-06	0.5839	-1.0194E-05	6.3964E-06
Sn	-1.3743E-07	0.3589	-2.7131E-07	7.8320E-08
Pb	4.9281E-07	0.4871	-1.3197E-07	1.1728E-07
Total	**2.6753E-01**	**0.0006**	**-**	**1.1086E-04**

Table 105: Elemental density sensitivities in k_{eff} for the HEU composition in Case 5.

Element	**Unconstrained Sensitivity, $S_{k,i}$**	**FSD, $S_{k,i}/\sigma(S_{k,i})$**	**Constrained Sensitivity, $S_{k,i}^{CPA}$**	**u_k/k**
U	1.6263E-01	0.0010	-	-
Li	-1.0137E-09	8.7695	-9.1525E-09	2.6421E-09
Be	-7.2896E-09	0.6306	-1.5428E-08	4.4538E-09
B	-3.4738E-07	0.1055	-4.0598E-07	2.5962E-07
C	3.9428E-06	0.3242	-6.2145E-05	6.0210E-05
Na	-3.2432E-08	1.5218	-1.1382E-07	3.2857E-08
Mg	-2.0764E-08	1.8686	-1.0215E-07	2.9489E-08
Al	9.0925E-07	0.7217	-1.0811E-05	7.9024E-06
Si	1.6582E-06	0.5368	-3.4804E-05	2.0037E-05
Ca	-7.4875E-09	6.7914	-1.7026E-07	4.9151E-08
V	1.8046E-08	19.5173	-1.6097E-06	4.6469E-07
Cr	2.2151E-08	7.7980	-9.5451E-07	8.2663E-07
Mn	6.9774E-07	0.6083	-2.7892E-07	5.6935E-08
Fe	-1.2304E-06	0.6042	-1.6857E-05	1.0359E-05
Co	-5.9582E-07	0.3578	-1.0028E-06	2.8947E-07
Ni	1.3752E-07	2.9841	-3.1180E-06	9.5469E-07
Cu	-6.7873E-07	0.2840	-1.3949E-06	3.6147E-07
Mo	-9.6081E-07	0.5626	-6.3867E-06	4.0076E-06
Sn	1.3302E-07	0.6300	5.1631E-08	1.4905E-08
Pb	2.3647E-08	5.6911	-3.5617E-07	3.1653E-07
Total	**1.6264E-01**	**0.0010**	**-**	**6.4920E-05**

Table 106: Elemental density sensitivities in k_{eff} for the HEU composition in Case 6.

Element	**Unconstrained Sensitivity, $S_{k,i}$**	**FSD, $S_{k,i}/\sigma(S_{k,i})$**	**Constrained Sensitivity, $S_{k,i}^{CPA}$**	**u_k/k**
U	3.6831E-01	0.0006	-	-
Li	1.4715E-08	1.6484	-3.7174E-09	1.0731E-09
Be	-2.2343E-08	0.3463	-4.0775E-08	1.1771E-08
B	-1.7772E-07	0.3009	-3.1043E-07	1.9852E-07
C	7.3019E-06	0.3506	-1.4237E-04	1.3793E-04
Na	-1.3558E-07	0.7585	-3.1990E-07	9.2347E-08
Mg	-9.2645E-08	0.9100	-2.7697E-07	7.9953E-08
Al	6.0052E-07	1.5904	-2.5942E-05	1.8963E-05
Si	3.5004E-06	0.5266	-7.9075E-05	4.5524E-05
Ca	2.7920E-08	3.1550	-3.4072E-07	9.8358E-08
V	1.1199E-06	0.6758	-2.5665E-06	7.4089E-07
Cr	2.6938E-07	1.3601	-1.9425E-06	1.6822E-06
Mn	8.5872E-07	0.8891	-1.3531E-06	2.7621E-07
Fe	6.8626E-07	2.0238	-3.4703E-05	2.1325E-05
Co	-4.4129E-07	0.8612	-1.3629E-06	3.9343E-07
Ni	6.5313E-07	1.2530	-6.7197E-06	2.0575E-06
Cu	-6.6060E-07	0.4712	-2.2826E-06	5.9150E-07
Mo	-1.0704E-06	0.9975	-1.3358E-05	8.3823E-06
Sn	-9.1856E-08	0.8656	-2.7618E-07	7.9725E-08
Pb	4.2981E-07	0.6353	-4.3035E-07	3.8246E-07
Total	**3.6833E-01**	**0.0006**	**-**	**1.4829E-04**

Table 107: Elemental density sensitivities in k_{eff} for the HEU composition in Case 7.

Element	Unconstrained Sensitivity, $S_{k,i}$	FSD, $S_{k,i}/\sigma(S_{k,i})$	Constrained Sensitivity, $S_{k,i}^{CPA}$	u_k/k
U	6.1755E-01	0.0005	-	-
Li	-2.8109E-08	0.0003	-5.9014E-08	1.7036E-08
Be	4.2959E-08	1.0712	1.2054E-08	3.4797E-09
B	-9.9533E-08	0.7087	-3.2205E-07	2.0595E-07
C	1.0432E-05	0.3352	-2.4052E-04	2.3303E-04
Na	1.3419E-07	1.0970	-1.7486E-07	5.0478E-08
Mg	3.1446E-07	0.6794	5.4082E-09	1.5612E-09
Al	2.5837E-06	0.5983	-4.1919E-05	3.0642E-05
Si	4.6095E-06	0.5722	-1.3384E-04	7.7055E-05
Ca	-2.0796E-08	9.1555	-6.3890E-07	1.8443E-07
V	3.8422E-07	2.0453	-5.7968E-06	1.6734E-06
Cr	4.5043E-07	1.1011	-3.2582E-06	2.8217E-06
Mn	-2.7482E-08	21.3472	-3.7361E-06	7.6262E-07
Fe	4.8198E-06	0.4125	-5.4518E-05	3.3501E-05
Co	-2.6994E-07	1.3429	-1.8152E-06	5.2400E-07
Ni	2.4707E-06	0.3996	-9.8913E-06	3.0286E-06
Cu	-9.3400E-08	5.0888	-2.8130E-06	7.2894E-07
Mo	1.0440E-06	1.5373	-1.9559E-05	1.2273E-05
Sn	1.2833E-07	1.3846	-1.8072E-07	5.2168E-08
Pb	-5.6972E-08	7.2568	-1.4992E-06	1.3323E-06
Total	**6.1758E-01**	**0.0005**	**-**	**2.4995E-04**

2.4.3 Hafnium Composition

The hafnium composition is based on the measured elemental composition reported in Table 52 of Section 1.3.2.2. The element composition measurements were performed with three samples of the ingot used to produce the plates and one sample from the product. There is a measured range in the impurities of $335\,\mu g\,g^{-1}$ to $710\,\mu g\,g^{-1}$, with an average of $688.3\,\mu g\,g^{-1}$. Zirconium is not treated as an impurity due to nature in which hafnium is refined. Table 108 presents the elemental composition for the hafnium based on these measurements, treating Hf as the remainder. For the elements with a range of reported values (C, Fe, N, and O), the uncertainty is based on the standard deviation of the measurements. For all other element, the uncertainty is assumed to be the precision (i.e., half of the least significant digit) of the reported value, which is ± 0.0005. Since the uncertainty in the precision represents a uniform tolerance interval, the standard uncertainty is $\pm 0.0005/\sqrt{12}$.

Table 108: Hafnium impurity content, elemental composition, and uncertainties.

Element	Range (ug/g)	Elemental Composition (Wt.%)	
		Average	Uncertainty
Hf[a]	-	9.72562E+01	-
Zr[b]	2.6 - 2.7 Wt.%	2.67500E+00	5.00000E-02
Al	25	2.50000E-03	1.44338E-04
C[b]	30 - 40	3.25000E-03	5.00000E-04
Cr	30	3.00000E-03	1.44338E-04
Cu	20	2.00000E-03	1.44338E-04
H	3	3.00000E-04	1.44338E-04
Fe[b]	140 - 160	1.52500E-02	9.57427E-04
Mo	10	1.00000E-03	1.44338E-04
Ni	25	2.50000E-03	1.44338E-04
Nb	50	5.00000E-03	1.44338E-04
N[b]	40 - 50	4.66667E-03	5.77350E-04
O[b]	170 - 210	1.96667E-02	2.30940E-03
Si	25	2.50000E-03	1.44338E-04
Ta	10	1.00000E-03	1.44338E-04
Sn	10	1.00000E-03	1.44338E-04
Ti	20	2.00000E-03	1.44338E-04
W	20	2.00000E-03	1.44338E-04
U	2	2.00000E-04	1.44338E-04
V	10	1.00000E-03	1.44338E-04

[a] Treated as the remainder.
[b] Uncertainty based on standard deviation of measurements.

Table 109 summarizes the hafnium composition uncertainty calculation parameters and sensitivity in k_{eff}. The calculated effect in k_{eff} is based on the sum of the effect in k_{eff} to the constrained sensitivities as described in Section 2.4. The standard uncertainty is based on the impurity content reported in Table 108. Table 109 is reproduced alongside the other evaluated uncertainties in Section 2.6.

Table 109: Summary of sensitivity in k_{eff} to uncertainties in the hafnium composition.

Case	Number of Plates	Parameter Value (Wt.%)	Calculated Effect in k_{eff}	Standard Uncertainty	Standard Uncertainty in k_{eff}
1	24	Varies (Table 108)	±0.00001	Varies (Table 108)	Negligible
2	15		±0.00001		Negligible
3	12		±0.00001		Negligible
4	9		±0.00002		Negligible
5	10		±0.00002		Negligible
6	13		±0.00001		Negligible
7	24		±0.00001		Negligible

The following tables report the unconstrained and constrained elemental density sensitivities for the hafnium composition, calculated as described in Section 2.4. These tables include: Table 110 for Case 1, Table 111 for Case 2, Table 112 for Case 3, Table 113 for Case 4, Table 114 for Case 5, Table 115 for Case 6, and Table 116 for Case 7.

Table 110: Elemental density sensitivities in k_{eff} for the hafnium composition in Case 1.

Element	**Unconstrained Sensitivity, $S_{k,i}$**	**FSD, $S_{k,i}/\sigma(S_{k,i})$**	**Constrained Sensitivity, $S_{k,i}^{CPA}$**	**u_k/k**
Hf	-1.8847E-04	1.0753	-	-
Zr	1.3438E-03	0.0319	1.3490E-03	2.5215E-05
H	2.2587E-05	0.2116	2.2592E-05	1.3044E-06
C	1.1999E-05	0.2429	1.2006E-05	1.8470E-06
N	-2.5034E-06	1.2299	-2.4976E-06	1.2016E-07
O	3.7227E-05	0.1826	3.7231E-05	2.6869E-06
Al	4.1066E-06	0.4556	4.1072E-06	1.9761E-06
Si	2.3081E-06	0.6857	2.3376E-06	1.4676E-07
Ti	1.7774E-06	0.8199	1.7794E-06	2.5683E-07
V	1.0555E-07	9.3337	1.1040E-07	6.3739E-09
Cr	1.3042E-08	105.7509	2.2731E-08	6.5620E-10
Fe	1.1315E-05	0.2904	1.1324E-05	1.4010E-06
Ni	-1.5085E-06	0.9195	-1.4704E-06	1.7266E-07
Cu	1.6246E-06	0.7616	1.6295E-06	9.4078E-08
Nb	8.2246E-07	2.5191	8.2440E-07	1.1899E-07
Mo	1.3706E-06	0.6674	1.3726E-06	1.9812E-07
Sn	5.2474E-07	1.3494	5.2862E-07	3.8150E-08
Ta	-1.3634E-06	0.5034	-1.3595E-06	9.8113E-08
W	-8.6605E-07	1.1989	-8.6566E-07	6.2474E-07
U	2.8626E-07	1.1825	2.8820E-07	4.1598E-08
Total	**1.2452E-03**	**0.1666**	**-**	**2.5585E-05**

Table 111: Elemental density sensitivities in k_{eff} for the hafnium composition in Case 2.

Element	**Unconstrained Sensitivity, $S_{k,i}$**	**FSD, $S_{k,i}/\sigma(S_{k,i})$**	**Constrained Sensitivity, $S_{k,i}^{CPA}$**	**u_k/k**
Hf	-3.6381E-02	0.0040	-	-
Zr	7.3881E-04	0.0392	1.7394E-03	3.2513E-05
H	7.3187E-06	0.3642	8.2539E-06	4.7654E-07
C	2.2749E-06	0.7842	3.4906E-06	5.3702E-07
N	1.4528E-06	1.2121	2.5750E-06	1.2389E-07
O	1.9080E-05	0.1941	1.9828E-05	1.4310E-06
Al	1.2510E-06	0.8532	1.3632E-06	6.5588E-07
Si	2.1072E-06	0.5527	7.8118E-06	4.9044E-07
Ti	2.2693E-06	0.4779	2.6433E-06	3.8153E-07
V	4.0164E-07	2.3912	1.3368E-06	7.7181E-08
Cr	1.0635E-06	0.9211	2.9338E-06	8.4693E-08
Fe	8.7702E-06	0.3314	1.0516E-05	1.3010E-06
Ni	3.2368E-07	2.8409	7.6804E-06	9.0189E-07
Cu	7.3067E-07	1.0396	1.6658E-06	9.6178E-08
Nb	-8.1160E-07	1.3797	-4.3753E-07	6.3152E-08
Mo	-4.0841E-08	12.6825	3.3323E-07	4.8098E-08
Sn	3.8000E-07	1.1458	1.1281E-06	8.1417E-08
Ta	-2.3925E-06	0.1578	-1.6443E-06	1.1867E-07
W	-2.2360E-06	0.3283	-2.1612E-06	1.5597E-06
U	1.2980E-07	1.7677	5.0387E-07	7.2727E-08
Total	**-3.5600E-02**	**-0.0042**	**-**	**3.2642E-05**

Table 112: Elemental density sensitivities in k_{eff} for the hafnium composition in Case 3.

Element	**Unconstrained Sensitivity, $S_{k,i}$**	**FSD, $S_{k,i}/\sigma(S_{k,i})$**	**Constrained Sensitivity, $S_{k,i}^{CPA}$**	**u_k/k**
Hf	-6.4623E-02	0.0016	-	-
Zr	4.2550E-04	0.0488	2.2029E-03	4.1177E-05
H	-1.6079E-06	1.2369	5.3233E-08	3.0734E-09
C	4.2039E-07	3.1407	2.5799E-06	3.9691E-07
N	3.6792E-06	0.4708	5.6726E-06	2.7292E-07
O	1.0026E-05	0.3146	1.1355E-05	8.1950E-07
Al	7.2700E-07	1.1854	9.2634E-07	4.4569E-07
Si	-6.8634E-08	11.2782	1.0064E-05	6.3187E-07
Ti	-6.0185E-07	1.3018	6.2617E-08	9.0380E-09
V	4.9646E-07	1.4046	2.1576E-06	1.2457E-07
Cr	1.2211E-06	0.5981	4.5434E-06	1.3116E-07
Fe	2.6721E-06	0.6344	5.7730E-06	7.1422E-07
Ni	-1.5463E-06	0.4846	1.1521E-05	1.3529E-06
Cu	-1.0273E-06	0.6061	6.3391E-07	3.6599E-08
Nb	1.3681E-06	0.7271	2.0326E-06	2.9338E-07
Mo	4.4750E-07	0.9515	1.1120E-06	1.6050E-07
Sn	7.1427E-08	4.3047	1.4004E-06	1.0106E-07
Ta	-3.4040E-06	0.0965	-2.0750E-06	1.4975E-07
W	-2.3842E-06	0.2890	-2.2513E-06	1.6248E-06
U	1.1067E-07	1.6194	7.7513E-07	1.1188E-07
Total	**-6.4187E-02**	**-0.0017**	**-**	**4.1258E-05**

Table 113: Elemental density sensitivities in k_{eff} for the hafnium composition in Case 4.

Element	**Unconstrained Sensitivity, $S_{k,i}$**	**FSD, $S_{k,i}/\sigma(S_{k,i})$**	**Constrained Sensitivity, $S_{k,i}^{CPA}$**	**u_k/k**
Hf	-1.0351E-01	0.0008	-	-
Zr	2.2870E-04	0.0705	3.0756E-03	5.7488E-05
H	-7.9613E-06	0.2314	-5.3006E-06	3.0603E-07
C	6.6518E-07	1.4383	4.1240E-06	6.3447E-07
N	-3.0412E-06	0.4631	1.5163E-07	7.2955E-09
O	6.7265E-06	0.3196	8.8550E-06	6.3906E-07
Al	-6.9797E-07	0.8259	-3.7869E-07	1.8220E-07
Si	1.1735E-06	0.4790	1.7404E-05	1.0926E-06
Ti	1.0920E-06	0.6139	2.1563E-06	3.1123E-07
V	1.0071E-06	0.5305	3.6677E-06	2.1176E-07
Cr	-2.1754E-07	2.4956	5.1038E-06	1.4733E-07
Fe	1.8379E-06	0.7641	6.8044E-06	8.4183E-07
Ni	-7.6042E-07	0.8398	2.0170E-05	2.3685E-06
Cu	4.7440E-07	1.0650	3.1351E-06	1.8100E-07
Nb	-2.5140E-07	2.8720	8.1286E-07	1.1733E-07
Mo	-8.6804E-07	0.3235	1.9623E-07	2.8323E-08
Sn	2.6165E-07	0.9131	2.3902E-06	1.7250E-07
Ta	-3.6656E-06	0.0663	-1.5370E-06	1.1093E-07
W	-3.8062E-06	0.1393	-3.5933E-06	2.5933E-06
U	-1.5025E-07	0.6946	9.1402E-07	1.3193E-07
Total	**-1.0329E-01**	**-0.0008**	**-**	**5.7622E-05**

Table 114: Elemental density sensitivities in k_{eff} for the hafnium composition in Case 5.

Element	**Unconstrained Sensitivity, $S_{k,i}$**	**FSD, $S_{k,i}/\sigma(S_{k,i})$**	**Constrained Sensitivity, $S_{k,i}^{CPA}$**	**u_k/k**
Hf	-1.4756E-01	0.0005	-	-
Zr	-4.8222E-05	0.2479	4.0103E-03	7.4959E-05
H	-5.8818E-06	0.2693	-2.0888E-06	1.2060E-07
C	-1.2067E-06	0.6090	3.7241E-06	5.7294E-07
N	-4.3838E-06	0.2165	1.6779E-07	8.0729E-09
O	8.4739E-07	1.8849	3.8818E-06	2.8014E-07
Al	1.8458E-07	2.3832	6.3974E-07	3.0779E-07
Si	9.3214E-08	4.8851	2.3230E-05	1.4585E-06
Ti	-6.3289E-07	0.6889	8.8431E-07	1.2764E-07
V	3.6645E-08	10.7637	3.8296E-06	2.2110E-07
Cr	-6.6084E-07	0.5845	6.9251E-06	1.9991E-07
Fe	-3.3011E-06	0.2860	3.7792E-06	4.6755E-07
Ni	-7.6679E-07	0.6052	2.9071E-05	3.4138E-06
Cu	-3.5764E-07	1.0410	3.4354E-06	1.9834E-07
Nb	2.4155E-07	2.2489	1.7587E-06	2.5385E-07
Mo	-3.1424E-07	0.7332	1.2030E-06	1.7363E-07
Sn	9.9818E-08	2.0743	3.1342E-06	2.2619E-07
Ta	-2.2523E-06	0.0918	7.8214E-07	5.6446E-08
W	-2.3103E-06	0.2279	-2.0069E-06	1.4483E-06
U	-2.2393E-08	3.7370	1.4948E-06	2.1576E-07
Total	**-1.4763E-01**	**-0.0005**	**-**	**7.5072E-05**

Table 115: Elemental density sensitivities in k_{eff} for the hafnium composition in Case 6.

Element	**Unconstrained Sensitivity, $S_{k,i}$**	**FSD, $S_{k,i}/\sigma(S_{k,i})$**	**Constrained Sensitivity, $S_{k,i}^{CPA}$**	**u_k/k**
Hf	-6.3541E-02	0.0018	-	-
Zr	5.1283E-04	0.0390	2.2605E-03	4.2252E-05
H	4.3192E-07	6.1963	2.0652E-06	1.1924E-07
C	6.6938E-07	2.3405	2.7927E-06	4.2965E-07
N	2.5464E-06	0.7029	4.5064E-06	2.1681E-07
O	1.6668E-05	0.1714	1.7975E-05	1.2972E-06
Al	9.6648E-07	0.9465	1.1625E-06	5.5930E-07
Si	7.5850E-07	0.9900	1.0722E-05	6.7314E-07
Ti	3.4145E-07	2.6349	9.9478E-07	1.4358E-07
V	3.6665E-07	2.0479	2.0000E-06	1.1547E-07
Cr	1.1796E-06	0.6507	4.4462E-06	1.2835E-07
Fe	1.5979E-06	1.1442	4.6468E-06	5.7489E-07
Ni	1.1302E-06	0.8178	1.3979E-05	1.6415E-06
Cu	-8.4410E-08	7.8477	1.5489E-06	8.9427E-08
Nb	-6.1146E-07	1.5399	4.1872E-08	6.0438E-09
Mo	-7.4459E-07	0.5736	-9.1257E-08	1.3172E-08
Sn	2.6768E-07	1.2802	1.5743E-06	1.1362E-07
Ta	-3.6116E-06	0.1074	-2.3049E-06	1.6634E-07
W	-2.9301E-06	0.2733	-2.7994E-06	2.0203E-06
U	-8.6438E-08	1.4386	5.6689E-07	8.1824E-08
Total	**-6.3009E-02**	**-0.0019**	**-**	**4.2369E-05**

Table 116: Elemental density sensitivities in k_{eff} for the hafnium composition in Case 7.

Element	**Unconstrained Sensitivity, $S_{k,i}$**	**FSD, $S_{k,i}/\sigma(S_{k,i})$**	**Constrained Sensitivity, $S_{k,i}^{CPA}$**	**u_k/k**
Hf	3.5163E-02	0.0034	-	-
Zr	2.7384E-03	0.0101	1.7712E-03	3.3107E-05
H	2.3256E-06	0.9580	1.4218E-06	8.2086E-08
C	1.3745E-05	0.1252	1.2570E-05	1.9338E-06
N	8.0956E-06	0.2151	7.0110E-06	3.3732E-07
O	7.6586E-05	0.0460	7.5863E-05	5.4749E-06
Al	5.0400E-06	0.2108	4.9315E-06	2.3727E-06
Si	4.9464E-06	0.1994	-5.6716E-07	3.5607E-08
Ti	1.1958E-06	0.7193	8.3424E-07	1.2041E-07
V	4.4428E-07	1.4317	-4.5959E-07	2.6535E-08
Cr	3.2891E-06	0.2428	1.4814E-06	4.2764E-08
Fe	1.5068E-05	0.1230	1.3381E-05	1.6555E-06
Ni	2.7921E-06	0.3482	-4.3184E-06	5.0710E-07
Cu	1.1474E-06	0.5509	2.4354E-07	1.4061E-08
Nb	3.2727E-06	0.3097	2.9112E-06	4.2019E-07
Mo	1.1164E-06	0.4675	7.5485E-07	1.0895E-07
Sn	9.3374E-07	0.3991	2.1064E-07	1.5202E-08
Ta	-1.2193E-06	0.2538	-1.9424E-06	1.4018E-07
W	-3.2883E-06	0.2177	-3.3606E-06	2.4253E-06
U	-1.2953E-07	0.8793	-4.9107E-07	7.0880E-08
Total	**3.8036E-02**	**0.0032**	**-**	**3.3833E-05**

2.4.4 Polyethylene Composition

The polyethylene composition is based on the measured elemental composition reported in Table 52 of Section 1.3.3.2. The elemental composition measurements were performed on a 246.97 µg sample of the polyethylene. Based on these measurements, there was less than 0.3 µg of impurities in the sample. Table 117 presents the elemental composition for the polyethylene based on these measurements. The reported elemental uncertainties are based on the standard deviation of the measurements. The remainder of the sample is assumed to be polyethylene (CH_2).

Table 117: Polyethylene elemental composition and uncertainties.

Element	Elemental Composition (Wt.%)	
	Average	Uncertainty
H[(a)]	1.43573E+01	-
C[(a)]	8.55467E+01	-
Na	1.43800E-03	±1.82000E−06
Al	2.39200E-03	±1.74000E−06
Si	1.17000E-04	±6.00000E−08
Cr	9.21350E-02	±7.08000E−06

[(a)] Treated as the remainder (CH_2).

Table 118 summarizes the polyethylene composition uncertainty calculation parameters and sensitivity in k_{eff}. The calculated effect in k_{eff} is based on the sum of the effect in k_{eff} to the constrained sensitivities as described in Section 2.4. All polyethylene materials were perturbed collectively, including the moderator (if present) and reflector parts. The standard uncertainty is based on the impurity content reported in Table 117. Table 118 is reproduced alongside the other evaluated uncertainties in Section 2.6.

Table 118: Summary of sensitivity in k_{eff} to uncertainties in the polyethylene composition.

Case	Parameter Value (Wt.%)	Calculated Effect in k_{eff}	Standard Uncertainty	Standard Uncertainty in k_{eff}
1	Varies (Table 117)	Negligible	Varies (Table 117)	Negligible
2		Negligible		Negligible
3		Negligible		Negligible
4		Negligible		Negligible
5		Negligible		Negligible
6		Negligible		Negligible
7		Negligible		Negligible

The following tables report the unconstrained and constrained elemental density sensitivities for the polyethylene composition, calculated as described in Section 2.4. These tables include: Table 119 for Case 1, Table 120 for Case 2, Table 121 for Case 3, Table 122 for Case 4, Table 123 for Case 5, Table 124 for Case 6, and Table 125 for Case 7.

Table 119: Elemental density sensitivities in k_{eff} for the polyethylene composition in Case 1.

Element	Unconstrained Sensitivity, $S_{k,i}$	FSD, $S_{k,i}/\sigma(S_{k,i})$	Constrained Sensitivity, $S_{k,i}^{CPA}$	u_k/k
H	1.7664E-02	0.0070	-	-
C	1.8538E-02	0.0035	-	-
Na	-3.2889E-07	0.4776	-8.4997E-07	1.0758E-09
Al	4.1242E-07	0.5322	-4.5436E-07	3.3051E-10
Si	-2.7550E-08	0.0012	-6.9947E-08	3.5870E-11
Cr	4.2332E-06	0.2924	-2.9153E-05	2.2403E-09
Total	**3.6206E-02**	**0.0039**	**-**	**2.5073E-09**

Table 120: Elemental density sensitivities in k_{eff} for the polyethylene composition in Case 2.

Element	Unconstrained Sensitivity, $S_{k,i}$	FSD, $S_{k,i}/\sigma(S_{k,i})$	Constrained Sensitivity, $S_{k,i}^{CPA}$	u_k/k
H	1.2397E-01	0.0028	-	-
C	4.0642E-02	0.0041	-	-
Na	7.8431E-07	0.7073	-1.5851E-06	2.0061E-09
Al	5.9621E-07	0.8500	-3.3451E-06	2.4333E-09
Si	3.3411E-08	2.8748	-1.5937E-07	8.1728E-11
Cr	1.2262E-05	0.2211	-1.3955E-04	1.0723E-08
Total	**1.6462E-01**	**0.0023**	**-**	**1.1178E-08**

Table 121: Elemental density sensitivities in k_{eff} for the polyethylene composition in Case 3.

Element	Unconstrained Sensitivity, $S_{k,i}$	FSD, $S_{k,i}/\sigma(S_{k,i})$	Constrained Sensitivity, $S_{k,i}^{CPA}$	u_k/k
H	1.5349E-01	0.0021	-	-
C	4.6483E-02	0.0032	-	-
Na	7.2563E-07	0.8882	-2.1527E-06	2.7246E-09
Al	1.0480E-06	0.5461	-3.7400E-06	2.7205E-09
Si	2.4038E-08	4.4411	-2.1016E-07	1.0777E-10
Cr	5.4589E-06	0.5282	-1.7896E-04	1.3752E-08
Total	**1.9998E-01**	**0.0018**	**-**	**1.4281E-08**

Table 122: Elemental density sensitivities in k_{eff} for the polyethylene composition in Case 4.

Element	Unconstrained Sensitivity, $S_{k,i}$	FSD, $S_{k,i}/\sigma(S_{k,i})$	Constrained Sensitivity, $S_{k,i}^{CPA}$	u_k/k
H	2.0612E-01	0.0018	-	-
C	5.3083E-02	0.0032	-	-
Na	1.0940E-07	6.4091	-3.6216E-06	4.5836E-09
Al	9.0539E-07	0.6519	-5.3008E-06	3.8559E-09
Si	7.4573E-08	1.5980	-2.2899E-07	1.1743E-10
Cr	6.6959E-07	4.3435	-2.3838E-04	1.8318E-08
Total	**2.5921E-01**	**0.0016**	**-**	**1.9273E-08**

Table 123: Elemental density sensitivities in k_{eff} for the polyethylene composition in Case 5.

Element	Unconstrained Sensitivity, $S_{k,i}$	FSD, $S_{k,i}/\sigma(S_{k,i})$	Constrained Sensitivity, $S_{k,i}^{CPA}$	u_k/k
H	3.3690E-02	0.0136	-	-
C	3.5002E-02	0.0074	-	-
Na	-4.3052E-08	19.6548	-1.0318E-06	1.3059E-09
Al	1.6351E-07	4.0632	-1.4812E-06	1.0774E-09
Si	1.7054E-08	8.9036	-6.3393E-08	3.2509E-11
Cr	-1.3924E-04	0.0274	-2.0259E-04	1.5567E-08
Total	**6.8553E-02**	**0.0077**	**-**	**1.5659E-08**

Table 124: Elemental density sensitivities in k_{eff} for the polyethylene composition in Case 6.

Element	Unconstrained Sensitivity, $S_{k,i}$	FSD, $S_{k,i}/\sigma(S_{k,i})$	Constrained Sensitivity, $S_{k,i}^{CPA}$	u_k/k
H	1.3153E-01	0.0029	-	-
C	4.5686E-02	0.0035	-	-
Na	1.4650E-06	0.4733	-1.0858E-06	1.3743E-09
Al	5.8533E-07	0.9904	-3.6578E-06	2.6608E-09
Si	1.5703E-07	0.8936	-5.0518E-08	2.5907E-11
Cr	1.5673E-05	0.2071	-1.4776E-04	1.1355E-08
Total	**1.7724E-01**	**0.0023**	**-**	**1.1743E-08**

Table 125: Elemental density sensitivities in k_{eff} for the polyethylene composition in Case 7.

Element	Unconstrained Sensitivity, $S_{k,i}$	FSD, $S_{k,i}/\sigma(S_{k,i})$	Constrained Sensitivity, $S_{k,i}^{CPA}$	u_k/k
H	-2.3359E-03	0.0296	-	-
C	1.5421E-02	0.0026	-	-
Na	3.5862E-07	0.5146	1.7027E-07	2.1550E-10
Al	2.2173E-07	0.6516	-9.1579E-08	6.6617E-11
Si	4.2499E-08	0.9510	2.7174E-08	1.3935E-11
Cr	3.7436E-06	0.1886	-8.3245E-06	6.3968E-10
Total	**1.3090E-02**	**0.0061**	**-**	**6.7843E-10**

2.4.5 Aluminum Composition

The aluminum composition is based on the handbook data reported for Al-6061 in Table 55 of Section 1.3.4. There is an average 2.695 Wt.% impurities in reported composition. The elemental compositions presented in Table 55 represent an upper and lower bound (Mg, Si, Cu, and Cr), a maximum upper bound with no lower bound (Fe, Zn, Mn, and Ti), or the main constituent as the remainder (Al). Table 126 presents the evaluated elemental composition for Al-6061. The uncertainty of the elemental composition is based on the range of the specification, assuming a lower bound of 0 if not given. The standard uncertainty assumes a uniform distribution within this range. Aluminum is treated as the remainder, including the other and unknown impurities.

Table 126: Aluminum elemental composition and uncertainties.

Element	Elemental Composition (Wt.%)	
	Average	Uncertainty
Al[(a)]	9.73050E+01	-
Mg	1.00000E+00	1.15470E-01
Si	6.00000E-01	1.15470E-01
Cu	2.75000E-01	7.21688E-02
Cr	1.95000E-01	8.94893E-02
Fe	3.50000E-01	1.01036E-01
Zn	1.25000E-01	3.60844E-02
Mn	7.50000E-02	2.16506E-02
Ti	7.50000E-02	2.16506E-02

[(a)] Treated as the remainder.

Table 127 summarizes the aluminum composition uncertainty calculation parameters and sensitivity in k_{eff}. The calculated effect in k_{eff} is based on the sum of the effect in k_{eff} to the constrained sensitivities as described in Section 2.4. The standard uncertainty is based on the impurity content reported in Table 126. Table 127 is reproduced alongside the other evaluated uncertainties in Section 2.6.

Table 127: Summary of sensitivity in k_{eff} to uncertainties in the aluminum composition.

Case	Parameter Value (Wt.%)	Calculated Effect in k_{eff}	Standard Uncertainty	Standard Uncertainty in k_{eff}
1	Varies (Table 126)	Negligible	Varies (Table 126)	Negligible
2		Negligible		Negligible
3		Negligible		Negligible
4		Negligible		Negligible
5		Negligible		Negligible
6		Negligible		Negligible
7		Negligible		Negligible

The following tables report the unconstrained and constrained elemental density sensitivities for the aluminum composition, calculated as described in Section 2.4. These tables include: Table 128 for Case 1, Table 129 for Case 2, Table 130 for Case 3, Table 131 for Case 4, Table 132 for Case 5, Table 133 for Case 6, and Table 134 for Case 7.

Table 128: Elemental density sensitivities in k_{eff} for the aluminum composition in Case 1.

Element	Unconstrained Sensitivity, $S_{k,i}$	FSD, $S_{k,i}/\sigma(S_{k,i})$	Constrained Sensitivity, $S_{k,i}^{CPA}$	u_k/k
Al	2.2414E-03	0.0233	-	-
Mg	4.7183E-05	0.1802	2.4148E-05	2.7884E-06
Si	4.3272E-07	12.6012	-1.3388E-05	2.5766E-06
Ti	1.8682E-06	0.8087	-4.4663E-06	1.1721E-06
Cr	6.0993E-07	4.3974	-3.8819E-06	1.7815E-06
Mn	3.1391E-07	5.2263	-7.7483E-06	2.2367E-06
Fe	-1.6055E-06	1.8353	-4.4848E-06	1.2947E-06
Cu	1.8068E-06	1.4284	7.9231E-08	2.2872E-08
Zn	5.8073E-06	0.3371	4.0797E-06	1.1777E-06
Total	**2.2978E-03**	**0.0233**	**-**	**4.3878E-06**

Table 129: Elemental density sensitivities in k_{eff} for the aluminum composition in Case 2.

Element	Unconstrained Sensitivity, $S_{k,i}$	FSD, $S_{k,i}/\sigma(S_{k,i})$	Constrained Sensitivity, $S_{k,i}^{CPA}$	u_k/k
Al	3.1181E-05	0.1844	-	-
Mg	2.4129E-03	0.0234	2.4126E-03	2.7859E-04
Si	3.7105E-06	1.0528	3.5183E-06	6.7709E-07
Ti	4.6758E-06	0.2971	4.5877E-06	1.2040E-06
Cr	1.6051E-06	1.1396	1.5426E-06	7.0792E-07
Mn	7.7241E-07	2.8087	6.6025E-07	1.9060E-07
Fe	2.3772E-06	1.0225	2.3371E-06	6.7466E-07
Cu	8.3489E-06	0.3011	8.3249E-06	2.4032E-06
Zn	2.4561E-06	0.6776	2.4321E-06	7.0209E-07
Total	**2.4681E-03**	**0.0231**	**-**	**3.0280E-06**

Table 130: Elemental density sensitivities in k_{eff} for the aluminum composition in Case 3.

Element	Unconstrained Sensitivity, $S_{k,i}$	FSD, $S_{k,i}/\sigma(S_{k,i})$	Constrained Sensitivity, $S_{k,i}^{CPA}$	u_k/k
Al	2.9089E-05	0.1764	-	-
Mg	2.2467E-03	0.0169	2.2464E-03	2.5940E-04
Si	1.2616E-05	0.2520	1.2437E-05	2.3935E-06
Ti	3.9077E-06	0.3406	3.8254E-06	1.0039E-06
Cr	2.1476E-07	6.8836	1.5647E-07	7.1805E-08
Mn	-2.8028E-06	0.6863	-2.9074E-06	8.3930E-07
Fe	3.3849E-06	0.6922	3.3475E-06	9.6635E-07
Cu	6.1160E-07	3.2641	5.8918E-07	1.7008E-07
Zn	1.5872E-06	0.8648	1.5648E-06	4.5171E-07
Total	**2.2953E-03**	**0.0168**	**-**	**2.9348E-06**

Table 131: Elemental density sensitivities in k_{eff} for the aluminum composition in Case 4.

Element	Unconstrained Sensitivity, $S_{k,i}$	FSD, $S_{k,i}/\sigma(S_{k,i})$	Constrained Sensitivity, $S_{k,i}^{CPA}$	u_k/k
Al	2.8459E-05	0.1418	-	-
Mg	1.9803E-03	0.0173	1.9800E-03	2.2863E-04
Si	8.2646E-06	0.3337	8.0891E-06	1.5568E-06
Ti	-8.2402E-07	1.4178	-9.0445E-07	2.3736E-07
Cr	1.5521E-06	0.9731	1.4950E-06	6.8611E-07
Mn	-4.9865E-06	0.3773	-5.0889E-06	1.4690E-06
Fe	-1.9998E-06	0.9212	-2.0363E-06	5.8783E-07
Cu	1.7804E-06	0.9746	1.7584E-06	5.0761E-07
Zn	1.9031E-06	0.6390	1.8812E-06	5.4305E-07
Total	**2.0144E-03**	**0.0173**	**-**	**2.4509E-06**

Table 132: Elemental density sensitivities in k_{eff} for the aluminum composition in Case 5.

Element	Unconstrained Sensitivity, $S_{k,i}$	FSD, $S_{k,i}/\sigma(S_{k,i})$	Constrained Sensitivity, $S_{k,i}^{CPA}$	u_k/k
Al	1.7228E-05	0.1773	-	-
Mg	1.0249E-03	0.0244	1.0247E-03	1.1833E-04
Si	7.4173E-06	0.2866	7.3111E-06	1.4070E-06
Ti	-3.7124E-06	0.2149	-3.7611E-06	9.8704E-07
Cr	-3.3319E-06	0.3341	-3.3664E-06	1.5449E-06
Mn	-7.4969E-06	0.1633	-7.5589E-06	2.1821E-06
Fe	-6.0332E-06	0.2697	-6.0553E-06	1.7480E-06
Cu	-5.7846E-06	0.2441	-5.7979E-06	1.6737E-06
Zn	-6.5529E-07	1.2505	-6.6857E-07	1.9300E-07
Total	**1.0226E-03**	**0.0249**	**-**	**3.9995E-06**

Table 133: Elemental density sensitivities in k_{eff} for the aluminum composition in Case 6.

Element	Unconstrained Sensitivity, $S_{k,i}$	FSD, $S_{k,i}/\sigma(S_{k,i})$	Constrained Sensitivity, $S_{k,i}^{CPA}$	u_k/k
Al	3.0446E-05	0.1619	-	-
Mg	2.0062E-03	0.0185	2.0059E-03	2.3162E-04
Si	1.1074E-05	0.2623	1.0886E-05	2.0951E-06
Ti	6.0309E-07	2.4150	5.1705E-07	1.3569E-07
Cr	1.3216E-06	1.2218	1.2606E-06	5.7851E-07
Mn	-2.1137E-06	0.9416	-2.2232E-06	6.4179E-07
Fe	4.4977E-06	0.4576	4.4586E-06	1.2871E-06
Cu	2.8484E-06	0.7363	2.8249E-06	8.1549E-07
Zn	1.7093E-06	0.8109	1.6858E-06	4.8666E-07
Total	**2.0566E-03**	**0.0184**	**-**	**2.7772E-06**

Table 134: Elemental density sensitivities in k_{eff} for the aluminum composition in Case 7.

Element	Unconstrained Sensitivity, $S_{k,i}$	FSD, $S_{k,i}/\sigma(S_{k,i})$	Constrained Sensitivity, $S_{k,i}^{CPA}$	u_k/k
Al	3.2286E-05	0.1893	-	-
Mg	1.8419E-03	0.0327	1.8415E-03	2.1264E-04
Si	8.1337E-06	0.6281	7.9346E-06	1.5270E-06
Ti	5.3425E-07	2.8467	4.4300E-07	1.1626E-07
Cr	3.0233E-06	0.6711	2.9586E-06	1.3577E-06
Mn	1.7525E-06	0.6788	1.6364E-06	4.7238E-07
Fe	3.9907E-06	0.6076	3.9492E-06	1.1400E-06
Cu	4.8112E-06	0.4922	4.7863E-06	1.3817E-06
Zn	2.1391E-06	0.7179	2.1142E-06	6.1031E-07
Total	**1.8985E-03**	**0.0321**	**-**	**2.8272E-06**

2.5 Temperature Uncertainty

The temperature of the experimental configurations and ambient temperature of the experiment room was measured for all cases. These temperature measurements are reported in Table 57 of Section 1.4. All experiments were conducted at slightly below 20.5 °C (293.6 K). The measured temperatures of the experimental configurations ranged from 15.5 °C (288.7 K) to 18.3 °C (291.5 K) while the ambient temperature of the room ranged from 13.3 °C (286.5 K) to 16.8 °C (289.0 K). On average, the ambient temperature of the room was −2.3 °C lower than the temperature of the Comet structure, ranging from −1.5 °C to −2.7 °C.

Table 135 reports the evaluated temperatures of the experimental configurations. These temperatures are based on RTD #3, which was in contact with the Comet structure. This temperature is expected to be more representative of the material temperature than the ambient air temperature which may fluctuate more quickly due to changes in the environment. The RTDs used to perform these measurements are confirmed to meet a ±2.0 °C tolerance annually. Therefore, the evaluated uncertainty in the temperatures of the experiment configurations is ±2.0 °C. Furthermore, this uncertainty largely captures the difference between the RTD #3 (Comet) and RTD #5 (ambient) temperatures.

Table 135: Temperatures of the experimental configurations.

Case	Temperature (°C)
1	16.0
2	16.6
3	18.3
4	16.4
5	16.7
6	15.5
7	16.0

2.5.1 Thermal Contraction

The thermal contraction uncertainty evaluates the effect of thermal contraction due to change in temperature. The thermal contraction is modeled using linear contraction in each dimension to capture the overall contraction of the volume. Linear contraction is defined as

$$\frac{\Delta L}{L} = \alpha_L \Delta T \tag{8}$$

where L is the dimension, ΔT is the change in temperature, and α_L is the linear coefficient of thermal expansion (CTE). Table 136 shows the linear coefficients of thermal expansion for uranium, hafnium, polyethylene, and aluminum.

Table 136: Typical linear coefficients of thermal expansion.

Material	CTE, α_L ($\frac{\mu m}{m\,^\circ C}$)
Uranium, U; Cast	19.0
Hafnium, Hf	5.9
Aluminum, Al	24.0
High Density Polyethylene, Extruded	110.0[a]

[a] Based on a reference value provided by the manufacturer.

Table 137 summarizes the calculation parameters and sensitivity in k_{eff} of thermal contraction due to uncertainty in temperature. The calculations use Eq. 8 with the CTE values from Table 136 to perturb each part within the experimental configurations by $\pm 10.0\,^\circ$C. The standard uncertainty is calculated using Eq. 3 with the evaluated uncertainty of $\pm 2.0\,^\circ$C. Table 137 is reproduced alongside the other evaluated uncertainties in Section 2.6.

Table 137: Summary of sensitivity in k_{eff} to thermal contraction due to uncertainties in temperature.

Case	Parameter Value (°C)	Parameter Variation in Calculation	Calculated Effect in k_{eff}	Standard Uncertainty	Standard Uncertainty in k_{eff}
1	16.0	±10.0	±0.00044	±2.0	±0.00009
2	16.6		±0.00111		±0.00022
3	18.3		±0.00112		±0.00022
4	16.4		±0.00148		±0.00030
5	16.7		±0.00014		Negligible
6	15.5		±0.00101		±0.00020
7	16.0		±0.00047		±0.00009

2.5.2 Doppler Broadening

The neutron cross section uncertainty evaluates the effect of Doppler Broadening in the incident neutron interaction cross sections due to change in temperature. The ACE-formatted neutron cross sections based on ENDF/B-VIII.0 distributed for use with MCNP® include the following temperatures (with ACE library identifier)[14]: 293.6 K (00c), 600 K (01c), 900 K (02c), 1200 K (03c), 2500 K (04c), 0.1 K (05c), and 250 K (06c). Of the available neutron cross section temperatures, 293.6 K (20.5 °C), referred to here as room temperature, and 250 K (−23.2 °C) are relevant to this analysis as they bound the measured experiment temperatures reported in Table 57 of Section 1.4.

In addition to Doppler Broadening of the neutron cross sections, the neutron collision kinematics must account for changes in temperature. In MCNP® 6.2, this is done using the free-gas thermal treatment (TMP) card. The free-gas thermal treatment card uses temperature in units of MeV, which can be converted from Kelvin using

$$kT = T \times 8.617 \times 10^{-8} \tag{9}$$

where kT is the temperature in MeV and T is the temperature in Kelvin. By default, MCNP® 6.2 uses 2.53×10^{-8} MeV which corresponds to room temperature.

Table 138 summarizes the calculation parameters and sensitivity in k_{eff} of the the neutron cross section due to uncertainty in temperature. The calculations vary the neutron cross sections and free gas thermal treatment between 293.6 K (2.530×10^{-8} MeV) and 250 K (2.154×10^{-5} MeV), representing a perturbation in temperature of 43.6 °C. The standard uncertainty is calculated using Eq. 3 with the evaluated uncertainty of ±2.0 °C. Table 138 is reproduced alongside the other evaluated uncertainties in Section 2.6.

Table 138: Summary of sensitivity in k_{eff} to the neutron cross sections with free-gas thermal treatment due to uncertainties in temperature.

Case	Parameter Value (°C)	Parameter Variation in Calculation	Calculated Effect in k_{eff}	Standard Uncertainty	Standard Uncertainty in k_{eff}
1	16.0	±43.6	±0.00013	±2.0	Negligible
2	16.6		±0.00031		Negligible
3	18.3		±0.00049		Negligible
4	16.4		±0.00058		Negligible
5	16.7		∓0.00059		Negligible
6	15.5		±0.00054		Negligible
7	16.0		±0.00026		Negligible

[14] J. L. Conlin et al. *Release of ENDF/B-VIII.0-Based ACE Data Files*. LA-UR-18-24034. Los Alamos National Laboratory, 2018. DOI: 10.2172/1438139.

2.5.3 Thermal Scattering Law

The thermal scattering law uncertainty evaluates the effect in k_{eff} due to changes in temperature of the thermal scattering laws. The thermal scattering laws in ENDF/B-VIII.0 relevant to these experimental configurations are polyethylene (^{1}H in CH_2) and aluminum (^{27}Al). This uncertainty evaluation is specific to the polyethylene thermal scattering law as the aluminum thermal scattering law does not have a significant effect in k_{eff}.

The ACE-formatted thermal scattering laws based on ENDF/B-VIII.0 for polyethylene distributed for use with MCNP® include the following temperatures (with ACE library identifier)[15]: 293.6 K (40t), 77 K (41t), 196 K (42t), 233 K (43t), 300 K (44t), 303 K (45t), 313 K (46t), 323 K (47t), 333 K (48t), and 343 K (49t). By default, MCNP® 6.2 uses thermal scattering laws at 293.6 K (20.5 °C), referred to here as room temperature. In MCNP® 6.2, thermal scattering laws replace the free-gas incident neutron interaction cross sections when the MT card is used and the thermal scattering law exists at the given energy of incident interaction. The polyethylene thermal scattering law is specific to the ^{1}H neutron cross section.

In addition to the temperatures distributed for MCNP®, thermal scattering laws for polyethylene were generated at the following temperatures[16]: 258 K, 263 K, and 268 K. These additional thermal scattering laws provide temperatures below room temperature, while being closer to the measured experiment temperature than the available 233 K thermal scattering law.

Table 139 reports the temperatures of the nine polyethylene thermal scattering laws evaluated as part of this uncertainty: room temperature (293.6 K); three temperatures above (300 K, 303 K, 313 K); three temperatures below (258 K, 263 K, 268 K); and two representing a large change in temperature from room temperature (233 K, 343 K).

Table 139: Thermal scattering law temperatures evaluated for polyethylene (^{1}H in CH_2).

Temperature (K)	Temperature (°C)
233.0	-40.1
258.0	-15.1
263.0	-10.1
268.0	-5.1
293.6[(a)]	20.5
300.0	26.9
303.0	29.9
313.0	39.9
343.0	69.9

[(a)] Room temperature.

Figure 33 shows a plot of Δk_{eff}, defined as the change in k_{eff} compared to room temperature, for the polyethylene

[15] The original ACE-formatted thermal scattering law library based on ENDF/B-VIII.0 distributed for MCNP® in 2018 included a processing error. This processing error was corrected and the ACE-formatted thermal scattering law library re-released in 2020. These calculations use the corrected thermal scattering law library. For more information, refer to: D. K. Parsons and C. A. Toccoli. *Re-Release of the ENDF/B VIII.0 S(α,β) Data Processed by NJOY2016*. LA-UR-20-24456. Los Alamos National Laboratory, 2020. DOI: 10.2172/1634930.

[16] These additional thermal scattering laws were provided by Ayman Hawari of North Carolina State University. They were generated using the Full Law Analysis Scattering System Hub (FLASSH) code. Dr. Hawari also provided the ^{1}H in CH_2 thermal scattering laws for the ENDF/B-VIII.0 library using the same methodology.

thermal scattering laws. The results are fit using linear least squares where the slope represents the sensitivity in k_{eff} to the temperature of the polyethylene thermal scattering law. Table 140 reports the parameters of a linear least squares fit to the five temperatures closest to the experiment temperature: 258 K, 263 K, 293.6 K, 303 K, and 313 K. All fits have a coefficient of determination exceeding 0.99, except Case 7 which is not sensitive to the polyethylene thermal scattering.

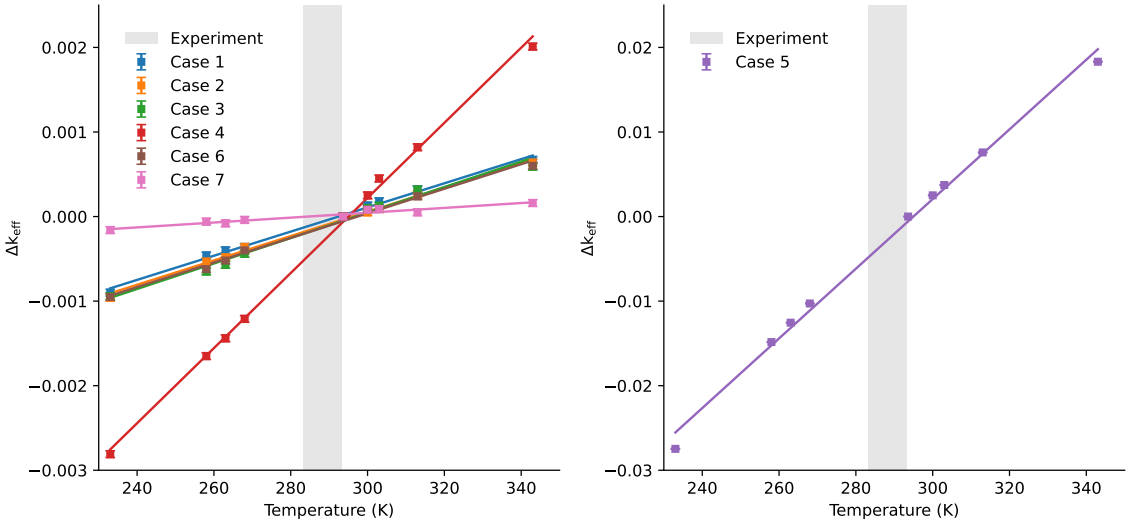

Figure 33: Effect of the polyethylene thermal scattering law at various temperatures. The plot includes error bars for the Monte Carlo statistical uncertainty (±0.00004) and the linear least-squares fit. The gray area represents the measured range in temperatures of the experimental configurations. Notice the y-axis scales, the right plot showing Case 5 is an order of magnitude large in Δk_{eff}.

Table 140: Parameters of the least squares fit for the change in k_{eff} due to the temperature of the polyethylene (^{1}H in CH_2) thermal scattering law.

Case	Slope (K^{-1})	y-Intercept	Coefficient of Determination, R^2
1	1.45870E-05	-4.25503E-03	0.99458
2	1.39195E-05	-4.11445E-03	0.99136
3	1.73982E-05	-5.12372E-03	0.99641
4	4.66869E-05	-1.37205E-02	0.99933
5	4.04586E-04	-1.18840E-01	0.99984
6	1.53793E-05	-4.54127E-03	0.99248
7	3.75293E-06	-1.06158E-03	0.89295

Table 141 summarizes the calculation parameters and sensitivity in k_{eff} of the polyethylene (^{1}H in CH_2) thermal scattering law due to uncertainty in temperature. The effect in k_{eff} is based on the slope of the linear least squares fit reported in Table 140. The standard uncertainty is calculated using Eq. 3 with the evaluated uncertainty of ±2.0 °C. Table 141 is reproduced alongside the other evaluated uncertainties in Section 2.6.

Table 141: Summary of sensitivity in k_{eff} to the polyethylene thermal scattering law due to uncertainties in temperature.

Case	Parameter Value (°C)	Calculated Effect in k_{eff}	Standard Uncertainty	Standard Uncertainty in k_{eff}
1	16.0	±0.00001/°C	±2.0	Negligible
2	16.6	±0.00001/°C		Negligible
3	18.3	±0.00002/°C		Negligible
4	16.4	±0.00005/°C		0.00009
5	16.7	±0.00040/°C		0.00081
6	15.5	±0.00002/°C		Negligible
7	16.0	±0.00000/°C		Negligible

2.6 Combined Uncertainty

Table 142 presents the total combined uncertainty for the experimental configurations. These combined uncertainties are broken down into individual parameters for mass, dimension, material, and temperature in Table 143 (Case 1), Table 144 (Case 2), Table 145 (Case 3), Table 146 (Case 4), Table 147 (Case 5), Table 148 (Case 6), and Table 149 (Case 7). These tables summarize the uncertainty calculations previously described in Sections 2.1, 2.2, 2.3, 2.4, and 2.5.

Table 142: Summary of calculated uncertainties for the experimental configurations.

Case	Standard Uncertainty in k_{eff}
1	±0.00146
2	±0.00157
3	±0.00153
4	±0.00123
5	±0.00146
6	±0.00141
7	±0.00136

All configurations are found to be acceptable for use as benchmark data.

2.6.1 Case 1

Table 143: Summary of sensitivity in k_{eff} to uncertainties in Case 1.

Parameter (unit of measured)	N	Parameter Value	Parameter Variation in Calculation	Calculated Effect in k_{eff}	Standard Uncertainty	Standard Uncertainty in k_{eff}
Mass Uncertainty						
HEU Mass (g)	26	135407.1	$\pm 6.0 \times 26$	± 0.00134	$\pm 1.7\sqrt{26}$	± 0.00007
Hafnium Mass (g)	24	37675.9	$\pm 14.4 \times 24$	± 0.00007	$\pm 0.1\sqrt{24}$	Negligible
Polyethylene Moderator Mass (g)	No polyethylene moderator plates.					-
Polyethylene Reflector Mass (g)	10	11032.2	± 0.5 %	± 0.00115	$\pm 3.5\sqrt{10}$	± 0.00007
Aluminum Insert Mass (g)	19	3907.1	$\pm 3.0 \times 19$	± 0.00036	$\pm 0.1\sqrt{19}$	Negligible
Membrane Mass (g)	-	2396.1	± 20.0	± 0.00003	± 0.3	Negligible
Structure Mass (g)	-	27159.7	± 10 %	± 0.00143	± 0.1 %	Negligible
Sum in Quadrature (Mass Uncertainty)						**±0.00010**
Dimensional Uncertainty						
HEU Plate Dimensions (cm)	26	Varies (Table 77)	± 0.02	± 0.00103	$\pm 0.002/\sqrt{26}$	Negligible
Hafnium Plate Dimensions (cm)	24	Varies (Table 79)	± 0.02	± 0.00039	$\pm 0.003/\sqrt{24}$	Negligible
Polyethylene Plate Dimensions (cm)	4	Varies (Table 81)	± 0.02	± 0.00006	$\pm 0.010/\sqrt{4}$	Negligible
Polyethylene Ref. Dimensions (cm)	3	Varies (Table 90)	± 0.02	± 0.00081	$\pm 0.006/\sqrt{6}$	± 0.00014
Aluminum Insert Dimensions (cm)	19	Varies (Table 84)	± 0.01	± 0.00003	$\pm 0.005/\sqrt{19}$	Negligible
Upper Core Stack Height (cm)	-	8.307	± 0.141	± 0.00217	± 0.031	± 0.00048
Lower Core Stack Height (cm)	-	7.713	± 0.128	± 0.00221	± 0.074	± 0.00128
Upper Reflector Ring Height (cm)	-	8.484	± 0.15875	± 0.00013	± 0.004	Negligible
Lower Reflector Ring Height (cm)	-	6.467	± 0.15875	± 0.00003	± 0.004	Negligible
Membrane Thickness (cm)	-	0.3175	± 0.0254	± 0.00119	± 0.0073	± 0.00034
Membrane Lift (cm)	-	0.508	± 0.127	± 0.00020	± 0.073	± 0.00006
Sum in Quadrature (Dimensional Uncertainty)						**±0.00142**

Table 143 (continued): Summary of sensitivity in k_{eff} to uncertainties in Case 1.

Parameter (unit of measured)	N	Parameter Value	Parameter Variation in Calculation	Calculated Effect in k_{eff}	Standard Uncertainty	Standard Uncertainty in k_{eff}
Composition Uncertainty						
^{235}U Enrichment (Wt.%)	26	93.232	±0.103	±0.00158	$\pm 0.103/\sqrt{26}$	±0.00031
HEU Impurities (Wt.%)	26	Varies (Table 99)	-	±0.00023	Varies (Table 99)	Negligible
Hafnium Impurities (Wt.%)	24	Varies (Table 108)	-	±0.00003	Varies (Table 108)	Negligible
Polyethylene Impurities (Wt.%)	-	Varies (Table 117)	-	Negligible	Varies (Table 117)	Negligible
Aluminum Impurities (Wt.%)	-	Varies (Table 126)	-	Negligible	Varies (Table 126)	Negligible
Sum in Quadrature (Composition Uncertainty)						**±0.00031**
Temperature Uncertainty						
Thermal Contraction (°C)	-	20.5	±10.0	±0.00044	±2.0	±0.00009
Neutron Cross Sections (°C)	-	20.5	±43.6	±0.00013	±2.0	Negligible
Thermal Scattering Laws (°C)	-	20.5	Refer to Section 2.5.3	1.4587E-5/°C	±2.0	Negligible
Sum in Quadrature (Temperature Uncertainty)						**±0.00009**
Sum in Quadrature (Total Uncertainty)						**±0.00146**

2.6.2 Case 2

Table 144: Summary of sensitivity in k_{eff} to uncertainties in Case 2.

Parameter (unit of measured)	N	Parameter Value	Parameter Variation in Calculation	Calculated Effect in k_{eff}	Standard Uncertainty	Standard Uncertainty in k_{eff}
Mass Uncertainty						
HEU Mass (g)	17	99330.7	$\pm 6.0 \times 17$	± 0.00093	$\pm 1.7\sqrt{17}$	± 0.00006
Hafnium Mass (g)	15	23608.2	$\pm 14.4 \times 15$	± 0.00060	$\pm 0.1\sqrt{15}$	Negligible
Polyethylene Moderator Mass (g)	15	5160.6	$\pm 0.9 \times 15$	± 0.00075	$\pm 0.1\sqrt{15}$	Negligible
Polyethylene Reflector Mass (g)	11	10350.3	$\pm 0.5\,\%$	± 0.00122	$\pm 3.0\sqrt{11}$	± 0.00007
Aluminum Insert Mass (g)	10	624.5	$\pm 3.0 \times 10$	± 0.00010	$\pm 0.1\sqrt{10}$	Negligible
Membrane Mass (g)	-	2396.1	± 20.0	± 0.00010	± 0.3	Negligible
Structure Mass (g)	-	27159.7	$\pm 10\,\%$	± 0.00116	$\pm 0.1\,\%$	Negligible
Sum in Quadrature (Mass Uncertainty)						**±0.00009**
Dimensional Uncertainty						
HEU Plate Dimensions (cm)	17	Varies (Table 77)	± 0.02	± 0.00066	$\pm 0.002/\sqrt{17}$	Negligible
Hafnium Plate Dimensions (cm)	15	Varies (Table 79)	± 0.02	± 0.00013	$\pm 0.003/\sqrt{15}$	Negligible
Polyethylene Plate Dimensions (cm)	19	Varies (Table 81)	± 0.02	± 0.00044	$\pm 0.005/\sqrt{19}$	Negligible
Polyethylene Ref. Dimensions (cm)	7	Varies (Table 90)	± 0.02	± 0.00047	$\pm 0.010/\sqrt{7}$	± 0.00007
Aluminum Insert Dimensions (cm)	10	Varies (Table 84)	± 0.01	± 0.00006	$\pm 0.005/\sqrt{10}$	Negligible
Upper Core Stack Height (cm)	-	7.675	± 0.213	± 0.00288	± 0.050	± 0.00068
Lower Core Stack Height (cm)	-	8.570	± 0.160	± 0.00257	± 0.083	± 0.00133
Upper Reflector Ring Height (cm)	-	7.913	± 0.15875	± 0.00022	± 0.004	Negligible
Lower Reflector Ring Height (cm)	-	7.272	± 0.15875	± 0.00010	± 0.004	Negligible
Membrane Thickness (cm)	-	0.3175	± 0.0254	± 0.00090	± 0.0073	± 0.00026
Membrane Lift (cm)	-	0.508	± 0.127	± 0.00004	± 0.073	Negligible
Sum in Quadrature (Dimensional Uncertainty)						**±0.00152**

Table 144 (continued): Summary of sensitivity in k_{eff} to uncertainties in Case 2.

Parameter (unit of measured)	N	Parameter Value	Parameter Variation in Calculation	Calculated Effect in k_{eff}	Standard Uncertainty	Standard Uncertainty in k_{eff}
Composition Uncertainty						
^{235}U Enrichment (Wt.%)	17	93.232	±0.103	±0.00125	$\pm 0.103/\sqrt{17}$	±0.00030
HEU Impurities (Wt.%)	17	Varies (Table 99)	-	±0.00017	Varies (Table 99)	Negligible
Hafnium Impurities (Wt.%)	15	Varies (Table 108)	-	±0.00003	Varies (Table 108)	Negligible
Polyethylene Impurities (Wt.%)	-	Varies (Table 117)	-	Negligible	Varies (Table 117)	Negligible
Aluminum Impurities (Wt.%)	-	Varies (Table 126)	-	Negligible	Varies (Table 126)	Negligible
Sum in Quadrature (Composition Uncertainty)						**±0.00030**
Temperature Uncertainty						
Thermal Contraction (°C)	-	20.5	±10.0	±0.00111	±2.0	±0.00022
Neutron Cross Sections (°C)	-	20.5	±43.6	±0.00031	±2.0	Negligible
Thermal Scattering Laws (°C)	-	20.5	Refer to Section 2.5.3	1.3920E-5/°C	±2.0	Negligible
Sum in Quadrature (Temperature Uncertainty)						**±0.00022**
Sum in Quadrature (Total Uncertainty)						**±0.00157**

2.6.3 Case 3

Table 145: Summary of sensitivity in k_{eff} to uncertainties in Case 3.

Parameter (unit of measured)	N	Parameter Value	Parameter Variation in Calculation	Calculated Effect in k_{eff}	Standard Uncertainty	Standard Uncertainty in k_{eff}
Mass Uncertainty						
HEU Mass (g)	14	82823.0	$\pm 6.0 \times 14$	± 0.00078	$\pm 1.7\sqrt{14}$	± 0.00006
Hafnium Mass (g)	12	18929.2	$\pm 14.4 \times 12$	± 0.00116	$\pm 0.1\sqrt{12}$	Negligible
Polyethylene Moderator Mass (g)	12	8266.2	$\pm 0.9 \times 12$	± 0.00033	$\pm 0.1\sqrt{12}$	Negligible
Polyethylene Reflector Mass (g)	14	11112.8	$\pm 0.5\,\%$	± 0.00113	$\pm 3.7\sqrt{14}$	± 0.00008
Aluminum Insert Mass (g)	7	173.8	$\pm 3.0 \times 7$	± 0.00003	$\pm 0.1\sqrt{7}$	Negligible
Membrane Mass (g)	-	2396.1	± 20.0	± 0.00005	± 0.3	Negligible
Structure Mass (g)	-	27159.7	$\pm 10\,\%$	± 0.00098	$\pm 0.1\,\%$	Negligible
Sum in Quadrature (Mass Uncertainty)						**±0.00010**
Dimensional Uncertainty						
HEU Plate Dimensions (cm)	17	Varies (Table 77)	± 0.02	± 0.00066	$\pm 0.002/\sqrt{17}$	Negligible
Hafnium Plate Dimensions (cm)	15	Varies (Table 79)	± 0.02	± 0.00013	$\pm 0.003/\sqrt{15}$	Negligible
Polyethylene Plate Dimensions (cm)	19	Varies (Table 81)	± 0.02	± 0.00044	$\pm 0.010/\sqrt{19}$	Negligible
Polyethylene Ref. Dimensions (cm)	8	Varies (Table 90)	± 0.02	± 0.00041	$\pm 0.010/\sqrt{6}$	± 0.00006
Aluminum Insert Dimensions (cm)	10	Varies (Table 84)	± 0.01	± 0.00001	$\pm 0.005/\sqrt{10}$	Negligible
Upper Core Stack Height (cm)	-	9.201	± 0.243	± 0.00207	± 0.054	± 0.00046
Lower Core Stack Height (cm)	-	8.881	± 0.245	± 0.00381	± 0.089	± 0.00138
Upper Reflector Ring Height (cm)	-	9.122	± 0.15875	± 0.00024	± 0.004	Negligible
Lower Reflector Ring Height (cm)	-	9.752	± 0.15875	± 0.00015	± 0.004	Negligible
Membrane Thickness (cm)	-	0.3175	± 0.0254	± 0.00083	± 0.0073	± 0.00024
Membrane Lift (cm)	-	0.508	± 0.127	± 0.00008	± 0.073	Negligible
Sum in Quadrature (Dimensional Uncertainty)						**±0.00148**

Table 145 (continued): Summary of sensitivity in k_{eff} to uncertainties in Case 3.

Parameter (unit of measured)	N	Parameter Value	Parameter Variation in Calculation	Calculated Effect in k_{eff}	Standard Uncertainty	Standard Uncertainty in k_{eff}
Composition Uncertainty						
^{235}U Enrichment (Wt.%)	14	93.232	±0.103	±0.00121	$\pm 0.103/\sqrt{14}$	±0.00032
HEU Impurities (Wt.%)	14	Varies (Table 99)	-	±0.00014	Varies (Table 99)	Negligible
Hafnium Impurities (Wt.%)	12	Varies (Table 108)	-	±0.00004	Varies (Table 108)	Negligible
Polyethylene Impurities (Wt.%)	-	Varies (Table 117)	-	Negligible	Varies (Table 117)	Negligible
Aluminum Impurities (Wt.%)	-	Varies (Table 126)	-	Negligible	Varies (Table 126)	Negligible
Sum in Quadrature (Composition Uncertainty)						**±0.00032**
Temperature Uncertainty						
Thermal Contraction (°C)	-	20.5	±10.0	±0.00112	±2.0	±0.00022
Neutron Cross Sections (°C)	-	20.5	±43.6	±0.00049	±2.0	Negligible
Thermal Scattering Laws (°C)	-	20.5	Refer to Section 2.5.3	1.7398E-5/°C	±2.0	Negligible
Sum in Quadrature (Temperature Uncertainty)						**±0.00022**
Sum in Quadrature (Total Uncertainty)						**±0.00153**

2.6.4 Case 4

Table 146: Summary of sensitivity in k_{eff} to uncertainties in Case 4.

Parameter (unit of measured)	N	Parameter Value	Parameter Variation in Calculation	Calculated Effect in k_{eff}	Standard Uncertainty	Standard Uncertainty in k_{eff}
Mass Uncertainty						
HEU Mass (g)	10	63890.9	$\pm 6.0 \times 10$	± 0.00054	$\pm 1.7\sqrt{10}$	± 0.00005
Hafnium Mass (g)	9	14214.7	$\pm 14.4 \times 9$	± 0.00193	$\pm 0.1\sqrt{9}$	Negligible
Polyethylene Moderator Mass (g)	9	12432.6	$\pm 0.9 \times 9$	± 0.00115	$\pm 0.1\sqrt{9}$	Negligible
Polyethylene Reflector Mass (g)	9	12046.3	$\pm 0.5\,\%$	± 0.00089	$\pm 3.9\sqrt{9}$	± 0.00006
Aluminum Insert Mass (g)	5	123.9	$\pm 3.0 \times 5$	± 0.00001	$\pm 0.1\sqrt{5}$	Negligible
Membrane Mass (g)	-	2396.1	± 20.0	± 0.00001	± 0.3	Negligible
Structure Mass (g)	-	27159.7	$\pm 10\,\%$	± 0.00093	$\pm 0.1\,\%$	Negligible
Sum in Quadrature (Mass Uncertainty)						**±0.00008**
Dimensional Uncertainty						
HEU Plate Dimensions (cm)	10	Varies (Table 77)	± 0.02	± 0.00020	$\pm 0.002/\sqrt{10}$	Negligible
Hafnium Plate Dimensions (cm)	9	Varies (Table 79)	± 0.02	± 0.00020	$\pm 0.003/\sqrt{9}$	Negligible
Polyethylene Plate Dimensions (cm)	11	Varies (Table 81)	± 0.02	± 0.00086	$\pm 0.010/\sqrt{11}$	± 0.00006
Polyethylene Ref. Dimensions (cm)	7	Varies (Table 90)	± 0.02	± 0.00046	$\pm 0.010/\sqrt{6}$	± 0.00007
Aluminum Insert Dimensions (cm)	5	Varies (Table 84)	± 0.01	± 0.00010	$\pm 0.005/\sqrt{5}$	Negligible
Upper Core Stack Height (cm)	-	9.673	± 0.123	± 0.00153	± 0.036	± 0.00045
Lower Core Stack Height (cm)	-	11.013	± 0.211	± 0.00251	± 0.087	± 0.00103
Upper Reflector Ring Height (cm)	-	9.752	± 0.15875	± 0.00016	± 0.004	Negligible
Lower Reflector Ring Height (cm)	-	9.791	± 0.15875	± 0.00010	± 0.004	Negligible
Membrane Thickness (cm)	-	0.3175	± 0.0254	± 0.00073	± 0.0073	± 0.00021
Membrane Lift (cm)	-	0.508	± 0.127	± 0.00010	± 0.073	Negligible
Sum in Quadrature (Dimensional Uncertainty)						**±0.00115**

Table 146 (continued): Summary of sensitivity in k_{eff} to uncertainties in Case 4.

Parameter (unit of measured)	N	Parameter Value	Parameter Variation in Calculation	Calculated Effect in k_{eff}	Standard Uncertainty	Standard Uncertainty in k_{eff}
Composition Uncertainty						
^{235}U Enrichment (Wt.%)	10	93.232	±0.103	±0.00089	$\pm 0.103/\sqrt{10}$	±0.00028
HEU Impurities (Wt.%)	10	Varies (Table 99)	-	±0.00011	Varies (Table 99)	Negligible
Hafnium Impurities (Wt.%)	9	Varies (Table 108)	-	±0.00006	Varies (Table 108)	Negligible
Polyethylene Impurities (Wt.%)	-	Varies (Table 117)	-	Negligible	Varies (Table 117)	Negligible
Aluminum Impurities (Wt.%)	-	Varies (Table 126)	-	Negligible	Varies (Table 126)	Negligible
Sum in Quadrature (Composition Uncertainty)						**±0.00028**
Temperature Uncertainty						
Thermal Contraction (°C)	-	20.5	±10.0	±0.00148	±2.0	±0.00030
Neutron Cross Sections (°C)	-	20.5	±43.6	±0.00058	±2.0	Negligible
Thermal Scattering Laws (°C)	-	20.5	Refer to Section 2.5.3	4.6687E-5/°C	±2.0	±0.00009
Sum in Quadrature (Temperature Uncertainty)						**±0.00031**
Sum in Quadrature (Total Uncertainty)						**±0.00123**

2.6.5 Case 5

Table 147: Summary of sensitivity in k_{eff} to uncertainties in Case 5.

Parameter (unit of measured)	N	Parameter Value	Parameter Variation in Calculation	Calculated Effect in k_{eff}	Standard Uncertainty	Standard Uncertainty in k_{eff}
Mass Uncertainty						
HEU Mass (g)	12	70336.1	$\pm 6.0 \times 12$	± 0.00033	$\pm 1.7\sqrt{12}$	Negligible
Hafnium Mass (g)	10	15799.5	$\pm 14.4 \times 10$	± 0.00282	$\pm 0.1\sqrt{10}$	Negligible
Polyethylene Moderator Mass (g)	10	41551.3	$\pm 0.9 \times 10$	± 0.00030	$\pm 0.1\sqrt{10}$	Negligible
Polyethylene Reflector Mass (g)	16	22372.7	± 0.5 %	± 0.00033	$\pm 5.0\sqrt{16}$	Negligible
Aluminum Insert Mass (g)	5	123.9	$\pm 3.0 \times 5$	± 0.00005	$\pm 0.1\sqrt{5}$	Negligible
Membrane Mass (g)	-	2396.1	± 20.0	± 0.00006	± 0.3	Negligible
Structure Mass (g)	-	27159.7	± 10 %	± 0.00017	± 0.1 %	Negligible
Sum in Quadrature (Mass Uncertainty)						**Negligible**
Dimensional Uncertainty						
HEU Plate Dimensions (cm)	12	Varies (Table 77)	± 0.02	± 0.00030	$\pm 0.002/\sqrt{12}$	Negligible
Hafnium Plate Dimensions (cm)	10	Varies (Table 79)	± 0.02	± 0.00044	$\pm 0.003/\sqrt{10}$	Negligible
Polyethylene Plate Dimensions (cm)	13	Varies (Table 81)	± 0.02	± 0.00051	$\pm 0.010/\sqrt{13}$	± 0.00014
Polyethylene Ref. Dimensions (cm)	13	Varies (Table 90)	± 0.02	± 0.00012	$\pm 0.010/\sqrt{6}$	Negligible
Aluminum Insert Dimensions (cm)	5	Varies (Table 84)	± 0.01	± 0.00009	$\pm 0.005/\sqrt{5}$	Negligible
Upper Core Stack Height (cm)	-	25.533	± 0.327	± 0.00363	± 0.084	± 0.00093
Lower Core Stack Height (cm)	-	23.774	± 0.361	± 0.00225	± 0.116	± 0.00072
Upper Reflector Ring Height (cm)	-	25.548	± 0.15875	± 0.00005	± 0.004	Negligible
Lower Reflector Ring Height (cm)	-	22.408	± 0.15875	± 0.00005	± 0.004	Negligible
Membrane Thickness (cm)	-	0.3175	± 0.0254	± 0.00059	± 0.0073	± 0.00017
Membrane Lift (cm)	-	0.508	± 0.127	± 0.00002	± 0.073	Negligible
Sum in Quadrature (Dimensional Uncertainty)						**±0.00120**

Table 147 (continued): Summary of sensitivity in k_{eff} to uncertainties in Case 5.

Parameter (unit of measured)	N	Parameter Value	Parameter Variation in Calculation	Calculated Effect in k_{eff}	Standard Uncertainty	Standard Uncertainty in k_{eff}
Composition Uncertainty						
^{235}U Enrichment (Wt.%)	12	93.232	±0.103	±0.00062	$\pm 0.103/\sqrt{12}$	±0.00018
HEU Impurities (Wt.%)	12	Varies (Table 99)	-	±0.00006	Varies (Table 99)	Negligible
Hafnium Impurities (Wt.%)	10	Varies (Table 108)	-	±0.00008	Varies (Table 108)	Negligible
Polyethylene Impurities (Wt.%)	-	Varies (Table 117)	-	Negligible	Varies (Table 117)	Negligible
Aluminum Impurities (Wt.%)	-	Varies (Table 126)	-	Negligible	Varies (Table 126)	Negligible
Sum in Quadrature (Composition Uncertainty)						**±0.00018**
Temperature Uncertainty						
Thermal Contraction (°C)	-	20.5	±10.0	±0.00014	±2.0	Negligible
Neutron Cross Sections (°C)	-	20.5	±43.6	±0.00059	±2.0	Negligible
Thermal Scattering Laws (°C)	-	20.5	Refer to Section 2.5.3	4.0459E-4/°C	±2.0	±0.00081
Sum in Quadrature (Temperature Uncertainty)						**±0.00081**
Sum in Quadrature (Total Uncertainty)						**±0.00146**

2.6.6 Case 6

Table 148: Summary of sensitivity in k_{eff} to uncertainties in Case 6.

Parameter (unit of measured)	N	Parameter Value	Parameter Variation in Calculation	Calculated Effect in k_{eff}	Standard Uncertainty	Standard Uncertainty in k_{eff}
Mass Uncertainty						
HEU Mass (g)	15	88396.9	$\pm 6.0 \times 15$	± 0.00075	$\pm 1.7\sqrt{15}$	± 0.00005
Hafnium Mass (g)	13	20484.2	$\pm 14.4 \times 13$	± 0.00113	$\pm 0.1\sqrt{13}$	Negligible
Polyethylene Moderator Mass (g)	26	9022.5	$\pm 0.9 \times 26$	± 0.00117	$\pm 0.1\sqrt{26}$	Negligible
Polyethylene Reflector Mass (g)	12	11421.0	$\pm 0.5\,\%$	± 0.00096	$\pm 4.1\sqrt{12}$	± 0.00007
Aluminum Insert Mass (g)	8	323.7	$\pm 3.0 \times 8$	± 0.00002	$\pm 0.1\sqrt{8}$	Negligible
Membrane Mass (g)	-	2396.1	± 20.0	± 0.00007	± 0.3	Negligible
Structure Mass (g)	-	27159.7	$\pm 10\,\%$	± 0.00077	$\pm 0.1\,\%$	Negligible
Sum in Quadrature (Mass Uncertainty)						**±0.00009**
Dimensional Uncertainty						
HEU Plate Dimensions (cm)	15	Varies (Table 77)	± 0.02	± 0.00065	$\pm 0.002/\sqrt{15}$	Negligible
Hafnium Plate Dimensions (cm)	13	Varies (Table 79)	± 0.02	± 0.00010	$\pm 0.003/\sqrt{13}$	Negligible
Polyethylene Plate Dimensions (cm)	32	Varies (Table 81)	± 0.02	± 0.00617	$\pm 0.010/\sqrt{32}$	± 0.00027
Polyethylene Ref. Dimensions (cm)	6	Varies (Table 90)	± 0.02	± 0.00048	$\pm 0.010/\sqrt{6}$	± 0.00008
Aluminum Insert Dimensions (cm)	8	Varies (Table 84)	± 0.01	± 0.00001	$\pm 0.005/\sqrt{8}$	Negligible
Upper Core Stack Height (cm)	-	8.001	± 0.273	± 0.00229	± 0.061	± 0.00051
Lower Core Stack Height (cm)	-	11.077	± 0.240	± 0.00346	± 0.083	± 0.00120
Upper Reflector Ring Height (cm)	-	8.030	± 0.15875	± 0.00027	± 0.004	Negligible
Lower Reflector Ring Height (cm)	-	9.774	± 0.15875	± 0.00022	± 0.004	Negligible
Membrane Thickness (cm)	-	0.3175	± 0.0254	± 0.00083	± 0.0073	± 0.00024
Membrane Lift (cm)	-	0.508	± 0.127	± 0.00002	± 0.073	Negligible
Sum in Quadrature (Dimensional Uncertainty)						**±0.00135**

Table 148 (continued): Summary of sensitivity in k_{eff} to uncertainties in Case 6.

Parameter (unit of measured)	N	Parameter Value	Parameter Variation in Calculation	Calculated Effect in k_{eff}	Standard Uncertainty	Standard Uncertainty in k_{eff}
Composition Uncertainty						
^{235}U Enrichment (Wt.%)	15	93.232	±0.103	±0.00132	$\pm 0.103/\sqrt{15}$	±0.00034
HEU Impurities (Wt.%)	15	Varies (Table 99)	-	±0.00015	Varies (Table 99)	Negligible
Hafnium Impurities (Wt.%)	13	Varies (Table 108)	-	±0.00004	Varies (Table 108)	Negligible
Polyethylene Impurities (Wt.%)	-	Varies (Table 117)	-	Negligible	Varies (Table 117)	Negligible
Aluminum Impurities (Wt.%)	-	Varies (Table 126)	-	Negligible	Varies (Table 126)	Negligible
Sum in Quadrature (Composition Uncertainty)						**±0.00034**
Temperature Uncertainty						
Thermal Contraction (°C)	-	20.5	±10.0	±0.00101	±2.0	±0.00020
Neutron Cross Sections (°C)	-	20.5	±43.6	±0.00054	±2.0	Negligible
Thermal Scattering Laws (°C)	-	20.5	Refer to Section 2.5.3	1.5379E-5/°C	±2.0	Negligible
Sum in Quadrature (Temperature Uncertainty)						**±0.00020**
Sum in Quadrature (Total Uncertainty)						**±0.00141**

2.6.7 Case 7

Table 149: Summary of sensitivity in k_{eff} to uncertainties in Case 7.

Parameter (unit of measured)	N	Parameter Value	Parameter Variation in Calculation	Calculated Effect in k_{eff}	Standard Uncertainty	Standard Uncertainty in k_{eff}
Mass Uncertainty						
HEU Mass (g)	23	124643.9	$\pm 6.0 \times 23$	± 0.00137	$\pm 1.7\sqrt{23}$	± 0.00008
Hafnium Mass (g)	24	37675.9	$\pm 14.4 \times 24$	± 0.00068	$\pm 0.1\sqrt{24}$	Negligible
Polyethylene Moderator Mass (g)	No polyethylene moderator plates.					-
Polyethylene Reflector Mass (g)	13	10850.5	± 0.5 %	± 0.00052	$\pm 3.1\sqrt{13}$	Negligible
Aluminum Insert Mass (g)	16	2626.6	$\pm 3.0 \times 16$	± 0.00033	$\pm 0.1\sqrt{16}$	Negligible
Membrane Mass (g)	-	2396.1	± 20.0	± 0.00006	± 0.3	Negligible
Structure Mass (g)	-	27159.7	± 10 %	± 0.00087	± 0.1 %	Negligible
Sum in Quadrature (Mass Uncertainty)						**±0.00008**
Dimensional Uncertainty						
HEU Plate Dimensions (cm)	23	Varies (Table 77)	± 0.02	± 0.00175	$\pm 0.002/\sqrt{23}$	Negligible
Hafnium Plate Dimensions (cm)	24	Varies (Table 79)	± 0.02	± 0.00014	$\pm 0.003/\sqrt{24}$	Negligible
Polyethylene Plate Dimensions (cm)	4	Varies (Table 81)	± 0.02	± 0.00003	$\pm 0.010/\sqrt{4}$	Negligible
Polyethylene Ref. Dimensions (cm)	9	Varies (Table 90)	± 0.02	± 0.00059	$\pm 0.010/\sqrt{6}$	± 0.00007
Aluminum Insert Dimensions (cm)	16	Varies (Table 84)	± 0.01	± 0.00005	$\pm 0.005/\sqrt{16}$	Negligible
Upper Core Stack Height (cm)	-	7.417	± 0.132	± 0.00186	± 0.029	± 0.00041
Lower Core Stack Height (cm)	-	7.701	± 0.128	± 0.00191	± 0.078	± 0.00117
Upper Reflector Ring Height (cm)	-	7.483	± 0.15875	± 0.00011	± 0.004	Negligible
Lower Reflector Ring Height (cm)	-	6.421	± 0.15875	± 0.00011	± 0.004	Negligible
Membrane Thickness (cm)	-	0.3175	± 0.0254	± 0.00140	± 0.0073	± 0.00040
Membrane Lift (cm)	-	0.508	± 0.127	± 0.00004	± 0.073	Negligible
Sum in Quadrature (Dimensional Uncertainty)						**±0.00130**

Table 149 (continued): Summary of sensitivity in k_{eff} to uncertainties in Case 7.

Parameter (unit of measured)	N	Parameter Value	Parameter Variation in Calculation	Calculated Effect in k_{eff}	Standard Uncertainty	Standard Uncertainty in k_{eff}
Composition Uncertainty						
^{235}U Enrichment (Wt.%)	23	93.232	±0.103	±0.00166	$\pm 0.103/\sqrt{23}$	±0.00035
HEU Impurities (Wt.%)	23	Varies (Table 99)	-	±0.00025	Varies (Table 99)	±0.00005
Hafnium Impurities (Wt.%)	24	Varies (Table 108)	-	±0.00003	Varies (Table 108)	Negligible
Polyethylene Impurities (Wt.%)	-	Varies (Table 117)	-	Negligible	Varies (Table 117)	Negligible
Aluminum Impurities (Wt.%)	-	Varies (Table 126)	-	Negligible	Varies (Table 126)	Negligible
Sum in Quadrature (Composition Uncertainty)						**±0.00035**
Temperature Uncertainty						
Thermal Contraction (°C)	-	20.5	±10.0	±0.00047	±2.0	±0.00009
Neutron Cross Sections (°C)	-	20.5	±43.6	±0.00026	±2.0	Negligible
Thermal Scattering Laws (°C)	-	20.5	Refer to Section 2.5.3	3.7529E-6/°C	±2.0	Negligible
Sum in Quadrature (Temperature Uncertainty)						±0.00009
Sum in Quadrature (Total Uncertainty)						**±0.00136**

3.0 BENCHMARK SPECIFICATIONS

3.1 Description of Model

The benchmark models include the experimental configuration and a simplified model of the Comet structure in vacuum (no air). The boundary of the benchmark model is outside of these components. The experiment room, including the air, is not part of the benchmark model. Therefore, their removal is analyzed as simplification biases in Section 3.1.1.6.

The experimental configuration consist of the upper and lower core stacks and reflector rings. The core stacks are made up of the HEU plates, hafnium plates, aluminum inserts, and polyethylene moderator plates, reflector plates, and the bottom reflector plate. The reflector rings are made up of the polyethylene reflector rings and caps. The Comet structure includes the stationary platform, movable platen, interface plate, adapter plate, adapter extension, and membrane. The adapter extension connects the adapter plate to the movable platen. The four standoffs connecting the interface plate to the stationary platform are not included in the models. The lower half of the experimental configuration sits in the adapter plate and the upper half of the experimental configuration sits on the membrane. These two halves are separated by the membrane, which sits on top of the interface plate.

A single benchmark model is presented for each experimental configuration. This model represents a simplified core stack using average part dimensions and bulk material densities to conserve mass. This representation simplifies the geometry and allows for regular units (typically defined by an HEU plate, hafnium plate and, if present, a polyethylene moderator plate and/or aluminum insert) that are uniform and repeatable.

3.1.1 Model Simplification and Bias

Given an unbiased model with calculated multiplication factor k_{eff} and a biased model, due to a simplification in component *i*, resulting in a calculated multiplication factor $k'_{eff,i}$, the simplification bias is defined as

$$\text{Bias}_i = k'_{\text{eff},i} - k_{\text{eff}} \tag{10}$$

Therefore, the simplification bias for component *i* is negative when the simplification results in a reduction in k_{eff}, and vice verse.

These model simplification and bias calculations use the same calculational parameters as Section 2.0. Therefore, the threshold for negligible is defined to be less than or equal to 0.00004 (4 pcm) in k_{eff}, which represents the propagated uncertainty in Δk_{eff} given a statistical uncertainty of ± 0.00003.

3.1.1.1 HEU Impurity

The impurities in the HEU are reported in Section 2.4.2. These impurities were measured to be between $486\,\mu g\,g^{-1}$ and $1671\,\mu g\,g^{-1}$, with an average of $885.5\,\mu g\,g^{-1}$. The largest elemental impurities are carbon (C), silicon (Si), aluminum (Al), and iron (Fe), making up just over 90% of the impurity content. Table 150 summarizes the effect in k_{eff} due to the removal of the HEU impurities. To improve the statistics in the calculation, all impurities are removed at once, with the resulting simplification bias reported in Table 157 of Section 3.1.2. In the benchmark models, the HEU impurities are modeled as void by reducing the HEU plate densities by 0.08855 %.

Table 150: Summary of simplification bias for the removal of the HEU impurities.

Case	Effect in k_{eff}
1	Negligible
2	Negligible
3	Negligible
4	Negligible
5	Negligible
6	Negligible
7	Negligible

3.1.1.2 Hafnium Impurity

The impurities in the hafnium are reported in Section 2.4.3. These impurities were measured to be between $335\,\mu g\,g^{-1}$ and $710\,\mu g\,g^{-1}$, with an average of $688.3\,\mu g\,g^{-1}$. Excluding zirconium (Zr), which is not considered an impurity for the purposes of this analysis[17], the largest elemental impurities are iron (Fe) and oxygen (O), making up just over 50% of the impurity content. Table 151 summarizes the effect in k_{eff} due to the removal of the hafnium impurities. To improve the statistics in the calculation, all impurities are removed at once, with the resulting simplification bias reported in Table 157 of Section 3.1.2. In the benchmark models, the hafnium impurities are modeled as void by reducing the hafnium plate densities by 0.06883 %.

Table 151: Summary of simplification bias for the removal of the hafnium impurities.

Case	Effect in k_{eff}
1	-0.00009 ± 0.00003
2	Negligible
3	Negligible
4	Negligible
5	Negligible
6	Negligible
7	-0.00018 ± 0.00002

3.1.1.3 Polyethylene Impurity

The impurities in the polyethylene are reported in Section 2.4.4. These impurities were measured to be $960.8\,\mu g\,g^{-1}$. The elemental impurities include Na, Al, Si, and Cr, none of which are significant neutron absorbers. Table 152 summarizes the effect in k_{eff} due to the removal of the polyethylene impurities. To improve the statistics in the calculation, all impurities are removed at once, with the resulting simplification bias reported in Table 157 of Section 3.1.2. In the benchmark models, the polyethylene impurities are modeled as void by reducing the polyethylene part densities by 0.09608 %. These parts include all the polyethylene parts described in Section 1.2.5.

[17]The chemical properties of hafnium and zirconium are nearly identical, meaning zirconium is typically present in hafnium.

Table 152: Summary of simplification bias for the removal of the polyethylene impurities.

Case	Effect in k_{eff}
1	Negligible
2	Negligible
3	Negligible
4	Negligible
5	0.00017 ± 0.00003
6	Negligible
7	Negligible

3.1.1.4 Aluminum Impurity

The impurities in the aluminum are reported in Section 2.4.5. This impurity content ranges from 1.4 Wt% to 4.2 Wt%, with an average of 2.695 Wt%. The largest elemental impurities include magnesium (Mg), silicon (Si), iron (Fe), copper (Cu), and chromium (Cr), making up just under 90% of the total impurity content. Table 153 summarizes the effect in k_{eff} due to the removal of the aluminum impurities, based on the average impurity content. Unlike the other impurity removal simplification biases, the impurities in the aluminum are not modeled as void since they are based on handbook data instead of measurement. Instead, a constant density of 2.7 $g\,cm^{-3}$ is modeled. To improve the statistics in the calculation, all impurities are removed at once, with the resulting simplification bias reported in Table 157 of Section 3.1.2.

Table 153: Summary of simplification bias for the removal of the aluminum impurities.

Case	Effect in k_{eff}
1	Negligible
2	Negligible
3	Negligible
4	Negligible
5	Negligible
6	-0.00012 ± 0.00004
7	Negligible

3.1.1.5 Temperature Correction

As described in Section 1.4, the measured temperatures of the experimental configurations during operation were typically around 15.0 °C. To simplify the model, these temperatures are corrected to 293.6 K (20.5 °C).

The bias in this simplification is determined based on the sensitivities calculated during the temperature uncertainty analysis described in Section 2.5. This analysis shows that the sensitivity in k_{eff} due to temperature results from thermal contraction and the polyethylene thermal scattering law. The sensitivity due to the neutron cross section data is negligible.

Table 154 summarizes simplification bias due to correcting the model temperature. The experiment temperature is evaluated in Section 2.5. This table is reproduced alongside the other simplification biases in Section 3.1.2.

Table 154: Summary of simplification bias for the temperature correction to 293.6 K (20.5 °C).

Case	Sensitivity in k_{eff} [a]	Temperature (°C)			Effect in k_{eff} [c]
		Model	Experiment	Difference[b]	
1	-0.00003/°C	20.5	16.0	4.5	-0.00013 ± 0.00010
2	-0.00010/°C		16.6	3.9	-0.00038 ± 0.00010
3	-0.00009/°C		18.3	2.2	-0.00021 ± 0.00010
4	-0.00010/°C		16.4	4.1	-0.00042 ± 0.00010
5	0.00039/°C		16.7	3.8	0.00148 ± 0.00010
6	-0.00009/°C		15.5	5.0	-0.00043 ± 0.00010
7	-0.00004/°C		16.0	4.5	-0.00019 ± 0.00009

[a] Sum of sensitivities in k_{eff} to thermal contraction (Section 2.5.1) and thermal scattering law (Section 2.5.3).
[b] (Model Temperature) - (Experiment Temperature)
[c] Uncertainty is due to uncertainty in the least squares fit.

3.1.1.6 Comet and Room Removal

As discussed in Section 1.2.2, the experimental configurations were assembled using Comet located at the National Criticality Experiments Research Center. Only the room, Comet, and air is considered in this simplification. Other components, such as Godiva-IV, the four start-up detectors, and the other contents of the room were not included as they are judged have a negligible effect in k_{eff}. These calculations were performed by Jacob Glesmann (LLNL).

Figure 34 shows a diagram of the room model, including Comet and an example experimental configuration. This room model is based on a previous study with additional measurement performed during this experiment[18]. The room is approximately 4.7 m tall with the stationary platform of Comet standing approximately 2.1 m from the floor. The closest wall and ceiling were measured relative to the interface plate. The interface plate was rigidly attached to the stationary platform of Comet by four 30.48 cm standoffs, described in Section 1.2.2.1. The ceiling was approximately 2.3 m from the top face of the interface plate and the nearest wall was approximately 3.1 m away from the side of the interface plate. The walls are modeled with a thickness of 0.3 m. The components of Comet are modeled using the engineering drawings provided in Appendix B.

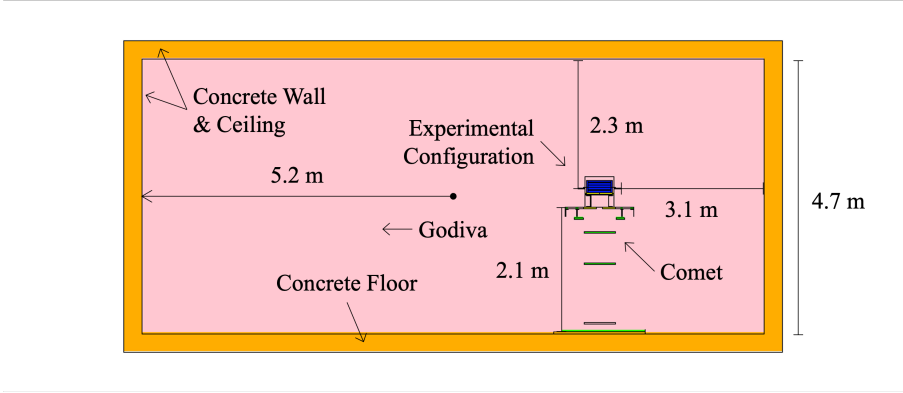

Figure 34: Diagram of the room containing Comet and the location of the experimental configurations.

[18] S. S. Kim. *12-Rad Zone Analysis for CAAS Placement at the Device Assembly Facility*. CSM 1531. Lawrence Livermore National Laboratory, 2008.

The room is filled with air (75.5 % nitrogen (N), 23.2 % oxygen (O), and 1.3 % argon (Ar), by weight)[19] modeled with a density of 0.001225 $g\,cm^{-3}$. The concrete walls are modeled as Portland Cement[19,20] with a density of 2.3 $g\,cm^{-3}$. The Comet components, separate of those already included in the benchmark model, are modeled as iron[21] with a density of 7.8 $g\,cm^{-3}$.

Table 155 summarizes the simplification bias due to removal of the room, air, and Comet. Cases 5 and 7 have a smaller effect in k_{eff} compared to the other cases. This is due to Case 5 being majority thermal and Case 7 having the top and bottom bunches of the hafnium plates. This table is reproduced alongside the other simplification biases in Section 3.1.2.

Table 155: Summary of simplification bias for removal of the room, Comet, and air.

Bias Component	**Case 1**	**Case 2**	**Case 3**	**Case 4**	**Case 5**	**Case 6**	**Case 7**
Baseline[(a)]	1.00219± 0.00003	1.00246± 0.00004	0.99955± 0.00004	0.99661± 0.00004	0.99995± 0.00004	0.99958± 0.00004	0.99678± 0.00003
Room Removed	1.00158± 0.00003	1.00178± 0.00004	0.99897± 0.00004	0.99620± 0.00004	0.99971± 0.00004	0.99901± 0.00004	0.99652± 0.00003
Difference[(b)]	-0.00061 ±0.00004	-0.00068 ±0.00006	-0.00058 ±0.00006	-0.00041 ±0.00006	-0.00024 ±0.00006	-0.00057 ±0.00006	-0.00026 ±0.00004
Air Removed	1.00140± 0.00003	1.00161± 0.00004	0.99889± 0.00004	0.99602± 0.00004	0.99969± 0.00004	0.99893± 0.00004	0.99651± 0.00003
Difference[(c)]	-0.00018 ±0.00004	-0.00017 ±0.00006	-0.00008 ±0.00006	-0.00018 ±0.00006	Negligible	-0.00008 ±0.00006	Negligible
Comet Removed	1.00092± 0.00003	1.00119± 0.00004	0.99848± 0.00004	0.99570± 0.00004	0.99957± 0.00004	0.99854± 0.00004	0.99630± 0.00003
Difference[(d)]	-0.00048 ±0.00004	-0.00042 ±0.00006	-0.00041 ±0.00006	-0.00032 ±0.00006	-0.00012 ±0.00006	-0.00039 ±0.00006	-0.00021 ±0.00004
Total[(e)]	**-0.00127 ±0.00004**	**-0.00127 ±0.00006**	**-0.00107 ±0.00006**	**-0.00091 ±0.00006**	**-0.00038 ±0.00006**	**-0.00104 ±0.00006**	**-0.00048 ±0.00004**

[(a)] The baseline model includes the average geometry experimental configuration (Section 3.1.1.8), the room, air, and Comet.
[(b)] (Room Removed) - (Baseline), the worth of the room.
[(c)] (Air Removed) - (Room Removed), the worth of the air.
[(d)] (Comet Removed) - (Air Removed), the worth of Comet.
[(e)] (Comet Removed) - (Baseline), the difference in k_{eff} with and without the room, air, and Comet.

[19] R. J. McConn Jr. et al. *Compendium of Material Composition Data for Radiation Transport Modeling*. PNNL-15870 Rev. 1. Pacific Northwest National Laboratory, 2011. DOI: 10.2172/1023125.

[20] Referred to as "Portland Concrete" in the reference.

[21] These components are A36 Steel which is greater than 98% iron.

3.1.1.7 Reflector Rings, Caps, and Bottom Reflector

The step joints on the reflector ring, cap, and bottom reflectors parts were removed to simplify the polyethylene reflector. Figure 35 Figure 36 show illustrations of these simplifications. The models represent the reflector rings and caps that make up the upper and lower reflector rings as a single volume, similar to the diagram in Figure 32 of Section 2.2.4. The total mass of the reflectors is conversed using a bulk density based on the measured mass and modeled volume.

In order to conserve the density of the bottom reflector, filling the step joint must be properly accounted for by adding a small amount of mass to the bottom reflector and removing the same amount of mass from the lower reflector ring. This mass is determined based on the volume of the step joint of the BOTREF-1 part. The dimensions of this step are reported in Table 18 and shown in Figure 12 of Section 1.2.5.4. The approximate mass of the step joint is 49.4 g, which is added to the bottom reflector and removed from the lower reflector ring. Additionally, the neutron source hole described in Section 1.2.5.4 is removed. This represents approximately 0.5 cm^3 which has a negligible effect on the calculated density of the bottom reflector.

The effect of these simplifications to the polyethylene reflector parts is analyzed as part of the average geometry simplification in Section 3.1.1.8.

3.1.1.8 Average Geometry

The upper and lower core stacks are geometrically simplified by representing each using either average or nominal dimension based on the part type. Each configuration uses a bulk density for the HEU, hafnium, and polyethylene materials. This bulk density is calculated to conserve the total measured mass of the parts that make up the experimental configuration. The aluminum inserts uses a nominal 2.70 $g\,cm^{-3}$ density.

All parts in the experimental configuration use nominal diameters, including the HEU plates, hafnium plates, polyethylene moderator and reflector plates, aluminum inserts, and polyethylene ring and bottom reflectors. The thickness of each part is based on the average thickness of the part type, as reported throughout Section 2.3. The top reflector, consisting of the polyethylene moderator and reflector plates, is simplified by combining the parts into a single top reflector plate.

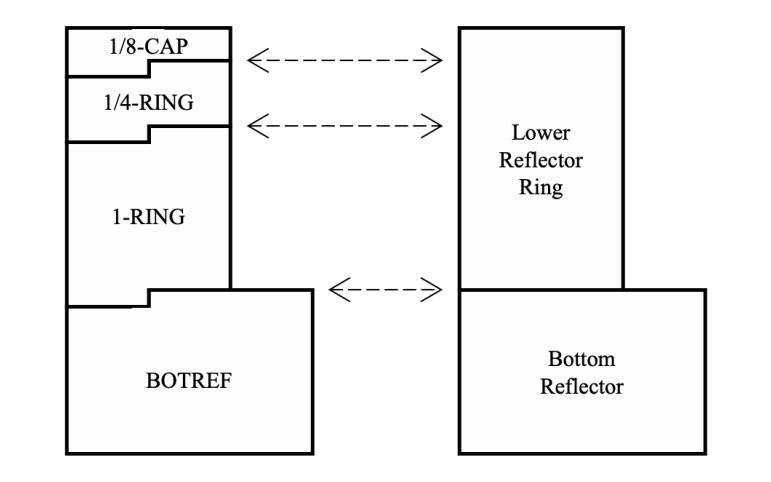

Figure 35: Example of the reflector simplification, showing the lower reflector rings and bottom reflector. The left shows the actual ring reflectors including the step joints while the right shows the model simplification which removes the step joints.

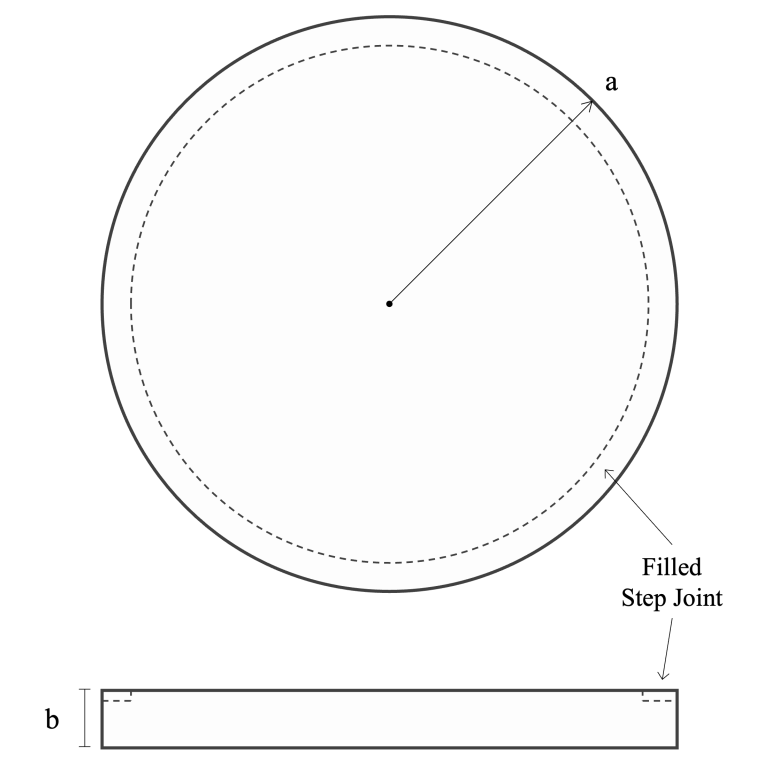

Figure 36: Simplifications to the bottom reflector plate, removing the step joint and neutron source hole. The dimensions are reported in Table 163 of Section 3.2.6.

Table 156 summarizes the simplification bias due to the average geometry and reflector simplifications. This table is reproduced alongside the other simplification biases in Section 3.1.2.

Table 156: Summary of simplification bias for the average geometry and reflector simplifications.

Case	Effect in k_{eff}
1	-0.00043 ± 0.00004
2	-0.00020 ± 0.00005
3	-0.00109 ± 0.00006
4	-0.00081 ± 0.00006
5	-0.00033 ± 0.00006
6	-0.00017 ± 0.00006
7	-0.00062 ± 0.00004

3.1.2 Summary of Bias Calculations

Table 157 presents the bias calculations for the benchmark model. The experimental k_{eff} will be adjusted by adding the total bias reported in this table. The dominant bias for all Cases, expect Case 5, is from removing the room, air, and Comet (Section 3.1.1.6). The dominant bias for Case 5 is due to the polyethylene thermal scattering law in the temperature correction (Section 3.1.1.5).

Table 157: Summary of bias calculation results due to model simplification.

Bias Component	Case 1	Case 2	Case 3	Case 4	Case 5	Case 6	Case 7
Impurity	−0.00015	−0.00009	−0.00012	−0.00006	+0.00019	−0.00013	−0.00013
Removal	±0.00003	±0.00003	±0.00002	±0.00003	±0.00003	±0.00003	±0.00002
Room and Comet	−0.00127	−0.00127	−0.00107	−0.00091	−0.00038	−0.00104	−0.00048
Removal	±0.00004	±0.00006	±0.00006	±0.00006	±0.00006	±0.00006	±0.00004
Temperature	−0.00013	−0.00038	−0.00021	−0.00042	+0.00148	−0.00043	−0.00019
Correction	±0.00010	±0.00010	±0.00010	±0.00010	±0.00010	±0.00010	±0.00009
Average	−0.00043	−0.00020	−0.00109	−0.00081	−0.00033	−0.00017	−0.00062
Geometry	±0.00004	±0.00005	±0.00006	±0.00006	±0.00006	±0.00006	±0.00004
Total	**−0.00198**	**−0.00194**	**−0.00249**	**−0.00220**	**−0.00096**	**−0.00177**	**−0.00142**
	±0.00013	**±0.00014**	**±0.00015**	**±0.00015**	**±0.00015**	**±0.00014**	**±0.00012**

3.2 Dimensions

3.2.1 Comet General Purpose Critical Assembly Machine

The model of Comet consists of six components, shown in Figure 37. The interface plate and stationary platform form the upper stationary platform, shown in Figure 4 of Section 1.2.2.1. The adapter plate, adapter extension, and movable platen form the lower movable platen, shown in Figure 5 of Section 1.2.2.2. The upper stationary platform is fixed in place, where the interface plate and stationary platform are separated by four 30.48 cm standoffs. The position of the lower movable platen varies along the vertical axis depending on the height of the lower half of the experiment. The membrane sits on top of the interface plate for all configurations, separating the upper and lower halves of the configurations.

Tables 158 and 159 report the part dimensions for the upper stationary platform and lower movable platen, respectively. Since the upper stationary platform is fixed in place across all models, Table 158 also reports the upper and lower z-planes that bound the extent, or thicknesses, of the parts. The same is done for the lower movable platen, but the positions along the vertical axis depend on the height of the lower half of the experimental configuration, so the values are reported in the relevant model sections. In addition to these tables, each component is described in detail in the following sections.

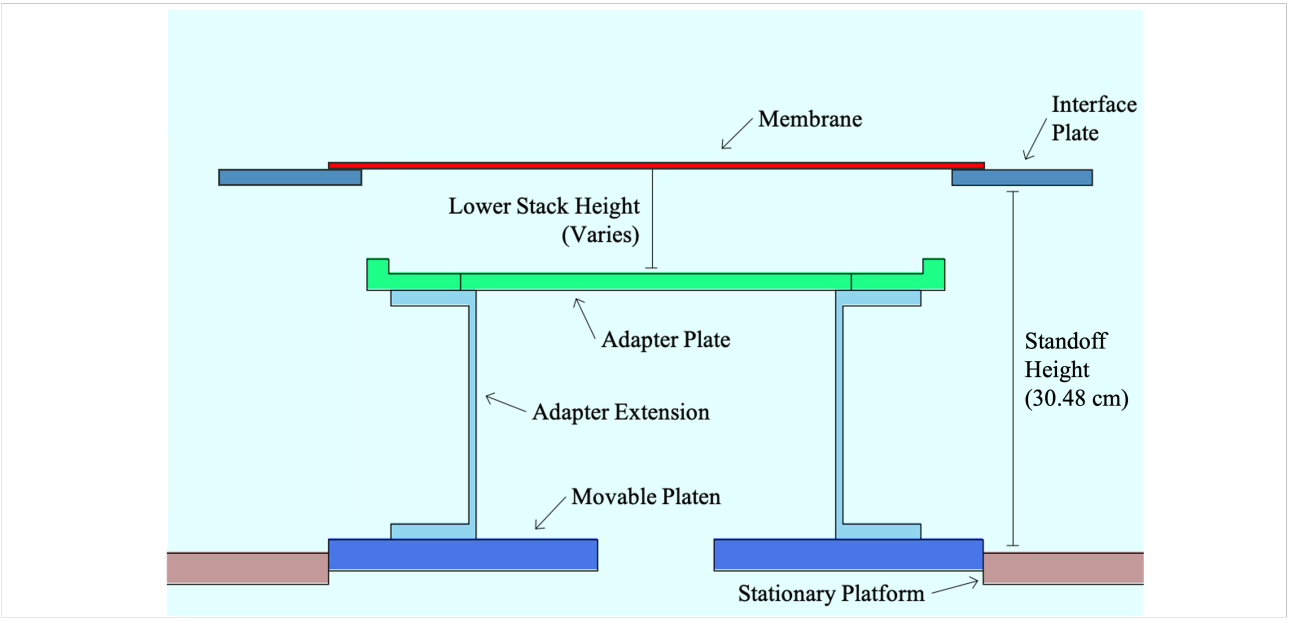

Figure 37: Comet structure components: membrane (red), interface plate (dark blue), adapter plate (teal), adapter extension (light blue), movable platen (blue), and stationary platform (brown).

Table 158: Model dimensions for the upper stationary platform of Comet.

Part	Density (g/cm^3)	Side Length (cm)	Inner Radius (cm)	Thickness (cm)	Lower z Plane (cm)	Upper z Plane (cm)
Membrane	2.65250	53.34000	-	0.31750	0.00000	0.31750
Interface Plate	2.7	71.12000	24.13000	1.27000	-1.27000	0.00000
Stationary Platform		114.30000	26.79700	2.54000	-34.29000	-31.75000

Table 159: Model dimensions for the lower movable platen of Comet.

Part		Density (g/cm^3)	Outer Radius (cm)	Inner Radius (cm)	Thickness (cm)	Lower z Plane (cm)	Upper z Plane (cm)
Adapter Plate	Lip	2.7	23.49500	21.78050	1.19380	See model-specific tables in each section.	
	Plate			15.87500	1.34620		
Adapter Extension			21.59000	14.60500	1.27000		
			15.24000		17.78000		
			21.59000		1.27000		
Movable Plate			26.67000	4.76250	2.54000		

3.2.1.1 Membrane

The membrane was modeled as shown in Figure 38. The membrane is a square aluminum sheet with a side length of 53.34 cm and thickness of 0.3175 cm. As shown in Figure 63 of Appendix B, there are four small holes in the corners of the membrane. These holes are removed in the model as they have a negligible impact on the calculation. The membrane is the same for all experimental configurations.

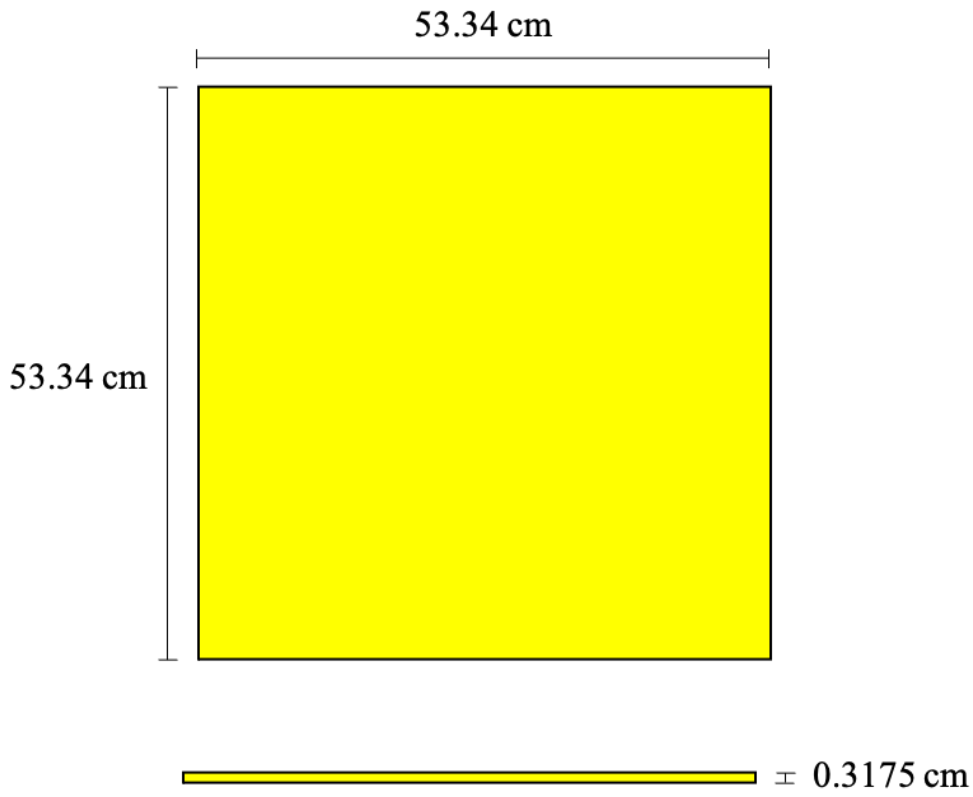

Figure 38: Membrane model dimensions (not to scale).

3.2.1.2 Interface Plate

The interface plate is modeled as shown in Figure 39. The interface plate is a square aluminum plate with a side length of 71.12 cm and thickness of 1.27 cm. There is a 48.26 cm diameter hole through the center of the interface plate. As shown in Figure 59 of Appendix B, there are various holes for affixing the standoffs to the interface plate and four protruding pegs to align the membrane. These components are removed in the model as they have a negligible impact on the calculation. The interface plate is the same for all experimental configurations.

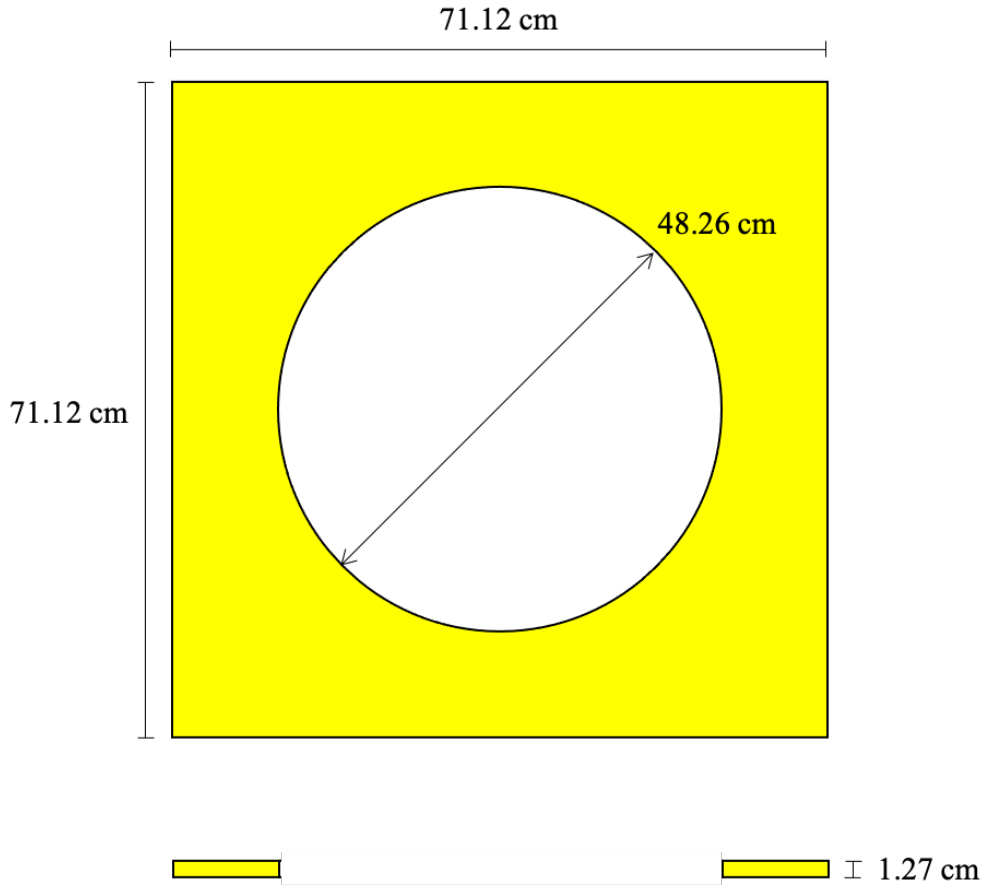

Figure 39: Interface plate model dimensions (figure not to scale).

3.2.1.3 Adapter Plate

The adapter plate is modeled as shown in Figure 40. The adapter plate is an annular cylinder with an outer lip and inner crossbars to hold the bottom reflector (BOTREF) in place. As shown in Figure 61 of Appendix B, there are various holes for affixing the adapter plate to the adapter extension. These holes are removed within the model as they have a negligible impact on the calculation. The adapter plate is the same for all experimental configurations.

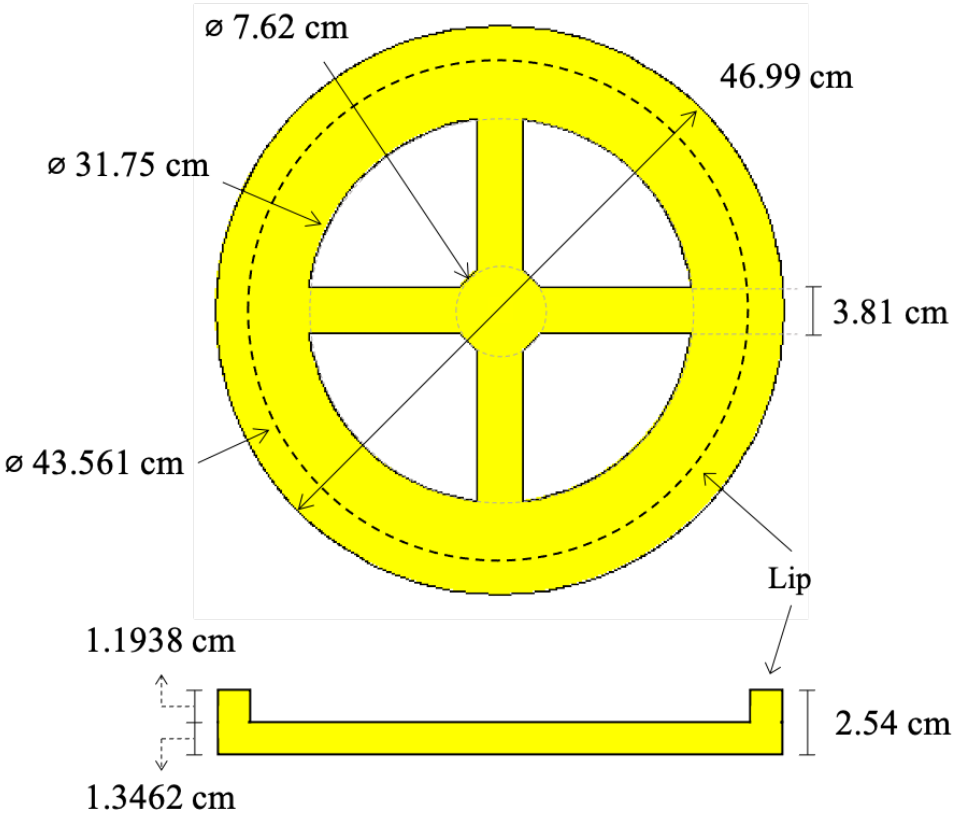

Figure 40: Adapter plate model dimensions (figure not to scale).

3.2.1.4 Adapter Extension

The adapter extension is modeled as shown in Figure 41. The adapter extension consists of a thin-walled aluminum cylinder with a top and bottom flange extending off the cylinder to affix the adapter extension to the adapter plate on top and the Comet movable platen on bottom. The annular cylinder has an inner diameter of 29.21 cm and a height of 20.32 cm with a wall thickness of 0.635 cm. The top and bottom lips have an outer diameter of 43.18 cm and thickness of 1.27 cm. As shown in Figure 62 of Appendix B, there are various holes for affixing the adapter extension to both the adapter plate and movable platen. These holes are removed within the model as they have a negligible impact on the calculation. The adapter extension is the same for all experimental configurations.

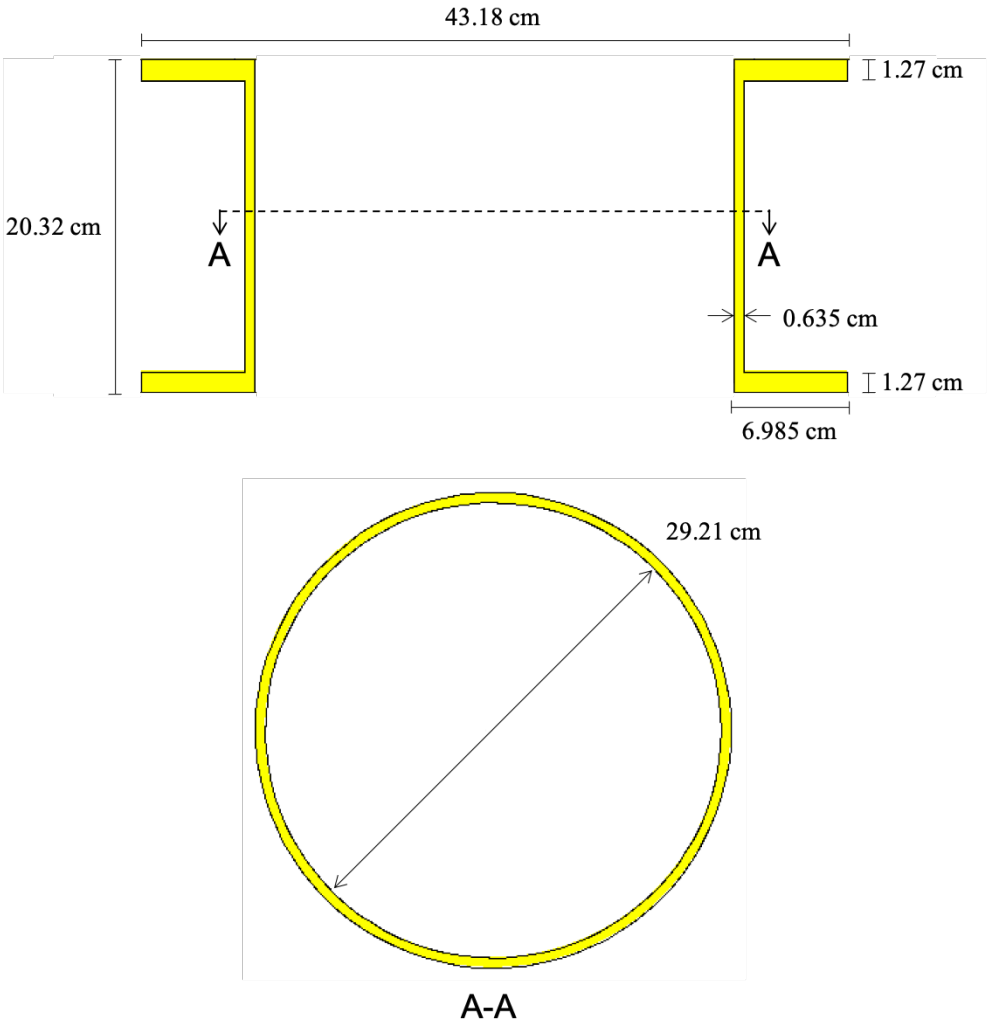

Figure 41: Adapter extension model dimensions (figure not to scale).

3.2.1.5 Comet Movable Platen

The Comet movable platen is modeled as shown in Figure 42. The platen is a circular aluminum plate with a diameter of 53.34 cm and thickness of 2.54 cm. There is a 9.525 cm diameter hole through the center of the platen. As shown in Figure 58 of Appendix B, there are various holes through the movable platen for fixturing. These holes are removed within the model as they have a negligible impact on the calculation. The movable platen is the same for all experimental configurations.

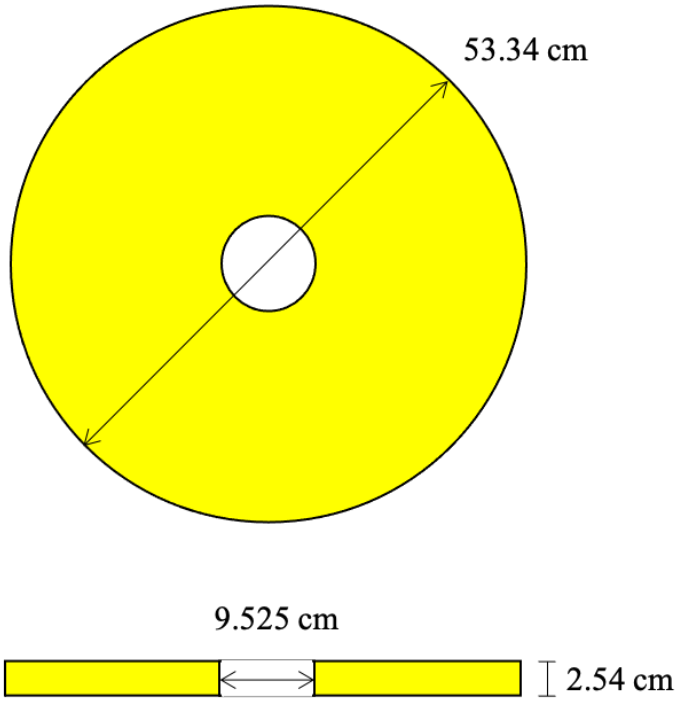

Figure 42: Comet movable platen model dimensions (figure not to scale).

3.2.1.6 Comet Stationary Platform

The Comet stationary platform is modeled as shown in Figure 43. The platform is a square aluminum plate with a side length of 114.3 cm and thickness of 2.54 cm. There is a 53.594 cm diameter hole through the center of the platform. As shown in Figure 57 of Appendix B, there are various holes through the stationary platform for fixturing and the four corners chamfered. These holes are removed, and the corners are filled within the model as they have a negligible impact on the calculation. The stationary platform is the same for all experimental configurations.

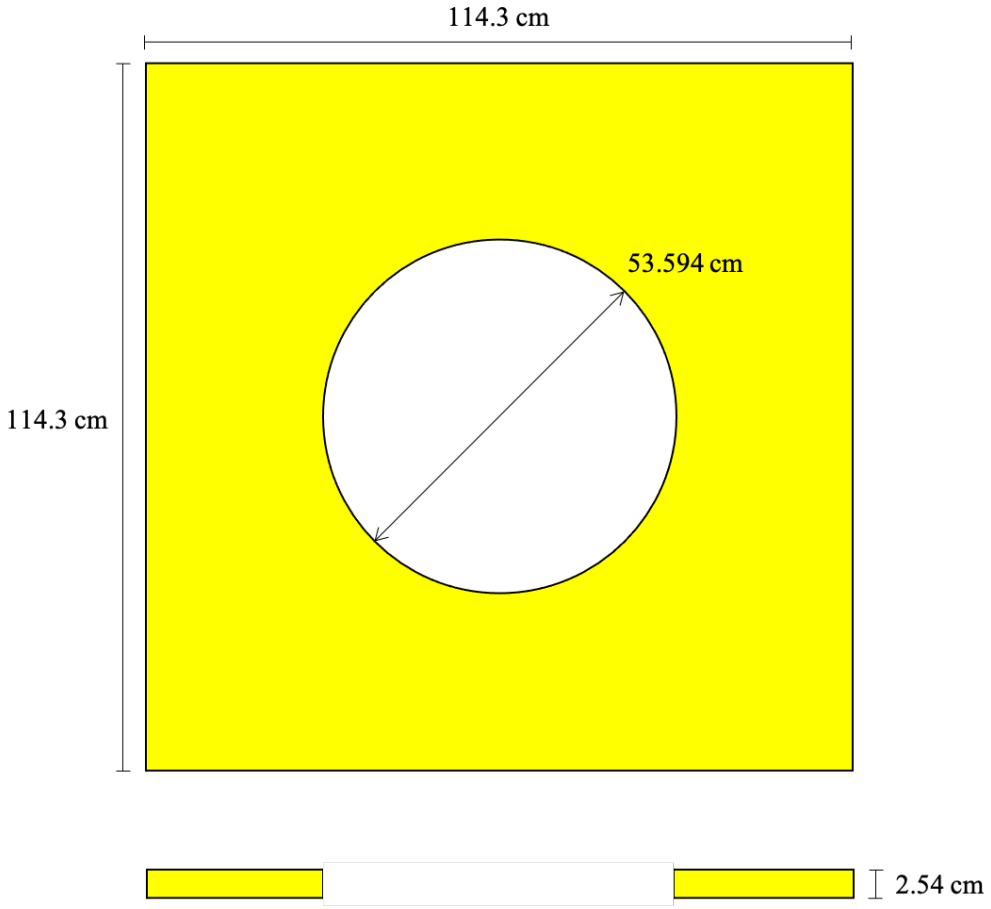

Figure 43: Comet stationary platform model dimensions (figure not to scale).

3.2.2 Highly Enriched Uranium Plates

The HEU plates are modeled as shown in Figure 44. There are five types of HEU plates: 15/0-HEU, 15/2.5-HEU, 15/6-HEU, 15/10-HEU, and 6/0-HEU. Each part type uses the nominal inner and outer radii. All part types use the same thickness, based on an average of all the measured plate thicknesses, as described in Section 2.3.1. Table 160 reports the dimensions of the HEU plates used in the benchmark models. The HEU plates are concentric with the vertical axis.

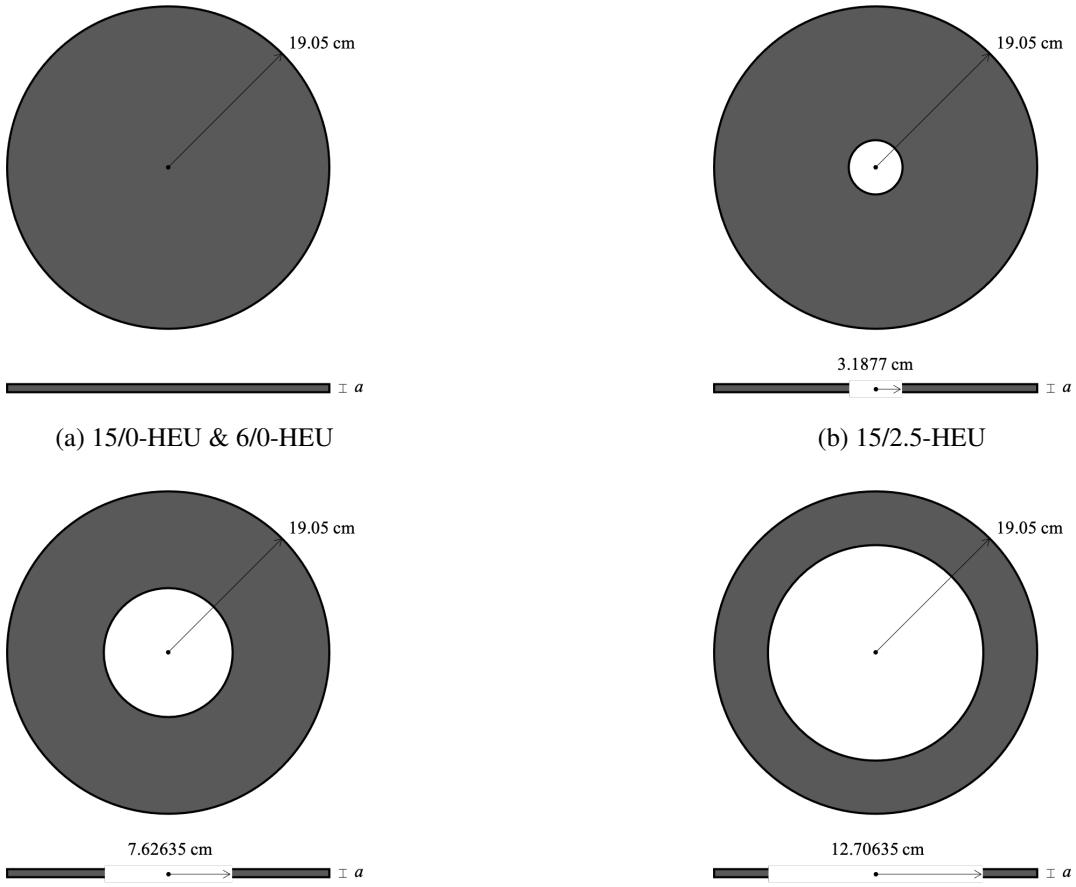

(a) 15/0-HEU & 6/0-HEU

(b) 15/2.5-HEU

(c) 15/6-HEU

(d) 15/10-HEU

Figure 44: HEU plate model (not to scale).

Table 160: HEU plate model dimensions (see Figure 44).

Part Type	Inner Radius (cm)	Outer Radius (cm)	Thickness, *a* (cm)
15/0-HEU	-	19.05000	0.31083
15/2.5-HEU	3.18770		
15/6-HEU	7.62635		
15/10-HEU	12.70635		
6/0-HEU	-	7.6200	

3.2.3 Hafnium Plates

The hafnium plates are modeled as shown in Figure 45. The plate uses a nominal radius of 19.05 cm and a thickness based on an average of all the measured plate thicknesses, as described in Section 2.3.2. Table 161 reports the dimensions of the hafnium plates used in the benchmark models. The hafnium plates are concentric with the vertical axis.

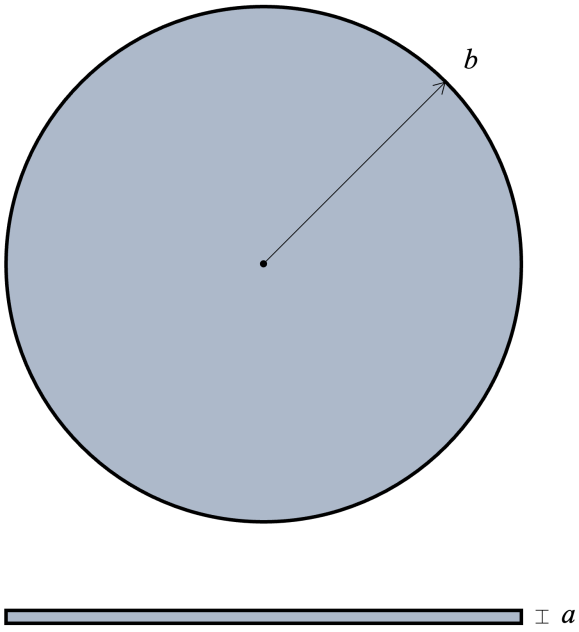

Figure 45: Hafnium plate model (not to scale).

Table 161: Hafnium plate model dimensions (see Figure 45).

Part Type	Thickness, *b* (cm)	Radius, *a* (cm)
HF	0.10637	19.05000

3.2.4 Polyethylene Moderator and Reflector Plates

The polyethylene moderator (MOD) and reflector (REF) plates are modeled as shown in Figure 46. There are seven types of polyethylene moderator and reflector plates: 1/8-MOD, 1/4-MOD, 1/2-MOD, 1.5-MOD, 1/32-REF, 1/16-REF, and 1-REF. The top reflector for each experimental configuration consists of a combination of these moderator and reflector plates. The benchmark models represent the top reflector as the sum of the individual part types. All part types use a nominal radius of 19.05 cm and an average thickness based on the part type, as described in Section 2.3.3. Table 162 reports the dimensions of the polyethylene moderator and reflector plates used in the benchmark models.

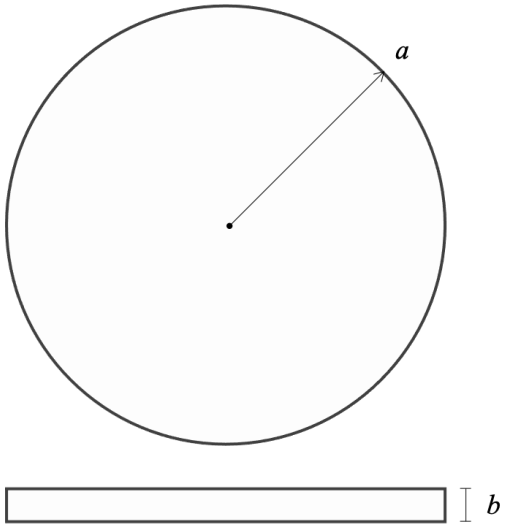

Figure 46: Polyethylene moderator and reflector plate model (not to scale).

Table 162: Polyethylene moderator and reflector plate model dimensions (see Figure 46).

Part Type	Thickness, *b* (cm)	Radius, *a* (cm)
1/8-MOD	0.32210	19.05000
1/4-MOD	0.64644	
1/2-MOD	1.28499	
1.5-MOD	3.83728	
1/32-REF	0.08369	
1/16-REF	0.17767	
1-REF	2.54127	

3.2.5 Polyethylene Reflector Rings and Caps

The polyethylene reflector rings surround the core stack to provide an additional 2.54 cm of radial reflection. These rings include male (top) and female (bottom) steps joints which mate with one another as the rings are stacked to provide structural support and reduce neutron streaming paths. The stack of reflector rings is finished using a reflector cap which only has the female (bottom) step joint to provide a flat top surface to the reflector stack.

The upper and lower reflectors are modeled as shown in Figure 47. The reflector rings use a nominal inner and outer radius of 19.177 cm and 21.717 cm, respectively. These dimensions are reported for each benchmark model in Section 3.2.8.

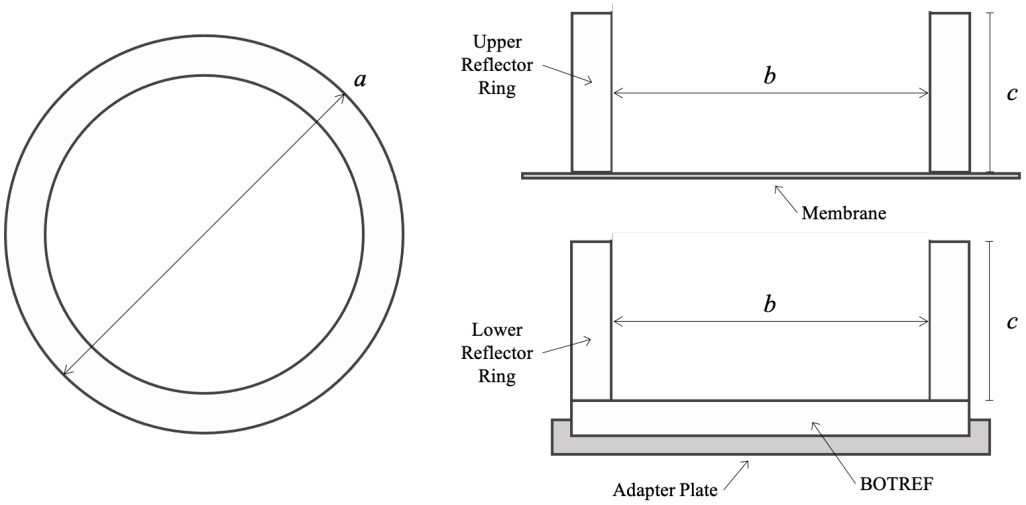

Figure 47: Polyethylene reflector ring model and dimensions. The left figure shows a cross section of the reflector which is an annular cylinder. The right figures show the upper ring reflector, which sits on top of the membrane, and the lower ring reflector, which sits on top of the bottom reflector within the adapter plate.

3.2.6 Polyethylene Bottom Reflector

The polyethylene bottom reflector (BOTREF) is modeled as shown in Figure 48. This model includes the simplifications described in Section 3.1.1. These simplifications include removal of the step joint and neutron source hole. Table 163 reports the dimensions of the bottom reflector used in the benchmark models.

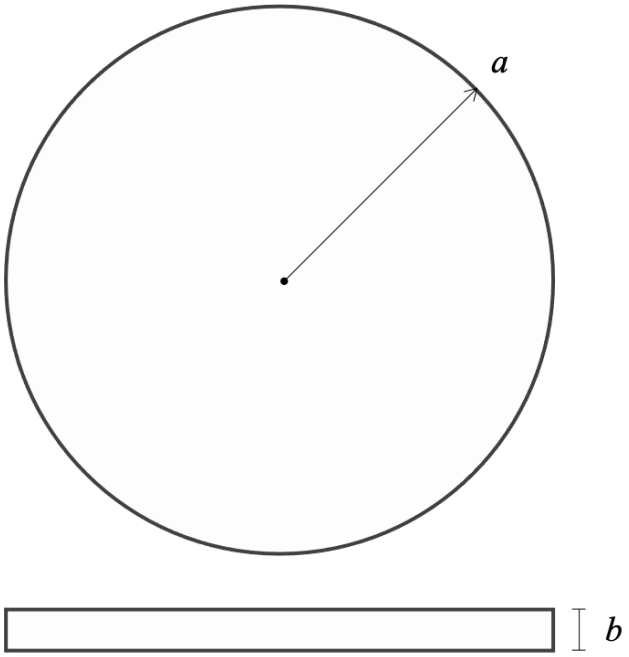

Figure 48: Polyethylene bottom reflector model (not to scale).

Table 163: Polyethylene bottom reflector model dimensions (see Figure 48).

Part Type	Radius, *a* (cm)	Thickness, *b* (cm)
BOTREF	21.71700	2.56794

3.2.7 Aluminum Inserts

The aluminum inserts are modeled as shown in Figure 49. There are three types of aluminum inserts, differentiated by their diameter, corresponding to the annuli of the 15/2.5-HEU, 15/6-HEU, and 15/10-HEU plates. The aluminum insert models are concentric with the vertical axis and fit within the center of the HEU plate annuli. Table 164 reports the dimensions of the aluminum inserts used in the benchmark models.

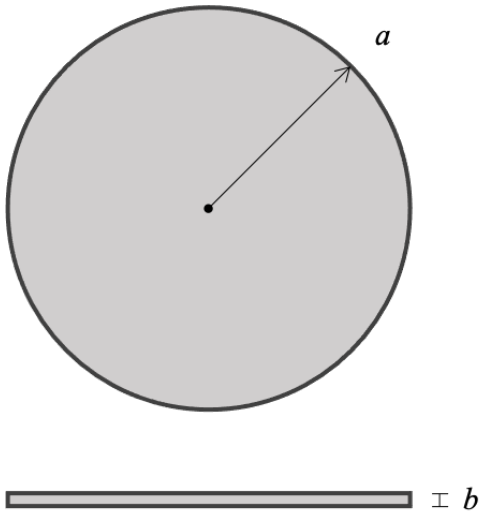

Figure 49: Aluminum insert model (not to scale).

Table 164: Aluminum insert model dimensions (see Figure 49).

Part Type	Thickness, *a* (cm)	Radius, *b* (cm)
2.5-DISK	0.31672	3.04800
6-DISK		7.49300
10-DISK		12.57300

3.2.8 Case Models

Each experimental configuration presents a benchmark model, with accompanying tables and figures to fully describe the experimental configuration including the dimensions, masses, and axial positions that describe each part. The origin of the benchmark models is at center of the top face of the interface plate. All axial positions reported in the following sections are relative to this origin. All parts are centered about the vertical axis (z-axis).

3.2.8.1 Case 1

The Case 1 model includes 25 HEU plates, 24 hafnium plates between each HEU plate, no HDPE moderator, and a nominal 1.15625 in. (2.936875 cm) top HDPE reflector. These 25 HEU plates consist of six 15/0-HEU plates, seven 15/2.5-HEU plates, five 15/6-HEU plates, and seven 15/10-HEU plates. Figure 50 shows a cross sectional view of the model. The aluminum parts (structural components, membrane, and inserts) are shown in yellow, the HEU plates in pink, the hafnium plates in green, and the polyethylene reflector in blue.

Figure 50 shows a diagram of the Case 1 model. Tables 166 and 167 report the upper and lower core stack dimensions, including: part densities (in g/cm^3), dimensions, and axial position (z-axis). Table 168 reports similar dimensions for the upper and lower reflector rings. Table 165 reports the axial positions of the Comet lower movable platen components specific to the Case 1 model, as reference in Table 159 of Section 3.2.1.

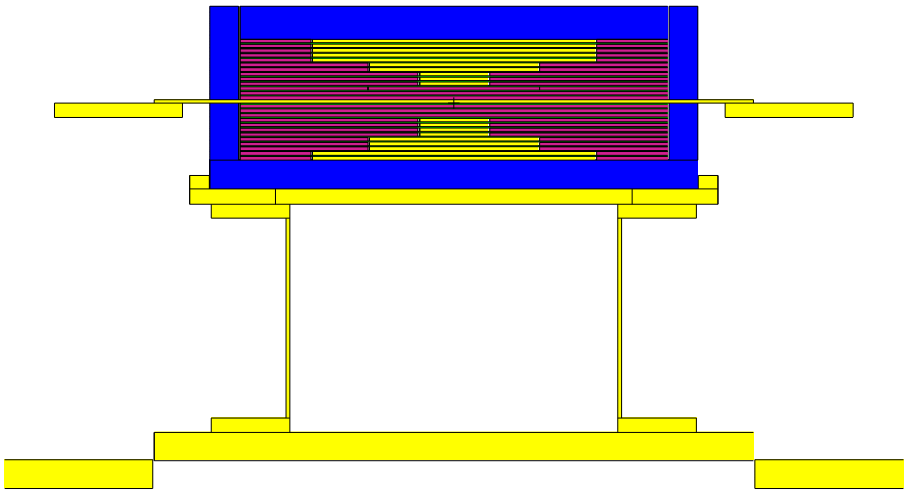

Figure 50: Case 1 model (HEU in pink, hafnium in green, polyethylene in blue, and aluminum in yellow).

Table 165: Case 1 model lower movable platen axial positions (see Section 3.2.1).

Part		Density (g/cm^3)	z-Plane (cm)	
			Lower	Upper
Adapter Plate	Lip	2.7	-7.62735	-6.43355
	Plate		-8.97355	-7.62735
Adapter Extension			-10.24355	-8.97355
			-28.02355	-10.24355
			-29.29355	-28.02355
Movable Platen			-31.83355	-29.29355

Table 166: Case 1 model upper core stack dimensions.

Layer	Part ID	Density (g/cm^3)	Radius (cm)		Thickness (cm)	z-Plane (cm)	
			Inner	Outer		Lower	Upper
26	Top Reflector	0.95576	-	19.05000	2.94707	5.69363	8.64070
25	10479	18.27667	12.70635	19.05000	0.31083	5.37691	5.68774
	10-DISK-7	2.70000	-	12.57300	0.31672		5.69363
24	HF-25	12.93639	-	19.05000	0.10637	5.27054	5.37691
23	10481	18.27667	12.70635	19.05000	0.31083	4.95382	5.26465
	10-DISK-6	2.70000	-	12.57300	0.31672		5.27054
22	HF-24	12.93639	-	19.05000	0.10637	4.84745	4.95382
21	10485	18.27667	12.70635	19.05000	0.31083	4.53073	4.84156
	10-DISK-5	2.70000	-	12.57300	0.31672		4.84745
20	HF-23	12.93639	-	19.05000	0.10637	4.42436	4.53073
19	10473	18.27667	12.70635	19.05000	0.31083	4.10764	4.41847
	10-DISK-4	2.70000	-	12.57300	0.31672		4.42436
18	HF-22	12.93639	-	19.05000	0.10637	4.00127	4.10764
17	10463	18.27667	12.70635	19.05000	0.31083	3.68455	3.99538
	10-DISK-3	2.70000	-	12.57300	0.31672		4.00127
16	HF-20	12.93639	-	19.05000	0.10637	3.57818	3.68455
15	10935	18.27667	7.62635	19.05000	0.31083	3.26146	3.57229
	6-DISK-5	2.70000	-	7.49300	0.31672		3.57818
14	HF-19	12.93639	-	19.05000	0.10637	3.15509	3.26146
13	10933	18.27667	7.62635	19.05000	0.31083	2.83837	3.14920
	6-DISK-4	2.70000	-	7.49300	0.31672		3.15509
12	HF-18	12.93639	-	19.05000	0.10637	2.73200	2.83837
11	10470	18.27667	3.18770	19.05000	0.31083	2.41528	2.72611
	2.5-DISK-7	2.70000	-	3.04800	0.31672		2.73200
10	HF-17	12.93639	-	19.05000	0.10637	2.30891	2.41528
9	10475	18.27667	3.18770	19.05000	0.31083	1.99219	2.30302
	2.5-DISK-6	2.70000	-	3.04800	0.31672		2.30891
8	HF-16	12.93639	-	19.05000	0.10637	1.88582	1.99219
7	10489	18.27667	3.18770	19.05000	0.31083	1.56910	1.87993
	2.5-DISK-5	2.70000	-	3.04800	0.31672		1.88582
6	HF-15	12.93639	-	19.05000	0.10637	1.46273	1.56910
5	11018	18.27667	7.62635	19.05000	0.31083	1.15190	1.46273
	Q2-16	18.27667	-	7.62000	0.31083		1.46273
4	HF-14	12.93639	-	19.05000	0.10637	1.04553	1.15190
3	11017	18.27667	-	19.05000	0.31083	0.73470	1.04553
2	HF-13	12.93639	-	19.05000	0.10637	0.62833	0.73470
1	11150	18.27667	-	19.05000	0.31083	0.31750	0.62833

Table 167: Case 1 model lower core stack dimensions.

Layer	Part ID	Density (g/cm^3)	Radius (cm)		Thickness (cm)	z-Plane (cm)	
			Inner	Outer		Lower	Upper
25	HF-12	12.93639	-	19.05000	0.10637	-0.10637	0.00000
24	11019	18.27667	-	19.05000	0.31083	-0.41720	-0.10637
23	HF-11	12.93639	-	19.05000	0.10637	-0.52357	-0.41720
22	11147	18.27667	-	19.05000	0.31083	-0.83440	-0.52357
21	HF-10	12.93639	-	19.05000	0.10637	-0.94077	-0.83440
20	11149	18.27667	-	19.05000	0.31083	-1.25160	-0.94077
19	HF-09	12.93639	-	19.05000	0.10637	-1.35797	-1.25160
18	10467	18.27667	3.18770	19.05000	0.31083	-1.67469	-1.36386
	2.5-DISK-4	2.70000	-	3.04800	0.31672		-1.35797
17	HF-08	12.93639	-	19.05000	0.10637	-1.78106	-1.67469
16	10464	18.27667	3.18770	19.05000	0.31083	-2.09778	-1.78695
	2.5-DISK-3	2.70000	-	3.04800	0.31672		-1.78106
15	HF-07	12.93639	-	19.05000	0.10637	-2.20415	-2.09778
14	10487	18.27667	3.18770	19.05000	0.31083	-2.52087	-2.21004
	2.5-DISK-2	2.70000	-	3.04800	0.31672		-2.20415
13	HF-06	12.93639	-	19.05000	0.10637	-2.62724	-2.52087
12	10491	18.27667	3.18770	19.05000	0.31083	-2.94396	-2.63313
	2.5-DISK-1	2.70000	-	3.04800	0.31672		-2.62724
11	HF-05	12.93639	-	19.05000	0.10637	-3.05033	-2.94396
10	10932	18.27667	7.62635	19.05000	0.31083	-3.36705	-3.05622
	6-DISK-3	2.70000	-	7.49300	0.31672		-3.05033
9	HF-04	12.93639	-	19.05000	0.10637	-3.47342	-3.36705
8	10457	18.27667	7.62635	19.05000	0.31083	-3.79014	-3.47931
	6-DISK-2	2.70000	-	7.49300	0.31672		-3.47342
7	HF-03	12.93639	-	19.05000	0.10637	-3.89651	-3.79014
6	10477	18.27667	7.62635	19.05000	0.31083	-4.21323	-3.90240
	6-DISK-1	2.70000	-	7.49300	0.31672		-3.89651
5	HF-02	12.93639	-	19.05000	0.10637	-4.31960	-4.21323
4	10458	18.27667	12.70635	19.05000	0.31083	-4.63632	-4.32549
	10-DISK-2	2.70000	-	12.57300	0.31672		-4.31960
3	HF-01	12.93639	-	19.05000	0.10637	-4.74269	-4.63632
2	10472	18.27667	12.70635	19.05000	0.31083	-5.05941	-4.74858
	10-DISK-1	2.70000	-	12.57300	0.31672		-4.74269
1	BOTREF-1	0.95576	-	21.71700	2.56794	-7.62735	-5.05941

Table 168: Case 1 model upper and lower reflector ring dimensions (see Section 3.2.5).

Layer	Density (g/cm^3)	Radius (cm)		Thickness (cm)	z-Plane (cm)	
		Inner	Outer		Lower	Upper
Upper	0.95576	19.17700	21.71700	8.32320	0.31750	8.64070
Lower				5.05941	-5.05941	0.00000

3.2.8.2 Case 2

The Case 2 model includes 16 HEU plates, 15 hafnium plates and 0.125 in. (0.3175 cm) nominal HDPE moderator plates between each HEU plate, and a nominal 0.875 in. (2.2225 cm) top HDPE reflector. These 16 HEU plates consist of six 15/0-HEU plates, seven 15/2.5-HEU plates, and three 15/6-HEU plates. Figure 51 shows a cross sectional view of the model. The aluminum parts (structural components, membrane, and inserts) are shown in yellow, the HEU plates in pink, the hafnium plates in green, and the polyethylene reflector in blue.

Figure 51 shows a diagram of the Case 2 model. Tables 170 and 171 report the upper and lower core stack dimensions, including: part densities (in g/cm^3), dimensions, and axial position (z-axis). Table 172 reports similar dimensions for the upper and lower reflector rings. Table 169 reports the axial positions of the Comet lower movable platen components specific to the Case 2 model, as reference in Table 159 of Section 3.2.1.

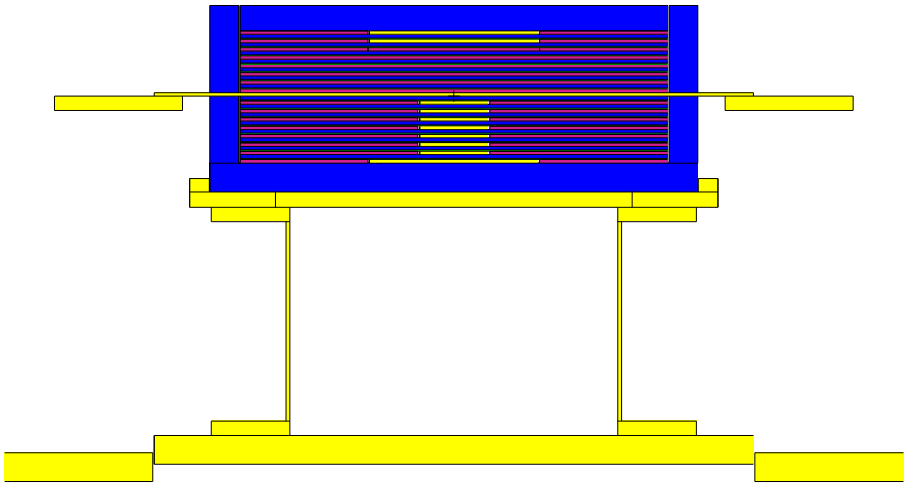

Figure 51: Case 2 model (HEU in pink, hafnium in green, polyethylene in blue, and aluminum in yellow).

Table 169: Case 2 model lower movable platen axial positions (see Section 3.2.1).

Part		Density (g/cm^3)	z-Plane (cm)	
			Lower	Upper
Adapter Plate	Lip	2.7	-8.52946	-7.33566
	Plate		-9.87566	-8.52946
Adapter Extension			-11.14566	-9.87566
			-28.92566	-11.14566
			-30.19566	-28.92566
Movable Platen			-32.73566	-30.19566

Table 170: Case 2 model upper core stack dimensions.

Layer	Part ID	Density (g/cm^3)	Radius (cm)		Thickness (cm)	z-Plane (cm)	
			Inner	Outer		Lower	Upper
23	Top Reflector	0.95313	-	19.05000	2.25353	5.81521	8.06874
22	10477	18.27669	7.62635	19.05000	0.31083	5.49849	5.80932
	6-DISK-3	2.70000	-	7.49300	0.31672		5.81521
21	1/8-MOD-15	0.93595	-	19.05000	0.32210	5.17639	5.49849
20	HF-15	12.96977	-	19.05000	0.10637	5.07002	5.17639
19	10935	18.27669	7.62635	19.05000	0.31083	4.75330	5.06413
	6-DISK-2	2.70000	-	7.49300	0.31672		5.07002
18	1/8-MOD-14	0.93595	-	19.05000	0.32210	4.43120	4.75330
17	HF-14	12.96977	-	19.05000	0.10637	4.32483	4.43120
16	11018	18.27669	7.62635	19.05000	0.31083	4.01400	4.32483
	Q2-16	18.27669	-	7.62000	0.31083		4.32483
15	1/8-MOD-13	0.93595	-	19.05000	0.32210	3.69190	4.01400
14	HF-13	12.96977	-	19.05000	0.10637	3.58553	3.69190
13	11150	18.27669	-	19.05000	0.31083	3.27470	3.58553
12	1/8-MOD-12	0.93595	-	19.05000	0.32210	2.95260	3.27470
11	HF-12	12.96977	-	19.05000	0.10637	2.84623	2.95260
10	11149	18.27669	-	19.05000	0.31083	2.53540	2.84623
9	1/8-MOD-11	0.93595	-	19.05000	0.32210	2.21330	2.53540
8	HF-11	12.96977	-	19.05000	0.10637	2.10693	2.21330
7	11019	18.27669	-	19.05000	0.31083	1.79610	2.10693
6	1/8-MOD-10	0.93595	-	19.05000	0.32210	1.47400	1.79610
5	HF-10	12.96977	-	19.05000	0.10637	1.36763	1.47400
4	11017	18.27669	-	19.05000	0.31083	1.05680	1.36763
3	1/8-MOD-9	0.93595	-	19.05000	0.32210	0.73470	1.05680
2	HF-09	12.96977	-	19.05000	0.10637	0.62833	0.73470
1	11147	18.27669	-	19.05000	0.31083	0.31750	0.62833

Table 171: Case 2 model lower core stack dimensions.

Layer	Part ID	Density (g/cm^3)	Radius (cm)		Thickness (cm)	z-Plane (cm)	
			Inner	Outer		Lower	Upper
25	1/8-MOD-8	0.93595	-	19.05000	0.32210	-0.32210	0.00000
24	HF-08	12.96977	-	19.05000	0.10637	-0.42847	-0.32210
23	10464	18.27669	3.18770	19.05000	0.31083	-0.74519	-0.43436
	2.5-DISK-7	2.70000	-	3.04800	0.31672		-0.42847
22	1/8-MOD-7	0.93595	-	19.05000	0.32210	-1.06729	-0.74519
21	HF-07	12.96977	-	19.05000	0.10637	-1.17366	-1.06729
20	10475	18.27669	3.18770	19.05000	0.31083	-1.49038	-1.17955
	2.5-DISK-6	2.70000	-	3.04800	0.31672		-1.17366
19	1/8-MOD-6	0.93595	-	19.05000	0.32210	-1.81248	-1.49038
18	HF-06	12.96977	-	19.05000	0.10637	-1.91885	-1.81248
17	10470	18.27669	3.18770	19.05000	0.31083	-2.23557	-1.92474
	2.5-DISK-5	2.70000	-	3.04800	0.31672		-1.91885
16	1/8-MOD-5	0.93595	-	19.05000	0.32210	-2.55767	-2.23557
15	HF-05	12.96977	-	19.05000	0.10637	-2.66404	-2.55767
14	10489	18.27669	3.18770	19.05000	0.31083	-2.98076	-2.66993
	2.5-DISK-4	2.70000	-	3.04800	0.31672		-2.66404
13	1/8-MOD-4	0.93595	-	19.05000	0.32210	-3.30286	-2.98076
12	HF-04	12.96977	-	19.05000	0.10637	-3.40923	-3.30286
11	10491	18.27669	3.18770	19.05000	0.31083	-3.72595	-3.41512
	2.5-DISK-3	2.70000	-	3.04800	0.31672		-3.40923
10	1/8-MOD-3	0.93595	-	19.05000	0.32210	-4.04805	-3.72595
9	HF-03	12.96977	-	19.05000	0.10637	-4.15442	-4.04805
8	10467	18.27669	3.18770	19.05000	0.31083	-4.47114	-4.16031
	2.5-DISK-2	2.70000	-	3.04800	0.31672		-4.15442
7	1/8-MOD-2	0.93595	-	19.05000	0.32210	-4.79324	-4.47114
6	HF-02	12.96977	-	19.05000	0.10637	-4.89961	-4.79324
5	10487	18.27669	3.18770	19.05000	0.31083	-5.21633	-4.90550
	2.5-DISK-1	2.70000	-	3.04800	0.31672		-4.89961
4	1/8-MOD-1	0.93595	-	19.05000	0.32210	-5.53843	-5.21633
3	HF-01	12.96977	-	19.05000	0.10637	-5.64480	-5.53843
2	10457	18.27669	7.62635	19.05000	0.31083	-5.96152	-5.65069
	6-DISK-1	2.70000	-	7.49300	0.31672		-5.64480
1	BOTREF-1	0.95313	-	21.71700	2.56794	-8.52946	-5.96152

Table 172: Case 2 model upper and lower reflector ring dimensions (see Section 3.2.5).

Layer	Density (g/cm^3)	Radius (cm)		Thickness (cm)	z-Plane (cm)	
		Inner	Outer		Lower	Upper
Upper	0.95313	19.17700	21.71700	7.75124	0.31750	8.06874
Lower				5.96152	-5.96152	0.00000

3.2.8.3 Case 3

The Case 3 model includes 13 HEU plates, 12 hafnium plates and 0.25 in. (0.635 cm) nominal HDPE moderator plates between each HEU plate, and a nominal 0.96875 in. (2.46063 cm) top HDPE reflector. These 13 HEU plates consist of six 15/0-HEU plates and seven 15/2.5-HEU plates. Figure 52 shows a cross sectional view of the model. The aluminum parts (structural components, membrane, and inserts) are shown in yellow, the HEU plates in pink, the hafnium plates in green, and the polyethylene reflector in blue.

Figure 52 shows a diagram of the Case 3 model. Tables 174 and 175 report the upper and lower core stack dimensions, including: part densities (in g/cm^3), dimensions, and axial position (z-axis). Table 176 reports similar information for the upper and lower reflector rings. Table 173 describes the axial positions of the Comet lower movable platen components specific to the Case 3 model, as reference in Table 159 of Section 3.2.1.

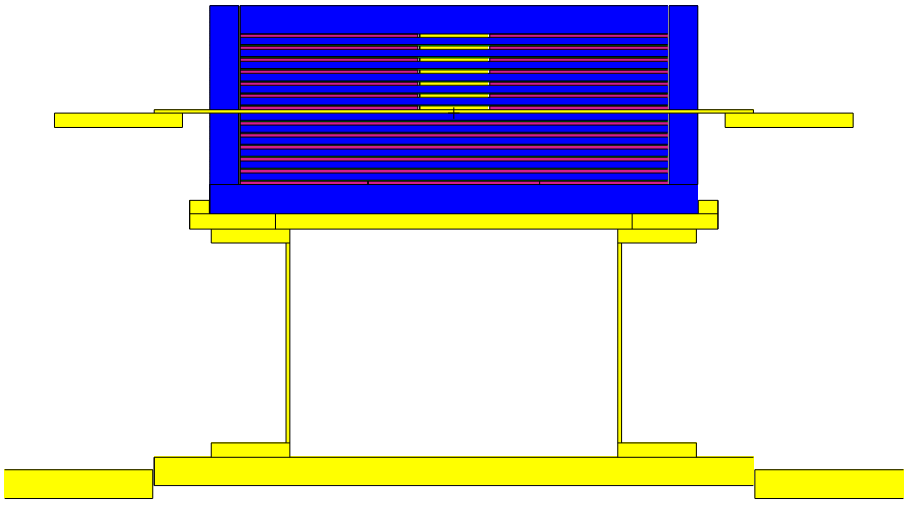

Figure 52: Case 3 model (HEU in pink, hafnium in green, polyethylene in blue, and aluminum in yellow).

Table 173: Case 3 model lower movable platen axial positions (see Section 3.2.1).

Part		Density (g/cm^3)	z-Plane (cm)	
			Lower	Upper
Adapter Plate	Lip	2.7	-8.94978	-7.75598
	Plate		-10.29598	-8.94978
Adapter Extension			-11.56598	-10.29598
			-29.34598	-11.56598
			-30.61598	-29.34598
Movable Platen			-33.15598	-30.61598

Table 174: Case 3 model upper core stack dimensions.

Layer	Part ID	Density (g/cm^3)	Radius (cm)		Thickness (cm)	z-Plane (cm)	
			Inner	Outer		Lower	Upper
20	Top Reflector	0.94305	-	19.05000	2.51489	7.05140	9.56629
19	10475	18.23772	3.18770	19.05000	0.31083	6.73468	7.04551
	2.5-DISK-8	2.70000	-	3.04800	0.31672		7.05140
18	1/4-MOD-12	0.93377	-	19.05000	0.64644	6.08824	6.73468
17	HF-12	12.99905	-	19.05000	0.10637	5.98187	6.08824
16	10464	18.23772	3.18770	19.05000	0.31083	5.66515	5.97598
	2.5-DISK-3	2.70000	-	3.04800	0.31672		5.98187
15	1/4-MOD-11	0.93377	-	19.05000	0.64644	5.01871	5.66515
14	HF-11	12.99905	-	19.05000	0.10637	4.91234	5.01871
13	10470	18.23772	3.18770	19.05000	0.31083	4.59562	4.90645
	2.5-DISK-9	2.70000	-	3.04800	0.31672		4.91234
12	1/4-MOD-5	0.93377	-	19.05000	0.64644	3.94918	4.59562
11	HF-10	12.99905	-	19.05000	0.10637	3.84281	3.94918
10	10489	18.23772	3.18770	19.05000	0.31083	3.52609	3.83692
	2.5-DISK-10	2.70000	-	3.04800	0.31672		3.84281
9	1/4-MOD-10	0.93377	-	19.05000	0.64644	2.87965	3.52609
8	HF-09	12.99905	-	19.05000	0.10637	2.77328	2.87965
7	10491	18.23772	3.18770	19.05000	0.31083	2.45656	2.76739
	2.5-DISK-4	2.70000	-	3.04800	0.31672		2.77328
6	1/4-MOD-4	0.93377	-	19.05000	0.64644	1.81012	2.45656
5	HF-08	12.99905	-	19.05000	0.10637	1.70375	1.81012
4	10467	18.23772	3.18770	19.05000	0.31083	1.38703	1.69786
	2.5-DISK-6	2.70000	-	3.04800	0.31672		1.70375
3	1/4-MOD-9	0.93377	-	19.05000	0.64644	0.74059	1.38703
2	HF-07	12.99905	-	19.05000	0.10637	0.63422	0.74059
1	10487	18.23772	3.18770	19.05000	0.31083	0.31750	0.62833
	2.5-DISK-5	2.70000	-	3.04800	0.31672		0.63422

Table 175: Case 3 model lower core stack dimensions.

Layer	Part ID	Density (g/cm^3)	Radius (cm)		Thickness (cm)	z-Plane (cm)	
			Inner	Outer		Lower	Upper
19	1/4-MOD-8	0.93377	-	19.05000	0.64644	-0.64644	0.00000
18	HF-06	12.99905	-	19.05000	0.10637	-0.75281	-0.64644
17	11149	18.23772	-	19.05000	0.31083	-1.06364	-0.75281
16	1/4-MOD-7	0.93377	-	19.05000	0.64644	-1.71008	-1.06364
15	HF-05	12.99905	-	19.05000	0.10637	-1.81645	-1.71008
14	11147	18.23772	-	19.05000	0.31083	-2.12728	-1.81645
13	1/4-MOD-6	0.93377	-	19.05000	0.64644	-2.77372	-2.12728
12	HF-04	12.99905	-	19.05000	0.10637	-2.88009	-2.77372
11	11019	18.23772	-	19.05000	0.31083	-3.19092	-2.88009
10	1/4-MOD-3	0.93377	-	19.05000	0.64644	-3.83736	-3.19092
9	HF-03	12.99905	-	19.05000	0.10637	-3.94373	-3.83736
8	11017	18.23772	-	19.05000	0.31083	-4.25456	-3.94373
7	1/4-MOD-2	0.93377	-	19.05000	0.64644	-4.90100	-4.25456
6	HF-02	12.99905	-	19.05000	0.10637	-5.00737	-4.90100
5	11150	18.23772	-	19.05000	0.31083	-5.31820	-5.00737
4	1/4-MOD-1	0.93377	-	19.05000	0.64644	-5.96464	-5.31820
3	HF-01	12.99905	-	19.05000	0.10637	-6.07101	-5.96464
2	11018	18.23772	7.62635	19.05000	0.31083	-6.38184	-6.07101
2	Q2-16	18.23772	-	7.62000	0.31083	-6.38184	-6.07101
1	BOTREF-1	0.94305	-	21.71700	2.56794	-8.94978	-6.38184

Table 176: Case 3 model upper and lower reflector ring dimensions (see Section 3.2.5).

Layer	Density (g/cm^3)	Radius (cm)		Thickness (cm)	z-Plane (cm)	
		Inner	Outer		Lower	Upper
Upper	0.94305	19.17700	21.71700	9.24879	0.31750	9.56629
Lower				6.38184	-6.38184	0.00000

3.2.8.4 Case 4

The Case 4 model includes 10 HEU plates, nine hafnium plates and 0.5 in. (1.27 cm) nominal HDPE moderator plates between each HEU plate, and a nominal 1.0 in. (2.54 cm) top HDPE reflector. These 10 HEU plates consist of five 15/0-HEU plates and five 15/2.5-HEU plates. Figure 53 shows a cross sectional view of the model. The aluminum parts (structural components, membrane, and inserts) are shown in yellow, the HEU plates in pink, the hafnium plates in green, and the polyethylene reflector in blue.

Figure 53 shows a diagram of the Case 4 model. Tables 178 and 179 report the upper and lower core stack dimensions, including: part densities (in g/cm^3), dimensions, and axial position (z-axis). Table 180 reports similar information for the upper and lower reflector rings. Table 177 describes the axial positions of the Comet lower movable platen components specific to the Case 4 model, as reference in Table 159 of Section 3.2.1.

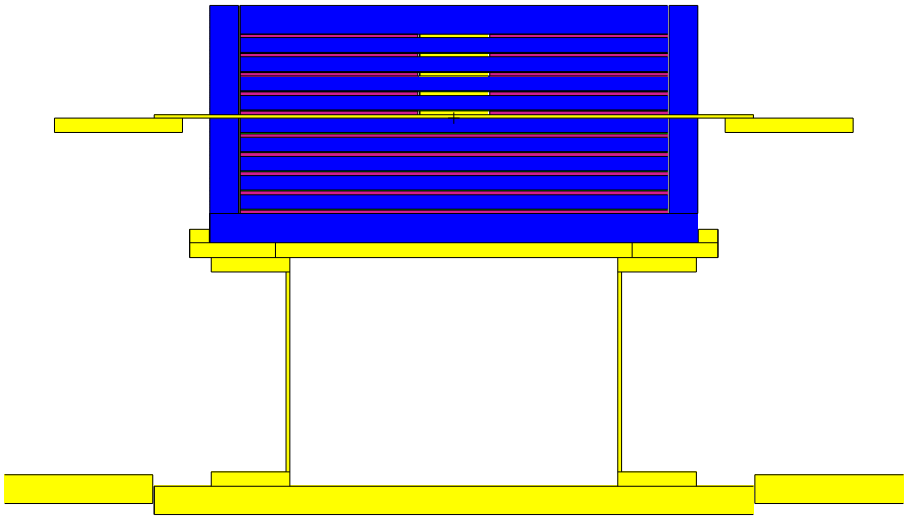

Figure 53: Case 4 model (HEU in pink, hafnium in green, polyethylene in blue, and aluminum in yellow).

Table 177: Case 4 model lower movable platen axial positions (see Section 3.2.1).

Part		Density (g/cm^3)	z-Plane (cm)	
			Lower	Upper
Adapter Plate	Lip	2.7	-11.07889	-9.88509
	Plate		-12.42509	-11.07889
Adapter Extension			-13.69509	-12.42509
			-31.47509	-13.69509
			-32.74509	-31.47509
Movable Platen			-35.28509	-32.74509

Table 178: Case 4 model upper core stack dimensions.

Layer	Part ID	Density (g/cm^3)	Radius (cm)		Thickness (cm)	z-Plane (cm)	
			Inner	Outer		Lower	Upper
14	Top Reflector	0.95200	-	19.05000	2.54127	7.46654	10.00781
13	10470	18.26915	3.18770	19.05000	0.31083	7.14982	7.46065
	2.5-DISK-5	2.70000	-	3.04800	0.31672		7.46654
12	1/2-MOD-9	0.94203	-	19.05000	1.28499	5.86483	7.14982
11	HF-09	13.01535	-	19.05000	0.10637	5.75846	5.86483
10	10489	18.26915	3.18770	19.05000	0.31083	5.44174	5.75257
	2.5-DISK-4	2.70000	-	3.04800	0.31672		5.75846
9	1/2-MOD-8	0.94203	-	19.05000	1.28499	4.15675	5.44174
8	HF-08	13.01535	-	19.05000	0.10637	4.05038	4.15675
7	10491	18.26915	3.18770	19.05000	0.31083	3.73366	4.04449
	2.5-DISK-3	2.70000	-	3.04800	0.31672		4.05038
6	1/2-MOD-7	0.94203	-	19.05000	1.28499	2.44867	3.73366
5	HF-07	13.01535	-	19.05000	0.10637	2.34230	2.44867
4	10467	18.26915	3.18770	19.05000	0.31083	2.02558	2.33641
	2.5-DISK-2	2.70000	-	3.04800	0.31672		2.34230
3	1/2-MOD-6	0.94203	-	19.05000	1.28499	0.74059	2.02558
2	HF-06	13.01535	-	19.05000	0.10637	0.63422	0.74059
1	10487	18.26915	3.18770	19.05000	0.31083	0.31750	0.62833
	2.5-DISK-1	2.70000	-	3.04800	0.31672		0.63422

Table 179: Case 4 model lower core stack dimensions.

Layer	Part ID	Density (g/cm^3)	Radius (cm)		Thickness (cm)	z-Plane (cm)	
			Inner	Outer		Lower	Upper
16	1/2-MOD-5	0.94203	-	19.05000	1.28499	-1.28499	0.00000
15	HF-05	13.01535	-	19.05000	0.10637	-1.39136	-1.28499
14	11147	18.26915	-	19.05000	0.31083	-1.70219	-1.39136
13	1/2-MOD-4	0.94203	-	19.05000	1.28499	-2.98718	-1.70219
12	HF-04	13.01535	-	19.05000	0.10637	-3.09355	-2.98718
11	11149	18.26915	-	19.05000	0.31083	-3.40438	-3.09355
10	1/2-MOD-3	0.94203	-	19.05000	1.28499	-4.68937	-3.40438
9	HF-03	13.01535	-	19.05000	0.10637	-4.79574	-4.68937
8	11019	18.26915	-	19.05000	0.31083	-5.10657	-4.79574
7	1/2-MOD-2	0.94203	-	19.05000	1.28499	-6.39156	-5.10657
6	HF-02	13.01535	-	19.05000	0.10637	-6.49793	-6.39156
5	11017	18.26915	-	19.05000	0.31083	-6.80876	-6.49793
4	1/2-MOD-1	0.94203	-	19.05000	1.28499	-8.09375	-6.80876
3	HF-01	13.01535	-	19.05000	0.10637	-8.20012	-8.09375
2	11150	18.26915	-	19.05000	0.31083	-8.51095	-8.20012
1	BOTREF-1	0.95200	-	21.71700	2.56794	-11.07889	-8.51095

Table 180: Case 4 model upper and lower reflector ring dimensions (see Section 3.2.5).

Layer	Density (g/cm^3)	Radius (cm)		Thickness (cm)	z-Plane (cm)	
		Inner	Outer		Lower	Upper
Upper	0.95200	19.17700	21.71700	9.69031	0.31750	10.00781
Lower				8.51095	-8.51095	0.00000

3.2.8.5 Case 5

The Case 5 model includes 11 HEU plates, 10 hafnium plates and 1.5 in. (3.81 cm) nominal HDPE moderator plates between each HEU plate, and a nominal 1.5 in. (3.81 cm) top HDPE reflector. These 11 HEU plates consist of six 15/0-HEU plates and five 15/6-HEU plates. Figure 54 shows a cross sectional view of the model. The aluminum parts (structural components, membrane, and inserts) are shown in yellow, the HEU plates in pink, the hafnium plates in green, and the polyethylene reflector in blue.

Figure 54 shows a diagram of the Case 5 model. Tables 182 and 183 report the upper and lower core stack dimensions, including: part densities (in g/cm^3), dimensions, and axial position (z-axis). Table 184 reports similar information for the upper and lower reflector rings. Table 181 describes the axial positions of the Comet lower movable platen components specific to the Case 5 model, as reference in Table 159 of Section 3.2.1.

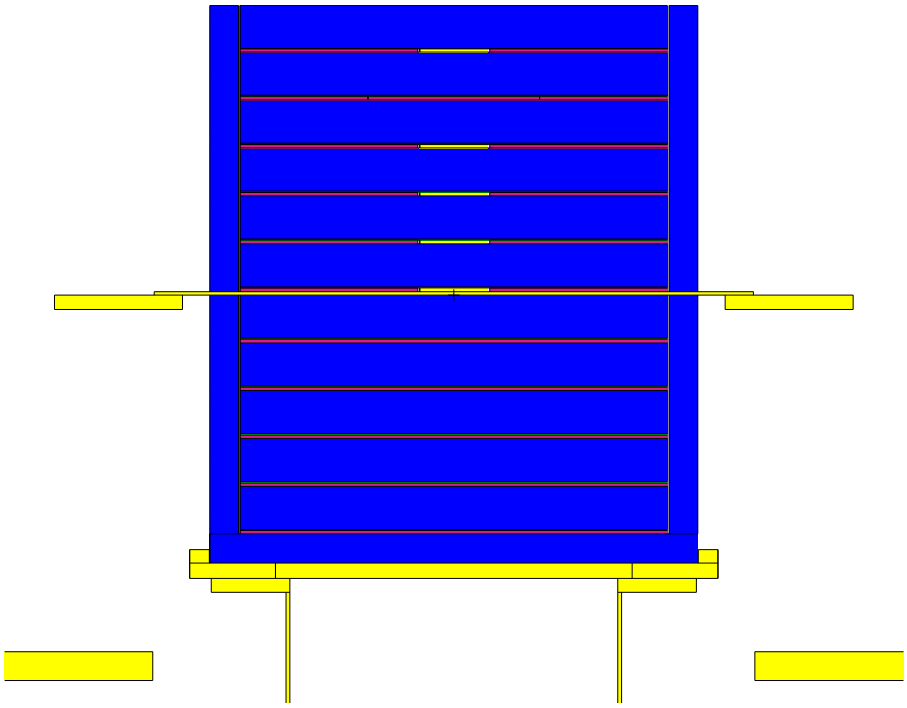

Figure 54: Case 5 model (HEU in pink, hafnium in green, polyethylene in blue, and aluminum in yellow).

Table 181: Case 5 model lower movable platen axial positions (see Section 3.2.1).

Part		Density (g/cm^3)	z-Plane (cm)	
			Lower	Upper
Adapter Plate	Lip	2.7	-23.84034	-22.64654
	Plate		-25.18654	-23.84034
Adapter Extension			-26.45654	-25.18654
			-44.23654	-26.45654
			-45.50654	-44.23654
Movable Platen			-48.04654	-45.50654

Table 182: Case 5 model upper core stack dimensions.

Layer	Part ID	Density (g/cm^3)	Radius (cm)		Thickness (cm)	z-Plane (cm)	
			Inner	Outer		Lower	Upper
17	Top Reflector	0.95477	-	19.05000	3.82626	21.93018	25.75644
16	10470	18.26062	3.18770	19.05000	0.31083	21.61346	21.92429
	2.5-DISK-5	2.70000	-	3.04800	0.31672		21.93018
15	1.5-MOD-11	0.94886	-	19.05000	3.83728	17.77618	21.61346
14	HF-10	13.01979	-	19.05000	0.10637	17.66981	17.77618
13	11018	18.26062	7.62635	19.05000	0.31083	17.35898	17.66981
	Q2-16	18.26062	-	7.62000	0.31083		17.66981
12	1.5-MOD-10	0.94886	-	19.05000	3.83728	13.52170	17.35898
11	HF-09	13.01979	-	19.05000	0.10637	13.41533	13.52170
10	10489	18.26062	3.18770	19.05000	0.31083	13.09861	13.40944
	2.5-DISK-4	2.70000	-	3.04800	0.31672		13.41533
9	1.5-MOD-9	0.94886	-	19.05000	3.83728	9.26133	13.09861
8	HF-08	13.01979	-	19.05000	0.10637	9.15496	9.26133
7	10491	18.26062	3.18770	19.05000	0.31083	8.83824	9.14907
	2.5-DISK-3	2.70000	-	3.04800	0.31672		9.15496
6	1.5-MOD-8	0.94886	-	19.05000	3.83728	5.00096	8.83824
5	HF-07	13.01979	-	19.05000	0.10637	4.89459	5.00096
4	10467	18.26062	3.18770	19.05000	0.31083	4.57787	4.88870
	2.5-DISK-2	2.70000	-	3.04800	0.31672		4.89459
3	1.5-MOD-7	0.94886	-	19.05000	3.83728	0.74059	4.57787
2	HF-06	13.01979	-	19.05000	0.10637	0.63422	0.74059
1	10487	18.26062	3.18770	19.05000	0.31083	0.31750	0.62833
	2.5-DISK-1	2.70000	-	3.04800	0.31672		0.63422

Table 183: Case 5 model lower core stack dimensions.

Layer	Part ID	Density (g/cm^3)	Radius (cm)		Thickness (cm)	z-Plane (cm)	
			Inner	Outer		Lower	Upper
16	1.5-MOD-6	0.94886	-	19.05000	3.83728	-3.83728	0.00000
15	HF-05	13.01979	-	19.05000	0.10637	-3.94365	-3.83728
14	11147	18.26062	-	19.05000	0.31083	-4.25448	-3.94365
13	1.5-MOD-5	0.94886	-	19.05000	3.83728	-8.09176	-4.25448
12	HF-04	13.01979	-	19.05000	0.10637	-8.19813	-8.09176
11	11149	18.26062	-	19.05000	0.31083	-8.50896	-8.19813
10	1.5-MOD-4	0.94886	-	19.05000	3.83728	-12.34624	-8.50896
9	HF-03	13.01979	-	19.05000	0.10637	-12.45261	-12.34624
8	11019	18.26062	-	19.05000	0.31083	-12.76344	-12.45261
7	1.5-MOD-3	0.94886	-	19.05000	3.83728	-16.60072	-12.76344
6	HF-02	13.01979	-	19.05000	0.10637	-16.70709	-16.60072
5	11017	18.26062	-	19.05000	0.31083	-17.01792	-16.70709
4	1.5-MOD-1	0.94886	-	19.05000	3.83728	-20.85520	-17.01792
3	HF-01	13.01979	-	19.05000	0.10637	-20.96157	-20.85520
2	11150	18.26062	-	19.05000	0.31083	-21.27240	-20.96157
1	BOTREF-1	0.95477	-	21.71700	2.56794	-23.84034	-21.27240

Table 184: Case 5 model upper and lower reflector ring dimensions (see Section 3.2.5).

Layer	Density (g/cm^3)	Radius (cm)		Thickness (cm)	z-Plane (cm)	
		Inner	Outer		Lower	Upper
Upper	0.95477	19.17700	21.71700	25.43894	0.31750	25.75644
Lower				21.27240	-21.27240	0.00000

3.2.8.6 Case 6

The Case 6 model includes 14 HEU plates, 13 hafnium plates, 26 0.125 in. (0.3175 cm) nominal HDPE moderator plates between each HEU plate, and a nominal 0.96875 in. (2.46063 cm) top HDPE reflector. These 14 HEU plates consist of six 15/0-HEU plates, seven 15/2.5-HEU plates, and one 15/6-HEU plate. Figure 55 shows a cross sectional view of the model. The aluminum parts (structural components, membrane, and inserts) are shown in yellow, the HEU plates in pink, the hafnium plates in green, and the polyethylene reflector in blue.

Figure 55 shows a diagram of the Case 6 model. Tables 186 and 188 report the upper and lower core stack dimensions, including: part densities (in g/cm^3), dimensions, and axial position (z-axis). Table 187 reports similar information for the upper and lower reflector rings. Table 185 describes the axial positions of the Comet lower movable platen components specific to the Case 6 model, as reference in Table 159 of Section 3.2.1.

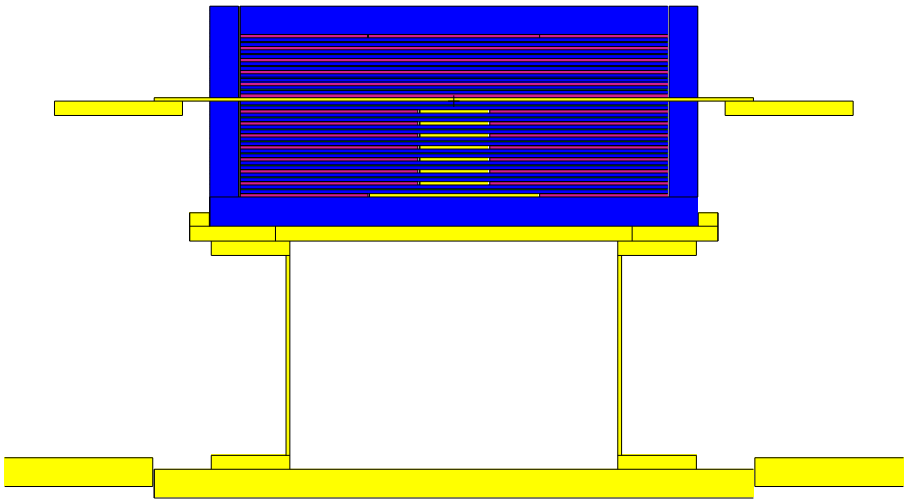

Figure 55: Case 6 model (HEU in pink, hafnium in green, polyethylene in blue, and aluminum in yellow).

Table 185: Case 6 model lower movable platen axial positions (see Section 3.2.1).

Part		Density (g/cm^3)	z-Plane (cm)	
			Lower	Upper
Adapter Plate	Lip	2.7	-11.10626	-9.91246
	Plate		-12.45246	-11.10626
Adapter Extension			-13.72246	-12.45246
			-31.50246	-13.72246
			-32.77246	-31.50246
Movable Platen			-35.31246	-32.77246

Table 186: Case 6 model upper core stack dimensions.

Layer	Part ID	Density (g/cm^3)	Radius (cm)		Thickness (cm)	z-Plane (cm)	
			Inner	Outer		Lower	Upper
22	Top Reflector	0.94203	-	19.05000	2.51489	5.93533	8.45022
21	11018	18.26705	7.62635	19.05000	0.31083	5.62450	5.93533
	Q2-16	18.26705	-	7.62000	0.31083		5.93533
20	1/8-MOD-31	0.94406	-	19.05000	0.32210	5.30240	5.62450
19	HF-13	12.98483	-	19.05000	0.10637	5.19603	5.30240
18	1/8-MOD-13	0.94406	-	19.05000	0.32210	4.87393	5.19603
17	11150	18.26705	-	19.05000	0.31083	4.56310	4.87393
16	1/8-MOD-30	0.94406	-	19.05000	0.32210	4.24100	4.56310
15	HF-12	12.98483	-	19.05000	0.10637	4.13463	4.24100
14	1/8-MOD-12	0.94406	-	19.05000	0.32210	3.81253	4.13463
13	11149	18.26705	-	19.05000	0.31083	3.50170	3.81253
12	1/8-MOD-29	0.94406	-	19.05000	0.32210	3.17960	3.50170
11	HF-11	12.98483	-	19.05000	0.10637	3.07323	3.17960
10	1/8-MOD-11	0.94406	-	19.05000	0.32210	2.75113	3.07323
9	11019	18.26705	-	19.05000	0.31083	2.44030	2.75113
8	1/8-MOD-28	0.94406	-	19.05000	0.32210	2.11820	2.44030
7	HF-10	12.98483	-	19.05000	0.10637	2.01183	2.11820
6	1/8-MOD-10	0.94406	-	19.05000	0.32210	1.68973	2.01183
5	11017	18.26705	-	19.05000	0.31083	1.37890	1.68973
4	1/8-MOD-27	0.94406	-	19.05000	0.32210	1.05680	1.37890
3	HF-09	12.98483	-	19.05000	0.10637	0.95043	1.05680
2	1/8-MOD-9	0.94406	-	19.05000	0.32210	0.62833	0.95043
1	11147	18.26705	-	19.05000	0.31083	0.31750	0.62833

Table 187: Case 6 model upper and lower reflector ring dimensions (see Section 3.2.5).

Layer	Density (g/cm^3)	Radius (cm)		Thickness (cm)	z-Plane (cm)	
		Inner	Outer		Lower	Upper
Upper	0.94203	19.17700	21.71700	8.13272	0.31750	8.45022
Lower				8.53832	-8.53832	0.00000

Table 188: Case 6 model lower core stack dimensions.

Layer	Part ID	Density (g/cm^3)	Radius (cm)		Thickness (cm)	z-Plane (cm)	
			Inner	Outer		Lower	Upper
33	1/8-MOD-26	0.94406	-	19.05000	0.32210	-0.32210	0.00000
32	HF-08	12.98483	-	19.05000	0.10637	-0.42847	-0.32210
31	1/8-MOD-8	0.94406	-	19.05000	0.32210	-0.75057	-0.42847
30	10464	18.26705	3.18770	19.05000	0.31083	-1.06729	-0.75646
	2.5-DISK-7	2.70000	-	3.04800	0.31672		-0.75057
29	1/8-MOD-25	0.94406	-	19.05000	0.32210	-1.38939	-1.06729
28	HF-07	12.98483	-	19.05000	0.10637	-1.49576	-1.38939
27	1/8-MOD-7	0.94406	-	19.05000	0.32210	-1.81786	-1.49576
26	10475	18.26705	3.18770	19.05000	0.31083	-2.13458	-1.82375
	2.5-DISK-6	2.70000	-	3.04800	0.31672		-1.81786
25	1/8-MOD-24	0.94406	-	19.05000	0.32210	-2.45668	-2.13458
24	HF-06	12.98483	-	19.05000	0.10637	-2.56305	-2.45668
23	1/8-MOD-6	0.94406	-	19.05000	0.32210	-2.88515	-2.56305
22	10470	18.26705	3.18770	19.05000	0.31083	-3.20187	-2.89104
	2.5-DISK-5	2.70000	-	3.04800	0.31672		-2.88515
21	1/8-MOD-23	0.94406	-	19.05000	0.32210	-3.52397	-3.20187
20	HF-05	12.98483	-	19.05000	0.10637	-3.63034	-3.52397
19	1/8-MOD-5	0.94406	-	19.05000	0.32210	-3.95244	-3.63034
18	10489	18.26705	3.18770	19.05000	0.31083	-4.26916	-3.95833
	2.5-DISK-4	2.70000	-	3.04800	0.31672		-3.95244
17	1/8-MOD-22	0.94406	-	19.05000	0.32210	-4.59126	-4.26916
16	HF-04	12.98483	-	19.05000	0.10637	-4.69763	-4.59126
15	1/8-MOD-4	0.94406	-	19.05000	0.32210	-5.01973	-4.69763
14	10491	18.26705	3.18770	19.05000	0.31083	-5.33645	-5.02562
	2.5-DISK-3	2.70000	-	3.04800	0.31672		-5.01973
13	1/8-MOD-21	0.94406	-	19.05000	0.32210	-5.65855	-5.33645
12	HF-03	12.98483	-	19.05000	0.10637	-5.76492	-5.65855
11	1/8-MOD-3	0.94406	-	19.05000	0.32210	-6.08702	-5.76492
10	10467	18.26705	3.18770	19.05000	0.31083	-6.40374	-6.09291
	2.5-DISK-2	2.70000	-	3.04800	0.31672		-6.08702
9	1/8-MOD-20	0.94406	-	19.05000	0.32210	-6.72584	-6.40374
8	HF-02	12.98483	-	19.05000	0.10637	-6.83221	-6.72584
7	1/8-MOD-2	0.94406	-	19.05000	0.32210	-7.15431	-6.83221
6	10487	18.26705	3.18770	19.05000	0.31083	-7.47103	-7.16020
	2.5-DISK-1	2.70000	-	3.04800	0.31672		-7.15431
5	1/8-MOD-19	0.94406	-	19.05000	0.32210	-7.79313	-7.47103
4	HF-01	12.98483	-	19.05000	0.10637	-7.89950	-7.79313
3	1/8-MOD-1	0.94406	-	19.05000	0.32210	-8.22160	-7.89950
2	10457	18.26705	7.62635	19.05000	0.31083	-8.53832	-8.22749
	6-DISK-1	2.70000	-	7.49300	0.31672		-8.22160
1	BOTREF-1	0.94203	-	21.71700	2.56794	-11.10626	-8.53832

3.2.8.7 Case 7

The Case 7 model includes 22 HEU plates, no HDPE moderator, a nominal 1.1875 in. (3.01625 cm) top HDPE reflector, and a nominal 0.48 in. (1.2192 cm) top and bottom hafnium reflector. These 22 HEU plates consist of six 15/0-HEU plates, seven 15/2.5-HEU plates, five 15/6-HEU plate, and four 15/10-HEU plates. Figure 56 shows a cross sectional view of the model. The aluminum parts (structural components, membrane, and inserts) are shown in yellow, the HEU plates in pink, the hafnium plates in green, and the polyethylene reflector in blue.

Figure 56 shows a diagram of the Case 7 model. Tables 190 and 191 report the upper and lower core stack dimensions, including: part densities (in g/cm^3), dimensions, and axial position (z-axis). Table 192 reports similar information for the upper and lower reflector rings. Table 189 describes the axial positions of the Comet lower movable platen components specific to the Case 7 model, as reference in Table 159 of Section 3.2.1.

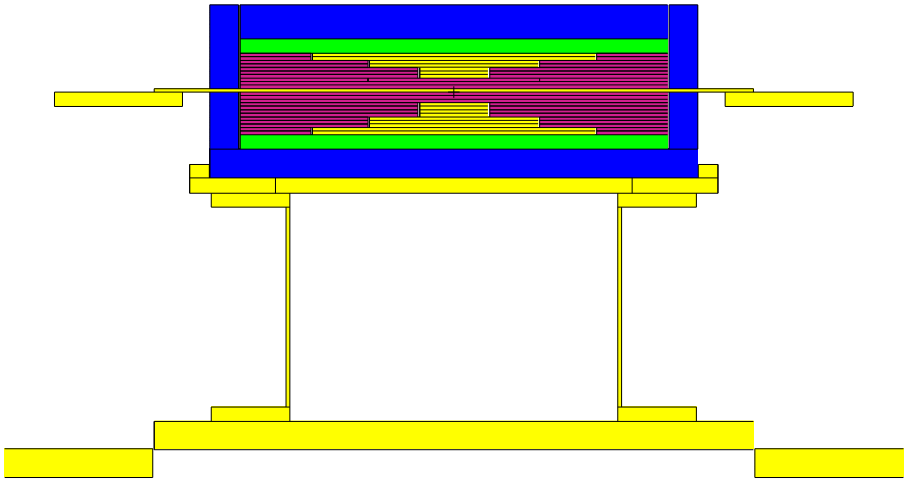

Figure 56: Case 7 model (HEU in pink, hafnium in green, polyethylene in blue, and aluminum in yellow).

Table 189: Case 7 model lower movable platen axial positions (see Section 3.2.1).

Part		Density (g/cm^3)	z-Plane (cm)	
			Lower	Upper
Adapter Plate	Lip	2.7	-7.62730	-6.43350
	Plate		-8.97350	-7.62730
Adapter Extension			-10.24350	-8.97350
			-28.02350	-10.24350
			-29.29350	-28.02350
Movable Platen			-31.83350	-29.29350

Table 190: Case 7 model upper core stack dimensions.

Layer	Part ID	Density (g/cm^3)	Radius (cm)		Thickness (cm)	z-Plane (cm)	
			Inner	Outer		Lower	Upper
12	Top Reflector	0.95427	-	19.05000	3.04105	4.74342	7.78447
11	Top HF	12.93639	-	19.05000	1.27639	3.46703	4.74342
10	10473	18.28140	12.70635	19.05000	0.31083	3.15031	3.46114
	10-DISK-4	2.70000	-	12.57300	0.31672		3.46703
9	10463	18.28140	12.70635	19.05000	0.31083	2.83359	3.14442
	10-DISK-3	2.70000	-	12.57300	0.31672		3.15031
8	10935	18.28140	7.62635	19.05000	0.31083	2.51687	2.82770
	6-DISK-5	2.70000	-	7.49300	0.31672		2.83359
7	10933	18.28140	7.62635	19.05000	0.31083	2.20015	2.51098
	6-DISK-4	2.70000	-	7.49300	0.31672		2.51687
6	10470	18.28140	3.18770	19.05000	0.31083	1.88343	2.19426
	2.5-DISK-7	2.70000	-	3.04800	0.31672		2.20015
5	10475	18.28140	3.18770	19.05000	0.31083	1.56671	1.87754
	2.5-DISK-6	2.70000	-	3.04800	0.31672		1.88343
4	10489	18.28140	3.18770	19.05000	0.31083	1.24999	1.56082
	2.5-DISK-5	2.70000	-	3.04800	0.31672		1.56671
3	11018	18.28140	7.62635	19.05000	0.31083	0.93916	1.24999
	Q2-16	18.28140	-	7.62000	0.31083		1.24999
2	11017	18.28140	-	19.05000	0.31083	0.62833	0.93916
1	11150	18.28140	-	19.05000	0.31083	0.31750	0.62833

Table 191: Case 7 model lower core stack dimensions.

Layer	Part ID	Density (g/cm^3)	Radius (cm)		Thickness (cm)	z-Plane (cm)	
			Inner	Outer		Lower	Upper
14	11019	18.28140	-	19.05000	0.31083	-0.31083	0.00000
13	11147	18.28140	-	19.05000	0.31083	-0.62166	-0.31083
12	11149	18.28140	-	19.05000	0.31083	-0.93249	-0.62166
11	10467	18.28140	3.18770	19.05000	0.31083	-1.24921	-0.93838
	2.5-DISK-4	2.70000	-	3.04800	0.31672		-0.93249
10	10464	18.28140	3.18770	19.05000	0.31083	-1.56593	-1.25510
	2.5-DISK-3	2.70000	-	3.04800	0.31672		-1.24921
9	10487	18.28140	3.18770	19.05000	0.31083	-1.88265	-1.57182
	2.5-DISK-2	2.70000	-	3.04800	0.31672		-1.56593
8	10491	18.28140	3.18770	19.05000	0.31083	-2.19937	-1.88854
	2.5-DISK-1	2.70000	-	3.04800	0.31672		-1.88265
7	10932	18.28140	7.62635	19.05000	0.31083	-2.51609	-2.20526
	6-DISK-3	2.70000	-	7.49300	0.31672		-2.19937
6	10457	18.28140	7.62635	19.05000	0.31083	-2.83281	-2.52198
	6-DISK-2	2.70000	-	7.49300	0.31672		-2.51609
5	10477	18.28140	7.62635	19.05000	0.31083	-3.14953	-2.83870
	6-DISK-1	2.70000	-	7.49300	0.31672		-2.83281
4	10458	18.28140	12.70635	19.05000	0.31083	-3.46625	-3.15542
	10-DISK-2	2.70000	-	12.57300	0.31672		-3.14953
3	10472	18.28140	12.70635	19.05000	0.31083	-3.78297	-3.47214
	10-DISK-1	2.70000	-	12.57300	0.31672		-3.46625
2	Bottom HF	12.93639	-	19.05000	1.27639	-5.05936	-3.78297
1	BOTREF-1	0.95427	-	21.71700	2.56794	-7.62730	-5.05936

Table 192: Case 7 model upper and lower reflector ring dimensions (see Section 3.2.5).

Layer	Density (g/cm^3)	Radius (cm)		Thickness (cm)	z-Plane (cm)	
		Inner	Outer		Lower	Upper
Upper	0.95427	19.17700	21.71700	7.46697	0.31750	7.78447
Lower				5.05936	-5.05936	0.00000

3.3 Material Data

3.3.1 Highly Enriched Uranium

The HEU composition is modeled with a ^{235}U enrichment of 93.232%, by weight. The impurities were removed from the HEU based on the simplification bias analyzed in Section 3.1.1.1. Table 193 reports the elemental and isotopic composition of the HEU material used in all benchmark models, renormalized following the removal of the impurities. Table 194 reports the densities of the HEU plates used in the benchmark models. These densities represent a bulk density per benchmark model, conserving the total HEU mass in each experimental configuration. Table 195 reports the atom densities for the HEU used in the benchmark models.

Table 193: HEU elemental and isotopic composition used in all benchmark models.

Element	Wt.%	Isotope	Wt.%	At.%
U	1.00000E+02	^{234}U	1.03046E+00	1.03556E+00
		^{235}U	9.32324E+01	9.32940E+01
		^{236}U	2.32202E-01	2.31369E-01
		^{238}U	5.50498E+00	5.43904E+00

Table 194: HEU plate density by case.

Case	Density (g/cm^3)
1	18.27667
2	18.27669
3	18.23772
4	18.26915
5	18.26062
6	18.26705
7	18.28140

Table 195: HEU plate atom densities by case.

Isotope	Atom Density (atoms-b/cm)			
	Case 1	**Case 2**	**Case 3**	**Case 4**
^{234}U	4.84602E-04	4.84603E-04	4.83570E-04	4.84403E-04
^{235}U	4.36579E-02	4.36579E-02	4.35649E-02	4.36399E-02
^{236}U	1.08272E-04	1.08272E-04	1.08041E-04	1.08227E-04
^{238}U	2.54525E-03	2.54526E-03	2.53983E-03	2.54421E-03
Total	**4.67960E-02**	**4.67961E-02**	**4.66963E-02**	**4.67768E-02**

Isotope	Atom Density (atoms-b/cm)		
	Case 5	**Case 6**	**Case 7**
^{234}U	4.84177E-04	4.84347E-04	4.84728E-04
^{235}U	4.36195E-02	4.36349E-02	4.36692E-02
^{236}U	1.08176E-04	1.08215E-04	1.08300E-04
^{238}U	2.54302E-03	2.54391E-03	2.54591E-03
Total	**4.67549E-02**	**4.67714E-02**	**4.68081E-02**

3.3.2 Hafnium

The hafnium composition is modeled based on the sample measurements, as described in Section 1.3.2.2. The impurities were removed from the hafnium based on the simplification bias analyzed in Section 3.1.1.2. Table 196 reports the elemental and isotopic composition of the hafnium material used in all benchmark models, renormalized following the removal of the impurities. Table 197 reports the densities of the hafnium plates used in the benchmark models. These densities represent a bulk density per benchmark model, conserving the total hafnium mass in each experimental configuration. Table 198 reports the atom densities for the hafnium used in the benchmark models.

Table 196: Hafnium elemental and isotopic composition used in all benchmark models.

Element	Wt.%	Isotope	Wt.%	At.%
Hf	9.73232E+01	^{174}Hf	1.57664E-01	1.57736E-01
		^{176}Hf	5.06664E+00	5.01046E+00
		^{177}Hf	1.81079E+01	1.78088E+01
		^{178}Hf	2.65663E+01	2.59805E+01
		^{179}Hf	1.32642E+01	1.28990E+01
		^{180}Hf	3.41604E+01	3.30354E+01
Zr	2.67684E+00	^{90}Zr	1.37724E+00	2.66578E+00
		^{91}Zr	3.00342E-01	5.74942E-01
		^{92}Zr	4.59078E-01	8.69254E-01
		^{94}Zr	4.65235E-01	8.62138E-01
		^{96}Zr	7.49516E-02	1.35995E-01

Table 197: Hafnium plate density by case.

Case	Density (g/cm^3)
1	12.93639
2	12.96977
3	12.99905
4	13.01535
5	13.01979
6	12.98483
7	12.93639

Table 198: Hafnium plate atom densities by case.

Isotope	Atom Density (atoms-b/cm)			
	Case 1	Case 2	Case 3	Case 4
^{174}Hf	7.06143E-05	7.07965E-05	7.09564E-05	7.10453E-05
^{176}Hf	2.24343E-03	2.24922E-03	2.25430E-03	2.25713E-03
^{177}Hf	7.97254E-03	7.99311E-03	8.01115E-03	8.02120E-03
^{178}Hf	1.16308E-02	1.16608E-02	1.16871E-02	1.17018E-02
^{179}Hf	5.77457E-03	5.78947E-03	5.80254E-03	5.80982E-03
^{180}Hf	1.47891E-02	1.48272E-02	1.48607E-02	1.48793E-02
^{90}Zr	1.19340E-03	1.19648E-03	1.19918E-03	1.20069E-03
^{91}Zr	2.57387E-04	2.58051E-04	2.58634E-04	2.58958E-04
^{92}Zr	3.89143E-04	3.90147E-04	3.91028E-04	3.91518E-04
^{94}Zr	3.85957E-04	3.86953E-04	3.87827E-04	3.88313E-04
^{96}Zr	6.08816E-05	6.10387E-05	6.11765E-05	6.12532E-05
Total	**4.47678E-02**	**4.48833E-02**	**4.49847E-02**	**4.50411E-02**

Isotope	Atom Density (atoms-b/cm)		
	Case 5	Case 6	Case 7
^{174}Hf	7.10696E-05	7.08788E-05	7.06143E-05
^{176}Hf	2.25790E-03	2.25184E-03	2.24343E-03
^{177}Hf	8.02394E-03	8.00239E-03	7.97254E-03
^{178}Hf	1.17058E-02	1.16744E-02	1.16308E-02
^{179}Hf	5.81180E-03	5.79620E-03	5.77457E-03
^{180}Hf	1.48844E-02	1.48445E-02	1.47891E-02
^{90}Zr	1.20110E-03	1.19787E-03	1.19340E-03
^{91}Zr	2.59046E-04	2.58351E-04	2.57387E-04
^{92}Zr	3.91652E-04	3.90600E-04	3.89143E-04
^{94}Zr	3.88445E-04	3.87402E-04	3.85957E-04
^{96}Zr	6.12741E-05	6.11095E-05	6.08816E-05
Total	**4.50564E-02**	**4.49354E-02**	**4.47678E-02**

3.3.3 Polyethylene

The polyethylene composition is modeled as CH_2. The impurities were removed from the polyethylene based on the simplification bias analyzed in Section 3.1.1.3. Table 199 reports the elemental and isotopic composition of the polyethylene material used in all benchmark models, renormalized following the removal of the impurities. Table 200 reports the densities of the polyethylene moderator and reflector used in the benchmark models. The polyethylene reflector consists of the top reflector plate, bottom reflector plate, and upper and lower reflector rings. These densities represent a bulk density per benchmark model, conserving the total polyethylene mass in each experimental configuration. Table 201 reports the atom densities for the polyethylene moderator used in the benchmark models. Table 202 reports the atom densities for the polyethylene reflector used in the benchmark models.

Table 199: Polyethylene elemental and isotopic composition used in all models.

Element	Wt.%	Isotope	Wt.%	At.%
H	1.43711E+01	^{1}H	1.43689E+01	6.66607E+01
		^{2}H	2.15566E-03	5.00403E-03
C	8.56289E+01	^{12}C	8.46870E+01	3.29956E+01
		^{13}C	9.41918E-01	3.38670E-01

Table 200: Polyethylene moderator and reflector densities by case.

Case	Density (g/cm^3)	
	Moderator	Reflector
1	-	0.95576
2	0.93595	0.95313
3	0.93377	0.94305
4	0.94203	0.95200
5	0.94886	0.95477
6	0.94406	0.94203
7	-	0.95427

Table 201: Polyethylene moderator atom densities by case, not present in Cases 1 and 7.

Isotope	Atom Density (atoms-b/cm)				
	Case 2	Case 3	Case 4	Case 5	Case 6
^{1}H	8.02850E-02	8.00978E-02	8.08060E-02	8.13923E-02	8.09802E-02
^{2}H	6.02676E-06	6.01271E-06	6.06587E-06	6.10988E-06	6.07895E-06
^{12}C	3.97394E-02	3.96467E-02	3.99972E-02	4.02874E-02	4.00835E-02
^{13}C	4.07889E-04	4.06938E-04	4.10535E-04	4.13514E-04	4.11421E-04
Total	**1.20438E-01**	**1.20158E-01**	**1.21220E-01**	**1.22099E-01**	**1.21481E-01**

Table 202: Polyethylene reflector atom densities by case.

Isotope	Atom Density (atoms-b/cm)			
	Case 1	**Case 2**	**Case 3**	**Case 4**
^{1}H	8.19840E-02	8.17587E-02	8.08934E-02	8.16613E-02
^{2}H	6.15430E-06	6.13739E-06	6.07243E-06	6.13008E-06
^{12}C	4.05803E-02	4.04688E-02	4.00405E-02	4.04206E-02
^{13}C	4.16520E-04	4.15375E-04	4.10979E-04	4.14881E-04
Total	**1.22987E-01**	**1.22649E-01**	**1.21351E-01**	**1.22503E-01**

Isotope	Atom Density (atoms-b/cm)		
	Case 5	**Case 6**	**Case 7**
^{1}H	8.18994E-02	8.08065E-02	8.18558E-02
^{2}H	6.14795E-06	6.06591E-06	6.14468E-06
^{12}C	4.05384E-02	3.99975E-02	4.05169E-02
^{13}C	4.16090E-04	4.10538E-04	4.15869E-04
Total	**1.22860E-01**	**1.21221E-01**	**1.22795E-01**

3.3.4 Aluminum

The aluminum composition is modeled as ^{27}Al. The other constituents of the Al-6061 alloy (Mg, Si, Cu, Cr, Fe, Zn, Mn, and Ti) were removed based on the simplification bias analyzed in Section 3.1.1.4. The density is modeled at the theoretical 2.7 $\mathrm{g\,cm^{-3}}$ (6.02623E-02 atom-b/cm) based on the additional simplification bias analyzed in Section 3.1.1.8.

3.4 Temperature Data

All benchmark cases use a temperature of 293.6 K (20.45°C).

3.5 Experimental and Benchmark-Model k_{eff}

As discussed in Section 2.1, the k_{eff} of the experimental configurations was calculated based on the measured reactor period. The experimental k_{eff} uncertainty was calculated by summing the combined modeling uncertainty (Section 2.6) and the experiment measurement uncertainty (Section 2.1) in quadrature. A calculation bias was determined based on the model simplification described in Section 3.1.1. The expected benchmark k_{eff} is determined by adding the bias to the experimental k_{eff}, summarized for the benchmark models in Table 157 of Section 3.1.1. The benchmark model uncertainty was calculated by summing the experimental k_{eff} uncertainty and the bias uncertainty in quadrature.

Table 203: Expected benchmark model k_{eff}.

Case	Experimental $k_{eff} \pm 1\sigma$	Bias in $k_{eff} \pm 1\sigma$	Benchmark Model k_{eff}
1	1.00101 ± 0.00146	-0.00198 ± 0.00013	0.99903 ± 0.00147
2	1.00102 ± 0.00157	-0.00194 ± 0.00014	0.99908 ± 0.00158
3	1.00185 ± 0.00153	-0.00249 ± 0.00015	0.99936 ± 0.00154
4	1.00063 ± 0.00123	-0.00220 ± 0.00015	0.99843 ± 0.00124
5	1.00081 ± 0.00146	0.00096 ± 0.00015	1.00177 ± 0.00147
6	1.00120 ± 0.00141	-0.00177 ± 0.00014	0.99943 ± 0.00142
7	1.00085 ± 0.00136	-0.00142 ± 0.00012	0.99943 ± 0.00137

4.0 RESULTS OF SAMPLE CALCULATIONS

Calculated fission fractions using MCNP® 6.2.2 with ENDF/B-VIII.0 cross sections are presented in Table 204. These calculated fission fractions are also shown in Table 1 of Section 1.0. These results show that the experimental configurations span the entire neutron energy spectrum: fast (Cases 1 and 7), intermediate (Cases 2, 3, and 6), mixed (Case 4), and thermal (Case 5).

Table 204: Fission fractions calculated using MCNP® 6.2.2 with ENDF/B-VIII.0 (United States).

Case	Calculated Fission Fractions		
	Thermal (<0.625 eV)	**Intermediate (0.625 eV - 100 keV)**	**Fast (>100 keV)**
1	0.057	0.179	0.764
2	0.085	0.511	0.404
3	0.155	0.551	0.294
4	0.311	0.487	0.203
5	0.598	0.279	0.123
6	0.129	0.575	0.296
7	0.015	0.136	0.849

Results are presented for MCNP® 6.2.2 using ENDF/B-VIII.0 cross section libraries[22,23] in Table 205 and MCNP® 6.2.2 using ENDF/B-VII.1 cross section libraries[24] in Table 206. Both tables include the associated calculated-over-experiment results, comparing to the benchmark model k_{eff} results reported in Table 203 of Section 3.5. Sample MCNP® 6.2.2 input files using ENDF/B-VIII.0 cross section libraries are included as attachments to Section A.1 of Appendix A.

Table 205: Sample k_{eff} and C/E results with combined experimental and calculational uncertainties using MCNP® 6.2.2 with ENDF/B-VIII.0 (United States).

Case	MCNP® 6.2.2 (Continuous Energy ENDF/B-VIII.0)	
	Calculated k_{eff}	**C/E**
1	1.00097 ± 0.00003	1.00194 ± 0.00147
2	1.00135 ± 0.00003	1.00227 ± 0.00158
3	0.99854 ± 0.00004	0.99918 ± 0.00154
4	0.99574 ± 0.00004	0.99731 ± 0.00124
5	0.99947 ± 0.00004	0.99770 ± 0.00147
6	0.99850 ± 0.00004	0.99907 ± 0.00142
7	0.99605 ± 0.00003	0.99662 ± 0.00137

[22] J. L. Conlin et al. *Release of ENDF/B-VIII.0-Based ACE Data Files*. LA-UR-18-24034. Los Alamos National Laboratory, 2018. DOI: 10.2172/1438139.

[23] D. K. Parsons and C. A. Toccoli. *Re-Release of the ENDF/B VIII.0 S(α,β) Data Processed by NJOY2016*. LA-UR-20-24456. Los Alamos National Laboratory, 2020. DOI: 10.2172/1634930.

[24] J. L. Conlin et al. *Release of ENDF/B-VII.1-based Continuous Energy Neutron Cross Section Data Tables for MCNP*. LA-UR-13-20240. Los Alamos National Laboratory, 2013.

Table 206: Sample k_{eff} and C/E results with combined experimental and calculational uncertainties using MCNP® 6.2.2 with ENDF/B-VII.1 (United States).

Case	MCNP® 6.2.2 (Continuous Energy ENDF/B-VII.1)	
	Calculated k_{eff}	C/E
1	1.00071 ± 0.00003	1.00168 ± 0.00147
2	0.99733 ± 0.00004	0.99825 ± 0.00158
3	0.99596 ± 0.00004	0.99660 ± 0.00154
4	0.99533 ± 0.00004	0.99690 ± 0.00124
5	1.00298 ± 0.00004	1.00121 ± 0.00147
6	0.99608 ± 0.00004	0.99665 ± 0.00142
7	0.99824 ± 0.00003	0.99881 ± 0.00137

Results are presented for COG 11.3 using ENDF/B-VIII.0 cross section libraries[25] in Table 207. The table includes the associated C/E results, comparing to the benchmark model k_{eff} results reported in Table 203 of Section 3.5. These results and inputs were provided by Eric Aboud of Lawrence Livermore National Laboratory.

Table 207: Sample k_{eff} and C/E results with combined experimental and calculational uncertainties using COG 11.3 with ENDF/B-VIII.0 (United States).

Case	COG 11.3 (Continuous Energy ENDF/B-VIII.0)	
	Calculated k_{eff}	C/E
1	0.99924 ± 0.00010	1.00021 ± 0.00147
2	1.00097 ± 0.00010	1.00189 ± 0.00158
3	0.99949 ± 0.00010	1.00013 ± 0.00154
4	0.99712 ± 0.00010	0.99869 ± 0.00124
5	1.00162 ± 0.00010	0.99985 ± 0.00147
6	0.99945 ± 0.00010	1.00002 ± 0.00142
7	0.99527 ± 0.00010	0.99584 ± 0.00137

[25] R. M. Buck and E. M. Lent. *COG User's Manual: A Multiparticle Monte CarloTransport Code, 5th Edition*. UCRL-TM-202590. Lawrence Livermore National Laboratory, 2002.

Results are presented for MC21 10.2 using ENDF/B-VIII.0 cross section libraries[26] in Table 208 and MC21 10.2 using ENDF/B-VII.1 cross section libraries in Table 209. Both tables include the associated C/E results, comparing to the benchmark model k_{eff} results reported in Table 203 of Section 3.5. These results were provided by Daniel Kelly of Naval Nuclear Laboratory.

Table 208: Sample k_{eff} and C/E results with combined experimental and calculational uncertainties using MC21 10.2 with ENDF/B-VIII.0 (United States).

Case	**MC21 10.2 (Continuous Energy ENDF/B-VIII.0)**	
	Calculated k_{eff}	**C/E**
1	1.00065 ± 0.00005	1.00162 ± 0.00147
2	1.00094 ± 0.00005	1.00186 ± 0.00158
3	0.99818 ± 0.00005	0.99882 ± 0.00154
4	0.99548 ± 0.00005	0.99705 ± 0.00124
5	0.99986 ± 0.00005	0.99809 ± 0.00147
6	0.99818 ± 0.00005	0.99875 ± 0.00142
7	0.99597 ± 0.00005	0.99654 ± 0.00137

Table 209: Sample k_{eff} and C/E results with combined experimental and calculational uncertainties using MC21 10.2 with ENDF/B-VII.1 (United States).

Case	**MC21 10.2 (Continuous Energy ENDF/B-VII.1)**	
	Calculated k_{eff}	**C/E**
1	1.00036 ± 0.00005	1.00133 ± 0.00147
2	0.99705 ± 0.00005	0.99797 ± 0.00158
3	0.99561 ± 0.00005	0.99625 ± 0.00154
4	0.99501 ± 0.00005	0.99657 ± 0.00124
5	1.00369 ± 0.00005	1.00192 ± 0.00147
6	0.99588 ± 0.00005	0.99645 ± 0.00142
7	0.99835 ± 0.00005	0.99892 ± 0.00137

[26] D. P. Griesheimer et al. "MC21 v.6.0 – A continuous-energy Monte Carlo particle transport code with integrated reactor feedback capabilities". *Annals of Nuclear Energy* 82 (2015), pp. 29–40. DOI: 10.1016/j.anucene.2014.08.020.

Results are presented for SCALE 6.3.1 using ENDF/B-VIII.0 cross section libraries[27] in Table 210 and SCALE 6.3.1 using ENDF/B-VII.1 cross section libraries in Table 211. Both tables include the associated C/E results, comparing to the benchmark model k_{eff} results reported in Table 203 of Section 3.5. These results and inputs were provided by William Marshall of Oak Ridge National Laboratory.

Table 210: Sample k_{eff} and C/E results with combined experimental and calculational uncertainties using SCALE 6.3.1 with ENDF/B-VIII.0 (United States).

Case	**SCALE 6.3.1 (Continuous Energy ENDF/B-VIII.0)**	
	Calculated k_{eff}	**C/E**
1	1.00160 ± 0.00010	1.00257 ± 0.00147
2	1.00233 ± 0.00010	1.00325 ± 0.00158
3	0.99989 ± 0.00010	1.00053 ± 0.00154
4	0.99751 ± 0.00010	0.99908 ± 0.00124
5	1.00125 ± 0.00010	0.99948 ± 0.00147
6	0.99986 ± 0.00010	1.00043 ± 0.00142
7	0.99713 ± 0.00010	0.99770 ± 0.00137

Table 211: Sample k_{eff} and C/E results with combined experimental and calculational uncertainties using SCALE 6.3.1 with ENDF/B-VII.1 (United States).

Case	**SCALE 6.3.1 (Continuous Energy ENDF/B-VII.1)**	
	Calculated k_{eff}	**C/E**
1	1.00137 ± 0.00010	1.00234 ± 0.00147
2	0.99819 ± 0.00010	0.99911 ± 0.00158
3	0.99733 ± 0.00010	0.99797 ± 0.00154
4	0.99716 ± 0.00010	0.99873 ± 0.00124
5	1.00378 ± 0.00010	1.00200 ± 0.00147
6	0.99732 ± 0.00010	0.99789 ± 0.00142
7	0.99941 ± 0.00010	0.99998 ± 0.00137

[27] W. A. Wieselquist and R. A. Lefebvre. *SCALE 6.3.1 User Manual*. ORNL/TM-SCALE-6.3.1. Oak Ridge National Laboratory, 2023. DOI: 10.2172/1959594.

5.0 REFERENCES

[1] J. D. Norris. *TEX-Hf: Integral Experiment Execution of Thermal/Epithermal eXperiments using Highly Enriched Uranium with Polyethylene and Hafnium (IER-532 CED-3b Report)*. LLNL-TR-850980. Lawrence Livermore National Laboratory, 2023. DOI: 10.2172/1992573.

[2] J. D. Norris. *TEX-HEU Baseline Assemblies: Highly Enriched Uranium Plates with Polyethylene Moderator and Polyethylene Reflector*. HEU-MET-MIXED-021, Rev. 0. International Handbook of Evaluated Criticality Safety Benchmark Experiments, NEA/NSC/DOC(95)03/II, Nuclear Energy Agency of the Organisation for Economic Co-operation and Development, 2020.

[3] R. D. Mosteller, R. W. Brewer, and J. L. Sapir. *The Initial Set of Zeus Experiments: Intermediate-Spectrum Critical Assemblies with a Graphite-HEU Core Surrounded by a Copper Reflector*. HEU-MET-INTER-006, Rev. 4. International Handbook of Evaluated Criticality Safety Benchmark Experiments, NEA/NSC/DOC(95)03/II, Nuclear Energy Agency of the Organisation for Economic Co-operation and Development, 2004.

[4] D. K. Hayes. *Zeus: Fast-Spectrum Critical Assemblies with an Iron-HEU Core Surrounded by a Copper Reflector*. HEU-MET-FAST-072, Rev. 1. International Handbook of Evaluated Criticality Safety Benchmark Experiments, NEA/NSC/DOC(95)03/II, Nuclear Energy Agency of the Organisation for Economic Co-operation and Development, 2006.

[5] R. D. Mosteller. *The Unmoderated Zeus Experiment: A Cylindrical HEU Core Surrounded by a Copper Reflector*. HEU-MET-FAST-073, Rev. 0. International Handbook of Evaluated Criticality Safety Benchmark Experiments, NEA/NSC/DOC(95)03/II, Nuclear Energy Agency of the Organisation for Economic Co-operation and Development, 2005.

[6] J. L. Sapir, B. J. Krohn, and R. D. Mosteller. *Big Ten: A Large, Mixed-Uranium-Metal Cylindrical Core with 10% Average U-235 Enrichment, Surrounded by a Thick U-238 Reflectors*. IEU-MET-FAST-007, Rev. 2. International Handbook of Evaluated Criticality Safety Benchmark Experiments, NEA/NSC/DOC (95)03/III, Nuclear Energy Agency of the Organisation for Economic Co-operation and Development, 2011.

[8] J. M. Goda. *HEU Data Jemima Plates 2019*. LA-UR-19-24229. Los Alamos National Laboratory, 2019.

APPENDIX A: TYPICAL INPUT LISTINGS

A.1 MCNP® 6.2.2 Input Listings

All cases listed use ENDF/B-VIII.0 nuclear data. Calculations are typically executed with 1,000 generations of 500,000 particles per generation, skipping the first 50 generations, resulting in a total of 475 million active histories.

A.1.1 Case 1

Input: MCNP® 6.2.2 Case 1

A.1.2 Case 2

Input: MCNP® 6.2.2 Case 2

A.1.3 Case 3

Input: MCNP® 6.2.2 Case 3

A.1.4 Case 4

Input: MCNP® 6.2.2 Case 4

A.1.5 Case 5

Input: MCNP® 6.2.2 Case 5

A.1.6 Case 6

Input: MCNP® 6.2.2 Case 6

A.1.7 Case 7

Input: MCNP® 6.2.2 Case 7

APPENDIX B: DESIGN DRAWINGS

The following sections include various as-designed part drawings for select components of TEX-Hf. Most of these drawings are part of NCERC Project Drawing (LA-UR-20-30439) provided by Los Alamos National Laboratory. The hafnium plate drawing was provided by Naval Nuclear Laboratory.

The interface plate (128Y1720909) is affixed to the Comet stationary platform using the 12 in. standoffs (128Y1720908 01). The lower adapter consists of two parts which are fastened to the Comet movable platen. The adapter plate (128Y1720900) provides the base which holds the bottom reflector. This plate is affixed to the movable platen with the lower adapter extension (128Y1720916).

The membrane (128Y1720910) and alignment plate (128Y1720901) provide the support and the alignment for the upper half of the experiment. These two plates sit on top of the interface plate using the four pegs.

The alignment brackets (128Y1720913) are a removable alignment fixture that attaches to the interface plate. The brackets hold and position a T-square to ensure the reflectors used in the experiments are in vertical alignment prior to final measurements. They are removed before the experiment measurements.

B.1 Comet Stationary Platform

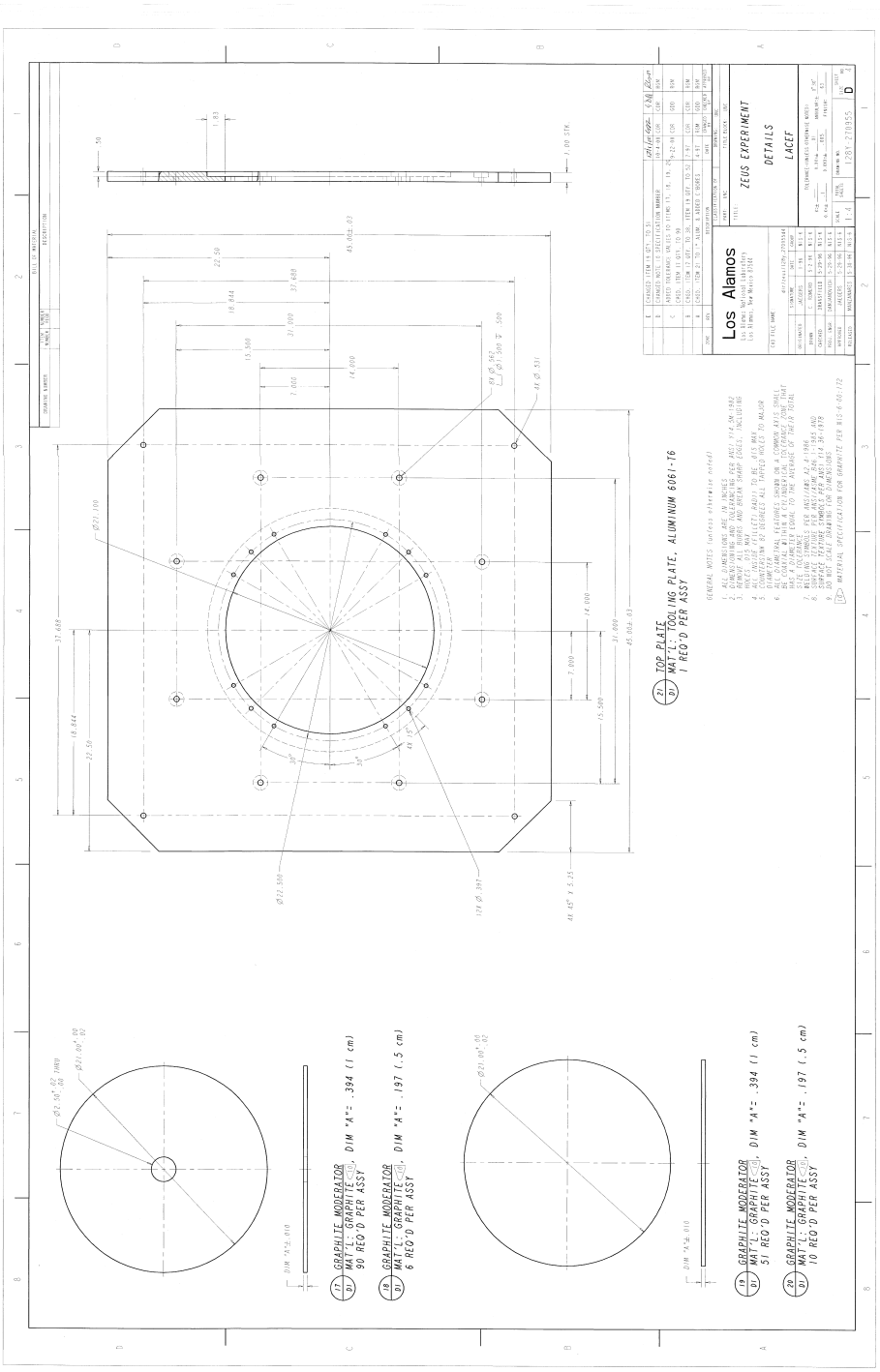

Figure 57: Drawing of the Comet stationary platform, referred to as the Top Plate in the drawing[28].

[28] Drawing No. 128Y-270955, Rev. E, "Zeus Experiment Details LACEF." Los Alamos National Laboratory, December 2000.

B.2 Comet Movable Platen

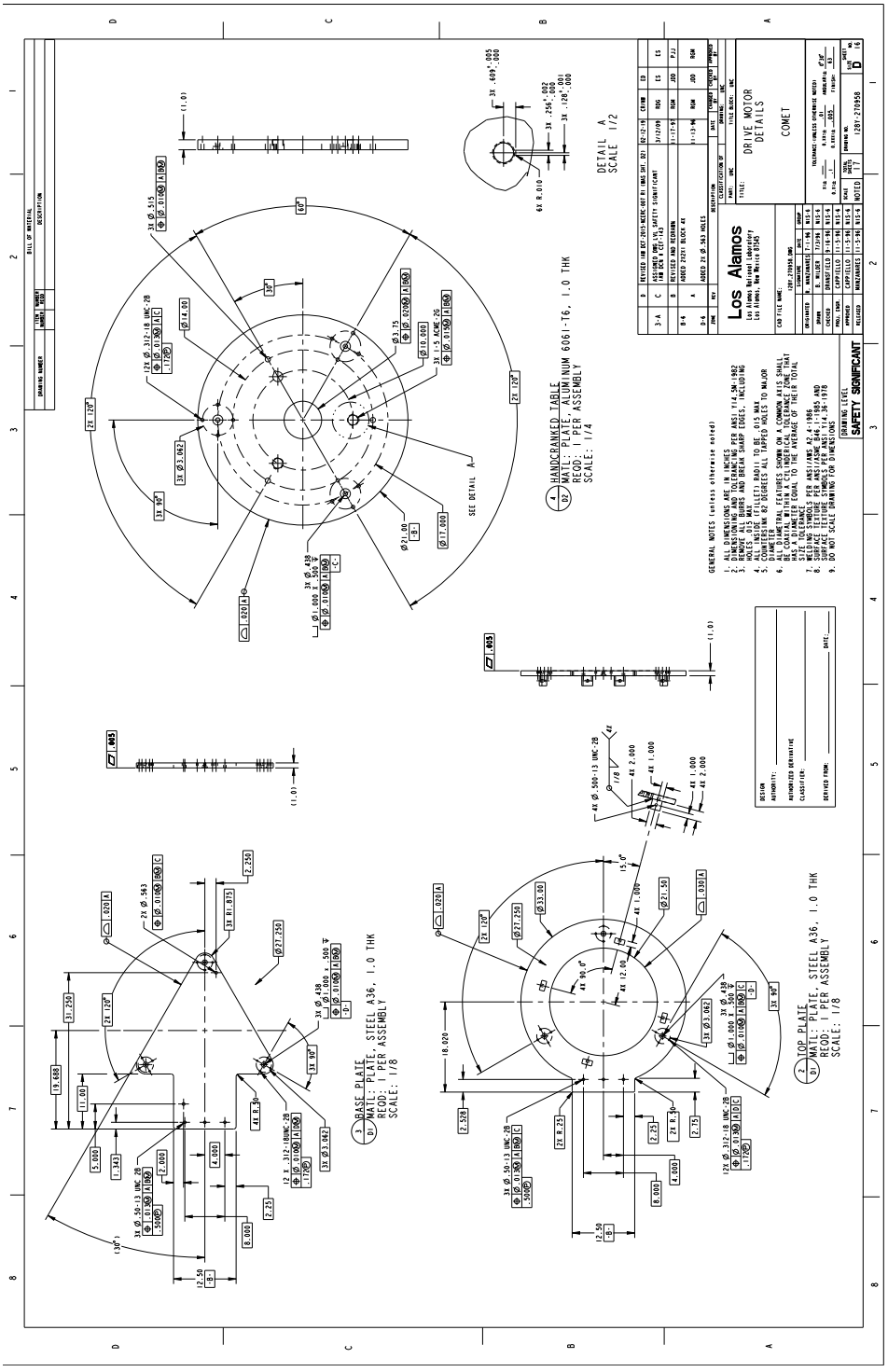

Figure 58: Drawing of the Comet movable platen, referred to as the Handcranked Table in the drawing[29].

[29] Drawing No. 128Y-270958, Rev. D, "Driver Motor Details Comet." Los Alamos National Laboratory, February 2019.

B.3 Interface Plate

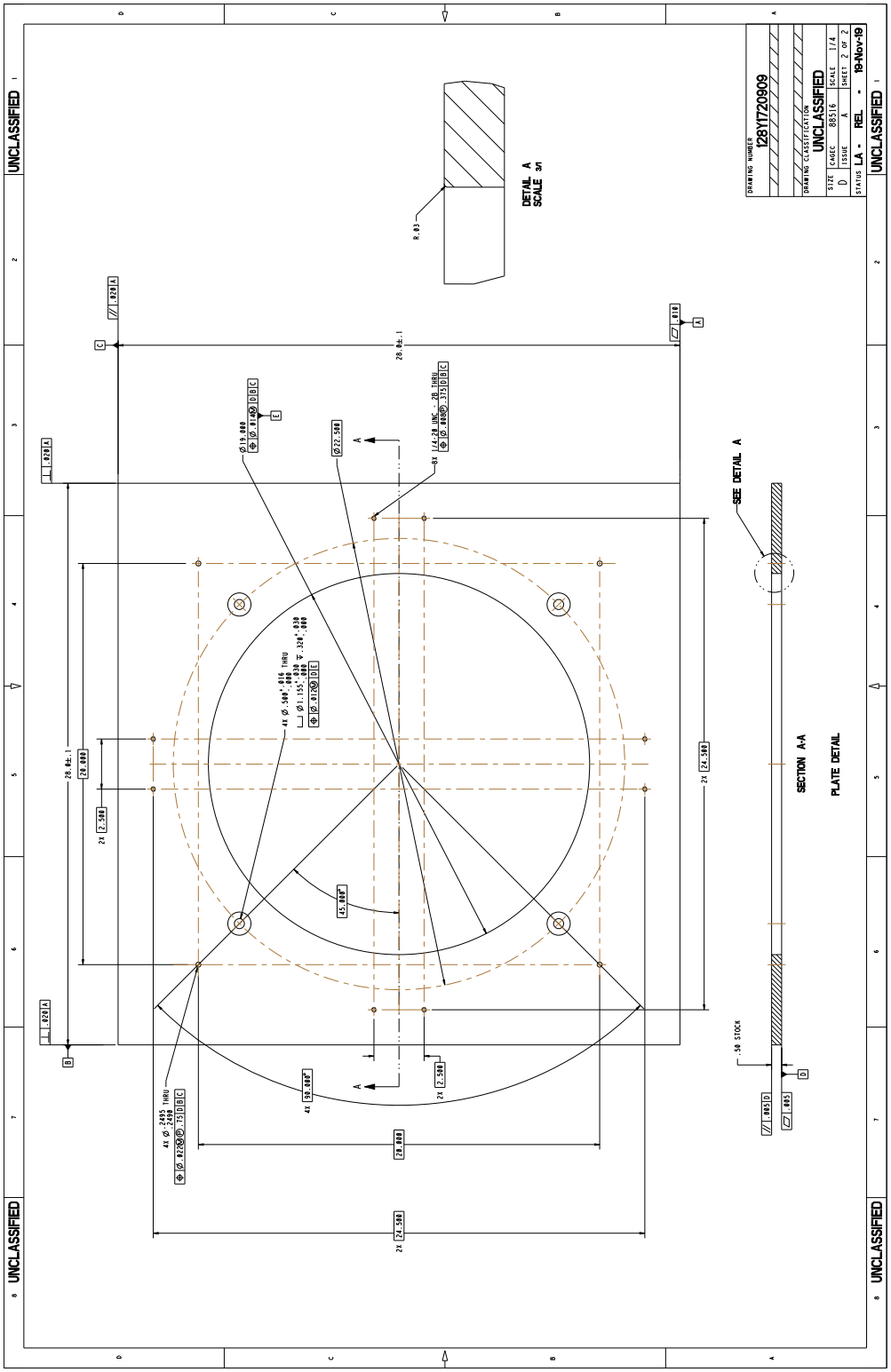

Figure 59: Drawing of the interface plate (dimensions in inches).

B.4 Standoffs

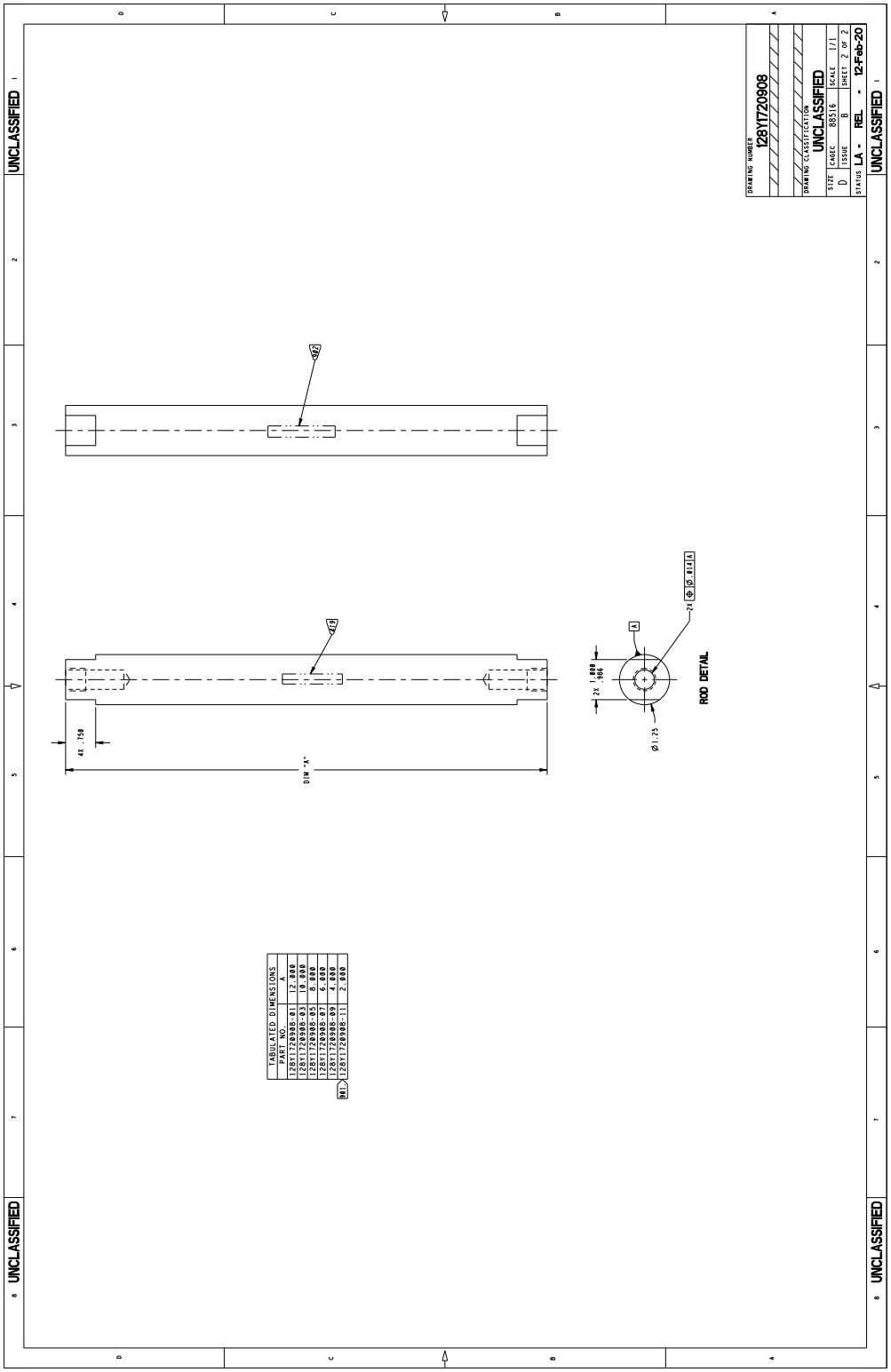

Figure 60: Drawing of the standoffs, DIM "A" is 12.000 (dimensions in inches).

B.5 Adapter Plate

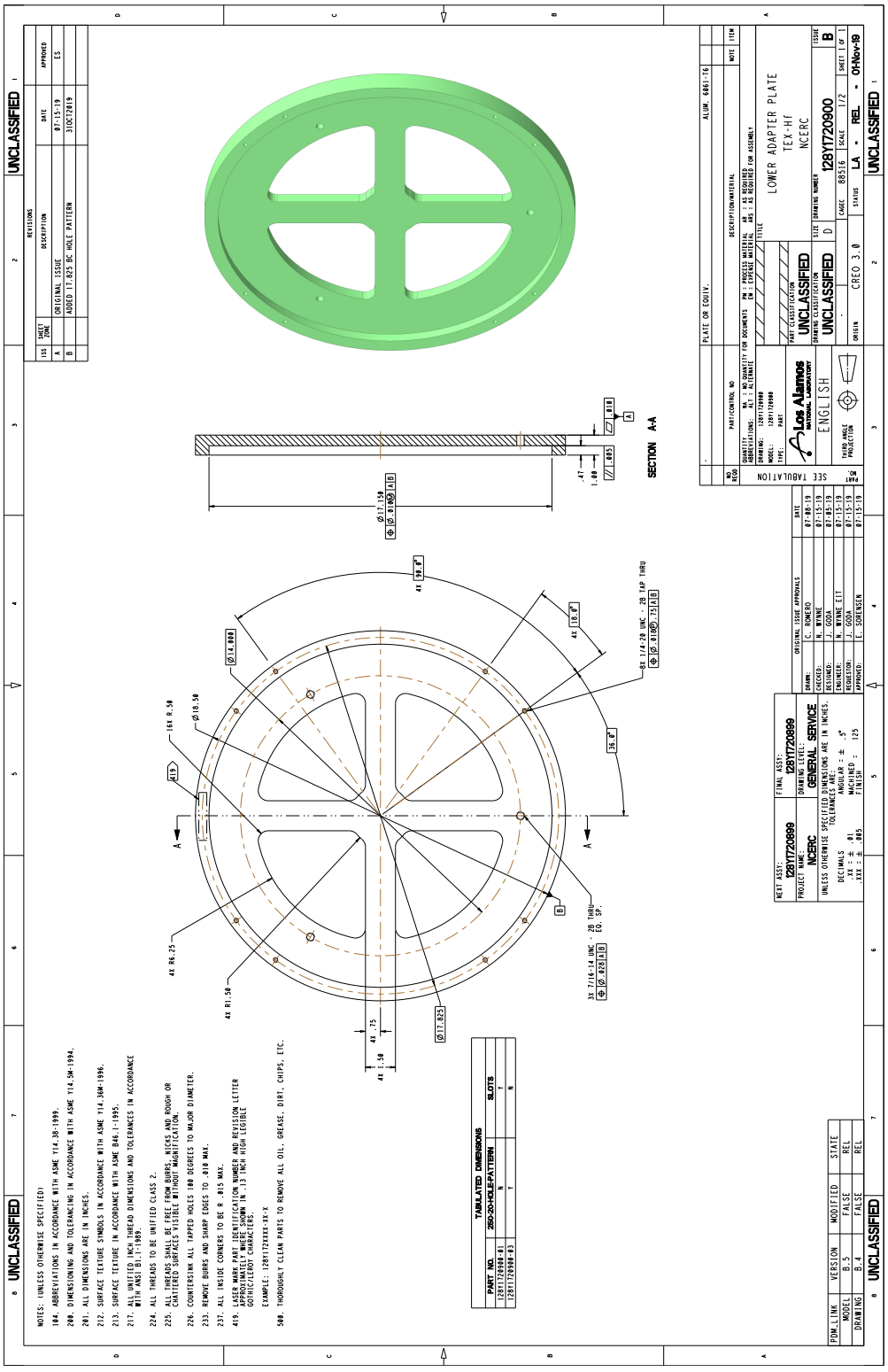

Figure 61: Drawing of the adapter plate, part of the lower adapter (dimensions in inches).

B.6 Adapter Extension

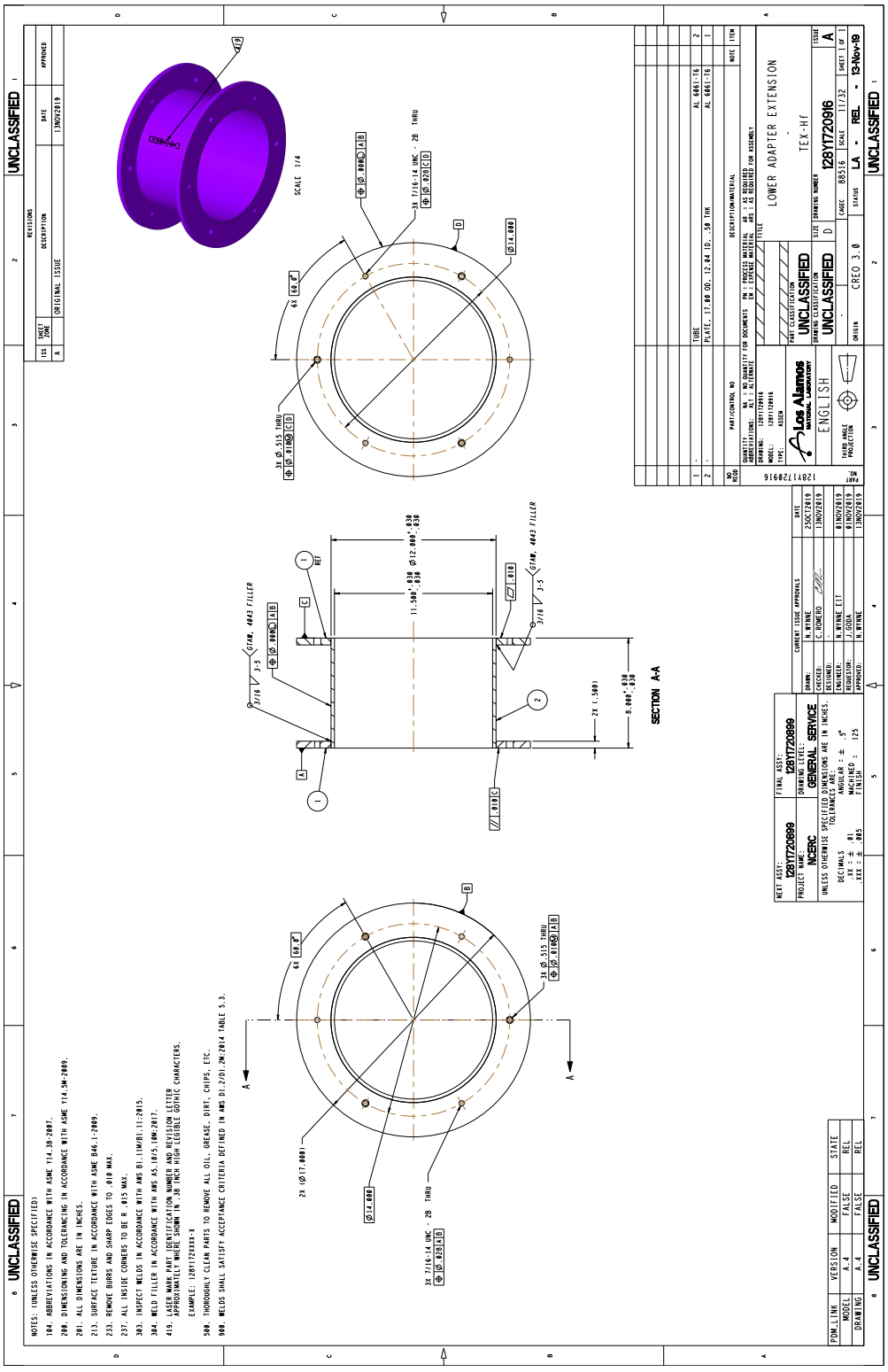

Figure 62: Drawing of the adapter extension, part of the lower adapter (dimensions in inches).

B.7 Membrane

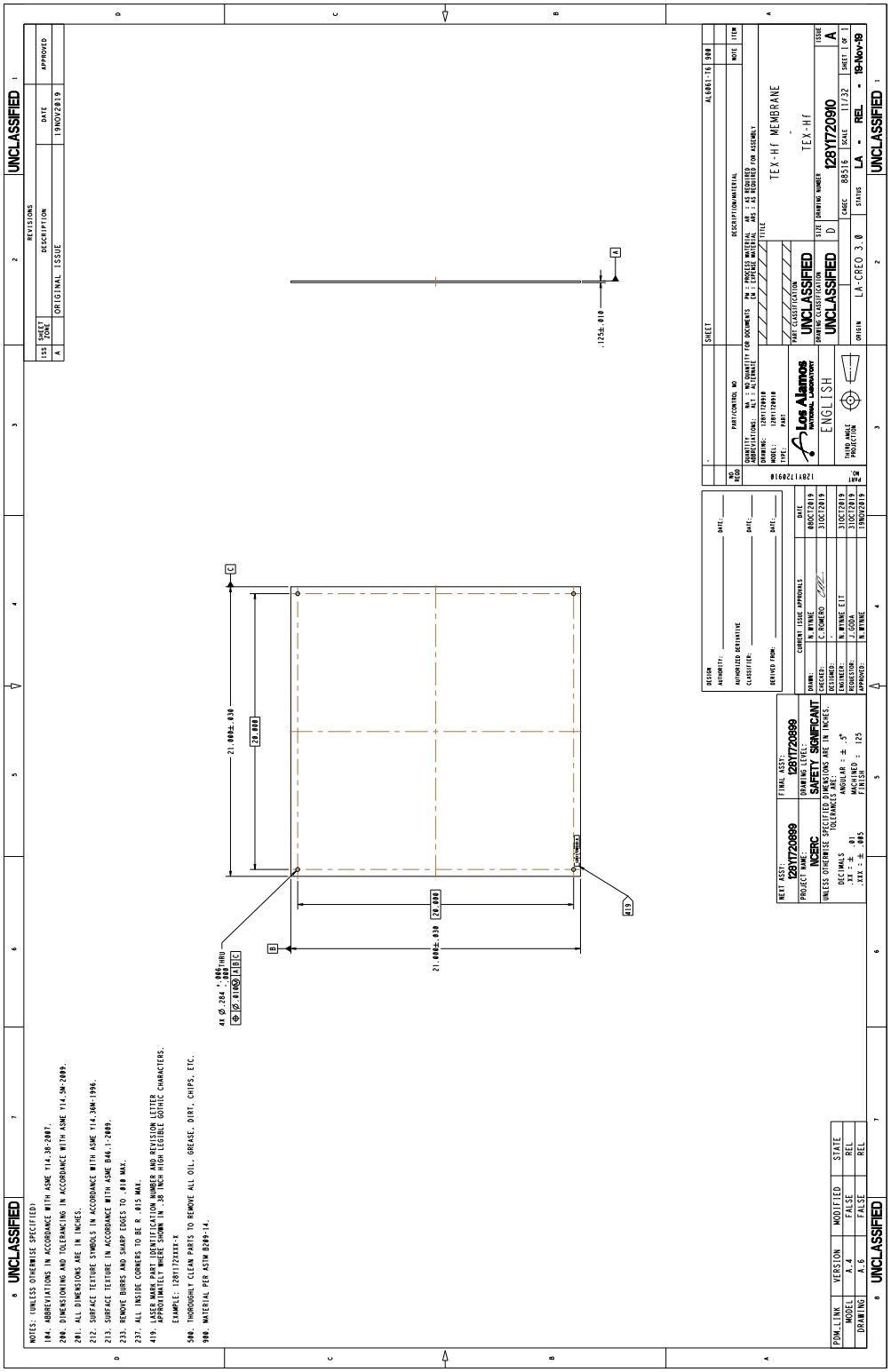

Figure 63: Drawing of the membrane (dimensions in inches).

B.8 Alignment Plate

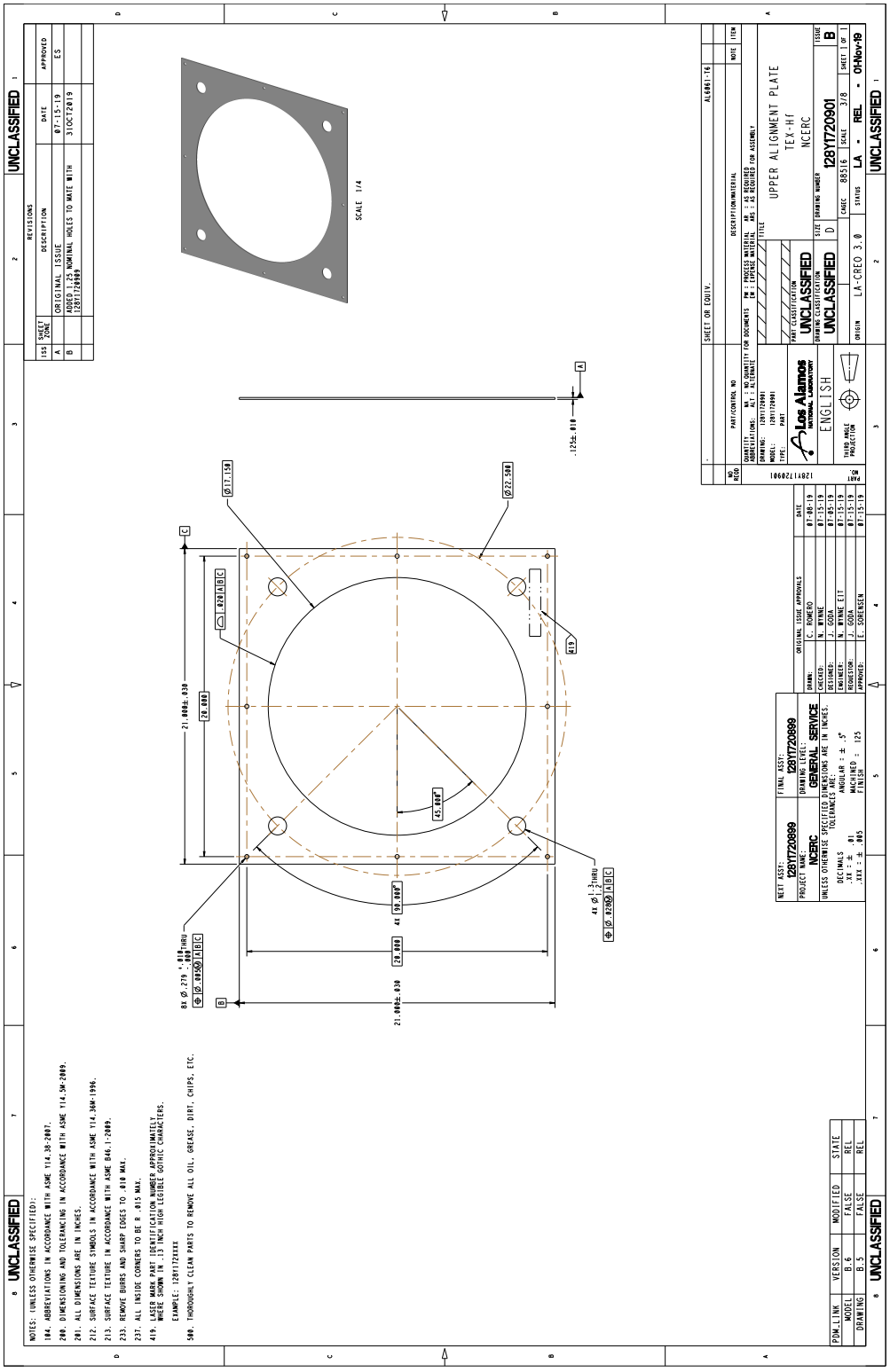

Figure 64: Drawing of the alignment plate, not present in experimental configurations (dimensions in inches).

B.9 Hafnium Plate

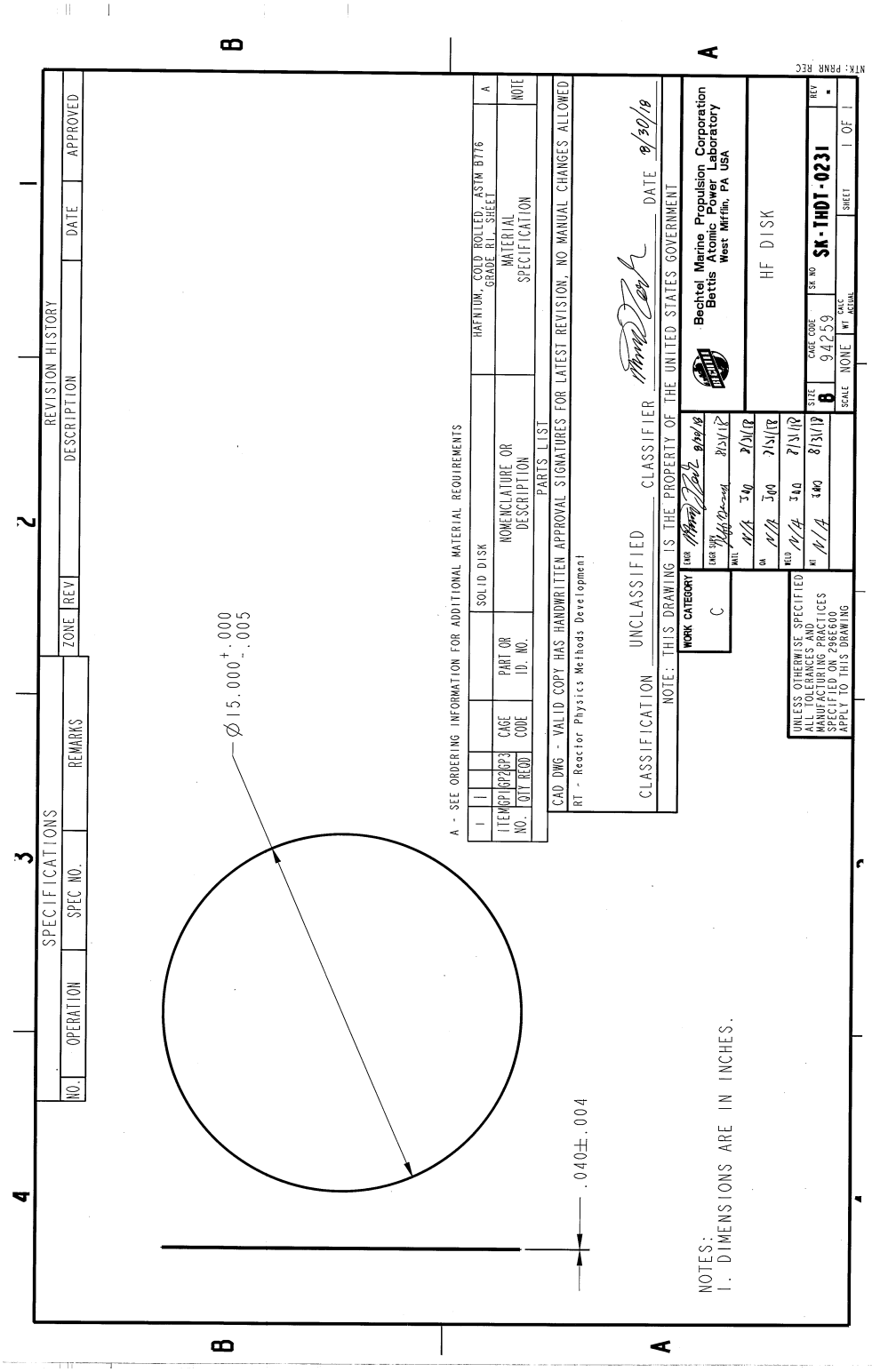

Figure 65: Drawing of the hafnium plate (dimensions in inches). Provided by Naval Nuclear Laboratory.

B.10 Polyethylene Moderator Plates

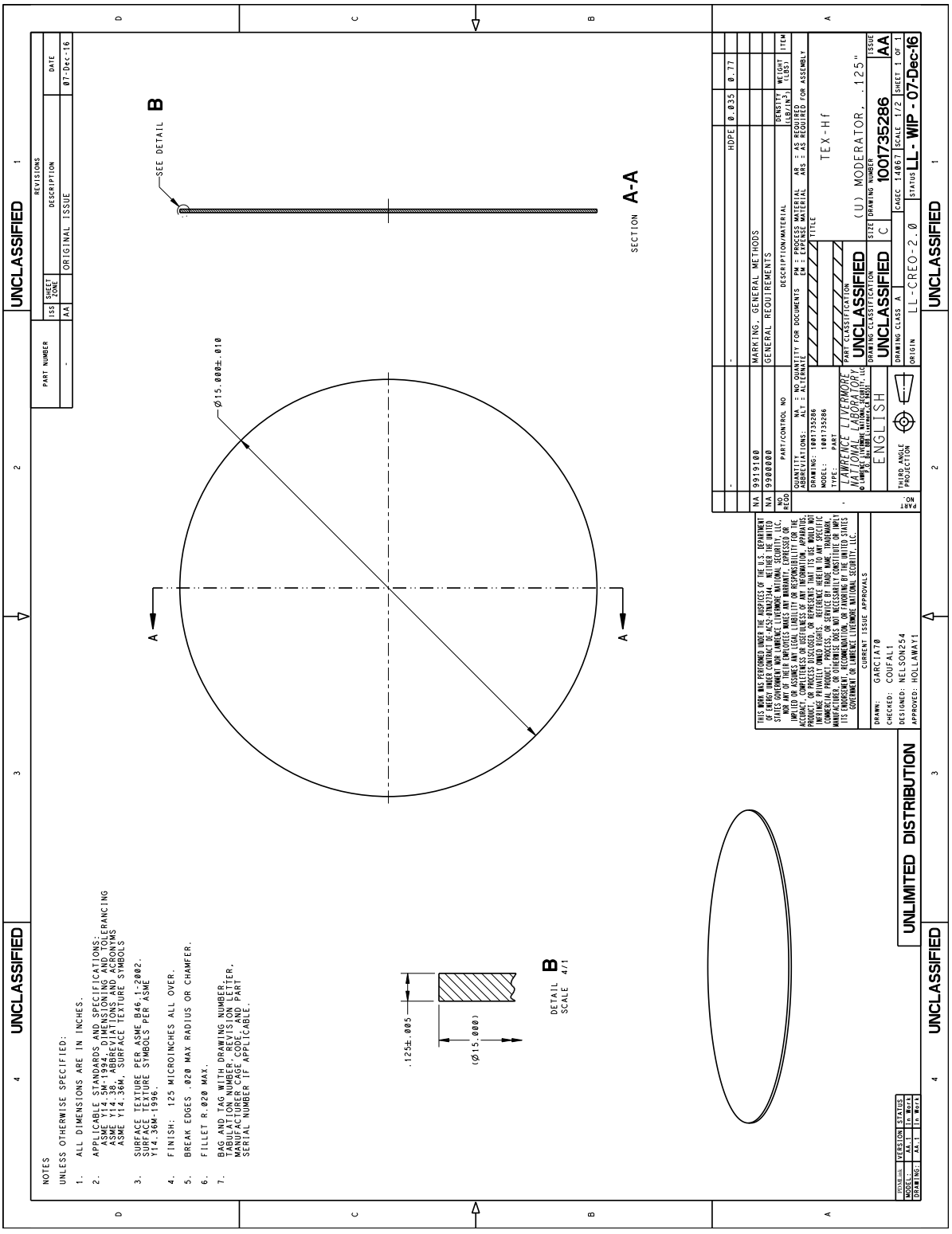

Figure 66: Drawing of the 1/8-MOD plate (dimensions in inches).

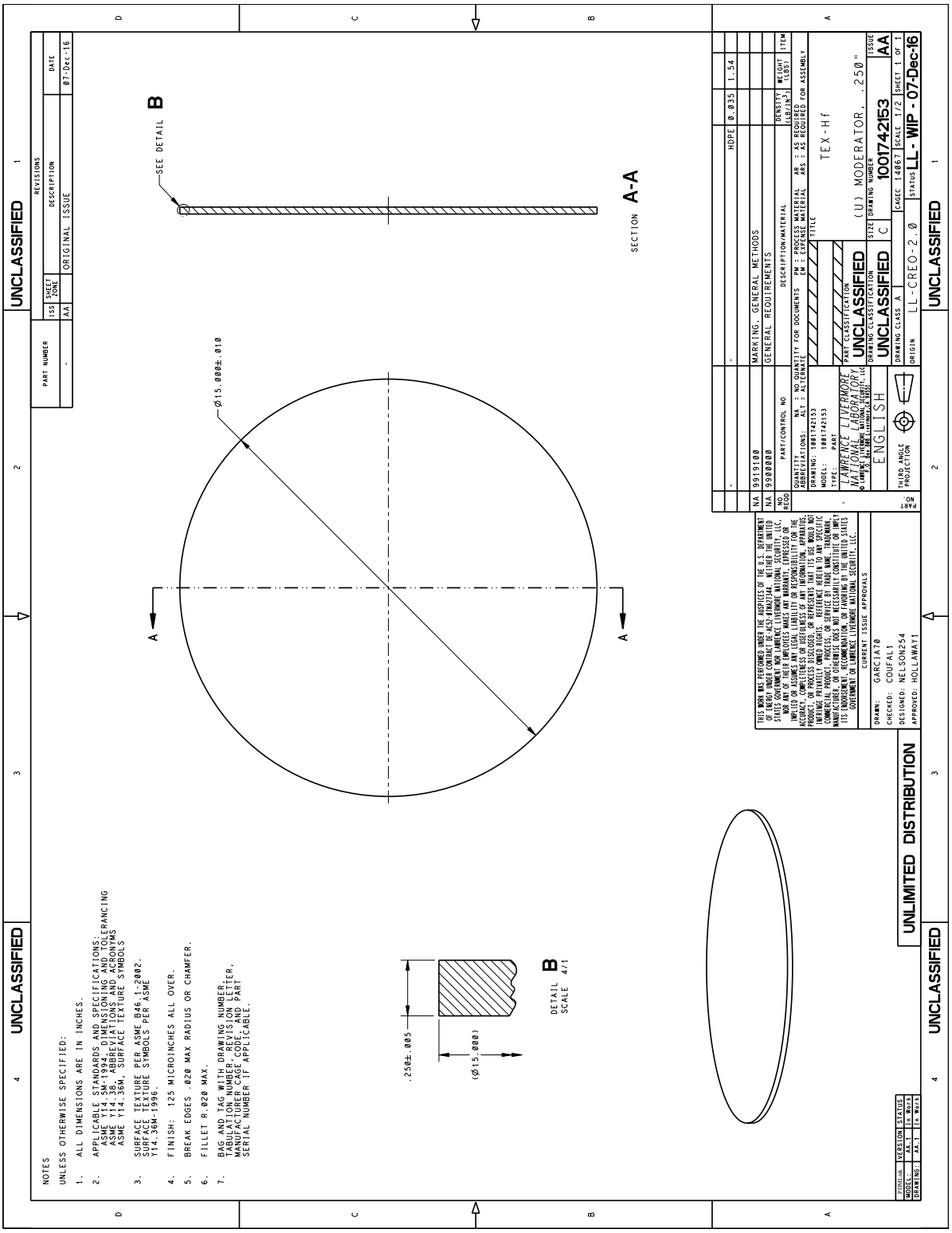

Figure 67: Drawing of the 1/4-MOD plate (dimensions in inches).

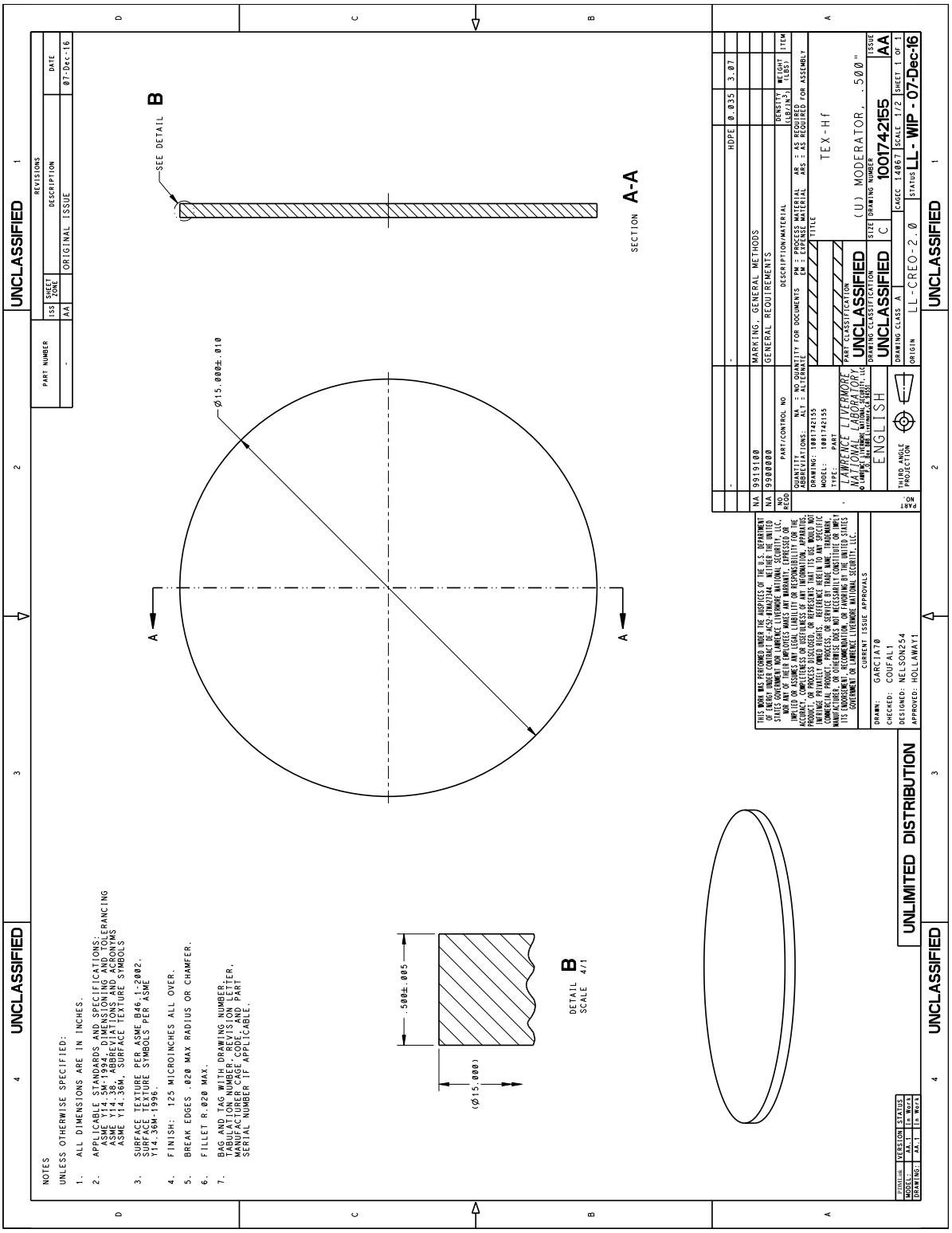

Figure 68: Drawing of the 1/2-MOD plate (dimensions in inches).

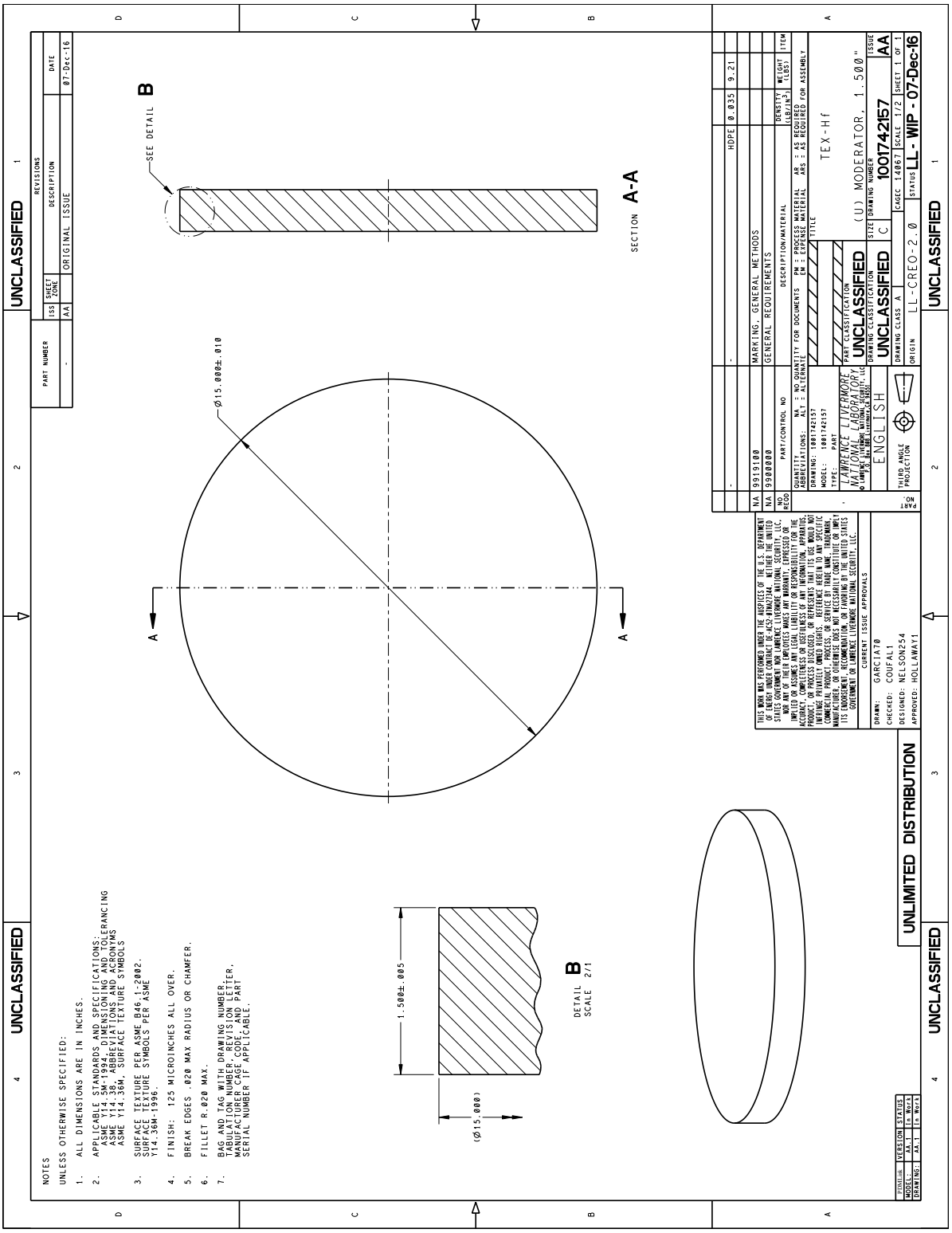

Figure 69: Drawing of the 1.5-MOD plate (dimensions in inches).

B.11 Polyethylene Reflector Rings

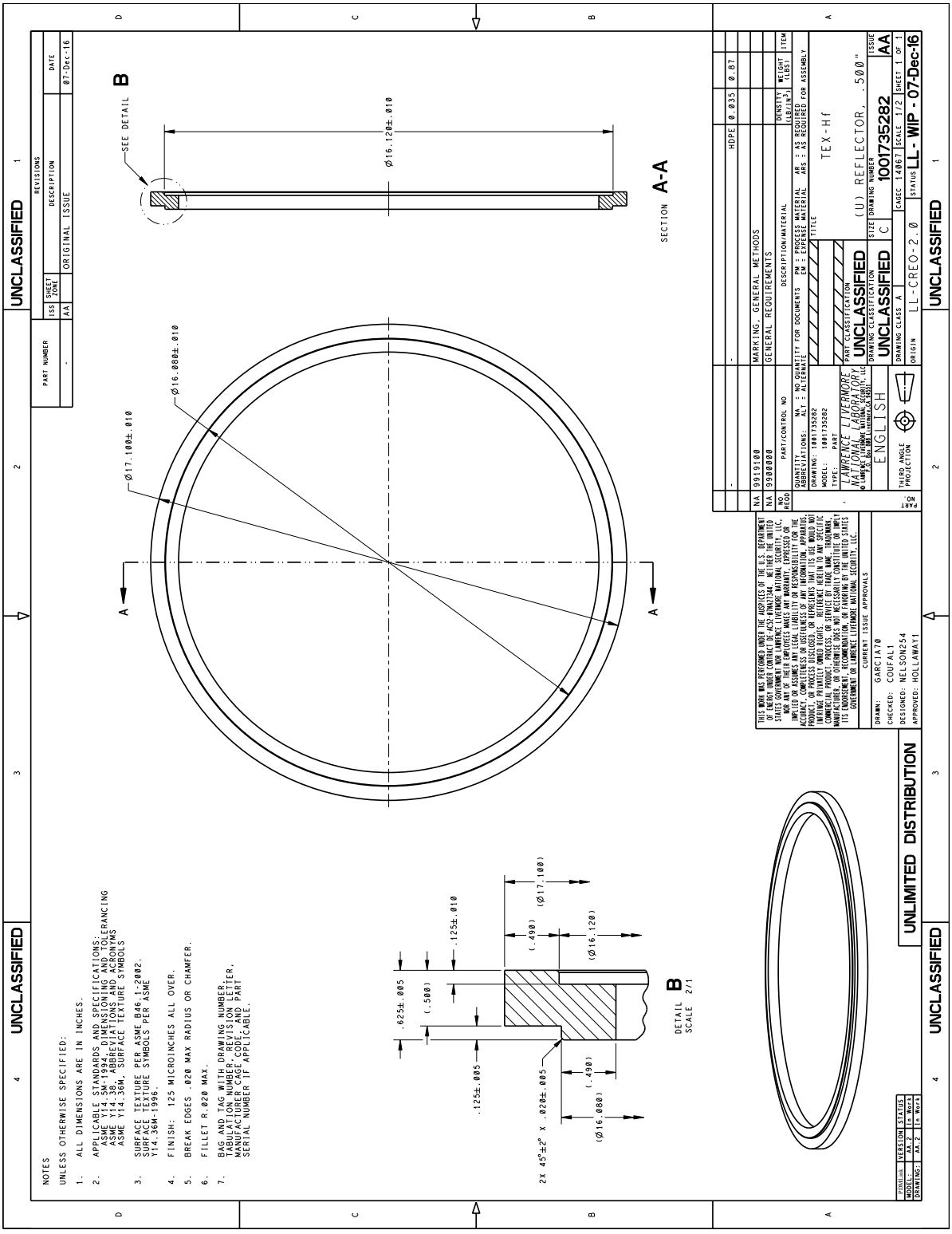

Figure 70: Drawing of the 1/2-RING part (dimensions in inches).

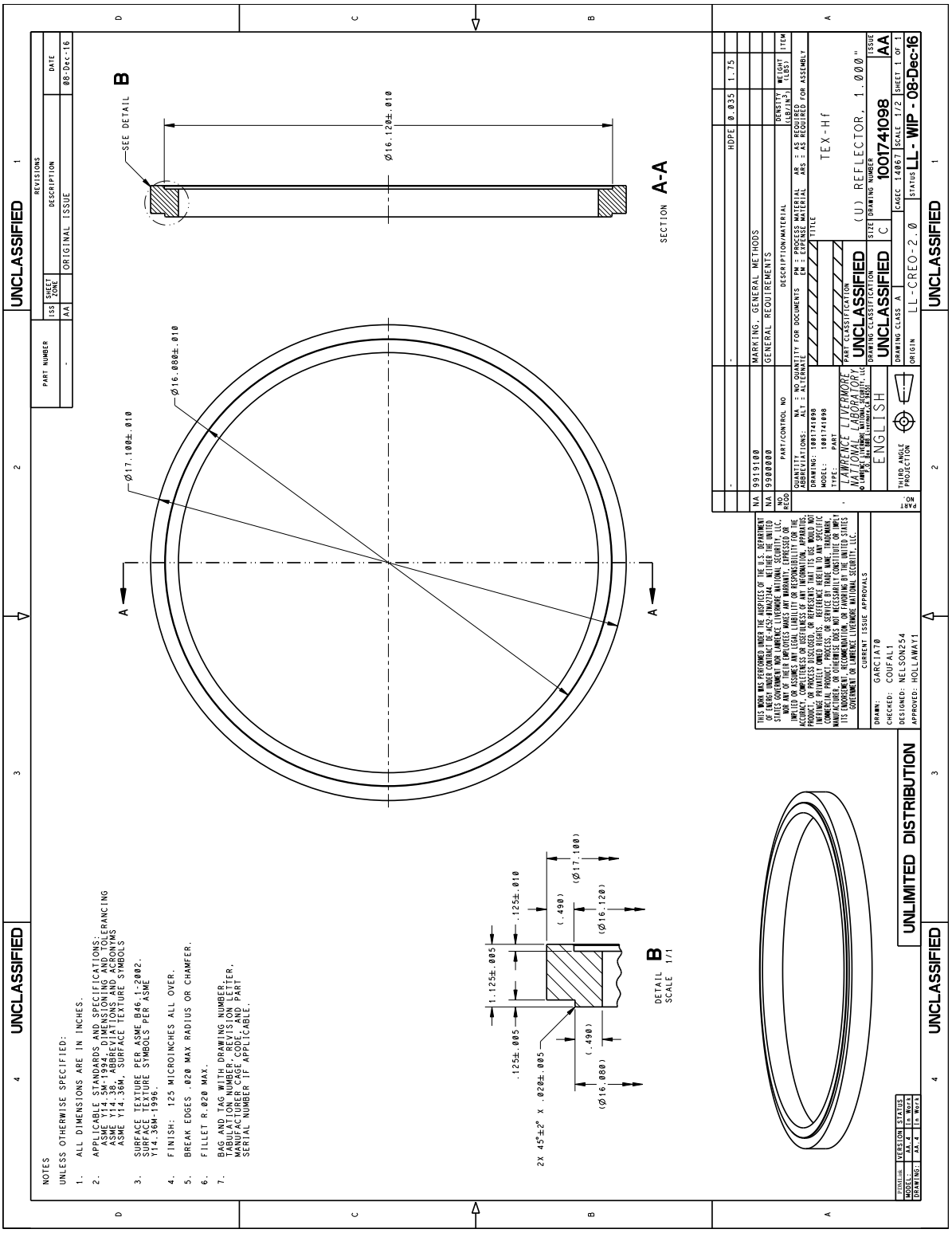

Figure 71: Drawing of the 1-RING part (dimensions in inches).

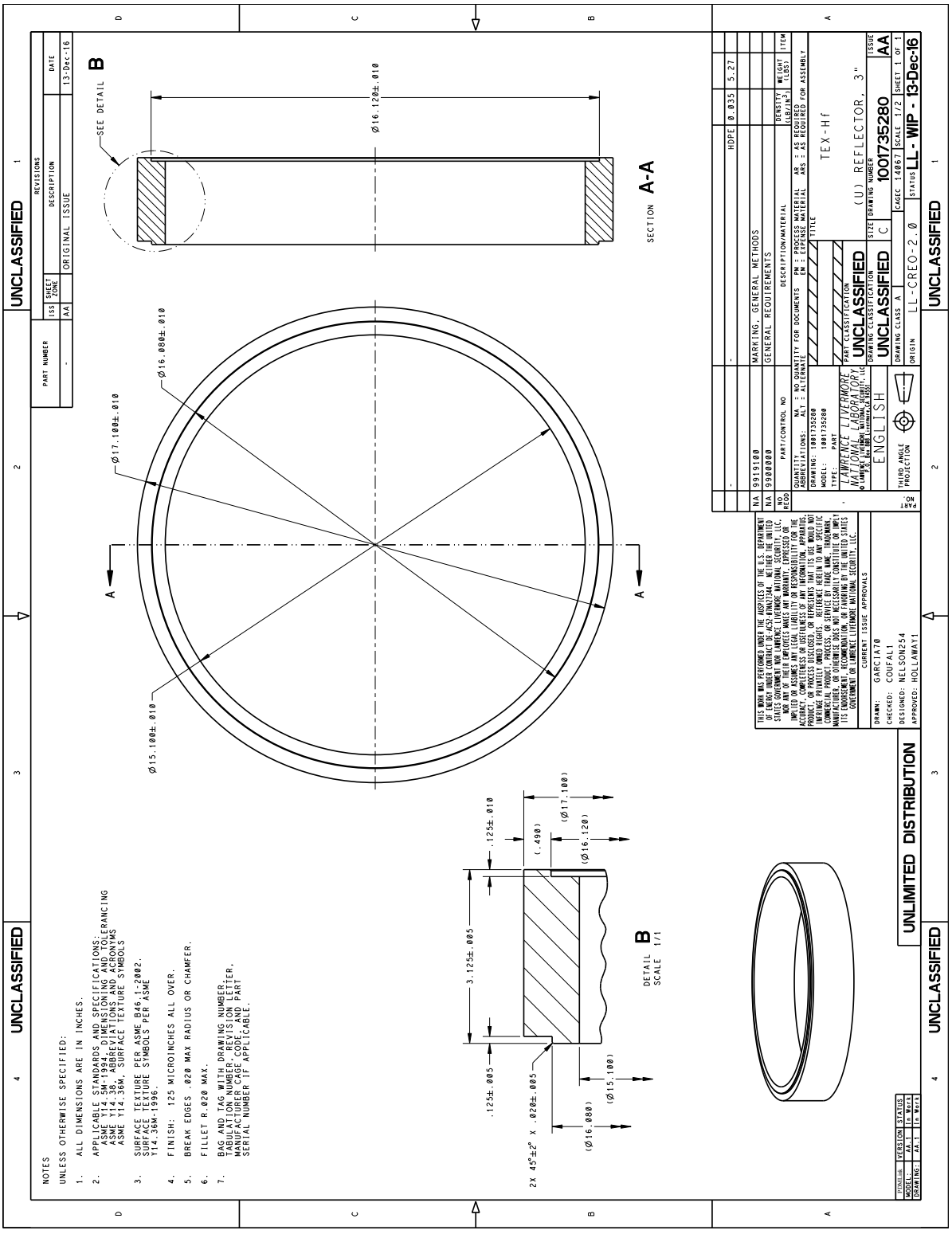

Figure 72: Drawing of the 3-RING part (dimensions in inches).